Prinsloo, Kevin Damian (2017) *Electrophysiological and behavioural consequences of cross-modal phase resetting.* PhD thesis.

https://theses.gla.ac.uk/8269/

Electrophysiological and behavioural consequences of cross-modal phase resetting

Kevin Damian Prinsloo

B.Sc. Psychology, M.Sc. Cognitive Neuroscience

Submitted in fulfilment of the requirements for the

Degree of Doctor of Philosophy

Institute of Neuroscience & Psychology

College of Medical, Veterinary and Life Sciences

University of Glasgow

November 2016

Abstract

This thesis examined the behavioural and electrophysiological signatures of cross-modal phase resetting. This functional connectivity is evident in the brains oscillations that are coordinated through synchronous rhythmic fluctuations. Neural oscillations are ubiquitous in the brain and the synchronised activity between neural populations is thought to be instrumental in the formation of transient coalitions of neurons that guide, modulate or drive behaviour. The key assumption is that this neural coordination is controlled intrinsically, although external input can affect the brains internal dynamics. This is achieved through phase resetting, the alignment of ongoing oscillations. This describes a mechanism whereby an event in one modality can reorganise or phase align oscillations in another, such that subsequent event in that modality are predictable. Through this mechanism, it is possible to investigate modulation of sensory gain across modalities, highlighting the role oscillations play in the discretisation observed in perception. Another well-studied model case for this fundamental operation is the interaction between motor and sensory areas. Motor action leads to predictable sensory consequences. The results of this thesis indicates that, cross-modal phase resetting is a candidate mechanism that could describe the interaction between sensory areas included motor regions.

Table of Contents

Electrophysiological and behavioural consequences of cross-modal phase resetting

1.1 List of figures

1.2. List of tables

1.3. Acknowledgements

1.4. Authors declaration

I declare that, except where explicit reference is made to the contribution of others, that this dissertation is the result of my own work and has not been submitted for any other degree at the University of Glasgow or any other institution.

Kevin Damian Prinsloo

Chapter 1

Introduction

Neural oscillations are ubiquitous in the brain and their synchronisation may provide the neural architecture to allow flexible communication within and between cortical areas. This rhythmic activity is a fundamental mechanism for enabling coordinated activity during cognitive processing (Buzsaki, 2006; György Buzsáki & Draguhn, 2004; Singer, 2013; VanRullen, 2016b; Ward, 2003). Hans Berger (1873-1941) was one of the first scientists to observe brain rhythms from recorded electrical activity from the scalp (Berger, 1929). Since then it has been proposed that spontaneous rhythms reflect the brains internal "state" and may have a fundamental influence on its response to incoming stimuli, as neuronal oscillations signal rhythmic variability in cortical excitability along the temporal and spatial dimensions (Buzsáki & Draguhn, 2004; Fries, 2005; Lakatos, Shah, Knuth, & Ulbert, 2005b)

A complete understanding of how different neural populations communicate is unknown and research continues to investigate the brains exceptionally complex system. At the microscopic level, one of the fundamental models that describe neural communication mechanisms is that of a neuron, which propagates its signals, that are encoded in an action potential (or the degree of action potential synchronisation), along its axon to all other anatomically connected neurons. Effective cognition, however, is flexible and therefore cannot be constrained by a fixed anatomical structure that exists between these neurons. A dynamic communication structure is required for the routing of these signals through these cortical networks. There is strong evidence that oscillations are involved in the process (Fries, 2005). Specifically, the phase locking of oscillations between neural ensembles. It is this synchronous oscillating between neural groups across close and distant regions that constitute the rhythmic modulations of neural excitability that affect the probability of signal propagation and sensitivity to synaptic input. Similarly, the neuro-dynamics of this functional connectivity is evident as activity fluctuations that are coordinated at the macroscopic level as well (Schnitzler & Gross, 2005). Both the micro- and macroscopic activity typically fall within delta (1-4 Hz), theta (4-8 Hz), alpha (8-16 Hz), beta (16-30 Hz), and gamma (30-100 Hz) range.

The existence of oscillatory brain rhythms in these specific narrow frequency bands are believed to be instrumental in the formation of transient coalitions of neurons that modulate or drive sensory cognitive functions (Buzsaki, 2006; Fries, 2015; Voloh & Womelsdorf, 2016). This supports the notion that certain mental processes operate rhythmically (Busch & VanRullen, 2010b; Landau & Fries,

2012a; Neuling, Rach, Wagner, Wolters, & Herrmann, 2012; Thut, Miniussi, & Gross, 2012a; VanRullen, 2016b). It has consistently been demonstrated that the phase of these periodic fluctuations are linked to the periodicities observed in perceptual performance (Thut, Miniussi, & Gross, 2012; VanRullen, VanRullen, 2016b). Emerging evidence points to multiple perceptual cycles that could indeed coexist in distinct brain networks, with different frequencies.

The brains neural oscillations have been linked to the notion that perception may be modulated in a discrete manner which can be measured in various frequency bands. This is one of the overarching theory that is being investigated by this thesis and will be discussed in greater detail below. The brains neural activity can be recorded with a variety of techniques from single-neuron recordings or at the macroscopic level, this include but not limited to, electrophysiological techniques such as magnetoencephalography (MEG) and electroencephalography (EEG). Frequency-specific activity emerges from neural interactions that are often localised to specific cortical layers of the neocortex (Wang, 2010). This thesis will contribute uniquely to the existing literature which demonstrates that the brains rhythms play a crucial role in sensory perceptual processing, including motor mechanisms (Buzsaki, 2006; Buzsáki & Draguhn, 2004; Thut et al., 2012; VanRullen, 2016b; VanRullen & Dubois, 2011), and that these rhythms can be modulated via internal cross-modal interactions (Kayser, Petkov, & Logothetis, 2008; Naue et al., 2011; Romei, Gross, & Thut, 2012; Schroeder & Lakatos, 2009a; Thorne & Debener, 2014; Voloh & Womelsdorf, 2016).

Oscillatory phase modulates perception

Modulation of sensory perception depends not only on the physical properties of the stimulus but also on the temporal dynamics of instantaneous state of the sensory system at the time of input. This instantaneous state, defined by ongoing neural oscillations, reflects the fluctuations in local field potential between high and low excitability states (Başar, 1998; Buzsaki, 2006; Fries, Nikolić, & Singer, 2007). This can which can be conceptualised as the peaks or troughs (or phases) of a sine wave (see figure 1.1). Changes in the phase of these rhythms over time reflect the dynamically evolving state of the brain and may contribute to this temporal modulation of sensory information processing. Such that, each oscillator has an optimal phase for processing associated with high neuronal excitability (Aoyagi et al., 1993; Schroeder & Lakatos, 2009). During a high excitability state when neurons are closer to their firing threshold, a near-threshold stimulus is more likely to be detected and subsequently acted upon (Henry & Obleser, 2012; Lakatos et al., 2009; Lakatos, Chen, O'Connell, Mills, & Schroeder, 2007). This is because inputs arriving during the optimal phase are 'amplified' (these generate relatively large responses); whereas input arriving at the non-optimal phase are 'supressed' (generating relatively small responses). This enables oscillations to have a pivotal role in perceptual processing (Lakatos et al., 2005; Schroeder & Wilson, 2010; VanRullen, 2016b).

Within this framework, depending on what phase a particular sensory brain area is in, would determine whether a stimulus is perceived and subsequently acted upon. However, studying this effect in behavioural experiments (without MEG or EEG) is difficult because the state at time of stimulus presentation is unpredictable. One method used to avoid the unpredictability in perceptual responses is to perturb the system, and eliminated the somewhat arbitrary state of the underlying phase of the cortex. (Klimesch, Hanslmayr, Sauseng, & Gruber, 2006; Makeig, Debener, Onton, & Delorme, 2004a; Voloh & Womelsdorf, 2016). Through the mechanism of phase reset, input from an external event cause the uniform random distribution, across trials, of the phase of MEG in one or more frequencies to partially collapse. Such an event causes a partial 'phase resetting' induced by the stimulus and contributes to the event-related response (ERF) with or without an increase in MEG power (Makeig et al., 2004). Research indicates that phase reset is more likely to occur in the trough of theta (4-6 Hz), alpha (4-8 Hz) and gamma (25-55 Hz) frequency ranges (Haegens, Händel, & Jensen, 2011; Jacobs, Kahana, & Ekstrom, 2007; Quyen & Bragin, 2007).

This seemingly direct link to the underlying physiology is less conclusive for oscillatory power. However, while fast fluctuations of neural activity reflected by changes in phase are important, changes in amplitude, which typically occur on the scale of hundreds of milliseconds to seconds, are also thought to be influential. It has been demonstrated that variability in the power of spontaneous oscillations in specific frequency bands predicts perceptual performance (Ergenoglu et al., 2004; Hanslmayr, Klimesch, & Sauseng, 2007; Thut, Nietzel, Brandt, & Pascual-Leone, 2006) and sensory-driven changes (Dijk, Schoffelen, & Oostenveld, 2008; Gross, Schnitzler, Timmermann, & Ploner, 2007). Ongoing pre-stimulus oscillatory power has been instrumental in demonstrating a variation in perceptual processing. For example, alpha amplitude reduction correlate with improved performance (e.g. Thut et al., 2006) and amplitude increments associated with impaired performance (e.g. Kelly et al., 2006).

These ongoing brain oscillations suggest that sensory systems operates in a discrete manner, sampling information in the sensory environment within these specific time-windows of high and low excitability states (VanRullen & Busch, 2011; VanRullen, 2016). Sensory perceptual sampling at the neuronal level may be characterised by the specific features in the amplitude and phase of neural oscillations. For example; previous findings show the amplitude of pre-stimulus alpha (8-12 Hz) oscillations (Ergenoglu et al., 2004; Hanslmayr, Klimesch, & Sauseng, 2007; Klimesch, Sauseng, & Hanslmayr, 2007; Romei, Gross, & Thut, 2012; Romei, Gross, & Thut, 2010; Romei, Rihs, Brodbeck, & Thut, 2008; Thut, Nietzel, Brandt, & Pascual-Leone, 2006); and the phase of occipital alpha rhythms, are associated with accuracy in perceptual discrimination of near-threshold visual stimuli (Buschman & Miller, 2009; Laura Dugué, Marque, & VanRullen, 2011; Hanslmayr et al., 2007; Mathewson, Gratton, & Fabiani, 2009; VanRullen, Guyonneau, & Thorpe, 2005); including the probability of neural firing

(Fries et al., 2007; Lakatos et al., 2005; VanRullen, Reddy, & Koch, 2005; Whittingstall & Logothetis, 2009). These findings reveal that alpha-band oscillations modulate incoming sensory information, whereby a phase correlated inhibitory influence gates neuronal firing in a cyclic manner as a function of time (Busch, Dubois, & VanRullen, 2009; Jensen & Mazaheri, 2010; Klimesch & Schack, 2004; Mathewson & Gratton, 2009; Sauseng, Klimesch, & Gruber, 2007; Sauseng, 2012; Thut et al., 2006).
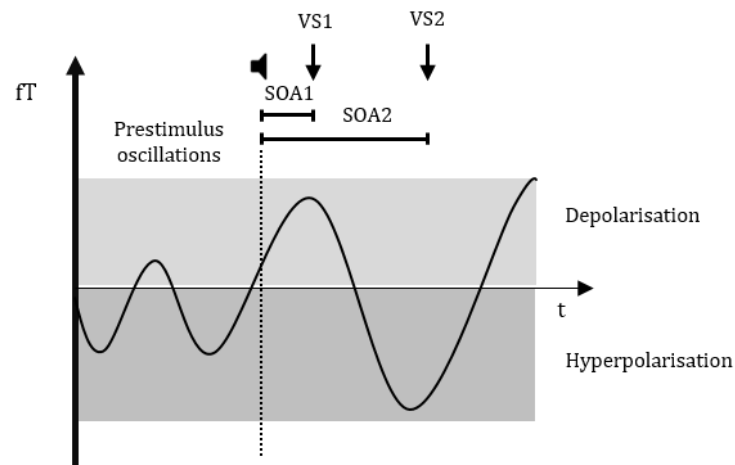
Figure 1.1. Schematic of phase-resetting influence on perception. The instantaneous neural oscillatory systems are present prior to stimulation and is at a higher probability of being below the threshold for neural firing to occur, the membrane voltage of visual neurons oscillate between states of depolarization (high excitability) and hyperpolarisation (low excitability). At the onset of the transient auditory stimulus (vertical dotted line), the phase of ongoing oscillations are either reset to a fixed value (phase-reset) or a visual oscillations is evoked. Whereby, if the target visual stimulus (V1) is presented during a state of more depolarization (after SOA1), the probability of accurately detecting and/or discriminating a near-threshold stimulus is higher because it can more readily exceed the firing threshold of visual neurons and evoked a brain response with specific perceptual consequences for conscious detection and subsequent reaction. If, however, the target stimulus (V2) occurs during the more hyperpolarized state (After SOA2), it is less likely to excite visual neurons

Rhythmic versus discrete perception

Having introduced neural oscillations their role perception suggests that the brain subsamples its environment in a discrete way. However, the notion of whether perception really does operate in a discrete way has been widely debated (*for reviews see*; Vanrullen, 2013; VanRullen & Koch, 2003; VanRullen, 2016b). Opponents argue that perception operates in a rather continuous way, and this debate has gained the term the "discrete vs. continuous perception". Researchers in support for the continuous nature of perception, argue that oscillations could drive a continuous sequence of sensory inputs into our perceptual systems forming a series of discrete cycles or "snapshots" (Harter, 1967; Pitts & McCulloch, 1947; Stroud, 1956). However, this view has become less accepted nowadays. The argument for rhythmic perception (also known as, cyclic or periodic perception – and these terms will

be used interchangeably throughout this thesis) implies that the oscillatory phase dynamics modulate perception rhythmically, where certain phases give rise to more efficient processing while at another phase the same process is less efficient. Discrete perception on the other hand, further necessitates that sensory perceptual events and neural processes are separated into discrete epochs ("snapshots"). By this account, events that are not perceived in one snapshot are differed to the next. Thus, oscillatory cycles modulate the temporal parsing of perceptual cycles. Within this framework, it is clear that neural oscillations are the optimal "candidate" mechanism that can reflect these perceptual cycles.

One illusion that demonstrates both sides of this argument is the continuous wagon wheel illusion (Purves & Paydarfar, 1996). In this illusion a continuous periodic motion stimulus can sometimes be perceived as moving in the opposite direction, known as temporal aliasing (VanRullen, Reddy, & Koch, 2006). In temporal aliasing, the signal (the wagon wheel) is a moving pattern, and the information processing system is taking temporally discrete samples with a sampling rate lower than the critical limit (of the system), then the system's representation of the signal is inaccurate. This critical limit has been found to exists around 13 Hz and thus, around alpha band. The perception of the illusion is represented in with a peak in the power spectrum of the EEG at the same frequency. This illusion occurs sporadically and requires some time to adapt, leading some researchers to argue that perception is dependent on spurious activation of low-level motion detectors, requiring sufficient adaptation time, after which they begin to dominate perception (Kline & Eagleman, 2008) suggesting that the visual system is continually sampling our environment. In contrast, another theory which could explain the causes of this illusion is that the visual system samples the environment in a series of snap shots suggesting that our environment is not continuously sampled, but rather is discretely sampled (VanRullen, Carlson, & Cavanagh, 2007). However, these two seemingly independent theories can be reconciled (VanRullen, 2016b). Any periodic modulation of sensory processing will result in distortions of perceived timing that would in fact resemble a discrete temporal framing. Vanrullen (2016b) argues that essentially the distinction between these concepts is a matter of degree, and fundamentally, any perceptual periodicities are principally relevant to the question of discrete perception.

Cross-modal phase reset

Conventional investigations into the mechanisms of perceptual processing have focused on activity within the primary sensory cortices as a function of their respective inputs. Research investigating multisensory stimulation have demonstrated that in addition to the preferred modality, extended cortical regions are modulated via cross-modal inputs related to nonpreferred modalities at the level of primary cortical areas (Kayser, Petkov, & Logothetis, 2008; Lakatos et al., 2009; Lakatos, Karmos, Mehta, Ulbert, & Schroeder, 2008). For example, stimulus input in one modality can cause a transient phase reorganisation of oscillations in another modality and eliminate the somewhat arbitrary state of

the underlying phase in the cortex. This in principle could lead to responses that are more predictable in the nonpreferred modality. This is often referred to as cross-modal phase resetting (CMPR) (Kayser et al., 2008; Lakatos et al., 2009).

By aligning the phase of separate oscillators, pre-synaptic potentials from one will arrive during a time when they can have maximal impact on a post-synaptic neuron (Fries, 2005; Voloh & Womelsdorf, 2016). Aligning the phase thereby results in predictable "windows" of integration, and provide a way for an upstream receiver to segregate information that should be processed from that which should be ignored simply by shifting the relative phase (Fries, 2009). For example, during a low excitability phase (when local circuitry is less sensitive to perturbation), relatively stronger incoming excitation is necessary to elicit a post-synaptic spike, whereas a relatively weaker excitation is sufficient during the period of high excitability (Vinck et al., 2010). Therefore, a low intensity stimulus could encode in the high excitability phase, and the opposite hold true for a high intensity stimulus (see figure 1.1). In other words, on the macroscopic level, this characterises the mechanism whereby cross-sensory interactions prompts an evoked response by the occurrence of an exogenous sensory stimulus shifting or realigning the phase of ongoing neural ensembles to a specific value with each event. This is an index of functional connectivity between the two regions. To this end, the processing of a subsequent stimulus in another modality is either facilitated or supressed and is dependent on the exact relation between phase of an oscillation and the occurrence of a second stimulus. Through this mechanism of aligning neural events across modalities in relation to an extraneous event suggests that this is a candidate mechanism for multisensory integration. Several lines of research suggest that transient auditory stimulation can modulate visual responses in the visual cortex, in doing so influencing early sensory-perceptual processing (Fort, Delpuech, Pernier, & Giard, 2002; Giard & Peronnet, 1999; Mercier et al., 2013b; Mishra & Martinez, 2007; Molholm, Ritter, & Murray, 2002; Naue et al., 2011; Raij et al., 2010; Romei, Gross, & Thut, 2012). This idea is central to this thesis.

Evidence for unimodal and cross-modal phase reset

Sounds have consistently been shown to enhance the perception and detection of visual target stimuli through this mechanism (Diederich, Schomburg, & Colonius, 2012; Fiebelkorn et al., 2011; Lakatos et al., 2009; Mercier et al., 2013; Naue et al., 2011; Romei et al., 2012). Visual input leads to widespread modulation of processing and some have found visual input alone may activate the auditory cortex (Raij et al., 2010). The exact underlying mechanisms however are still up for debate. In the dominant model, CMPR would not lead to increased signal amplitude (as measured with MEG or EEG) in the target sensory area (e.g. auditory input does not increase amplitude of visual activity) but rather realigns –or resets- ongoing activity to a state of high or low excitability. Through this mechanism, the visual system is systematically prepared for the expected imminent visual input, leading to potential gains in efficiency or sensitivity in sensory perceptual processing (Thorne, De Vos,

Viola, & Debener, 2011). Therefore, an exogenous auditory stimulus, such as a salient transient tone, is able to reset ongoing activity and thereby reveal the oscillatory modulation in perceptual performance.

One of the first influential and fundamental studies to demonstrate pure phase resetting, was an investigation of multisensory interactions in primary auditory cortex (A1) in the macaque using somatosensory and auditory stimuli (Lakatos et al., 2007). In this study Lakatos et al. demonstrated that somatosensory related responses in A1 are characterized by a low amplitude supragranularly weighted current source density (CSD) modulation combined with no transient multiunit activity (MUA) correlate, indicating that while somatosensory input does alter the net local neuronal excitability (attributed by an organized post-stimulus CSD pattern in the averaged response) it does not alter the amount of net post-stimulus transmembrane current, and therefore does not "trigger" neuronal firing. In contrast to these findings, they also found that auditory, preferred modality stimuli result in an increase of net transmembrane current in all cortical layers, that aggregates to an evoked type response (*but see section below: **conceptual issues***). Coincidently, this type of response is similarly characterised by a phasic MUA response caused by an increase in synaptic currents. As a result, phase-reset and evoked type responses are functionally different. Phase-reset is modulatory since it does not trigger suprathreshold neural firing, whereas evoked activity is a driving type of response, which results in significant increase in post-stimulus MUA indicating that specific information (e.g. frequency, location, intensity, etc.) about the stimulus is being transmitted.

They found that these two different types of responses have different spectral signatures. Here in the time-frequency domain, phase reset was restricted to enhancement of physiological responses at specific SOAs that correspond to cycles of the dominant delta, theta and gamma frequencies observed in the spectral profile of spontaneous auditory activity (Lakatos et al., 2005). The biased post-stimulus phase distribution (i.e., phase locking) was accompanied by little or no pre- to post stimulus increase in oscillatory amplitude, which is the hallmark of oscillatory phase resetting (Delorme & Makeig, 2004; Shah et al., 2004; *but see conceptual issues section below*). Opposed to this, they found that evoked type or driving responses were characterised by a sharp onset de-novo generated waveform, which in the time-frequency domain is represented by a spectrally distributed amplitude increase, coupled with a biased phase distribution similarly spanning the whole spectrum due to the sharp onset. It is noteworthy that these findings do not necessarily indicate that auditory, preferred modality stimuli do not reset ongoing oscillations, but that signatures of phase reset are "masked" by larger amplitude evoked activity.

In a further study, they demonstrated through electrophysiological recordings in A1 from the macaque, that a somatosensory stimulus alone has a minimal effect on the amplitude of local field

potentials (LFP) but systematically aligns the phase of individual trials with a specific phase angle known to elicit maximal stimulus driven responses (Lakatos et al., 2007). Here they found evidence for a perceptual facilitation in the primary visual cortex following an auditory induced phase-reset. These findings suggest a supramodal coordination of theta-band oscillatory activity. Lakatos et al. (2009), in a follow on study, showed that visual stimuli modulated primary auditory activity via phase resetting. Notably, phase reset followed only when sensory stimuli were attended to or inherently salient, in contrast to evoked typed responses. Kayser et al. (2008) further demonstrated that oscillatory phase in auditory cortex can also be reset by visual input, and the opposite hold true whereby auditory regions can phase align visual oscillations.

Thorne *et al.* (2011) using a combined reaction time- (RT) electroencephalography (EEG) paradigm, found similar results using an auditory frequency discrimination task. Here a short audiovisual stream was presented where two responses were recorded, the initial stimulus response and another to the target. Their findings revealed significant increases in phase concentration in alpha (8-12 Hz) and beta-band (13-30 Hz) when the visual stimulus preceded the auditory stimulus by a 30 to 75 ms lag. By implementing a variable SOA, it was possible to show that visual perception systematically varied in a cyclic pattern time-locked to the auditory stimuli. Naue et al. (2011) provided complimentary evidence in a similar RT-EEG paradigm. They demonstrated how auditory stimuli can modulate visual discrimination of brief flashes of light to the left and right eye preceded by a binaural auditory stimulus with varying SOAs. Auditory stimuli were presented at 40 to 70 ms in increments of 5 ms, prior to the light flashes. They found that the amplitude of beta-band (28.9 Hz) response was modulated as a function of SOA. Although manual RTs decreased with increasing SOA, they were not able to discern oscillatory effects, this could be due to the SOA range not being sufficiently long enough to reveal any oscillatory signatures.

Romei et al. demonstrated that auditory stimulation can decrease the threshold of perceived phosphenes induced by a single pulse of transcranial magnetic stimulation (TMS) when applied over the occipital pole (Romei, Murray, & Merabet, 2007). Excitability of low-level visual cortices is pre-perceptual and stimulus selective (Romei, Murray, Cappe, & Thut, 2009) and demonstrated both physiological and perceptual periodic fluctuations in visual alpha (~10 Hz) which followed an auditory induced-phase reset (Romei et al., 2012). Romei *et al.* (Romei, Gross, and Thut., 2012) presented brief sounds while simultaneously recording EEG and visual perceptual performance was assessed via visual excitability using TMS to induced phosphenes.. In the first of two experiments, phosphene perception rate showed a periodic fluctuation at ~10 Hz phase-aligned to the sound. In a second study combining TMS and EEG, on trials where TMS was administered revealed the same fluctuations of phosphene perception at a ~10 Hz pattern of EEG-derived measure of occipital cortex reactivity to the TMS pulses. On no-TMS trials, there was alpha phase-locking over both the auditory cortex and

posterior parietal-occipital regions implicating the visual cortex. These independently recorded variables were significantly correlated. This was taken as evidence that cross-modal phase locking of oscillatory visual cortex activity can show both physiological and perceptual properties consistent with auditory induced resetting of visual alpha activity. Importantly, perceptual and physiological periodicities were recorded on separate trials and revealed that electrophysiological fluctuations were representative of physiological substratum of the periodicities observed in the perceptual data. This was taken as evidence that cross-modal phase locking of oscillatory visual cortex activity can show both physiological and perceptual properties consistent with auditory induced resetting of visual alpha activity.

Busch *et al.* (2009) used EEG to demonstrate how auditory stimuli can modulate visual perception of near-threshold brief flashes of light to the left and right hemifields preceded by a binaural auditory stimulus. In this signal detection paradigm on average only half the stimuli were perceived although all stimuli were identical. The results show that the trial-by-trial variability of perception was systematically phase-locked to the tone onset at theta (4-7 Hz) and at alpha (8-12 Hz). This suggests that pre-stimulus phase angle of alpha-band activity predicts target detection performance. This notion was further support by Mathewson *et al.* (2009) who found that for undetected trials, the phase at stimulus onset was difference from that of detected trials. These findings demonstrate that mechanism whereby at certain phases of alpha and theta cycles, visual target detection of near threshold stimuli was higher compared to other phases. These accumulating findings provide the underpinnings of the inhibitory role of alpha activity, and is evidence towards the model of pulsed inhibition as described in detail by Jensen & Mazaheri (2010).

Mercier and colleagues (2013), using a simple detection task with data measured from intracranial recording from patients with epilepsy, found an auditory-driven phase reset in visual cortices. Here theta and alpha bands showed increased phase coherence to audio-visual stimuli relative to audio or visual presented separately. Fiebelkorn et al. (2013), were also able to show both physiological and perceptual phase related effects recorded from EEG using long auditory and visual SOAs between 2.5 and 5 s. The data show phase-detection relationships were not confined to small set of certain frequencies, but rather were shown across a wide range of frequencies from low delta to high beta (1-30 Hz). Stimulus detection was found to depend on the modulation of high-frequency phase from lower-frequency phase. Target detection was dependent not only on specific higher frequencies but was dependent on low-frequency phase.

Until recently, the majority of studies investigating neural oscillations and the CMPR model have primarily come from electrophysiological measures such as EEG and MEG. However, electrophysiology is not the only tool that can be used to probe perceptual rhythms. Increasing new evidence using purely

psychophysical and behavioural measures are contributing to the literature (Diederich et al., 2012; Diederich et al., 2014; Fiebelkorn et al., 2011; VanRullen & Dubois, 2011). Early research report oscillations in perceptual accuracy (e.g. detection thresholds) and reaction time (Harter & White, 1968; Latour, 1967; Poppel & Logothetis, 1986; Venables, 1960). These are often reported in 'alpha' frequency range. For example, Diederich et al. (Diederich et al., 2012) used saccadic reaction onset times to visual stimuli preceded by an extraneous auditory stimulus across a range of 200 ms in steps of 2 ms to probe for underlying oscillatory activity, time-locked to the auditory stimulus. They found a reduction in mean response times which revealed a cyclic temporal profile. Using spectral analyses on the detrended mean response times, as a function of SOA, they found that performance was modulated in a cyclic way showing an oscillatory frequency in the 20-40 Hz frequency band. Spectral analysis of the trend in the response profile revealed an additional behavioural response at an oscillation between 7 and 12 Hz. In a follow up study, Diederich et al. (2014) presented suprathreshold non-target auditory stimuli followed by a visual target stimulus at specific SOA. However, here SOA ranged from 0 to 404 ms in increments of 4 ms, allowing them to detect lower frequencies that included the theta range. Furthermore, they recorded EEG simultaneously and provided direct evidence for an auditory induced phase resetting with specific consequences on visual target detection at 7 Hz (theta). In both studies, RTs to near-threshold visual target were reduced when the visual stimulus was presented in the optimal phase of theta.

Consistent with these results another study using a purely psychophysical approach found an auditory induced facilitation of visual target detection of a near-threshold stimulus presented at varying SOAs (Fiebelkorn et al., 2011). They found that hit rates of visual-target detection were modulated as a function of SOA (that ranged from 500 ms to 6000 ms), phase locked to the auditory stimulus. Applying spectral analyses across the different SOAs, they found that the temporal profile of performance fluctuated at intervals that correspond to the wavelengths of delta and taken as indirect measurement in support for CMPR. In contrast to Diederich and colleagues, the emphasis was on a wide range of SOAs rather than small incrementing steps. This precluded identification of specific frequencies, but nonetheless identified periodicities in the response profile. This suggests that effects of phase reorganisation persist for the full six seconds tested. Furthermore, de Graaf et al. (Graaf, Gross, Paterson, & Rusch, 2013) reported a rhythmic modulation in hit rate following a 5.3 Hz and 10.6 Hz visual stimulation.

In summary, the above reviewed research provides ample evidence for the periodic nature of perception, termed the *perceptual cycles* theory. These perceptual cycles represent clear support for a discretisation of information in the brain, both at the neuronal level and perceptual level. However, the majority of these studies focus of brief momentary stimuli presentations; in **Chapter 2** and **Chapter 3,** I will provide evidence for a modulation of visual motion perception following a task irrelevant

auditory stimulus. VanRullen (2016) recently published a review article, and summarised the entire body of research as a spectral distribution of reported perceptual cycles, separated into visual and other modalities (including cross-modal interactions). The data shows that the majority of research report a primary peak at 10 Hz with a second at 7 Hz. This would suggest that similar neural mechanisms could support perceptual cycles in distinct modalities. Taken together the literature highlights a role for alpha (~ 10 Hz) for sensory periodicities, while theta (~ 7 Hz) rhythm can contribute to higher-level, attentional cycles. **Chapter 2** and **Chapter 3** will contribute to the existing literature and demonstrate a role of neural oscillations play in the integration of temporal information over time. In **Chapter 3**, demonstrates that these cross-modal findings are not constrained within sensory modalities, but can involve motor-sensory interactions.

Cyclic modulation in cortical excitability

As early as 1933, George Bishop reported that the physiological importance of the brains oscillatory activity, in conjunction with stimulating the optic nerve he detected recurring or cyclic excitability variations in the visual cortex of the rabbit (Bishop, 1932). In the last couple of decades there has been a wealth of both human and animal research that demonstrates that neural excitability is inexorably linked to oscillatory phase (Bishop, 1932; Busch et al., 2009; Mathewson et al., 2009; Ploner, Gross, Timmermann, & Pollok, 2006; Rinzel & Ermentrout, 1998; Romei, Gross, & Thut, 2012; Schroeder et al., 2008; Whittingstall & Logothetis, 2009). Within this framework, the exact phase reset of ongoing oscillations following sensory input, in A1 for example, determines the effect of phase reset on subsequent, driving responses, if the subsequent ongoing oscillatory activity is reset to a high excitability phase. This concept is discussed in detail above, but here it is worth expanding on the findings from Lakatos et al. (2007); they found phase reset of ongoing oscillations in A1 to their high excitability phase following somatosensory stimulation contralateral to the recording area, which when delivered simultaneously with auditory stimuli produced an enhanced auditory response. In contrast, ipsilateral somatosensory stimuli reset ongoing oscillations to their opposite or low excitability phase and when paired with auditory stimuli resulted in suppressed auditory responses. An additional mechanism determining the effect of phase reset on a subsequent driving type input is the temporal relationship between phase reset and incoming-evoked responses. In other words, there are more optimal and less optimal periods following the phase resetting event (in this study the somatosensory stimulus) for multisensory enhancement that are represented at immediate post-reset and there are further attributed to periods of delta-, theta-, and gamma-band oscillations.

Studies combining ongoing oscillations with evoked responses (ERF/ERP) have revealed an inverse relationship between spontaneous oscillatory amplitudes and event-related responses in several modalities. These include visual evoked potential (Brandt & Jansen, 1991; Rahn & Basar, 1993a) somatosensory evoked potentials (Ploner et al., 2006), auditory evoked potentials (Rahn & Basar,

1993b), and TMS-evoked phosphenes (Romei, Brodbeck, Michel, & Amedi, 2008; Romei, Brodbeck, et al., 2008). Including an inverse relationship between occipital alpha activity and visual perception (Dijk, Schoffelen, & Oostenveld, 2008; Hanslmayr et al., 2007; Romei, Rihs, Brodbeck, & Thut, 2008; Romei, Brodbeck, et al., 2008; Thut et al., 2006). These studies scrutinise the interaction between perception and neural mechanisms that underlie the excitation of visual ensembles by transient sounds. For example, brief sounds can facilitate the excitability of the visual cortex whereby increasing the threshold of detection of TMS induced phosphenes (Romei et al., 2009, 2007; Romei et al., 2012). Specifically, auditory induced modulations in visual cortices and subsequent visual processing exhibited direct neural underpinnings in oscillatory activity, as auditory stimulation induced phase-locking in the alpha-band oscillations over parieto-temporal areas (Romei et al., 2012). The networks in the visual cortex constitutes the alpha rhythm (Klimesch, Sauseng, Hanslmayr, & Gruber, 2007), and the nature of alpha oscillations provide a candidate proxy to the excitability of the visual areas (Busch & VanRullen, 2010; Dijk et al., 2008; Thut, Miniussi, & Gross, 2012; Thut et al., 2006). Furthermore, studies inducing changes in alpha phase using rhythmic transcranial magnetic stimulation (rTMS; Dugué, Marque, & VanRullen, 2011), and oscillatory transcranial direct stimulation (Neuling et al., 2012) have demonstrated how the selective realignment of phase supports the idea that particular phases correspond to temporal windows of increased excitation that improve sensory processing.

Trial-by-trial variablity in pre-stimulus activity (i.e. baseline) is shown to covary with the variability of iminent stimulus processing in specific frequency bands over posterior cortical regions (Dijk et al., 2008; Hanslmayr et al., 2007; Romei, Gross, & Thut, 2010). The phase of pre-stimulus oscillations seem to be implicated in the perceptual fate of the upcoming visual input. Some studies demonstrate a relationship between pre-stimulus EEG, ERP amplitudes, and response latencies (Başar, Başar-Eroğlu, Karakaş, & Schürmann, 1999; Başar, 1998). Others focus on the relationship between ongoing neurophysiology and cognitive processes (Busch, Dubois, & VanRullen, 2009b; de Graaf et al., 2013; Vanrullen et al., 2011). Experimental tasks that probe perception of near threshold stimuli are able to integrate both these approaches. Animal studies, are a prime example showing that a subset of neurons preferentially fire during specific phases of the ongoing local field potential (LFP; Lakatos, Karmos, Mehta, Ulbert, & Schroeder, 2008; Lőrincz, Kékesi, Juhász, & Crunelli, 2009). It is increasingly reported that evoked responses (N1 and P1) to identical visual stimulation varies as a function of the phase of ongoing oscillations at the time of stimulation (Barry, Blasio, & Pascalis, 2014; Barry, Pascalis, Hodder, & Clarke, 2003; Jansen & Brandt, 1991; Kruglikov & Schiff, 2003; Lakatos et al., 2008; Mathewson, Gratton, & Fabiani, 2009; Sachdev & Ebner, 2004). For example, Haig & Gordon (1998) showed a cyclic modulation of the amplitude of the M3 evoked component that was phase-locked to alpha oscillatory phase. Their findings show that late ERP components (P3) are influenced by the phase of ongoing oscillations.

Basic priniples of oscillations

Apart from the role of an oscillation, a question of similar importance that is shrouded in ambiguity is where these oscillations actually come from. Although the membrane potential of single neurons inherently demonstrate regular fluctuations (Llinás, 1988), it appears that it is rather the interplay between many different neurons that produce the oscillations that are relevant for the perception in behaviour (Buzsáki & Draguhn, 2004). Neural oscillations as they are commonly measure, are the synchronised activity of neural populations (Uhlhaas, Roux, & Singer, 2009). Interestingly, different neural population exhibit different preferred frequencies in which they oscillate (Hutcheon & Yarom, 2000). Neural oscillations can be recorded at various frequencies over different spatial locations, some of which will appear in this thesis. **Chapter 1** and **Chapter 2**, demonstrate their reflection in psychophysical data. Whereas **Chapter 2** and **Chapter 3**, will show oscillations recorded from the scalp with MEG. Other methods include intracranial recordings as local field potentials or their second spatial derivative, current source density on the cortical surface (ECoG). The later of these methods have laid the foundation on CMPR primarily been carried out in the animal literature as discussed previously (Kayser & Logothetis, 2007; Lakatos et al., 2009). Oscillations recorded from MEG have been associated with neural firing (Whittingstall & Logothetis, 2009).
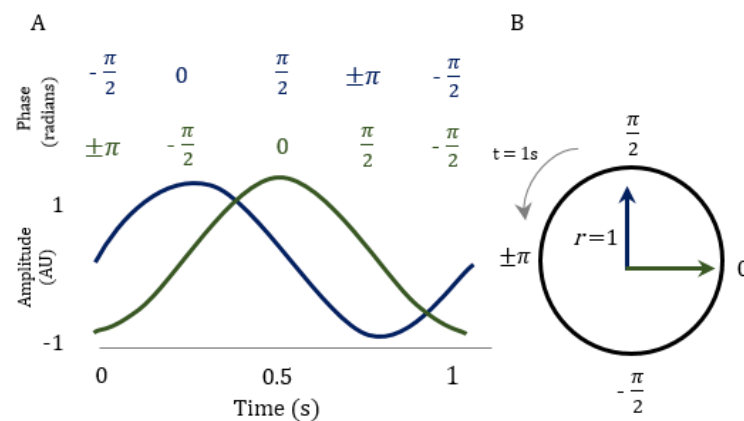
Figure 1.2. Oscillatory phase. A) Two phase-shifted oscillations (Blue and green; frequency 1 Hz, amplitude AU) differ in phase (upper panel, in radians) at each arbitrary moment in time. **B)** Oscillatory phase on a unit circle represented in the complex plane. The radius r reflects the amplitude and the angle reflects phase. Signals shown here correspond to the blue and green waves at the time t=0.5 s in A. Note, that their phase shift is now visible as the angle between them.

Oscillatory phase is defined as a fraction of a complete period that has elapsed with respect to an arbitrary reference (Canavier, 2015). Most commonly, a cosine wave is used as a reference (curve fitting procedures fitting cosine models, Chapter 2 and 3). Figure 1.2a shows two 1 Hz waves, which are shifted by $\frac{\pi}{2}$. These two waves differ in time at each arbitrary point due to the phase shift. Alternatively, an oscillation can be conceptualised as a rotating vector in a complex plane, where the

radius r (or absolute value) represents the amplitude and phase, the angle of an oscillations (Figure 1.2b). Within this framework, every revolution of a full 360° cycle (or 2π) by the vector represents a single cycle of the oscillation. The example shown in Figure 1.2a, the two signals (blue and green) at time t = 0 s, is shown again in Figure 1.2b, rather here this is in the complex plan on a unit circle.

As previously introduced, oscillations in the brain vary across a broad range of frequencies. In general, frequency varies inversely as a function of spatial scale upon which that oscillation is maintained. Neurons that are closer together tend to have the strongest interconnections; this is due to the short conduction times for synaptic transmission. Therefore, fast oscillations (> 80 Hz) are typically confined to networks for a few thousands neurons, whereas slow delta (0.5-3Hz), theta (3-8 Hz) and alpha (8-12 Hz) rhythms can be effectively synchronized regionally across large areas of the cerebral cortex. The relationship between frequency and the spatial scale of coherence leads to a characteristic of regional brain measurements by which the power of an oscillation decreases directly as a function of its frequency, the 1/f distribution. In principle, this 1/f distribution is largely attributed to the focal characteristics of higher oscillations and the attributes of waveform summation. Accordingly, after summation over a specific region, focal waveforms at different phases will partially cancel each other out.

A variety of signal processing methods are used to estimate amplitude (or power, the squared amplitude) or phase of an oscillation. Whichever method, the intended outcome is a decomposition of the complex recorded signal into different frequency bands, each defined by amplitude and phase. After transformation, the spectra density of the signal is computed, this is used to define the relative contributions of various frequencies to the observed signal in an epoch. The outcome produces plots which exhibit a $1/f$ law (Buzsaki, 2006; Cohen, 2014). Oscillations that are present in the signal are thus expected to manifest themselves in the spectral plots as "peaks" deviating from the $1/f$ structure. Whereas broadband increases in power typically reflect asynchronous activity (Miller, Honey, Hermes, Rao, & Ojemann, 2014). As a results of lower frequencies contributing more power, peaks in higher frequencies may not be apparent on visual inspection (Buzsaki, 2006; Cohen, 2014). This can be solved by scaling the spectral density by f, in order to detect peaks.

The MEG signal is thought to originate from dendrites of the pyramidal neurons (Buzsaki, 2006; Cohen, 2014). The magnetic field of individual action potentials are not typically measurable using MEG. These neurons have dendrites that are oriented in parallel to other neurons in large cortical columns. This is in opposition to the stellate neuron whose dendrites are arranged symmetrically around the soma. In the instance of the stellate neuron, electromagnetic fields generated by multiple dendrites will cancel because of its symmetric orientation. The electromagnetic signal is generated when the postsynaptic dendrite receives excitatory or inhibitory neurotransmitter across the synapse

resulting in an excitatory postsynaptic potential (EPSP) or inhibitory postsynaptic potential (IPSP). Before this takes place, the action potential in a pyramidal neuron maintains a negative voltage of about -70 mV (hyperpolarization) between the cell body and the extracellular fluid by actively transporting positively changed Na+ and Ca+ ions out of the cell body and negatively charged Cl- ions into the cell body. When excitatory neurotransmitters (e.g. glutamate) binds with ligand-gated ion channels at the synapse, the channels open and allow the influx of positive ions into the post-synaptic cell, partially reducing the polarization and increasing the probability of firing. Conversely, inhibitory neurotransmitters (e.g. gamma-aminobutyric acid), open negative ion channels, increasing polarization. If the post-synaptic cell reaches a critical threshold, voltage sensitive Na+ or Ca+ channels in the axon open, resulting in an action potential, propagated along the axon resulting in the release of neurotransmitters to the post-synaptic cell across the synapse. A secondary volume, current travels in the opposite direction in the extracellular space. The pre-synaptic cell shifts to a hyperpolarized state by closing Na+ channels and opening K+ channels, resulting in the efflux of K+ and hyperpolarization of the cell, preventing the cell from firing again for a brief refractory period.
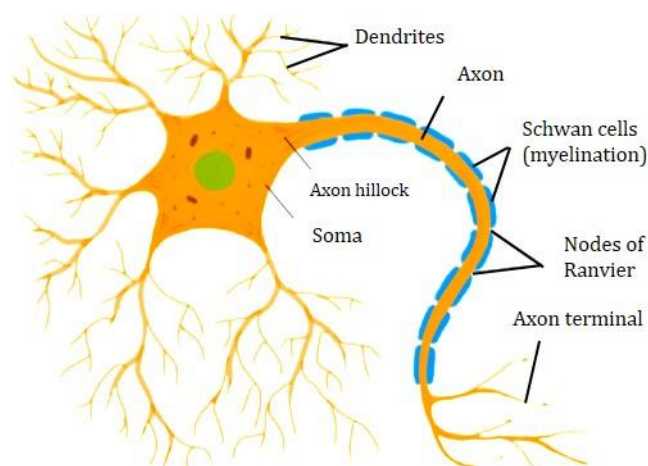
Figure 1.3. Schematic of morphology of a neuron.

Slower and more sustained oscillations occur due to the interconnectivity of populations of neurons. Many network oscillations in the brain, particular gamma (30-80 Hz) oscillations, involve the concerted activity of coupled populations of inhibitory interneurons. Many interneurons are connected directly electrically via synaptic gap junctions, increasing the probability of simultaneous firing between neighbouring cells. Complex interconnectivity of GABA interneurons with each other and principal excitatory pyramidal cells can lead to temporal windows of pyramidal activity counter-phase to the activity of the local interneuron cluster (Bartos, Vida, & Jonas, 2007). This precise

rhythmic timing of pyramidal activity can greatly enhance the efficiency of communication between separate local circuits through synchronous spike timing (Womelsdorf, Schoffelen, & Oostenveld, 2007), a process known as "communication through neural coherence" (Fries, 2005). As inhibitory interneuron ensembles can be triggered and phase-locked by a single neuronal input (Miles, 1990), functional phase locking can occur between distant cortical sites (Traub, Whittington, Stanford, & Jefferys, 1996). Although, the majority of cross-regional phase coupling is mediated by slower frequencies which in turn modulates gamma activity (Engel, Gerloff, Hilgetag, & Nolte, 2013; Liebe, Hoerzer, Logothetis, & Rainer, 2012; Sauseng & Griesmayr, 2010), to allow for the longer windows of integration required for sustained long range coupling. The exact frequency and direction of coupling in the brain depends on the region and task.

Phase reset model

Phase-resetting characteristics can be measured for a single oscillating neuron (Farries & Wilson, 2012; Wang, Musharoff, & Canavier, 2013) or network of neurons (Akam, Oren, Mantoan, & Ferenczi, 2012; Zhang & Lewis, 2013). Establishing that a phase reset has occurred first requires signal processing tools to measure that an oscillations was present (Sauseng, Klimesch, & Gruber, 2007). One general procedure for detecting an oscillation requires signal filtering based on *a priori* knowledge and a transformation of the signal using time-frequency analyses using one of a variety of methods (Bruns, 2004). The majority of studies concerning the functional role of oscillations have primarily focused on oscillatory amplitude in particular frequency bands. However, oscillations are not only defined by frequency and amplitude but also by phase (see figure 1.2).

Figure 1.4 shows an oscillatory where phase is defined and shows how it can be reset, using a simple network oscillator model (Wilson & Cowan, 1972), that consists of the average firing rates of two neural populations, one excitatory (E) and one inhibitory (I). In the model, the phase ϕ evolves from 0 to 1 (this is also commonly represented by the modulo 2π instead) in proportion to the elapsed time ($\phi = t/2\pi$) for an undistributed oscillator, but can be phase reset by an external stimulus. Here, the advance or delay is quantified as the phase resetting $\Delta\phi$ in a phase transmission curve (PTC) with the new phase a function of the old phase $\phi_{new} + \phi_{old} + \Delta\phi$. In figure 1.4.C, the new phase is established within a single cycle, but in principle, more cycles may be required. A continuous PTC is shown for a near-threshold stimulus (the type of stimuli that is used on Chapters 2 and 3) shown in Figure 1.4.D2. The discontinuity results from the abrupt transition between the delays due to prolonging an existing peak (Figure 1.4.C1) and advances due to initiating a new peak (Figure 1.4.C2). Here, the figure shows that both PTCs reflect partial resetting, although E2 is more complete than that of E1. Many coding mechanisms require full resetting; this is depicted, as the PTC being flat and the new phase is independent of the old phase. Full resetting is not assured for arbitrary stimuli to a given oscillator. LFP and M/EEG measure the synchronisation of neural ensembles collectively. Numerous

studies investigating phase resetting (and by extension CMPR) have used a variety of methodologies to investigate this model. This in part, is due to the inherent measurement limitations involved in determining genuine phase reset (Thorne & Debener, 2014). This is because transient sensory responses are evoked in both the visual and auditory cortex, making it difficult to differentiate between transient responses, and genuine cross modal phase resetting (Makeig et al., 2004; Shah et al., 2004; Sauseng et al., 2007).
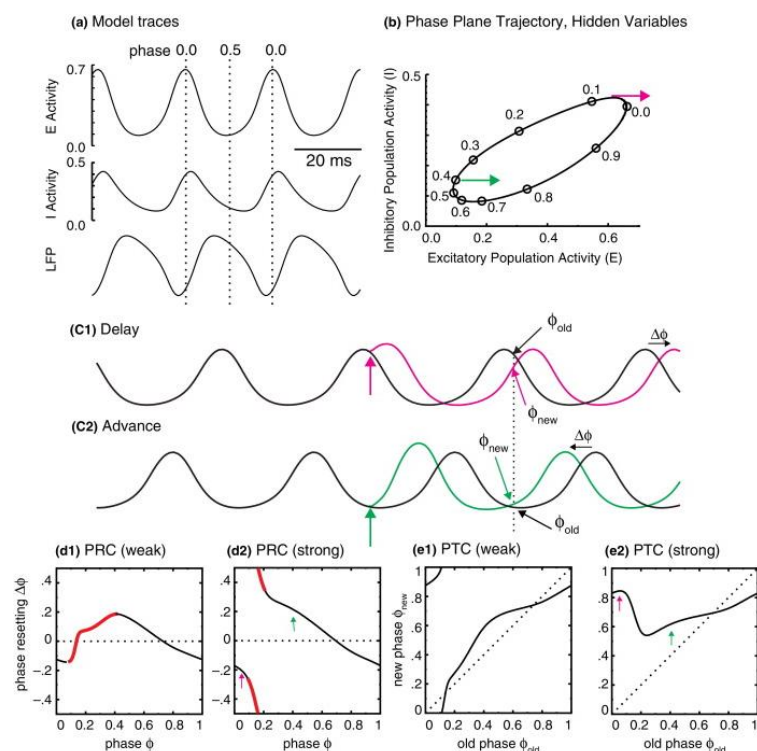
Figure 1.4. Schematic explaining phase resetting using the Wilson-Cowan model. **A)** Excitatory (E) and inhibitory (I) activity and the simulated local field potential (LFP). Phase 0 is the peak of the E activity. B) Phase is marked on the circle in the plane of firing rates of the two populations. Green and magenta arrows indicate the direction of an external excitation (applied to the excitatory population). **C)** An external perturbation (vertical coloured arrows) phase shifts the perturbed (coloured) traces for the excitatory population compared to unperturbed (black) traces by the amount shown by the horizontal arrows. **C1)** an input at phase 0.05 causes a delay. **C2)** an input at phase 0.4 causes and advance. The old phase just prior to the stimulus is repeated on the unperturbed (black) waveform at multiples of the cycle period (vertical dashed line) after the input, but the new phase on the coloured traces at that point differs from the old phase by the phase shift. **D)** The PRC plots the phase shift as a function of the phase of the input perturbation. Slopes outside the stabilizing range (−2 to 0) are indicated in red. (**D1**) Weak input. (**D2**) Strong input. The arrows correspond to the perturbations in **B** and **C. E.** The phase transition curve plots the new phase (modulo one) versus the old phase. **E1**. For a weak input, the range of new phases is equal to that of old phases. **E2**. For a strong input, the range of new phases can be much smaller than the range of old phases. (reproduced with permission; Canavier, 2015).

Conceptual issues: neural generator of phase reset

As early as 1974 (Sayers, Beagley, & Henshall, 1974), the oscillatory phase reset mechanism from sensory inputs was proposed whereby the brain aligns a specific phase of its neural oscillations to these inputs. This notion did not gain scientific interest until a controversial paper by Makeig (Makeig, Westerfield, & Jung, 2002), where he argues that sensory ERPs are attributable to the reorganisation or reset of the phase of neural oscillations in particular frequency bands by sensory related inputs. This sparked a decade long debate, in which research groups endeavoured to elucidate what – if any- portion of the sensory ERP is due to phase reset (Barry, 2009; Başar et al., 1999; Brandt, 1997; David, Harrison, & Friston, 2005; Fell et al., 2004; Gruber, Klimesch, & Sauseng, 2005; Hanslmayr et al., 2007; Klimesch, Sauseng, Hanslmayr, et al., 2007; Klimesch et al., 2004; Kruglikov & Schiff, 2003; Makeig, Westerfield, Jung, & Enghoff, 2002; Mäkinen, Tiitinen, & May, 2005; Mazaheri & Jensen, 2006; Mazaheri & Picton, 2005; Naruse, Matani, Hayakawa, & Fujimaki, 2006; Penny, Kiebel, Kilner, & Rugg, 2002; Rizzuto et al., 2003; Sauseng et al., 2007; Shah et al., 2004).

The pure phase reset model, argues that there is simply a phase resetting of ongoing oscillations to a specific value in each trial, without any amplitude increase in the post stimulus time-window compared to the baseline period. To this end post stimulus M/EEG oscillations are aligned or "phase-locked" across trials, as a result positive and negative peaks do not average out and are detectable in the average responses a speaks and troughs of the ERF/P (Başar, 1980; Klimesch, Sauseng, Hanslmayr, et al., 2007; Makeig, Westerfield, Jung, et al., 2002a; Sayers et al., 1974). This theory contradicts the long held assumption that neural responses are newly generated in response to an external stimulus (i.e., "evoked response"), are a superposition on the ongoing M/EEG and are characterised by an amplitude increase from pre-to-post stimulus time-windows in each trial (Jervis, Nichols, Johnson, & Allen, 1983; Mäkinen et al., 2005). In recent years, this debate has become less polarised following substantial findings from intracranial recordings, which show that there is a non-linear relationship between these mechanisms (Lakatos, Schroeder, & Leitman, 2013; Lakatos, Shah, Knuth, & Ulbert, 2005; Peter Lakatos et al., 2009, 2013, 2007, 2008; Mäkinen et al., 2005). These studies reconcile both hard arguments and demonstrate that it is both phase reset and evoked typed neural activity that contribute to the ERF/P.

In addition, recent evidence suggests that ERF/Ps recorded on the scalp are a combination of evoked activity and phase reset of ongoing oscillatory activity (Barry, 2009; Olivier David, Kilner, & Friston, 2006; Delorme & Makeig, 2004; Gomez-Ramirez, Kelly, & Molholm, 2011; Min, Busch, Debener, & Kranczioch, 2007; Telenczuk & Nikulin, 2010); although the relative contribution from each is still very much debated since due to volume conduction and summation of synchronous neural activity, even pure phase reset involving several different neural ensembles exhibit an evoked type, "added"

post-stimulus activity (Sauseng, Klimesch, & Gruber, 2007). Nonetheless, due to elimination of volume conduction and the existence of high temporal resolution measures, intercortical recordings on the mesoscopic scale can distinguish between stimulus related phase reset and evoked type activity.

Magnetoencephalography

The first biomagnetic signal measurements were magnetocardiographic (MCG), recorded by Baule & McFee (1963). Here two coils with a ferrite core and when wired to create a series of opposite polarity, they formed a gradiometer that could detect biomagnetic fields. Considerable improvements to this concept was made by David Cohen, he used a low-noise amplifier and a magnetically shielded room (Cohen, 2004). Using this set-up, Cohen attempted to record the first MEG measurement in 1968, although signal-to-noise was extremely poor. Then in 1969 a new type of sensor was created by Jim Zimmerman, known as super-conducting quantum interference device (SQUID; Wikswo, 1995). By 1971, commercially manufactured SQUIDS had become available, which Cohen utilised to record the first MEG recording, figure 1.4 (Cohen, 1972).
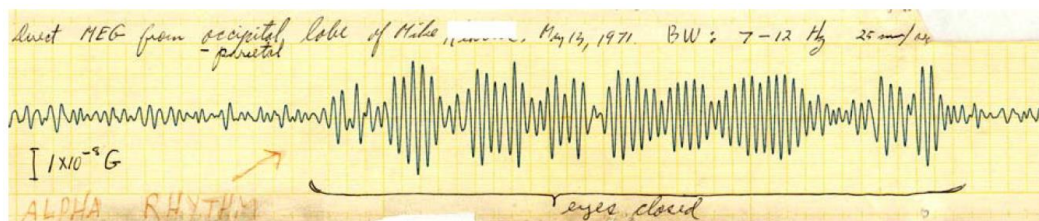
Figure 1.5. The first MEG measurement. MEG signal recorded in 1971 (*taken from* Cohen, 2004))

Traditionally, it was thought that only the primary current is detectable outside of the head but more recent analyses have cast doubt on this view and suggest that volume currents, in some instances, may be more prominent at the sensor level than primary currents (Uitert & Johnson, 2004). It is estimated that approximately 100,000 synchronised dendritic currents (±1nAm) are required to detect a field outside of the head. If there are a suitable number or EPSPs as compared to IPSPs that reach the axon hillock, an action potential is initiated down the axon to the dendrite of the next neuron. This process within the axon is similar to that of the dendrite but happens on a much faster time scale. Furthermore, the magnetic field generated by an action potential is representative to a current quadrupole where there is a flowing 'train' of cell depolarisation followed by repolarisation. The magnetic field generated by an action potential falls off as $\frac{1}{r^3}$ as compared to $\frac{1}{r^2}$ for a current dipole. This decrease in field propagation coupled with the rapid nature of action potentials, which makes synchronised firing less likely, results in the majority of MEG signal being generated by dendritic rather than axonal currents. Even with the synchronous activity of 100,000 dendrites, the magnetic field outside of the head is extremely small, ±100fT. This is far smaller than the earth's magnetic field and

typically electronic equipment found in most laboratories. SQUIDS can be arranged either as a magnetometer, an axial gradiometer or planar gradiometer. Magnetometers are the simplest of pick up coils, which consist of a wire with a single loop that measures the magnetic field (figure 1.5., B) through the loop. An axial gradiometer consists of two coils arranged atop one-another and the magnetic field gradient can be measured from the difference between the two, thus enhancing noise cancellation. Finally, planar gradiometers also consist of two coils, but these are aligned on the same horizontal plane. These too measure the magnetic field gradient but in the orthogonal orientation to axial gradiometers. As the strength of B follows the inverse square law (Figure 1.5), which dictates that closer sources have a larger field, external environmental noise can be removed.
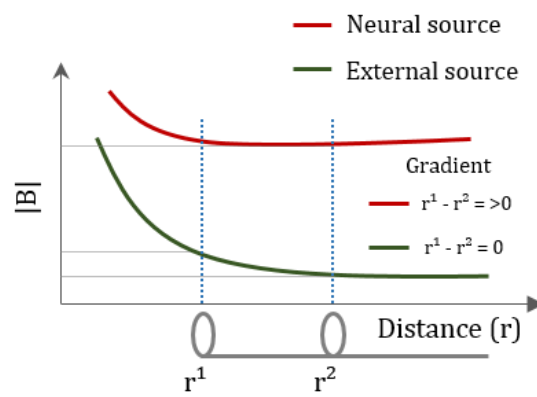
Figure 1.6. MEG field gradient. Schematic of the magnetic field gradient from external and neural sources as detected by axial-gradiometer

The neuromagnetic fields being measured are many orders of magnitude smaller than typical ambient magnetic fields (e.g., geomagnetic field of the planet Earth). MEG equipment must be sensitive enough to measure the relevant neurological fields, but insensitive to much larger noise signals. MEG systems employ specific design features to overcome potential sources of noise. Firstly, environmental noise fields are greatly attenuated by housing the complete measuring instrument in a magnetically shielded room. Secondly, SQUID magnetometers are utilised for their superior noise performance. Finally, the output from the SQUIDs are amplified using low-noise instrumentation amplifiers. These features can lead to spectral noise densities of less than $5fT/\sqrt{Hz}$. Many systems implement analogue and digital noise reduction improve further the signal-to-noise ratio. During MEG, the output from every magnetometer (or a subset of them) is recorded over time. Stimuli (auditory or visual) often presented to the participant during the recording to investigate neurological responses. Spontaneous brain activity can also be measured. MEG spatial resolution can be better than 3 mm (Cohen, 1972; Hämäläinen, Hari, Ilmoniemi, Knuutila, & Lounasmaa, 1993; Hari, 1993). However, this depends on several factors including the analysis method, number of sensors, the location of the activity and the presence of noise. Temporal resolutions in MEG range down to 1 ms or less.

Thesis overview

Chapter 2 abstract: Behavioural oscillations reflect sensory perceptual consequences of cross-modal phase reset

Cortical oscillations are implicated in the gating of information flow. Oscillations are linked to variety of cognitive processes such as visual sensory perception which cycles at the characteristic frequencies of brain rhythms. The inherent fluctuations in the phase of neural oscillations are thought to be linked to the periodicities observed in sensory perception. Previous research has shown that the presentation of a brief sensory event in one modality can affect activity within hierarchically organised early sensory cortical regions in another modality. This modulation by cross-modal input through resetting the phase of ongoing intrinsic oscillations has been demonstrated in animal and human research. Here we investigated this mechanism and evaluate whether auditory induced phase resetting of primary sensory visual oscillations would affect perceptual performance. 24 Participants performed an apparent motion discrimination task of a dynamic dot pattern presented at one of 18 delays (SOAs) following a brief tone. If the target stimulus was presented at the optimal phase of the auditory-induced phase reset of visual cortical oscillations, then this should have specific behavioural consequences in sensory perception. The second aim of the experiment was to probe the underlying visual systems sampling frequency. To this end, the phase detection relationships were probed at various coherent motion stimulation lengths (i.e. temporal integration windows). Signal processing methods revealed a systematic variation in perceptual accuracy across the SOAs. Revealing a cyclic modulation that was explained by fitting 4-9 Hz sine models, consistent with an auditory phase resetting of visual theta-alpha oscillations. In conclusion, these data provide evidence for the discrete sampling of perception that is modulation through cross-modal interaction. Specifically, we demonstrate the role low frequencies oscillations play in the integration of temporal information over time. Finally, we show that a transient exogenous tone can modulate visual motion perception.

Chapter 3 abstract: Auditory driven cross-modal phase reset of visual oscillations predicts visual motion perception.

This chapter was a partial replication of the previous chapter. In the study we extend these finding using MEG. To this end, the underlying oscillatory dynamics were investigated. Results clearly show a significant cyclic pattern in behavioural *d*-prime accuracy performance and an oscillatory modulation in the ERF component in alpha frequency in the visual cortex. These findings are in-line with occipital alpha-oscillations underlying the periodicity in visual perception. This offers support that visual ERF component may serve as a proxy for cortical excitability that is modulated by tone-onset. Cross-modal phase resetting modulates intrinsic brain-rhythms and subsequently influences sensory perception.

Chapter 4 abstract: Cross modal enhancement for multisensory predictions of self-generated stimuli.

The first two experiments support the view that CMPR is a versatile, flexible and efficient mechanism for sensory gain control. The process of selective attention is an attribute of the biased competition model that assumes that attention influences visual processing by enhancing the input gain for the group of low-level neurons associated with an attended behaviourally relevant stimulus over those groups of neurons related to the unattended stimulus. Another well-studied model case for this fundamental operation is the interaction between motor and sensory areas. Motor action leads to predictable sensory consequences. This predictive coding is associated with attentional neuromodulatory gain control in sensory processing, which reflects encoding of precision by the excitability of neural populations that report prediction errors. The very fact that the sensory consequences are predictable, changes the way they are processed in the brain and the associated percept. Specifically, self-induced sensory stimuli lead to reduced activation in sensory cortex. The exact mechanisms are yet unclear. However, inter-areal phase resetting is a potential mechanism, which may index the forward model account of motor-to-somatosensory prediction account to different sensory modalities. This experiment demonstrates that CMPR may be a candidate mechanism that could index the interactions between motor and sensory modalities. Here we demonstrate the role of neural oscillations play in sensory attenuation for self-generated unisensory and multisensory stimuli.

Chapter 2

Behavioural oscillations reflect sensory perceptual consequences of cross-modal phase reset

2.1 Introduction

Research has demonstrated a mechanism whereby a transient tone can modulate the phase of visual oscillations whereby enhancing perceptual salience for detecting or discriminating subsequent visual stimuli (Fiebelkorn et al., 2011; Naue et al., 2011; Romei et al., 2012; Watkins, Shams, Josephs, & Rees, 2007; Watkins, Shams, Tanaka, Haynes, & Rees, 2006). For example, a tone has been shown to improve detection of near threshold lights (McDonald, Teder-Sälejärvi, & Hillyard, 2000; Noesselt et al., 2010), or enhance the detection of phosphene perception (Romei et al., 2012). This suggests that the underlying neuronal oscillatory systems have direct consequences on behaviour. Research suggests that this inter-regional communication can be achieved through oscillatory synchrony between modalities (Diederich, Schomburg, & Colonius, 2012; Fiebelkorn et al., 2011; Graaf et al., 2013; Song, Meng, Chen, Zhou, & Luo, 2014). However, the majority of studies investigating this mechanism within the framework of multisensory integration use brief, momentary stimuli, and focus either on the spatial domain (Eimer & Driver, 2000; Landau & Fries, 2012a) or detection of a single transient near-threshold stimulus (Fiebelkorn et al., 2011; Kayser et al., 2008; Naue, Rach, Strüber, & Huster, 2011; Romei, Gross, & Thut, 2012). What is less known, is the interaction between the auditory modality on spatiotemporal visual motion perception.

Previous studies have demonstrated that different presentations of sounds can affect the precision or quality of a visual motion percept, similarly when the sound in not task relevant (Kim, Peters, & Shams, 2012; Sekuler, Sekuler, & Lau, 1997). For example, brief sounds can alter bi-stable visual motion precepts (Sekuler, Sekuler, & Lau, 1997) and task-irrelevant acoustic motion can enhance visual motion detection (Kim, Peters, & Shams, 2012). This suggests that there is a dynamic interaction between auditory and visual motion evidence and that it is task dependent. One candidate mechanism that could account for these inter-regional connections, is cross-modal phase resetting. Studies which investigate this possible mechanism have suggested that the direction of cross-modal interactions depends, at least in part, on the structure of the stimuli; that is, the modality that carries a signal which is more discontinuous (and hence more salient) becomes the influential or modulating modality (Luo, Liu, & Poeppel, 2010; Shinsuke Shimojo & Shams, 2001). Where a transient, and therefore more

discontinuous and structured, stimulus alters the perception of a continuous visual stimuli regardless of its modality (Sekuler et al., 1997; Shimojo, Watanabe, & Scheier, 2001; Watanabe & Shimojo, 2001; Katsumi Watanabe, 2001). However, the exact neural mechanism associated with auditory induced enhancement of dynamic visual motion detection remains poorly understood, with only sparse behavioural evidence.

Behavioural studies have failed to find conclusive evidence for sensory interaction between the two modalities within the framework of auditory to visual motion perception. For example, in a motion detection task of near threshold auditory and visual stimuli researchers (Alais & Burr, 2004; Wuerger, Hofbauer, & Meyer, 2003) found that detection accuracy could be explained rather by statistical (probability summation) or maximum likelihood integration of the two modalities, rather than through sensory interactions. In the current study using a purely behavioural approach, we investigated whether an exogenous salient tone (task irrelevant) could modulate the detection of motion in a near-threshold visual stimulus. Here the results are interpreted as evidence of inter-areal phase resetting. Similar to other behavioural studies we concentrate on purely psychophysical measures. Which enables inferences to be made on the underlying oscillatory activity, and will also inform on the psychological and perceptual consequences of visual motion discrimination and detection. Several studies (Mercier et al., 2013; Naue et al., 2011; Romei et al., 2012) introduced in the main introduction have shown that a transient sound can modulate the amplitude and phase of low frequency oscillation over occipital areas. Within this framework, we could investigate whether behavioural oscillations are evident, that may underlie an auditory induced enhancement of the temporal integration of motion perception.

The current study

The current paradigm required participants to detect and discriminate, at near-threshold stimulus, the direction of apparent coherent motion in a circular dynamic random dot kinematogram (RDK). At the start of each trial, the RDK remained as dynamic moving dots "noise", with no coherent motion until at one of eighteen SOAs, which followed a salient exogenous tone that was not task relevant. At this point, a defined percentage of dots in the circular random dot pattern would appear to rotate coherently, for a set number frames, producing the phenomenon a global coherent motion. The motion sequences rotated either clockwise, anticlockwise or not at all and participants were required to report the direction of coherent motion. The assumption is that the auditory stimulus would phase-reset the underlying visual oscillations to approximately the same phase on each trial and behavioural performance would change in a sinusoidal manner across SOAs following the tone-onset. By these means, we gain systematic control over visual cortical excitability. This would index an enhancement of perceptual sensitivity, as measured by *d*-prime (*d'*), for visual motion perception governing multisensory integration at the neuronal level.

In our signal detection paradigm, we predicted that, by presenting the target coherent motion at varying delays post-auditory-onset, we are able to reveal the temporal profile of discrimination (of the direction of visual motion) and detection (of motion or no motion) accuracy performance as a function of SOA. We would expect that depending on when the target coherent motion is presented (i.e. SOAs) would determine whether that coherent motion was accurately perceived or not. In other words, if the target motion falls within the optimal phase of the visual systems sampling rhythms, participants will have a higher probability of accurately detecting and discriminating the direction of coherent motion. Signal detection measures (McNicol, 2005) allows for the separation of perceptual level and decision-level of near-threshold visual motion stimuli, in equation 2 (Methods section) with d' parameter reflecting the participants accuracy to discern a sensory event from its background (perceptual level), and β parameter reflecting the participants decision criterion of response level (decision level). To this end, if these psychophysical measures were analogous to the modulation in cortical excitability indexed by oscillatory phase, then we would expect to see a cyclic modulation in performance accuracy time-locked to the tone-onset. We predict that if perception is rhythmically modulated this could be taken as evidence in support for the CMPR mechanism. Importantly and in contrast to previous studies, here accuracy in behavioural performance relies on the temporal integration of motion displacement frames. The present study therefore gives insight into the role phase has on visual motion perception, quantified here in behavioural oscillations which are a proxy of the underlying neural oscillatory mechanism.

Previous research has found contrasting evidence for the frequency of phase detection relationships in a multisensory context. Considerable evidence demonstrates how pre-stimulus phase of ongoing oscillations contribute to the perceptual consequences, for example if a near-threshold stimulus is detected. What is less established however, is the relative contribution that different frequencies have on perception. Some previous work (Busch et al., 2009; Dugué, Marque, & VanRullen, 2015; Lakatos et al., 2009; Mathewson et al., 2009; Romei et al., 2010, 2012) indicate frequencies between 4-14 Hz, while others (Besle et al., 2011; Fiebelkorn et al., 2011; Gomez-Ramirez et al., 2011; Lakatos et al., 2008; Schürmann, Başar-Eroglu, Kolev, & Başar, 2001) emphasis 1-2 Hz low delta-band frequencies to be particularly relevant to visual perception and awareness. It is noteworthy that the central difference between these findings is due to the manipulation of attention in experimental paradigms. Findings that report delta-band tend to manipulate attention in contrast to those in the alpha/theta range that have not. Frequently, studies manipulating attention appear to report lower frequencies entraining higher frequencies via functionally interconnected attentional-related brain areas.

Taken together it is clear that neural oscillations exist in multiple frequency bands and as a product their perceptual consequences should display similar periodicities (VanRullen, 2016b; VanRullen &

Koch, 2003). By this account, we would argue that there is no one central sampling rhythm simultaneously affecting all aspects of perceptual experience often reported as the critical alpha (10 Hz) sampling frequency. Multiple perceptual waves could indeed coexist within the brains networks, with different periodicities. To this end, the second aim of our experiment was to explore the specificity of the phase detection relationships at varying lengths of target visual stimulation. Specifically, we investigated the perceptual consequences of increasing numbers of displacement frames of target coherent motion. To achieve this there were three experimental conditions consisting of a, 5-frames, 10-frames, 25-frames. Using a 100 Hz monitor these would result in temporal coherent motion stimulation lengths of 50, 100, 250 ms respectively. Importantly, the task difficulty remains constant across the experimental conditions the percentage of moving dots was individually titrated for each condition and participant. Such that the coherence level was set to near-threshold for each participant, such that on 75% of the trials, coherent motion could be detected and on the other 25%, coherent motion could go undetected.

To successfully perceive global coherent motion, the visual system must integrate information across frames of spatiotemporal information for each successive frame displacement (Eagle & Rogers, 1996; Lappin & Bell, 1976; Maloney, Mitchison, & Barlow, 1987; Swettenham, Anderson, & Thai, 2010). Whereby consecutive frame displacements are retrospectively perceived as continuous motion (Morand, Gross, & Thut, 2015; Ramachandran & Anstis, 1986). This integration of information over time is under attentional control (Cavanagh & Mather, 1989). Considerable evidence indicates that attention samples information rhythmically (Busch & VanRullen, 2010; Fiebelkorn, Saalmann, & Kastner, 2013; Gross & Schmitz, 2004; Landau & Fries, 2012; VanRullen, 2006; VanRullen, Carlson, & Cavanagh, 2007). If it is by discrete processing that we sample our environment, then the displacement frames are bound together by the visual sensory system to produce the effect of global coherent motion at some points and not others, resulting in an oscillatory phase-detection relationship, representative of the underlying neuronal oscillations.

Visual neural ensembles enable the integration of inputs over a range of intervals that correspond to half cycles of oscillatory activity at various frequencies (Schroeder, Lakatos, & Kajikawa, 2008). Therefore, a 10 Hz oscillation would integrate inputs that arrive within the duration of their ideal phase (half the period of a 10 Hz oscillations is 50 ms). Consistent with this idea, the three experimental manipulations, 2 Hz, 5 Hz and 10 Hz would correspond to temporal integration windows of 250 ms, 100 ms and 50 ms respectively. Such that, these would integrate over their corresponding intervals of half cycles of ideal phase. Within this framework, by manipulating the length of coherent motion frames, we could investigate any behavioural sensory consequence induced by this "frequency-tagging" type approach. The target coherent motion has a defined temporal frequency and here we explore the elicited effects of quasi-sinusoidal brain responses. There are two possible outcomes,

either the varying lengths of coherent motion will induce visual neural ensembles to oscillations at the stimulus frequency (fundamental frequency), which will be reflected as a corresponding frequency-code reflected in behavioural perceptual performance. Alternatively, the underlying visual sampling frequency will remain stable irrespective of coherent motion stimulation lengths.

2.2 Methods

Participants

Twenty-four right-handed volunteers participated in the study (10 male, mean age 21.6 ± 1.1 years). All participants provided informed written consent and received a monetary compensation for their participation. One participant was excluded for further analysis due to technical issues concerning behavioural threshold performance. None had been diagnosed with a hearing disability or had a history of significant neurological or psychiatric illness. Participants had normal to corrected-to-normal vision. Handedness was defined by the Annett Hand Preference Questionnaire (Annett, 1970). Experiments were approved by the local ethical committee (University of Glasgow, The College of Science and Engineering) and conducted in conformity with the declaration of Helsinki.

Design and procedure

Participants performed an apparent motion discrimination task. Using a three forced choice design procedure, participants were required to indicate the direction of apparent coherent motion (henceforth, motion) in the RDK stimulus. The target onset of apparent coherent motion was presented at near-threshold. The three possible motion conditions were; coherent clockwise-, coherent anticlockwise- and/or no coherent-motion (control) condition. For the purposes of simplicity, both coherent motion directions will henceforth be referred to as the motion condition (MC), since data from these were concatenated to form one condition, and the incoherent motion condition (control) will be referred to the as no-motion condition (NMC). Reponses were made with the right hand using a nonmagnetic response pad (Lumitouch). They were instructed to respond either by pressing with their right index finger (placed on right most key), middle finger (placed on middle key) and ring finger (placed on left most key) for coherent anticlockwise motion, no-coherent motion, and coherent clockwise motion responses respectively.

The experimental paradigm and stimuli are illustrated in Figure 2.1. Each trial started with the presentation of a circular random dot kinematogram (RDK) around a central fixation point. Dots appeared as 'noise' flashing on and off with an incoherent motion for a period of 0-300 ms, and remained for a jittered period (300-780 ms, intervals of 10 ms), after which depending on the type of condition either a binaural tone was present (tone condition) or not (no-tone condition). Following the

cessation of the tone or no-tone condition, the random dots remain as incoherent motion until one of 18 possible stimulus-onset-asynchrony (SOAs) time points (310-490 ms, intervals of 10 ms), after which, a certain percentage of dots either rotated in a clockwise- or anticlockwise manner or remained as incoherent motion (control). The experiment consisted of three experimental conditions (described below) with 3 blocks in each lasting for approximately 6-7 mins in length. The design was created in such a way that blocks were continuous. A block consisted of 144 trials, where each SOA delay point was repeated 8 times. There were 48 trials per motion direction condition, where 18 trials were no-tone trials and 126 were tone trials. No-tone trials formed 12.4 % of the total trials. The three experimental conditions manipulated the number of successive frames in the apparent motion sequence. Critically, this manipulation targeted the length of the temporal integration window in the RDK stimulus where information is integrated into a single percept over time. Each RDK frame was one refresh rate of the 100 Hz monitor (1 frame equal to 10 ms). The three experimental conditions were, five RDK frames, ten RDK frames and twenty-five RDK frames. These will be referred to as 5-frames, 10-frames and 25-frames. Here the temporal framing integration window was 50 ms, 100 ms and 250 ms for each experimental condition respectively.

Stimuli

Stimuli were presented on a Sun Microsystems® 21-inch Flat-Screen Trinitron CRT colour monitor (X7136A FD, spatial resolution 1280 x 1024 pixels and refresh rate of 100 Hz). A chinrest maintained a constant viewing distance of 90cm to the screen. Tone were delivered binaurally via a set of headphones (Beyerdynamic®, DT770 PRO Headset-250 OHM). Sound stimuli levels were calibrated using a condenser using microphone and sound level meter. Sounds were presented at a self-adjusted comfortable level of approximately 65 dB SPL. Stimuli were generated off-line using Matlab 2013.b (The MathWorks®) and controlled using routines from Psychophysics toolbox (Brainard, 1997). To create a dynamic dot pattern, 1000 dots (white) with a 0.06° diameter and consistent separation formed a concentric-form random array, were centred around the fixation spot (0.15°), covered 7° of visual angle (with the centre 0.4° devoid of dots) and were presented on a uniform black screen (0.1 cd/m² background luminance). A random dot pattern sequence was created whereby the oriented dots were aligned along a common trajectory, creating the effect of a dynamic Glass pattern (Ramachandran & Anstis, 1983, 1986; Ramachandran & Anstis, n.d.). This alignment generates a global structure pattern of coherent motion, a fraction of dots moved at 15°/s for either 5-frames, 10-frames or 25-frames depending on the conditions (10 ms/frames), and a titrated percentage (individual participant titration performed before each block) of dots were randomly replaced after each frame. Each trial commenced with a dot array as the first frame, the second frame was constructed by displacing 40% of dots in the first frame with a new random distribution for dots. A fraction of dots would displace a threshold amount of dots in the first frame 4 arc min distance in coherent clockwise, coherent anticlockwise, or no-coherent motion, this would be repeated for a four-frame apparent motion. This

fraction of dots moved coherently either clockwise- or anticlockwise to produce the target motion, theoretically conceptualised as apparent motion, while the other dots contained only random dot motion, with no coherent motion direction.

The direction of coherent apparent and random motion was randomised for each trial. The coherence level was adjusted for each subject to attain a threshold detection rate of around 75 ± 5%, as previously reported by Kim, Peters, & Shams (2012), auditory enhancement of visual motion detection in such a task is largest at intermediate levels of performance. This coherent apparent motion detection threshold was initially established in a separate session in which the patterns of the different coherences were systematically tested to measure psychometric curves. Then for the actual experiment this coherent motion detection level was adapted before the beginning of each experimental block. This ensured that the performance of coherence motion detection was kept constant over time. Across participants coherence levels were comparable (75 ± 15%; mean ± S.E.M; corresponding to 75% of dots moving in the same direction) and this varied of approximately 6% over time (subject average standard deviation).

Stimulus onset asynchrony (SOA) - 18 possible delay points of apparent motion onset following tone.10 ms Intervals for jitter and SOA
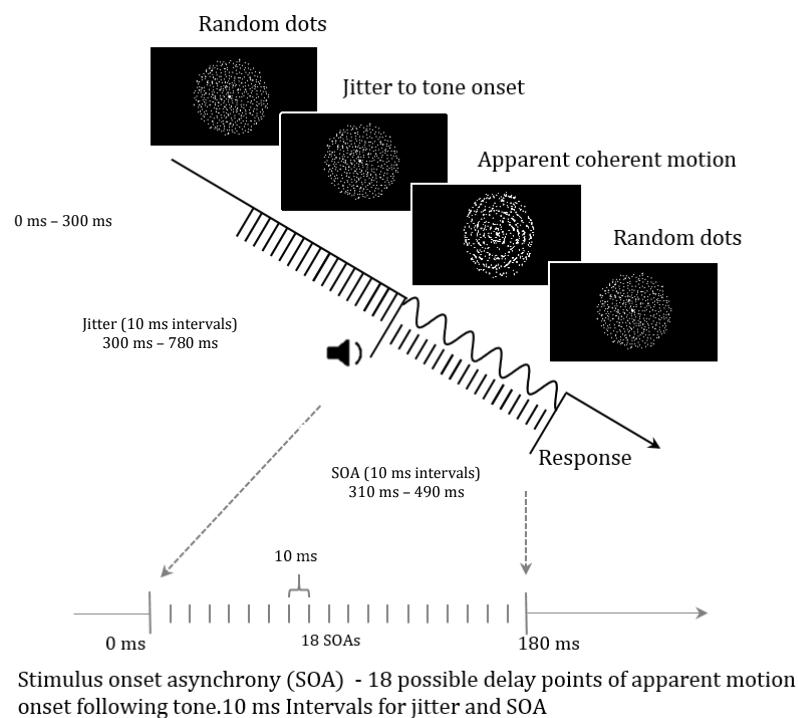
Figure 2.1. Experimental design. RDK stimulus remained as random no coherent motion and presented on for a minimum of 300ms, and continued for a randomised jittered interval between 300 and 700 ms to the onset of the binaural tone. Then at one of eighteen SOAs, following the tone-onset, the dots in the RDK stimulus would appear to rotate in a coherent notion for a set number of frames. This producing the phenomenon a global coherent motion, which either rotated clockwise or anticlockwise, or remain as no coherent motion. The SOAs are at intervals of 10 ms.

2.2.1   Data analyses

Preprocessing behavioural data

To remove outliers' only trials with reaction times between 200 and 1400 ms were used for analysis. Accuracy discrimination (as calculated below using signal detection theory) was the dependent variable.

Signal detection theory

The data were divided into cases where participants correctly discriminated the true direction of coherent motion in the dot pattern (hit) or incorrectly discriminated the direction of rotation (miss). Signal detection theory can be applied when there are two possible stimulus types – *signal* and *noise* – which must be discriminated (Green & Sets, 1966; Macmillan & Creelman, 2005). This measure takes the standardised (z-) value of the proportion of hits minus the standardised value of the proportion of false alarms (*d'*). This is necessary because an increase in hit-rate does not provide any information whether false alarms also increased due to a shift in response bias. Therefore, accuracy rate as characterised by *d*-prime (*d'*) served as the dependent variable of interest. This provides a more reliable indication of apparent motion discrimination ability in which hit-rate is corrected for the false positive rate. Equation 1 represents how *d'*-prime was implemented:

$$d' = z\big(\mathrm{P}(\gamma|s)\big) - z\big(\mathrm{P}(\gamma|n)\big)$$

(1)

where d' is the d'-prime statistic, with $z\big(\mathrm{P}(\gamma|s)\big)$ the z-score of hits rates (correct responses), and $z\big(\mathrm{P}(\gamma|n)\big)$ being the z-score of the false positives, and finally the z-transforms of these two rates (where the z scores represent the area under a normally distributed curve with a mean of 0 and a standard deviation of 1 for the Hits and False Alarms ratios). Because the z transform reaches infinity when percentages are equal to 0 or 100, datasets with values of 0 and 100% were assigned values of 1 and 99%, respectively (Macmillan & Creelman, 2005). Response criterion was calculated as the normalized sum of hit and false alarm rates multiplied by − .5 for each SOA across conditions (i.e., 5-Frames, 10-Frames, 25-Frames). The formula corresponded to

$$c = -0.5[\, z\big(\mathrm{P}(\gamma|s)\big) + z\big(\mathrm{P}(\gamma|n)\big)\,]$$

(2)

The criterion provided information about the participants' response bias in judging the target onset of RDK as coherent motion or no coherent motion, with a more conservative or liberal bias across SOAs (and conditions). A more conservative bias corresponds to positive criterion values. Instead, a more

liberal bias corresponds to negative criterion values. Unbiased responses are obtained when the criterion value is close to zero. As changes in sensitivity (d') and response bias (criterion) are independent, signal detection theory distinguishes between discriminative and motivational components in perceptual decision-making. Criterion scores obtained were subjected to a Wilcoxon signed ranks test to evaluate any significant deviation of these values from 0. Further, we evaluated whether there was a significant difference in response bias across the three conditions.

Cyclic modulation in behavioural performance

Group-level statistics. The behavioural experiment focused on the temporal profile of d' as a function of the visual motion discrimination accuracy over the variable delay time points (18 SOAs) between tone onset and onset of target stimulus (coherent motion). To investigate whether there was a cyclic pattern in d' performance, a curve-fitting procedure (cosinusoidal curve) was applied with custom software in MATLAB using the robust nonlinear least-squares method. Group-averaged d' was analysed for each experimental condition seperately after linearly detrending the data to remove linear effects across SOAs and retain any cyclic patterns around the mean. Next, the optimal fitting cosine curves to the data were computed from a variable frequency between 0 Hz – 25 Hz . For each frequency, the coefficient of determination, R^2, provided a goodness-of-fit measure. Bootstrapping was used to statistically evaluate the R-squared group mean. Using this statistical method, random permutations of the 18 SOAs over the 2000 iterations were computed and a model cosinusoidal curve was fitted to the resulting behavioural pattern contained within the data each time. This generated a null distribution of 2000 R-squared values.

The R-squared value acquired from the original data was compared to the null-distribution generated by the bootstrapping and used to evaluate whether the model fell in the upper 95th percentile. To this end, if this was the case, it would be by definition then an indication that the model cosine significantly explained variance in the group data. The cosine function was fitted with equation 2, where y the dependant variable represents the residuals following detrending of d' accuracy, x the independent variable is the time points of SOA delay from tone-onset and the target stimulus (dot rotation), and coefficients a, b, c, and a represent the amplitude, phase lag, and frequencyrespectively. Coefficients a,b,c are determined by numerical optimisation.

$$y = a * \cos(c * 2\pi * x + b)$$

(3)

Individual participant statistics. Using similar methods as describes on the group-level a secondary analyses was performed where model cosine fits were implemented on the behavioural data of

individual participants. Here, rather than averaging data over the group, models for each individual participant were first fitted and then these were statistically bootstrapped. Finally a second-level anlyses using a RM-ANOVA was computed on the cosine model fitting R-squared values for each SOA across all three experimental conditions.

Statistical comparisons across condtions

In all the experimental conditions a repeated-measures analyses of variance (RM-ANOVA) was implemented. In principle, although this test cannot specifically inform on the periodicity within the data as it can only test for equality of class means. Here, the variability is computed between SOA time bins and the variability computed within groups, if there is rhythmicity evident in the data, however, the variability among SOA time bins will be larger than the variability within SOA time bins ($F > 1$). Although, the ANOVA can guide the inferences about a lack of uniformity further evaluation will provide direct evidence for the existence of any particular rhythmicity in sensory perceptual performance. Significant results were further explored using two-tailed paired-samples *t*-tests.

The data from the bootstrapping procedure, which was conducted on the curve fitting models, were compared cross conditions. In order to test for significant differences in fitting frequencies between conditions, individual participant peak fitting frequencies were obtained by applying a jackknife approach (Kiesel, Miller, Jolicœur, & Brisson, 2008; Miller, Ulrich, & Schwarz, 2009; Smulders, 2010). The jackknifing procedure was used to scale the peak fitting frequency at subsets of the grand-average fitting frequency of the cosine fitting models. Subsets were generated by using data from an iteration of *n*-1 participants (*N*-different-leave-one-out subsets) of the original sample included in the grand-average cosine model fitting of *d'*. By doings so the standard error of the estimated peak fitting frequencies were derived. In order to test for significant differences between peak fitting frequencies across the three conditions, estimates of the individual participant peak fitting frequencies ($o_1 \dots, o_n$) were calculated from the sub average scores ($j_1 \dots, j_n$) using the following equation (Smulders, 2010);

$$o_i = n\bar{J} - (n-1)j_i$$

(4)

Next, an RM-ANOVA was conducted to examine the differences in the peak fitting frequency estimates across conditions and participants. Significance was tested using a two-tailed criterion and a 95% confidence interval.

Average Power Spectral Density estimation

In order to investigate the amount of power contribution in the d-prime curve fitting models, the power spectral density (PSD) was computed, which is a measure of the magnitude of a signal of a given frequency within the average time-series. Power is equivilant to the squared amplitude of a signal and is used here to quantify the strength of the oscillations within a given frequency band. The integral of the PSD over a given frequency band computes the average power in the signal over that frequency band. A Welch spectral estimator (Percival & Walden, 1993) was applied to obtain the PSD (MATLAB Signal Processing Toolbox function, *spectrum.welch;* using a discrete Fourier transform with a Hamming window segmented length of 64. The signal is real-valued so the PSD is one-sided and this contains the total power of the signal in the frequency interval from DC (0 Hz) to half of the sampling rate (Nyquist rate of 50 Hz).

Oscillatory phase concentration

Phase concentration was calculated across subject separately. The complex Fourier-spectra was computed by applying a non-overlapped fixed Hanning tapered window, short time Fast Fourier Transform (FFT). The window had a length of 18 data points, each point representing one of the 18 SOAs and was padded with zeros up to 64 data points. The absolute value (magnitude) of the Fourier coefficients represents the amplitude of the spectral components, with its square as the power spectrum. This expresses how much periodicity is visible in the SOAs at each particular frequency. The frequencies of interest ranges from 1 to 25 Hz in steps of 1 Hz. Phase was measured by taking the mean normalised complex Fourier spectrum with respect to subject's d-prime curve fitting across SOAs and frequency. The phase time series assumes values within $(-\pi, \pi]$ radians with a cosine phase such that $-/+\pi$ radians correspond to the troughs and 0 radians to the peak. These were carried out in Matlab using custom programming code established on standard mathematical and signal analysis functions.

Statistical significance of phase consistency was then determined by taking the instantaneous Rayleigh Z score (against a hypothetical uniform distribution) and associated P value using the circ_rtest function found in the Circular statistics toolbox (Berens, 2009). The function calculates the mean resultant vector length for the phase distribution (von Mises distribution), which indicates the direction (preferred phase) and magnitude of directionality (length) of a given distribution by first averaging direction vectors:

$$\bar{r} = \frac{1}{n} \sum_r r_i$$

(5)

Then the preferred phase angle:

$$\cos a + i \sin a = \exp(ia)$$

<div align="right">(6)</div>

And finally calculating the length of the mean resultant vector:

$$R = \|\bar{r}\|$$

<div align="right">(7)</div>

This results in a value between 0 and 1, with 0 indicating no directionality, and 1 indicating the maximum directionality. A limitation of using the mean resultant vector length as the dependent vairable is that it is affected by the number of samples contained within the phase-angle distribution. Therefore, a bootstrapping procedure was implemented on the mean resultant vector length for each participant's d' accuracy by randomly sub-sampling from the distribution a 1000 times taking the mean from the bootstrapped distribution to obtain a normalised mean resultant vector length.

2.3 Results

Behavioural performance

We assessed the temporal profile of visual perceptual performance over the 18 SOAs (delay time points) between tone onset and target stimulus was assessed. Figure 2.2 shows box plots of the d' performance and reaction times (RT) for each subject across the conditions. This enabled visual inspection of the data to identify outliers and determine which data sets to exclude for further analyses. Participants were excluded if the average d' performance was consistently below or above the peri-threshold level set between 65% and 80% accuracy. Based on these criteria subject eighteen was excluded for having consistently low accuracy scores and slow RTs. Individual trials with RTs outside the specified criterion of 200 and 14000 ms, were excluded. These data show the variability between subject performance within and across conditions. Table 1-3 shows the Hit Rate, False Alarm, and Response Bias(c) shows the data for each SOA across the conditions. A non-parametric contrast (Wilcoxon signed ranks test) between the mean values of c against zero (no response bias) revealed that these were significantly greater than zero for all conditions (5-Frames: $Z = -3.725, p < 0.05$; 10-Frames: $Z = -3.724, p < 0.05$; and   25-Frames: $Z = -3.724, p < 0.05$). This indicates that participants were biased to respond that there was coherent motion; however, this bias was in the same direction across all conditions. Indicating that the d' scores were not confounded by a difference in response bias.

Table 1. 5-Frames descriptive statistics. Hit rates (HIT), false alarm rates (FA) and bias criterion (c)

SOA	HIT % (S.E.M.)	FA % (S.E.M.)	c (S.E.M.)
10 ms	73 (±2.44)	6 (± 1.18)	0.51 (± 0.05)
20 ms	76 (±2.15)	3 (± 0.78)	0.58 (± 0.05)
30 ms	71 (±2.32)	5 (± 1.09)	0.59 (± 0.05)
40 ms	75 (±2.10)	5 (± 1.15)	0.53 (± 0.06)
50 ms	72 (±2.50)	5 (± 0.93)	0.54 (± 0.05)
60 ms	72 (±2.01)	5 (± 0.85)	0.55 (± 0.05)
70 ms	73 (±2.11)	9 (± 1.63)	0.4 (± 0.04)
80 ms	75 (±2.69)	9 (± 1.94)	0.38 (± 0.04)
90 ms	76 (±2.28)	10 (± 2.04)	0.36 (± 0.05)
100 ms	75 (±2.47)	11 (± 1.92)	0.34 (± 0.04)
110 ms	75 (±2.39)	11 (± 1.86)	0.31 (± 0.04)
120 ms	74 (±2.08)	9 (± 1.61)	0.4 (± 0.05)
130 ms	74 (±2.16)	4 (± 0.85)	0.57 (± 0.05)
140 ms	73 (±2.85)	5 (± 1.34)	0.56 (± 0.05)
150 ms	72 (±2.51)	6 (± 1.19)	0.5 (± 0.05)
160 ms	72 (±2.14)	5 (± 0.91)	0.55 (± 0.05)
170 ms	75 (±2.43)	3 (± 0.72)	0.57 (± 0.05)
180 ms	76 (±2.48)	4 (± 0.92)	0.51 (± 0.05)

Cells contain the mean and standard error of the mean (S.E.M.) averaged across participants. Trials time-locked to tone onset.

Table 2. 10-Frames descriptive statistics. Hit rates (HIT), false alarm rates (FA) and bias criterion (c)

SOA	HIT % (S.E.M.)	FA % (S.E.M.)	c (S.E.M.)
10 ms	78 (± 2.89)	5 (± 1)	0.46 (± 0.06)
20 ms	76 (± 2.84)	4 (± 0.93)	0.49 (± 0.06)
30 ms	78 (± 3.32)	5 (± 1.08)	0.43 (± 0.05)
40 ms	78 (± 2.49)	4 (± 1.16)	0.5 (± 0.05)
50 ms	79 (± 2.81)	5 (± 0.87)	0.42 (± 0.06)
60 ms	78 (± 2.09)	3 (± 0.69)	0.54 (± 0.05)
70 ms	79 (± 2.75)	7 (± 1.57)	0.37 (± 0.06)
80 ms	83 (± 2.55)	8 (± 1.8)	0.25 (± 0.05)
90 ms	81 (± 2.24)	8 (± 1.86)	0.3 (± 0.04)
100 ms	79 (± 2.37)	9 (± 1.61)	0.28 (± 0.05)
110 ms	80 (± 2.32)	7 (± 1.58)	0.31 (± 0.04)
120 ms	78 (± 2.23)	9 (± 1.73)	0.32 (± 0.05)
130 ms	80 (± 2.43)	6 (± 0.98)	0.38 (± 0.04)
140 ms	82 (± 2.04)	3 (± 0.66)	0.45 (± 0.04)
150 ms	79 (± 2.33)	4 (± 0.85)	0.49 (± 0.06)
160 ms	80 (± 2.38)	5 (± 0.97)	0.41 (± 0.06)
170 ms	79 (± 2.86)	3 (± 0.91)	0.48 (± 0.07)
180 ms	79 (± 2.03)	4 (± 0.95)	0.47 (± 0.05)

Cells contain the mean and standard error of the mean (S.E.M.) averaged across participants. Trials time-locked to tone onset.

Table 3. 25-Frames descriptive statistics. Hit rates (HIT), false alarm rates (FA) and bias criterion (c)

SOA	HIT % (S.E.M.)	FA % (S.E.M.)	c (S.E.M.)
10 ms	76 (± 2.56)	5 (± 1.18)	0.54 (± 0.06)
20 ms	76 (± 3.42)	3 (± 0.71)	0.53 (± 0.07)
30 ms	77 (± 2.77)	4 (± 0.82)	0.52 (± 0.07)
40 ms	71 (± 3.02)	6 (± 1.07)	0.53 (± 0.07)
50 ms	74 (± 2.9)	6 (± 1.21)	0.52 (± 0.06)
60 ms	76 (± 2.55)	6 (± 1.29)	0.5 (± 0.07)
70 ms	72 (± 2.76)	10 (± 2.34)	0.42 (± 0.06)
80 ms	71 (± 3.25)	9 (± 1.85)	0.44 (± 0.06)
90 ms	75 (± 2.66)	8 (± 2.09)	0.47 (± 0.07)
100 ms	72 (± 2.57)	10 (± 1.94)	0.42 (± 0.06)
110 ms	77 (± 3.09)	8 (± 2.06)	0.42 (± 0.07)
120 ms	75 (± 2.85)	10 (± 1.84)	0.36 (± 0.06)
130 ms	73 (± 2.82)	7 (± 1.15)	0.46 (± 0.06)
140 ms	76 (± 2.27)	4 (± 0.95)	0.5 (± 0.05)
150 ms	75 (± 2.46)	5 (± 1.19)	0.52 (± 0.05)
160 ms	73 (± 2.84)	6 (± 1.12)	0.52 (± 0.06)
170 ms	76 (± 2.75)	4 (± 1.06)	0.52 (± 0.06)
180 ms	73 (± 2.46)	6 (± 1.14)	0.51 (± 0.05)

Cells contain the mean and standard error of the mean (S.E.M.) averaged across participants. Trials time-locked to tone onset.

Table 4 shows the results of average apparent motion discrimination accuracy (hit rate and d prime) for each experimental condition. These data indicate that all subjects, including those with high false alarm rates, were nonetheless able to differentiate apparent motion in the three forced choice task. In all three experimental conditions a repeated-measures analyses of variance (RM-ANOVA) was implemented to assess the variability of apparent motion discrimination accuracy (d') across the 18 SOAs as a function over time relative to tone onset. Three RM-ANOVA were run for the three experimental conditions on apparent motion discrimination accuracy with factors SOA (18-factors) across subjects (23) there were significant main effects of SOA for the 5-frames ($F_{17,391} = 2.51$, $p < 0.001, \eta_p^2 = 0.1$) the 10-frames condition ($F_{17,391} = 2.10$, $p < 0.05, \eta_p^2 = 0.08$), and for the 25-frames condition $F_{17,391} = 3.58$, $p < 0.001, \eta_p^2 = 0.14$),. An overall RM-ANOVA across all the experimental conditions (SOA [18] x Condition [3]) revealed a significant main effect of condition $F_{2,46} = 3.31$, $p = 0.043, \eta_p^2 = 0.13$), a significant main effect of SOA ($F_{17,391} = 5.01, < 0.001, \eta_p^2 = 0.18$, and no significant (marginally significant) interaction (SOA*Condition) ($F_{34,782} = 1.40$, $p = 0.07, \eta_p^2 = 0.06$).

Table 4. Grand average. Hit rates (HIT, percentage correct), false alarm rates (FA, percentage) and d' (c, bias response) for each SOA

	HIT % (S.E.M.)	d' (c)	FA % (S.E.M.)
5-Frames	78.72(1.25)	2.29(0.33)	8.26(0.98)
10-Frames	81.02(1.11)	1.90(0.05)	16.45(1.11)
25-Frames	54.33(1.18)	2.15(0.92)	2.56(0.38)

Cells contain the mean and standard error of the mean (S.E.M.) averaged across participants for Hit and FA. Trials time-locked to tone onset.
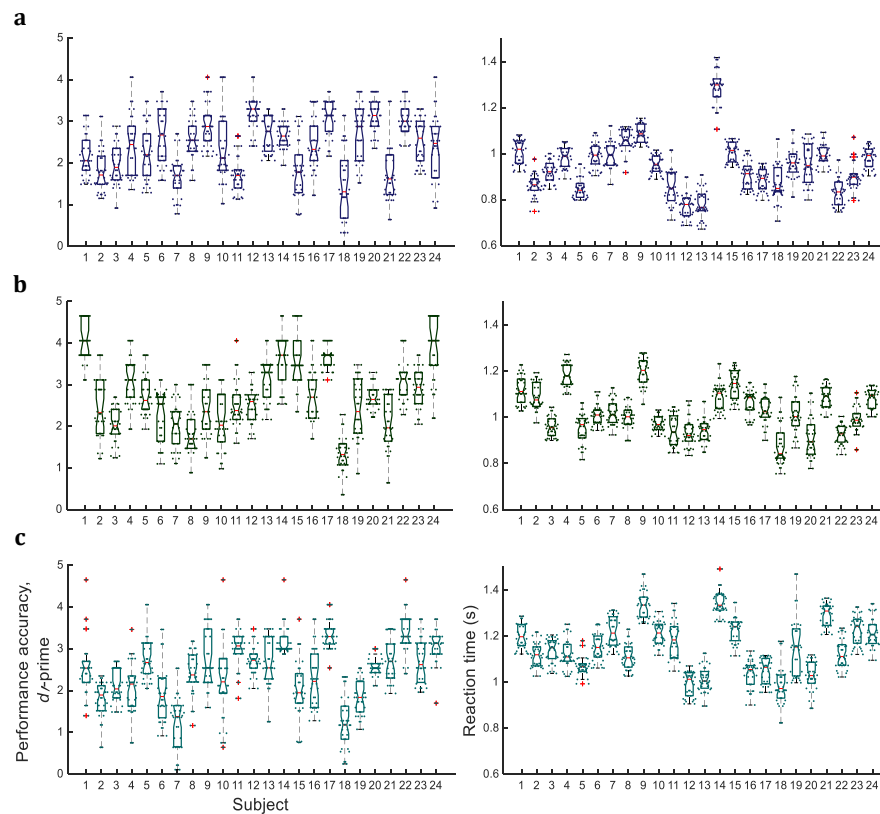
Figure 2.2. Descriptive Statistics. Box plots illustrating the individual subject performance data. Left panel represents the d' detection accuracy. Right panel represents reaction time (RT) data. a) 5-Frames, b) 10-Frames, c) 25-Frames. Lines in boxes represent medians, the box ends at the 25th and 75th percentiles, whiskers 10th/90th percentiles. Individual SOA data are superimposed dots for each subject. Outliers (>1.5 times the interquartile distance) are plotted with crosses.
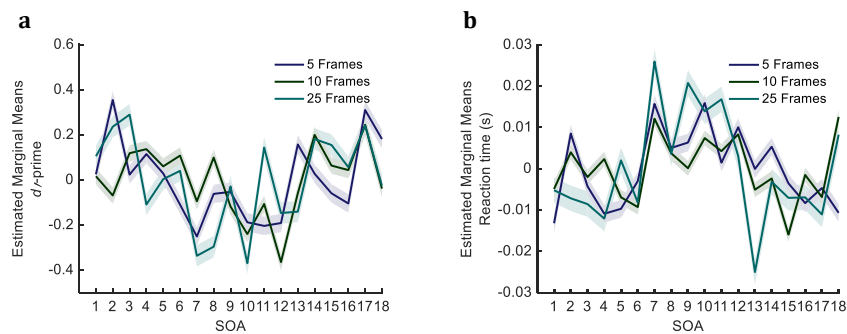
Figure 2.3. Estimated marginal means. Line plots illustrating estimated marginal means at the group-level across SOAs. **a1)** accuracy expressed as detrended d' scores and **b)** reaction times Solid lines show the data where shading demarcates standard error. For d' scores **a)** SEM = 0.002, SEM = 0.001, SEM = 0.003, respectively. Standard error for detrended reaction times **b)** SEM = 0.039, SEM = 0.035, SEM = 0.039, respectively.

Periodicity in perceptual discrimination performance

To investigate the effects of the varying onset of the target stimulus presentation (coherent motion) over the 18 SOAs time-locked to tone-onset (180 ms post-tone window) a curve fitting function (cosinusoidal curve) was applied to data. This test determined if there are periodic fluctuations evident in *d'* discrimination accuracy as a function over time relative to tone onset. To assess the significance of the model fit and the presence of periodicity, a bootstrapping statistical approach were combined with the cosinusoidal model fitting procedures (see Methods). Critically, this procedure tests the existence of a significant cyclic modulation in sensory perceptual performance, where the periodic fluctuations observed in the data could be attributed to stimulus-locked (tone-onset) oscillatory activity. This would provide support for CMPR. The results of this analyses revealed a significant modelled cosine function for all three conditions at the group and single subject levels. Figure 2.4 illustrates the time-course of visual task performance timelocked to tone onset for all three conditions (after linear detrending), with best-fitting cosine models superimposed in red.

Statistics. Using boostrapping procedures revealed that in the 5-frames condition the best fitting cosine model was 6 Hz (r^2 = 0.6) with a range of significant frequencies between 4-8 Hz (95% CI). In the 10-frames condition the best fitting cosine model was 9 Hz (r^2 = 0.5) with a range of significant frequencies between 6-10 Hz (95% CI). Finally, for the 25-frames condition, the best significant model fit was 7 Hz (r^2 = 0.4) with a range of significant frequencies between 4-8 Hz (95% CI). These data statistically confirm the presence of a cyclic modulation in visual task performance at group level. Single subject data not shown here, yield similar results. Figure 2.4 (left hand column) shows the results of the bootstrapping with all conditions superimposed. On visual inspection, we can see that there are very slight differences between the conditions. It appears that the 5-Frames and 25-Frames yielded similar best fitting models at 6-7 Hz, while the 25-frames condition revealed a slightly higher

best cosine model fit at 9 Hz. These conditions have in common significant range of frequencies between 4-10 Hz. In order to test any significant difference between conditions individual subjects peak model fitting frequencies were obtained by means of a Jackknife procedure (see methods). This results in a peak frequency for each individual subject for each condition. These data were then analysed for significant differences using a RM-ANOVA two-sided. The results show no significant main effect of condition ($F_{2,46} = .49$, $p > 0.05, ns, \eta_p^2 = 0.02$). This would indicate that there is no significant difference in best fitting frequency for different number of displacement frames at target coherent motion in the RDK stimulus.
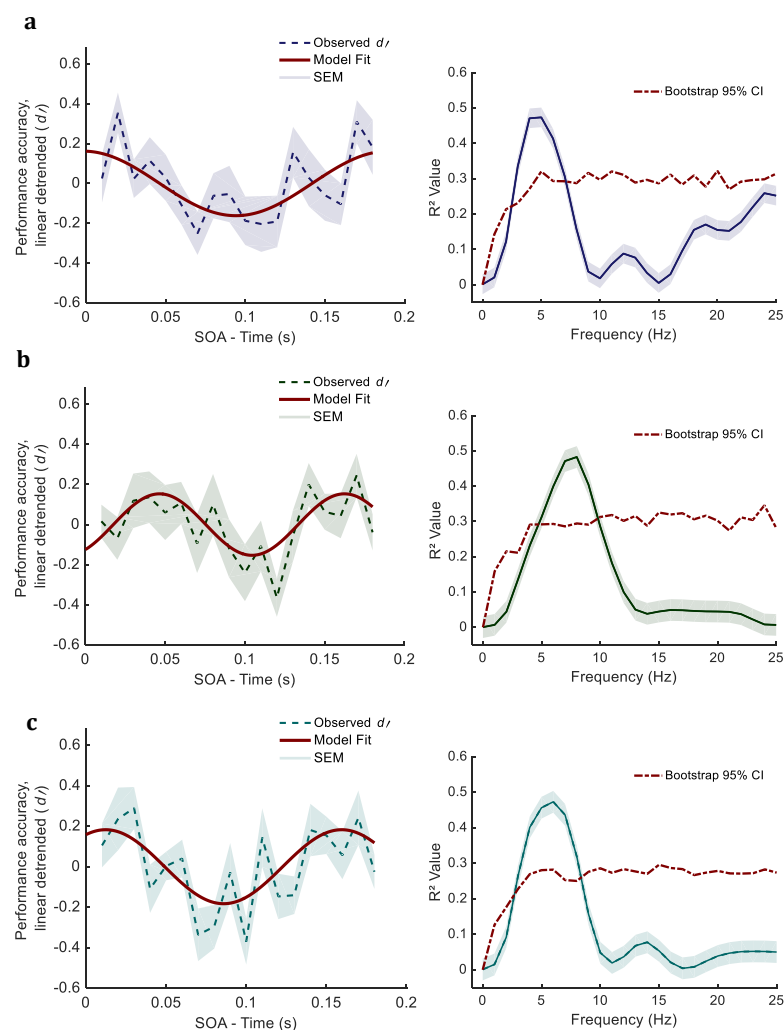
Figure 2.4. Group Avg. Cosine Functions. *Left panel* shows cosine model fits (red sloid line) superimposed on d' data (dotted line). *Right panel* shows the bootstrapping significance r-square model fits. **a)** 5-frames, **b)** 10-frames condition, **c)** 25-frames conditions respectively. Group average d' accuracy (linearly detrended) for apparent motion discrimination for all conditions over 2 cycles post-tone onset. The best fitting cosine model superimposed in red. **a)** 5 Hz (r2 = 0.5), **b)** 8 Hz (r2 = 0.5), **c)** 6 Hz (r2 = 0.4), show the optimal significant cosine functions. Shaded area represent standard error of the mean (SEM) after the removal of baseline between subject variance (within-subject error bars (Cousineau, 2005).

Power Spectral Density estimate

In order to further assess the existence of periodicity in sensory perceptual performance as evidence of CMPR, we transformed the d' data into their frequency-domain representations (see Methods). Figure 2.5b illustrates the power spectrum density (PSD) computed on average d' time courses within the range 1-50 Hz (for visualisation and comparison purposes we plot only frequencies from 1-25 Hz), all three conditions superimposed. All conditions show similar results in lower frequencies (6-9 Hz) compared to the r-square values obtained from bootstrapping. The 5-Frames and 25-Frames conditions show peaks at 6 Hz. The 10-Frames conditions there is a peak at 23 Hz, with a second smaller peak at 9 Hz.
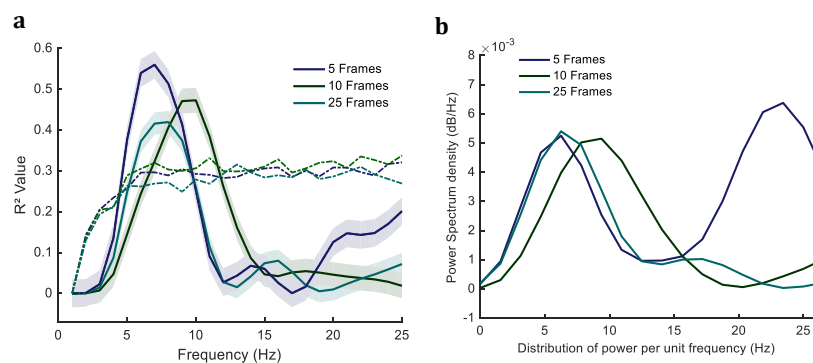
Figure 2.5. Power spectral density and R-square fit. a) R^2 values for cosine model fitting across frequencies. Three conditions superimposed. Peak fitting frequencies at 5-10 Hz. Solid lines indicate the 95% confidence interval bootstrapped permutation. **b)** Using standard short-time Fourier transform, power spectrum of d-prime temporal profile. All the conditions show similar peaks at 6-9 Hz frequency; 5-Frames peak = 6 Hz, 10-Frames peak = 23 Hz, 25-Frames peak 6 Hz. The 10-Frames conditions does show a second peak at 9 Hz, closer to the other peaks.

Oscillatory phase concentration

Phase concentration was computed across participants averaged *d'* and calculated for each condition. Importantly, in contrast to conventional methods for measuring phase over single trials figure 2.6 shows the phase of average performance for each participant depicted on as a single data point on the circumference of the unit circle (right panel). This gives an indirect measure of oscillatory phase concentration following the auditory accessory stimulus. The results confirmed a statistically significant non-uniformity ($p < 0.05$) in the phase distribution for each condition. In the 5- and 25-frames conditions there is significant phase concentration between 1-6 Hz frequency (*z*-score range = 3.1 -7.2, with a peak at 4 Hz). Whereas the 10-frames conditions a 10-11 Hz phase concentration (*z*-score range = 3.3 -3.4, with a peak at 11 Hz). Across all conditions there was high PLV of .4 to .6, which indicate the direction (preferred phase) and magnitude of directionality (length) of the given distribution. These data reveal tentative evidence for cross-modal phase resetting.
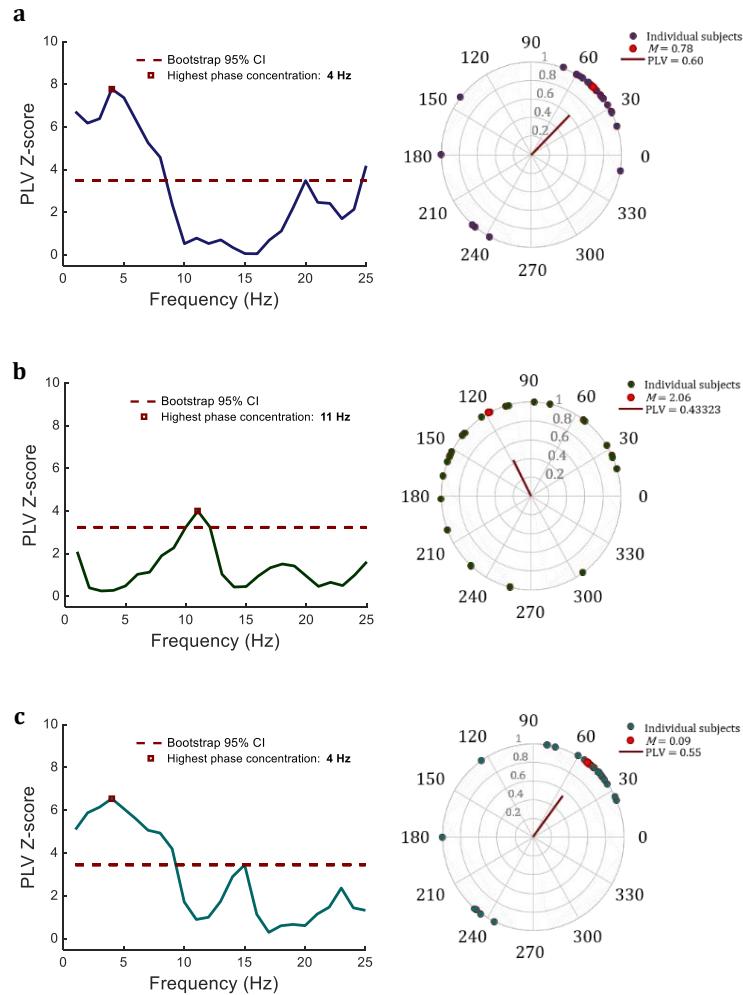
Figure 2.6. Phase concentration. *Left panel*; Rayleigh's Z-scores across subjects on d' cosinusoidal model fits as a function of frequency. Red squares indicate the highest phase concentration. Horizontal red dotted line indicated the 95% confidence interval cut-off (Z score = 3.8) *Right panel*; Circular plot representing the highest phase concentration frequency, with individual participants' phase angle values on the circumference of the unit circle (theta phase in degrees). Red dot and line represents the mean and resultant vector length respectively for the phase coherence of d' across participants. The vector length here measures the consistency of phase locking around the mean angle (M), with 0 being random and 1 being zero variance. The vector direction indicates the preferred phase of visual task performance (*d'*), and length indicates magnitude of phase resetting, the mean resultant (PLV). a) 5-frames, Z score = 4 Hz, PLV = .6 (M = .78), b) 10-frames, Z-score = 11 Hz, PLV = .4 (M = .2), c) 25-frames, Z score = 4 Hz, PLV = .5 (M = .09).

2.4 Discussion

Research suggests that an event in one modality can phase align oscillations in another modality through the mechanism of CMPR of ongoing oscillations. However, most previous studies have focused on using a single briefly flashed stimulus, and focus on the spatial domain. These paradigms make it problematic to discern phase resetting due to transient evoked responses or through internally driven oscillatory modulations (Makeig, Westerfield, Jung, & Enghoff, 2002b; Sauseng, Klimesch, Gruber, & Hanslmayr, 2007). Far less understood, is the interaction of the auditory modality and visual motion. Furthermore, behavioural evidence for an auditory induced enhancement of visual motion perception as investigated within the context of cross-modal phase resetting is sparse. In the present study, using a continuous dynamic stimulus, we contribute new evidence. The first aim of the experiment was to investigate an auditory-driven modulation of visual perceptual performance. Next, within the framework of the perceptual cycles theory (VanRullen, 2016b), we investigated the sensory perceptual consequences of increasing the duration of coherent motion in the RDK. We aimed to explore the effects of a "frequency tagging" type effect that may be reflect as quasi-sinusoidal behavioural responses. The temporal profile of visual perceptual performance was analysed over varying delays, time-locked to a transient auditory stimulus. We predicted that evidence for a systematic phase reorganisation in underlying visual oscillations, would manifest itself behaviourally as a cyclic modulation in perceptual performance phase-locked to the tone-onset. Our data revealed that this was indeed the case.

The present data offer a behavioural marker for an auditory induced facilitation of visual cortical excitability. Our findings are consistent with data described in the animal literature (e.g., Lakatos et al., 2009, 2007; Kayser et al., 2008; Kayser & Logothetis, 2007 Magri et al., 2009) and human neurophysiological research (e.g. Fiebelkorn, Foxe, Butler, & Molholm, 2011; McDonald, Störmer, Martinez, Feng, & Hillyard, 2013; Naue et al., 2011; Romei et al., 2012; Thorne & Debener, 2014). Although we attribute our findings as sensory consequence of CMPR as the most parsimonious explanation, using purely psychophysical measures, it is not possible to provide unambiguous evidence for CMPR. To this end, it is also possible then that the existence of auditory-timelocked periodicity is a product of an additional oscillatory component superimposed on the instantaneous visual oscillations rather than from phase reset of pre-existing oscillations (Fiebelkorn, Foxe, & Butler, 2011; VanRullen & Dubois, 2011).

The manifestations of oscillations in behavioural performance have only recently been investigated (Diederich et al., 2012; Diederich et al., 2014; Fiebelkorn et al., 2011; Graaf, Gross, Paterson, Rusch, et al., 2013; Landau & Fries, 2012). These findings suggest that the underlying neuronal oscillatory systems have direct consequences on behaviour. However, there is sparse behavioural evidence for

the CMPR mechanism using a continuous visual stimulation that is spatiotemporally informative. First, we demonstrate that perception of a near threshold visual motion is modulated by oscillatory phase induced by a task irrelevant tone. Here we provide analogous interpretations to those provided by neurophysiological research. Second, our findings suggest that visual oscillatory systems are not modulated by increasing the length of sequential frame displacement in the RDK stimulus.

Cross-modal phase modulation of visual motion perception

The periodicity observed in the behavioural response profile provides an indication for an auditory induced phase resetting of visual behavioural performance. Using a continuously dynamic RDK, presented prior to an exogenous tone, it was possible to preclude any transient effects that could be induced by the presentation of a sudden visual stimulus. Moreover, the low-level visual features in the stimulus remained constant for the duration of the epoch. Without having any direct electrophysiological evidence, we speculate here that the periodicity observed in behaviour could be attributed to CMPR mechanism. If there were no inter-regional phase modulation, then visual accuracy and detection performance would not reveal any systematic fluctuations, such that visual performance would be at chance level at each SOA.

The temporal integration of continuous sensory information into a temporally extended perception becomes evident when using tasks with spontaneous near-threshold apparent coherent motion in RDK stimuli. Apparent motion in RDKs, are created by displacing a display of randomly presented dots by a certain amount in a given direction. Consequently, there must be spatial and temporal integration of dots displacement over an extended area of the visual field in order to signal the veridical direction of the pattern. If the displacement is relatively small and all dots shift in the same direction (100 % coherence), the motion percept is smooth and continuous. As the displacement approaches the maximum displacement value (Dmax), direction discrimination of the apparent motion is still possible but less coherent. As the displacement exceeds Dmax, motion direction is not reliably determined because the perceived motion appears to be incoherent, even though the dots are still moving with 100% coherence. Short-range motion perception is involved in complex patterns, small displacements, and temporal interval processes (Braddick, 1974). Experiments using psychophysics have proposed that Dmax increases with a decrease in dot probability (Ramachandran & Anstis, 1986) and an decrease in motion coherence (Todd & Norman, 1991, 1995). Consequently, direction discrimination of motion coherence in RDKs benefit from spatial summation (Movshon & Thompson, 1978). Therefore, the observer must identify the direction of the signal dots in the relative proportion of signal to noise in the stimulus.

Our data revealed behavioural oscillations that waxed and waned in periods of optimal and nonoptimal windows of performance, supporting the perceptual cycles theory for the discretisation of

perception through neural oscillations. The results of which provide a highly plausible link between perception and the neural oscillatory substrate (Lakatos, Shah, & Knuth, 2005; Schroeder & Lakatos, 2009; VanRullen & Dubois, 2011). The interpretations of the data are focused on the results obtained from the fitting procedures, rather than that of the PSD (see, results and limitations below). The data revealed a rhythmicity in behavioural performance that appeared to cycle at wavelengths corresponding to 4-10 Hz frequency. Specifically, the 5- and 10-frames conditions revealed similar best fitting frequencies at 6 Hz and 7 Hz respectively. Whereas the 25-frames condition the best fitting, model was slightly higher at 9 Hz frequency. Interestingly, when statistically comparing the differences between peak fitting frequencies across conditions, there was no significant difference.

These findings highlight the role that low frequency oscillations play in the sensory integration of information over time. Interestingly, we find that there is no significantly different perceptual consequences on task performance from varying the lengths of coherent motion stimulation. According to previous research, we might have predicted the 5-frames condition to yield the most optimal behavioural performance. In this condition the target coherent motion lasted for a period of 50 ms, which coincides with the widely reported resonant sampling frequency of the visual system denoted as the alpha rhythms (Basar & Schurmann, 1997; Ergenoglu et al., 2004; Foxe & Snyder, 2011; Graaf et al., 2013; Romei et al., 2012; Spaak, Lange, & Jensen, 2014). Therefore, the 5-frames condition is apt to probe visual alpha at the highest sampling resolution as compared to the other spatiotemporal window lengths. The rational here is that a 50 ms spatiotemporal integration window falls neatly within the bounds of half the wavelength of a 10 Hz oscillation, where processing is at its optimum (Jensen & Mazaheri, 2010; Romei et al., 2012; Schroeder et al., 2008).

Our data reveals low frequency (4-10 Hz) modulations in behavioural performance. Until recently, the majority of research has reported oscillations in the alpha as critical in visual perception (Wolfgang Klimesch, Fellinger, & Freunberger, 2011; Lange, Oostenveld, & Fries, 2013; Mathewson & Lleras, 2011; Romei et al., 2008; Vincenzo Romei, Driver, Schyns, & Thut, 2011). Although the alpha (8-12 Hz) rhythm remains widely implicated in visual perception, progressively more research is demonstrating functional associations of perception involving other frequency bands, as reported here in 4-8 Hz theta frequency range (Diederich et al., 2014; Dugué et al., 2015; Vanrullen, 2013; VanRullen & Dubois, 2011; Mathewson & Lleras, 2011). For example, VanRullen and colleagues have demonstrated the relative contribution that ongoing pre-stimulus EEG oscillations have on perceptual consequences. In one of their studies (Busch et al., 2009), they presented brief flashes of light at near-threshold detection, where the luminance of the flashes were calibrated so that the exact same stimulus would be perceived on approximately half of the trials, but go undetected on the other half. They found significant pre-stimulus phase concentration at ~7 Hz (theta range) on those trials where flashes were accurately detected. Using the data from prefrontal EEG electrodes, they were able to predict the subsequent

responses of each subject above chance. Specifically up to 16% of the trial-by-trial variants in perception were accounted for by estimating those trial which had am optimal phase angle with those in the opposite phase. Using EEG, Thorne and colleagues (2011) similarly show that much like delta, theta- low-alpha band oscillatory activity can also influence behavioural performance. Numerous EEG studies and neurophysiological recordings reveal that theta-band (3-8 Hz) rhythms have been implicated in the mediation of perception and attention (e.g., Landau & Fries, 2012; Luo, Liu, & Poeppel, 2010).

Experimental data concerning the theta-band oscillations indicate a role in cognitive processing and in the cortico-hippocampal interaction (for a review see, Miller, 1991). Theta rhythms constitute the cycles of selection, where the process of selection is made and then desynchronising gamma-band oscillations for selecting one item at a time within a cycle, in return this enables sampling for successive relevant items and resulting in a rhythmic sampling (Fries, 2009). Furthermore, theta ($\sim$ 7Hz) rhythms may contribute to higher-level attentional cycles (Dugué et al., 2015; Vanrullen, 2013; Voloh & Womelsdorf, 2016). This is consistent with EEG recordings positing a role for low frequency rhythms associated with spatiotemporal integration (Von Stein & Sarnthein, 2000; Varela, Lachaux, Rodriguez, & Martinerie, 2001). Evidence from animal research has already suggested at a supramodal coordination of theta-band oscillatory activity (Lakatos et al., 2009). Taken together these studies support our data for a role that pre-stimulus theta brain oscillations have in spatiotemporal integration and cross-modal modulations thereof.

Phase locking value results show that the 5-frames and 25-frames were consistent with the results obtained from the curve fitting models. Our data revealed significant phase coherence across participants within the 1-9 Hz frequency range. In contrast to conventional methods for measuring phase concentration, in the current study phase-locking value was computed on the d-prime cosine models, which was an average of all trials for an individual participant, rather than at the single trial level (Canavier, 2015; Fisher, 1995). Measurement limitations imposed on behavioural paradigms necessitate the averaging over trials to reveal oscillatory components, which constitutes the data. Nonetheless, we observed consistent phase coherence across participants; this might give some indication of consistent phase coherence across individual trials, albeit indirect. This is compatible with the notion of CMPR, although our interpretations here are speculative at this point. Finding that there is alpha phase reset may not be surprising as it is consistent with the proposal that alpha represents a pulsed inhibition of ongoing cortical activity where alpha phase reflect states of high and low excitability leading to a modulation in perception (Hanslmayr, Gross, Klimesch, & Shapiro, 2011; Jensen & Mazaheri, 2010; Klimesch, Sauseng, & Hanslmayr, 2007b). One possible explanation for the 10-frames exhibiting different results could be attributed to individual participant variability within the data, contributing a driving factor in the phase analyses that are sensitive to these differences when

analysed. Taken together, our findings are in line with those reported previously by Romei et al. (2010, 2012). Here they which showed a preferential phase for optimal perception, phase modulated by a task irrelevant auditory stimulus. In contrast, they report alpha-band (11 Hz) modulations at delays of 75-130 ms and 180-225 ms post tone-onset.

Spatiotemporal integration

The second aim of the experiment was to probe the effects of visual perceptual performance by varying the number of successive frames in the coherent motion sequence. In order to perceive a single percept of coherent motion in the stimulus, participants must integrate the spatiotemporal information over time for each successive frame. Within the context of our paradigm, we define spatiotemporal integration as the accumulation of information gain from consecutive frame displacements in the kinematogram, which are sequentially integrated to form a unitary percept of coherent visual motion (Cleary & Braddick, 1990; Morand et al., 2015; Ramachandran & Anstis, 1983b; Ramachandran & Anstis, 1986). In principle, according to the discrete perceptual cycles theory we could expect that performance accuracy in detecting or discriminating the direction of the visual motion is contingent of the phase of the underlying visual system sampling frequency. Visual neural ensembles enable the integration of inputs over a range of intervals that correspond to half cycles of oscillatory activity at various frequencies (Schroeder et al., 2008). Within this framework then, performance accuracy would be at its highest if the complete coherent motion sequence falls within the period when the underlying cortical excitability is at its most optimal phase for information processing. For example in the current paradigm, the 5-frames condition corresponds to a coherent motion sequence of 50 ms; this coincidently this is proportionate to half the wavelength of an alpha (10 Hz) oscillation, the ideal half of the full wavelength, indicating that the full sequence can fit neatly into the period where sensory information processing is most optimal. However, this is assuming the visual sampling frequency is within the alpha frequency range. Interestingly, this would suggest that by increasing the number of displacement frames in the RDK, whereby essentially extending the length of apparent motion, would result in a motion sequence that is greater in length than the period of highest cortical excitability where signal processing is most optimal (see figure 2.7.b1 and 2.7. c1). If this were the case, we would expect that performance accuracy would decline with increasing coherent motion frames.

An alternative prediction is that visual system will adapt to the varying lengths of the coherent motion. This could be reflected by a 'frequency tagging' type response in the behavioural data. In other words, by manipulating the time window of coherent motion integration, each condition is optimal at different sampling frequencies of visual cortical substrate. This then, could manifest as a modulation in discrimination accuracy at those particular frequencies. We might speculate then, that the visual systems sampling frequency systematically adapts in order to optimally process the increase in the

number of displacing frames. Referred to as *Model 2* as illustrated in Figure 2.7. (*Right panel*). This idea can be likened to the "oscillatory selection" hypothesis (Schroeder & Lakatos, 2009) that proposes that the phase of cortical excitability represents a fundamental mechanism for tuning the brain to the temporal dynamics of task-relevant event patterns. It is noteworthy that these studies manipulate attention whereby entraining neocortical oscillations over longer periods of time then the RDK displacement frames used in the current paradigm (Besle et al., 2011). Alternatively, *Model 1*, (*Left panel*), if alpha frequency band is indeed the visual systems resonant sampling frequency, then behavioural periodicity should remain stable across all experimental conditions. Our data show that this is the case. There appears to be very little effect on increasing the length of the spatiotemporal integration window on behavioural performance. This suggests that while each condition covers increasing cycle lengths of the visual systems perceptual sampling frequency, behavioural performance cycles as measured by curve fitting procedures, revealed a consistent results across conditions at 4-10 Hz (theta-alpha) frequency irrespective of temporal integration window.
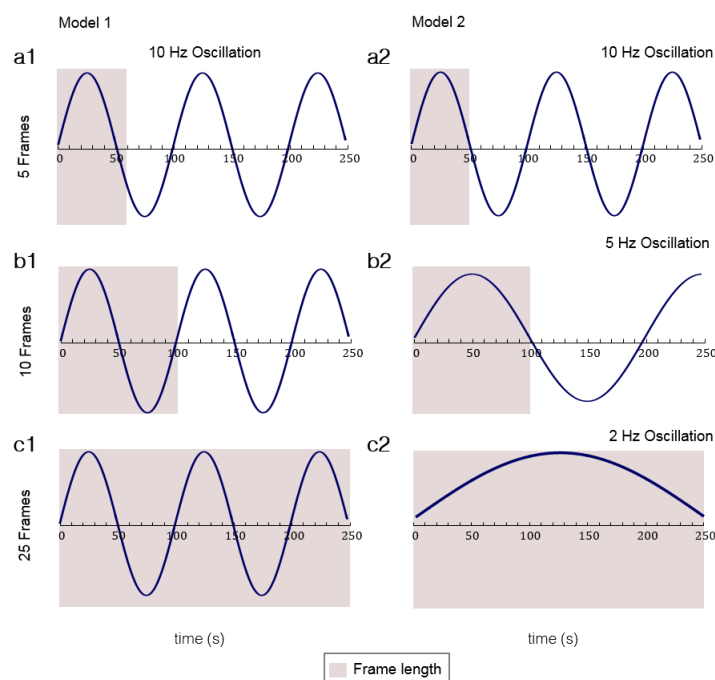
Figure 2.7. Modelling visual alpha sampling frequency. Schematic demonstrating the sampling of visual oscillations in two models, over the three experimental conditions. **a)** 5-frames, **b)** 10-frames condition, **c)** 25-frames condition. The left panel, model 1, shows a model where alpha-band (10 Hz) oscillations are the resonant sample frequency for visual perception. Whereas, the right panel, model 2 demonstrates the length of sampling frequency if visual oscillations adapted to the length of sequential processing stream. Shaded area demarcates the three experimental lengths of the coherent motion sequences. The blue sine waves represent the relative length of the visual oscillations sampled.

The notion that sensory evidence is integrated linearly and continuously is impacted by the capacity limits of perceptual information processing (Marois & Ivanoff, 2005), this bottleneck feature accounts for the refractory period in perception at a few hundreds of milliseconds during which relevant sensory information can be missed (Raymond, Shapiro, & Arnell, 1992). One prominent theory providing an explanation for this refractory period is that visual perception is constrained to sample incoming stimuli discretely in rhythmic frames (VanRullen & Koch, 2003). Whereby incoming sensory information is processed optimally at specifics phases within the sampling cycle of sensory visual oscillations (Busch & VanRullen, 2010). This rhythmic sampling framework proposes that slow cortical oscillations in theta-alpha can sub serve attentional selection by modulating rhythmically the gain of information processing, and often reported in primary sensory cortices (Lakatos, Karmos, Mehta, Ulbert, & Schroeder, 2008; Schroeder & Lakatos, 2009). The current findings show that not only are these slow frequencies reflected in the behavioural data, but also these seem to be independent on the length of the time windows of integration across the three experimental conditions. This suggests that evidence accumulation rate during decision-making exhibits a slow rhythmic fluctuations are critically dependent on the high excitability phase.

In this study it is important to note that individual subjects' threshold was keep constant across all conditions. In other words, the task would not be any easier with additional frames being presented in the 10- and 25-frames conditions, as each block was titrated accordingly. Performance accuracy was kept constant at approximately at 75% chance level. This meant that performance in each condition is attributed rather to the phase angle of visual reset oscillations and, if it were shown in these data, the number of frames in the RDK stimulus and not that of level of difficultly or ease across the conditions. This experiment therefore presents evidence consistent with the idea of periodic fluctuations in processing and perception. Although possible, it is not at present clear whether these periodic fluctuations necessarily form the limit of temporal resolution or represent a dedicated quantization of sensory input over time, as has been previously suggested (Varela et al., 1981).

Limitations and caveats

Several psychophysical studies using time-resolved behavioural measurements reveal rhythmic fluctuations (de Graaf et al., 2013; Diederich, Schomburg, & Colonius, 2012; Fiebelkorn, Foxe, & Butler, 2011; Landau & Fries, 2012; Song, Meng, Chen, Zhou, & Luo, 2014; VanRullen & Busch, 2011) directly in behavioural performances (behavioural oscillations). Here they reason that the underlying neural oscillations have direct consequences in behaviour. It is important to note, however, that due to the inherent temporal limitations of conventional psychophysical methods, the majority of studies assess fluctuations in perception at a much coarser temporal scale and therefore are limited in their capacity to use spectral analyses to measure oscillations in behavioural data (Theunissen & Doupe, 1998; Vanrullen & Dubois, 2011b). For example, cross-modal stimuli are typically presented using only a few

SOAs with temporal spacings of only a few increments (e.g. 30, 50, 65, 100 ms), or large intervals 50 – 100 ms (Fiebelkorn, Saalmann, & Kastner, 2013; Kayser, Petkov, & Logothetis, 2008; Mercier et al., 2013b; Romei et al., 2012; Thorne, Vos, & Viola, 2011). Consequently, predicted curve models are based on inter- or extrapolation (Thorne et al., 2011). Therefore, in principle, most psychophysical methods are somewhat restricted to the lower end of the frequency spectrum.

Inferences are often made on few repeating cycles of behavioural rhythms. However, it is not always possible to increase the sampling points in these paradigms. Increase the number of SOAs would require more trials, which would substantially increase the length of the experiment. By contrast, if more SOAs are added, but sampled with fewer trials, this would result in increased signal-to-noise ratio (SNR). Measuring neurophysiological reverent spectrotemporal dynamics in behavioural outcomes is gaining prominence. For example, Song et al. (2014) provided evidence for a rhythmic component in visual attention, which was cued to one of two possible locations. Using a reaction time (RT) task, participants had to detect a target stimulus as fast as possible following the spatial cue. Critically, the time between cue and target onset (SOA) was variable as in our study. Here the cue reset attentional sampling where the difficulty of target detection was not constant with respect to time, but was dependent or covaried with respect to SOA. They were able to characterise finer changes in the rhythmicity of attention using time-frequency analyses due to having a higher sampling rate. Further, they found that RT distribution oscillated in theta phase-locked to cue onset. These finding further corroborated those in a similar study by Landau and Fries (2012) that show an attentional sampling in the theta-band (3-4 Hz) that coupled changes in alpha-power (5-25 Hz), in-line with phase-amplitude coupling of neural oscillations.

In our data the temporal profile of behavioural performance does not capture repeating cycles of slow oscillations. Each condition captures approximately either one and a half cycles of theta-band and two cycles of alpha-band, the frequencies associated with posterior visual perception as discussed earlier. Commensurate with other psychophysical studies it is a known limitation that exists within the literature where inferences are made on few repeating behavioural rhythms. The current data were fitted using cosinusoidal models, it could be argued though that non-periodic model may also fit the data, one example being a quadratic function. Therefore, it could be argued that in the current paradigm we would need more repeating cycles in the d-prime data in order to confidently infer an accurate reflection of the underlying oscillations. Future experiments would address this limitation and capture longer rhythmic behavioural oscillations.

We consider it likely that the broadband cosinusoidal model fit to the d-prime data represent a variety of cognitive processes that are captured in the psychophysical signal. These fluctuations in performance are nested not only with primary sensory processing but encapsulate higher order

processing including, perceptual decision making, spatiotemporal integration of information over time and attention. In the current data set this can be seen as two frequency bands that constitute the d-prime data, which exemplifies a common caveat in behavioural paradigms, the difficulty discerning multiple frequencies which constitute a perceptual task. Perception is a multisensory process, where inputs are modulated by motor sampling strategies and routines (Schroeder & Wilson, 2010). Moreover, motor output is modulated by motor cortical oscillatory rhythms in delta (1-3 Hz), theta (5-7 Hz), alpha (8-12 Hz), and beta bands (13-30 Hz), the motor system's imposition on these rhythms on sensory inflow and outflow possibly contributes towards the behavioural data profile. For this reason, it is common practise in studies to carry out *post hoc* analyses to assess the correlates between recorded brain oscillations and behavioural data in order to support the notion for oscillations playing a key role in the gating of perception processing.

2.5 Conclusion

Our findings show manifestations of oscillations in behavioural performance at physiologically relevant rhythms as demonstrated in neurophysiological recordings. We suggest low frequency oscillations have a role in the spatiotemporal integration of information over time. We further add to the growing literature in support for the CMPR model. Taken together our findings demonstrate a behavioural proxy of the neuronal substrate. These results are consistent with the hypothesis that low-frequency band oscillations reflect fluctuations in cortical excitability in neural ensembles that periodically modulate perceptual processes.

Chapter 3

Auditory driven cross-modal phase reset of visual oscillations predicts visual motion perception

3.1 Introduction

Conventional investigations into the mechanisms of sensory perceptual processing have focused on activity within the primary sensory cortices as a function of their respective inputs. Multisensory stimulation paradigms have demonstrated that in addition to the preferred modality, extended cortical regions are modulated via cross-modal inputs related to nonpreferred modalities at the level of primary cortical areas (Kayser, Petkov, & Logothetis, 2008; Lakatos et al., 2009; Lakatos, Karmos, Mehta, Ulbert, & Schroeder, 2008) often referred to as cross-modal phase resetting (CMPR). Several lines of research suggest that transient auditory stimulation can modulate visual responses in the visual cortex, in doing so influencing early sensory-perceptual processing (Fort, Delpuech, Pernier, & Giard, 2002; Giard & Peronnet, 1999; Mercier et al., 2013b; Mishra & Martinez, 2007; Molholm, Ritter, & Murray, 2002; Naue et al., 2011; Raij et al., 2010; Romei, Gross, & Thut, 2012).

The first experiment sort to explored the behavioural signatures of multisensory interactions within the framework of cross-modal phase resetting. The data provide evidence which supports the mechanism for an auditory driven modulation of visual motion perception. This study investigated the sensory perceptual consequences from varying the lengths of apparent coherent motion sequence. The results revealed behavioural performance was modulated in low-frequency oscillations, and suggests a possible role for these neural rhythms in the integration of sensory information over time. Additionally, it was found that increasing the length of temporal integration windows did not significantly affect perception performance. This suggest that participants are able to integrate spatiotemporal information over windows with varying lengths of stimulation between 2 Hz and 10 Hz. Specifically, participants were able to perform the task consistently irrespective of condition, suggesting that evidence accumulation reaches an optimal level within only a few frames (at least 50 ms) of the coherent motion sequence. To this end, the current experiment explored the neural mechanisms that constitute the CMPR mechanism using an adaption of the previous experimental paradigm. In this study, we expand on the previous findings using MEG to further explore the underlying neural oscillatory systems involved. As discovered in the previous chapter, there was no effect elicited by manipulating the length of coherent motion, therefore, in the present study we used five frames integration window, as this would be sufficiently optimal to perform the task.

The current study

Several lines of research from animal and human EEG studies have provided complimentary evidence in support for the CMPR mechanism (e.g. Lakatos et al., 2007; Romei et al., 2012). Some with direct evidence, extending from animal studies, while others provide indirect measure using psychophysical measures. For example, there is an emerging body of research that shows behavioural oscillations in purely psychophysical data which are taken to represent the underlying neural systems involved in sensory perceptual processing (Benedetto & Spinelli, 2016; Diederich et al., 2012; Diederich et al., 2014; Fiebelkorn, Foxe, & Butler, 2011; Song, Meng, Chen, Zhou, & Luo, 2014). Most electrophysiological studies investigating the CMPR use brief, momentary stimuli, and focus either on the spatial domain (Eimer & Driver, 2000; Landau & Fries, 2012a) or detection of a single transient near-threshold stimulus (Fiebelkorn et al., 2011; Kayser et al., 2008; Naue, Rach, Strüber, & Huster, 2011; Romei, Gross, & Thut, 2012). While purely psychophysical studies probe the rhythmicity in perception at a much courser temporal scale and are restricted to measurements in the lower frequency spectrum. Moreover, contributing research using MEG neurophysiological recordings is sparse. To address this, we aimed to contribute new MEG neurophysiological and psychophysical evidence in support of cross-sensory interactions. To achieve this we used continuous dynamic visual stimulation that is spatio-temporally informative prior to target stimulation onset.

Instantaneous pre-stimulus oscillatory phase will be different on each successive repetition of trials of an experiment, where averaged performance across these trials will reveal no perceptual modulation (Vanrullen et al., 2011). In the present experiment, we circumvent this problem by consistently presenting a salient auditory stimulus at the start of each trial as a method used to avoid the unpredictability of in visual perceptual responses. To this end, a brief single tone can cause a transient phase reorganisation of visual oscillations and eliminate the uniform random distribution of oscillatory phase in the visual cortex. This in principle would lead to responses that are more predictable. The current experiment used the same paradigm as in the previous chapter. Although, in the present study we used five frames of apparent coherent motion only.

Hypotheses

We predict a replication of the behavioural performance as previously reported. Next, we hypothesised that if there were evidence for a cyclic modulation in sensory perceptual performance, this would be indexed by a cyclic modulation in ERF amplitudes time-locked to tone-onset. Further offering support for the notion of a cyclic modulation in cortical excitability that impacts on sensory perceptual performance. Finally, we predict a brain-behaviour correlation that suggest a neural correlate for the behavioural oscillations.

3.2 Methods

Participants

Twenty right-handed volunteers participated in the study (11 male, mean age 24.4 ± 5.3 years). All participants provided informed written consent and received a monetary compensation for their participation. Two participants were excluded for further analysis due to technical issues concerning behavioural threshold performance. None had been diagnosed with a hearing disability or had a history of significant neurological or psychiatric illness. Participants had normal to corrected-to-normal vision. Handedness was defined by the Annett Hand Preference Questionnaire (Annett, 1970). Experiments were approved by the local ethical committee (University of Glasgow, The College of Science and Engineering) and conducted in conformity with the declaration of Helsinki.

Design and procedure

Participants performed an apparent motion discrimination task. Using a three-alternative forced choice design procedure, participants were required to indicate the direction of apparent coherent motion (henceforth, motion) in a dot kinematogram stimulus. The target onset of motion was presented at near-threshold. The three possible motion conditions were; coherent clockwise-, coherent anticlockwise- and/or no coherent-motion (control) condition. For the purposes of simplicity, both coherent motion directions will henceforth be referred to as the motion condition (MC), since data from these were concatenated to form one condition, and the no-coherent motion condition (control) will be referred to the as no-motion condition (NMC). Responses were made with the right hand using a nonmagnetic response pad (Lumitouch). They were instructed to respond either by pressing with their right index finger (placed on right most key), middle finger (placed on middle key) and ring finger (placed on left most key) for coherent anticlockwise motion, no-coherent motion, and coherent clockwise motion responses respectively.

The experimental paradigm is illustrated in Figure 3.1. Each trial started with the presentation of a circular random dot kinematogram (RDK) around a central fixation point. Dots appeared as 'noise' flashing "on and off" with no coherent motion for a fixed jittered period (300-700 ms, intervals of 16.67 ms), after which a binaural tone was presented. The dots would then remain as no-coherent motion until one of 18 possible stimulus-onset-asynchrony (SOAs) time points (700-1033.34 ms, intervals of 16.67 ms), where a titrated percentage of dots either rotated in a clockwise- or anticlockwise manner for four monitor refresh frames or remained as no coherent motion (control). The experiment consisted of 8 blocks of approximately 6- 7 mins in length. The design was constructed in such a way that trials were continuous, where the next trial started immediately after the response. A block comprised 60 trials of each of the three apparent motion conditions: no motion, leftward motion, and

rightward motion (180 trials in total) presented in pseudorandomised order. For each apparent coherent motion condition all 18 SOAs were repeated three times. In the remaining 6 trials (a total of 18 across the conditions, i.e. 10%) a no-tone catch trial was presented. These catch trials were used as a control condition.

Stimuli

Stimuli were presented through a DLP projector (PT-D7700e-K, Panasonic®) placed outside the shielded room onto a screen situated 1.90 m away from the participant via an in-room mirror. Stimuli were generated off-line using Matlab 2013.b (The MathWorks®) and controlled using routines from Psychophysics toolbox (Brainard, 1997). Sound stimuli were delivered binaurally via a sound pressure transducer through two 5 m long plastic tubes terminating in plastic insert earpieces. Sound stimuli levels were calibrated using a condenser using microphone and sound level meter. Sounds were presented at a self-adjusted comfortable level of approximately 65 dB SPL.

For detailed description of the RDK stimulus see **Chapter 2** (see Chapter 2, Methods Section, Stimuli).
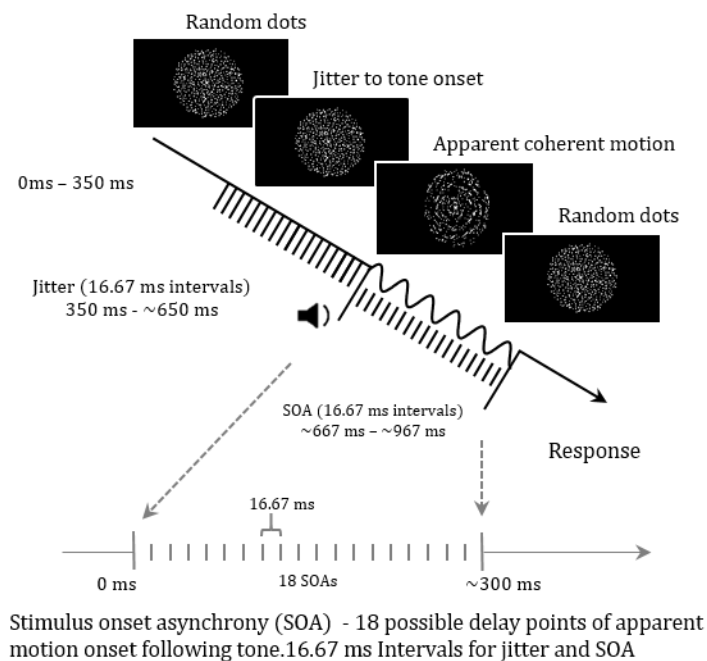
Figure 3.1. Experimental design. Random dots will be presented on the screen for a minimum of 300ms, after which will remain for a jittered period until the binaural presentation of a tone. The jitter period between 300 to 700 ms to tone onset. Following the tone-onset the random dots will rotate either clockwise anticlockwise or remain as random dots (no move condition) and this will take place at one of 18 SOAs time-locked to the auditory stimulus. The SOAs are at intervals of 16.67 ms according to the 60 Hz refresh rate.

3.2.1   Behavioural Data

The behavioural analyses pipeline is identical to that in **Chapter 2** (see Chapter 2 Methods Section).

3.2.2   MEG Analyses

Data acquisition

Neural activity was recorded continuously during each block from participants in a comfortable sitting position using a 4D Neuroimaging Magnes® 3600 WH system (Neuroimaging Inc., San Diego) with 248 magnetometers in a magnetically shielded room. The acquisition sample rate was 1017 Hz. The MEG signal was high pass filtered at 0.1 Hz and digitised at 508 Hz. Data from three bad channels were excluded from the data. Participants were asked to remain as still as possible and were continuously monitored by video camera. They were also instructed to minimize blinking during the presentation of visual stimuli, and instead to synchronize their blinks with the simultaneous button press for selecting responses. Eye movements were monitored using a SR-research remote Eyelink system (FL-890, SR Research Ltd.). Calibration of eye fixation was performed at the beginning of each run using a 9-point fixation procedure.

Data analysis of the MEG signal was performed using the FieldTrip software package (Oostenveld & Fries, 2010); see http://fieldtrip.fcdonders.nl/) and in-house Matlab code.

Preprocessing

The preprocessing of the MEG signal was performed using the following procedures. First, the signal was epoched in trials of 3.5 s in length time-locked to the tone onset (1 s pre-stimulus). Each trial was assign to a different condition based on SOA delay time points (forming 18 conditions). Trials were further split into tone trials and no-tone trails including coherent motion and no-coherent motion. Secondly, before visually inspecting MEG traces for artefacts, the DC offset and linear trends were removed to facilitate visualisation. Four excessively noisy sensors were discarded from all subjects' analysis. Additionally, trials contaminated with physiological (eye blinks, eye movements) or non-physiological (squid jumps) were discarded. Thirdly, signals recorded from by the MEG reference channels were used to linearly remove electromagnetic interference from outside the scanner, implemented using the "ft_denoise_pca" function in FieldTrip (Johnson, Hirschkoff, & Buchanan, 2003) and post-acquisition, data were DC offset to ensure a zero mean signal on all sensors. Finally, trials containing large signal variance which corresponded to cardiac artefacts were projected out of the MEG signal using Independent Component Analyses ("fastica" algorithm implemented in FieldTrip).

Sensor-level analysis

Before calculating the event-related averaging, preprocessed data were bandpass filtered in the range of 1–30 Hz. Event-related fields (ERFs) were baseline corrected to the 500 ms period immediately preceding the stimulus onset for each condition (tone and no-tone). Subsequently, the ERFs were realigned in time according either to tone onset or to coherent apparent motion onset while retaining the baseline intervals time-locked to the stimulus onset for each condition (Figure 3.2). To avoid differences in the noise when comparing unequal number of trials from different conditions, these were matched by randomly selecting a subsample of trials from the more numerous condition to equate trial numbers across them.
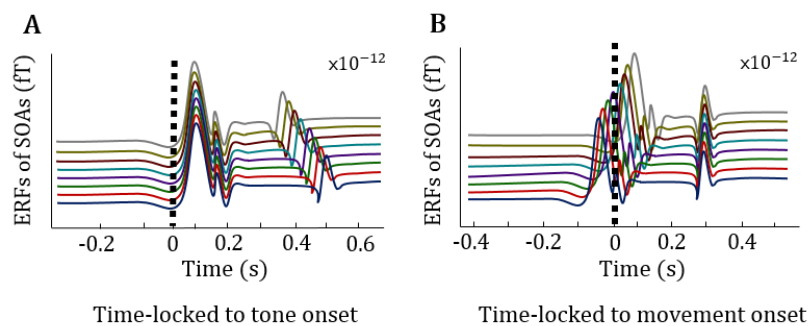
Figure 3.2. Schematic of realigned ERFs. Data were analysed in time according to either, A) timelocked to tone-onset or, B) timelocked to coherent movement-onset. For illustrative purposes, only eight simulated ERFs are shown to represent the 18 different SOAs.

From the fields measured by the magnetometers, the approximation of the MEG planar gradient was computed using Fieldtrip's *ft_megplanar* function. Considering planar gradient data simplifies the interpretation of the sensor-level results, as the maximal signals are located above neural sources (Bastiaansen & Knösche, 2000; Hari, Salmelin, & Makela, 1997). For the ERFs, the combined resulting horizontal and vertical planar gradients were calculated by singular value decomposition per channel location using the fields from the sensors and both first- and second-order neighbouring sensors (maximum distance of 7.4 cm) and using the "sincos" approach implemented in Fieldtrip. This projected the data along the largest magnitude direction above a given source (Hämäläinen, Hari, & Ilmoniemi, 1993). For the spectral analyses, we computed metrics separately for the horizontal and vertical planar gradients, and combined the two by computing the sum.

ERF analysis

All non-rejected trials were sorted according to the respective conditions; coherent-motion (coherent clockwise-, coherent anticlockwise-motion) and no coherent-motion conditions; tone and

no-tone conditions, and finally data were further divided into correct and incorrect trials based on behavioural response classification. The ERFs elicited for each stimulus category were then computed separately for each participant and averaged in the time range between -300 ms and 300ms, and subsequently, the grand-average across all participants.

Identification of auditory and visual activation

Loci of auditory and visual evoked activation were defined statistically by comparing the difference of between coherent-motion and no-coherent-motion conditions using nonparametric cluster-based permutation *t*-tests (Maris & Oostenveld, 2007). This randomisation testing uses a cluster-based threshold correction method to control for the type I error rate in the context of multiple comparisons. This achieved by identifying clustering neighbours that show significant differences over sensors, time, and/or frequency rather than performing separate tests on each sensor, sample frequency pair. Here, data was selected where the difference between the two conditions whose sensor- time-pairs *t*-statistics exceeded the critical *p*-value of 0.025% for two-sided testing.

The selected sensor- time-pairs were then grouped into clusters wherein each cluster, the sensor-time-pairs form an arrangement that is connected spatially and temporally. Such that, if the sensor-time-pair *t*-statistics exceeded the statistical threshold were neighbouring spatially and temporally, then these sensor- time-pairs were grouped together as a cluster. Next, each cluster was assigned a cluster-level statistic, calculated by the sum of the sensor- time-specific statistics. That is, the cluster-level statistic is contingent on the size of the cluster and the magnitude of the sensor- time-specific *t*-statistics with in that cluster. To control for the Type-I error rate across all spatiotemporal data, the cluster-level statistics were evaluated under the randomisation null distribution of the maximum cluster-statistic. Therefore, using only the maximum cluster-level statistic as the test statistic, allows the control of the Type-I error rate rather than multiple tests for every sensor- time-pair. The permutation distribution was approximated by randomising the order of the coherent-motion and no-coherent-motion conditions within every participant. Finally, by creating a reference distribution from 1000 random draws, the *p*-values were estimated by the proportion from this randomisation null distribution in which maximum cluster-level test statistic exceeded the observed maximum cluster-level test statistic. This proportion of estimation is statistically known as the Monte Carlo *p*-value. Here, the Monte Carlo *p*-value provides an accurate estimation of the true *p*-value where a one-sided randomisation test was performed. The results of these statistics would allow the demarcation of significant sensor-clusters to be used as regions of interest (ROI) for further analyses.

Cyclic modulation in ERF components

To assess evidence for a cyclic modulation in the ERF components as a function of SOA, spectral analysis was performed. This test determined if there are periodic fluctuations evident in the ERF amplitude values across each stimulus delay phase-locked to apparent motion onset. Figure 10b shows the critical time-window demarcated in red, this marks the period of spectral-decomposition computed across the 18 SOAs. These were carried out in Matlab using custom programming code established on standard mathematical and signal analysis functions. It is important to note that for this analysis spectra were computed not across time but across SOA – so across the 18 evoked responses and for each participant independently. At each latency relative to the motion onset the 18 data points (from the 18 SOA conditions) were multiplied with a Hamming window and padded with zeros to a total length of 64 data points. FFT was applied and the power spectrum was computed as the square of absolute values of the complex spectrum. The frequencies of interest were integer values between 1 and 33 Hz. The time steps of interest were from -500 ms to 500 ms in 1 ms steps (for illustrative purposes only 200 ms to 400 ms and frequencies between 1 and 20 Hz are shown). The power spectrum at each latency expresses how much periodicity is visible in the SOAs. To quantify statistical significance, the time-frequency results of the power spectra between the motion conditions was subjected to nonparametric cluster-based permutation test procedure, as described in more detail in the previous section Pre-stimulus phase difference

Pre-stimulus phase

Phase-locking value was measured separately for each condition grouped into correct and incorrect trials. Because trial numbers are known to influence phase measures crucially (Hanslmayr et al., 2013), trial numbers were equated across the two conditions with the lowest number of trials per SOA and randomly selecting the same number of trials from the remaining condition. To exclude potential effects due to a specific trial selection, we performed trial selection by means of random subsampling 2000 times. We compute spectro-temporal decompositions of single trials by a applying a multi-taper convolution method with a Hanning window of half the wavelength of the frequency investigated. The frequencies of interest were integer values between 1 and 20 Hz. The time steps of interest were from -0.5 to 0.5 s in 0.1 ms steps. For each participants', trial r, frequency f, and time point t, we normalized the complex Fourier spectrum $F_{s,r,f,t}$ of the DFT by dividing it by its absolute (abs) value, thus normalizing the signal by its amplitude:

$$F_{s,r,f,t}^{nrom} = \frac{F_{s,r,f,t}}{abs(F_{s,r,f,t})}$$

From these normalised values, the normalised phase was calculated for each participant s, trial r, frequency f, and time point t:

$$\phi_{s,r,f,t}^{norm} = a \tan\left(\frac{Im\ (F_{s,r,f,t}^{norm})}{Re\ (F_{s,r,f,t}^{norm})}\right)$$

Where Im and Re are the imaginary and real part, respectively, of the DFT.

To analyse statistically whether the prestimulus phase angles differed between correct and incorrect trials, the phase of these two sets of trial groups for each time-frequency element at the within-subject level by means of the circular Watson-Williams test. The Watson-Williams two- or multi-sample test is a circular analogue of the two-sample t-test or the one-factor analysis of variance (ANOVA) in the linear scale (Fisher, 1995). This test defines whether the mean direction of two or more groups are identical or not. The Watson-Williams test assumes the von Mises distribution, which ranges from $-\pi$ to $+\pi$ on the unit circle. The concentration parameter k of the von Mises distribution (circular analogue of the normal distribution) describes the spread of the data, Such that, a higher value of k corresponds to a narrower concentration about the circular mean. Circular statistics were computed using MATLAB 2013a (MathWorks, Natick, MA) and CircStat Version 2012a (Berens, 2009). The concentration parameter has been proven to be robust against deviations from these assumptions (Berens, 2009). Results are reported as circular mean ± circular SD. This function implements the procedure described by Zar (1999).

To assess the consistency of phase angle differences over subjects, we performed a nonparametric randomization test identifying clusters in time-frequency space demonstrating a similarly directed phase angle difference relative to a null distribution (see methods above). The null hypothesis is that the phases are randomly distributed and uniformly distributed, showing no difference between the correct and incorrect trials. That is, for each participant, we assigned to each trial group random phases (equating the number of trials for each participant) and then repeated the above-mentioned statistical analysis. Next, a comparison (random) of phase angles between both trial groups for each time-frequency element at the within-subject level was analysed by applying the Watson–Williams test. This procedure was repeated 2000 times (each time with new, randomly chosen phases), resulting in 2000 F-values for each time-frequency element. Subsequently, we used the median of all 2000 F-values for each time-frequency element, resulting in a time-channel map of F-values for each participant, which constitutes the null distribution. We then statistically compared the F-values of the test distribution with the F-values of the null distribution for each time-frequency element by means of a dependent-samples t-test, resulting in a time-frequency map of t-values. Positive t-values for a specific time-frequency element demonstrate a larger phase angle difference compared with randomly distributed phase angles, and vice versa for negative t-values. To investigate whether the phase angle

differences between perceptual conditions were significantly different from randomly distributed phases, we applied a cluster-based randomization approach (described in detail above).

Correlation analyses

To establish the relationship between the spectral profile of the behavioural performance data (*d'* fitting) and the evoked response profile of MEG fluctuations in ERF amplitude values as a function of SOA, we performed a Spearman's correlation. First, in the behavioural data, single subject detection *d'* (DP-DT-1) temporal profile were subjected to a Jackknife resampling method to accurately estimate the optimal fitting cosine models at each frequency. The details of the Jacknife procedure are described in **Chapter 2.** A Spearman's rank correlation was performed on both behavioural and MEG spectrums. To correct for multiple comparisons the false discovery rate (FDR) procedure was applied (Matlab function fdr_bh.m) (Benjamini & Hochberg, 1995; Benjamini & Yekutieli, 2001). Significance level of correlation coefficients were set at 0.01. A further clustering threshold was set of a minimum of five consecutive data points that were required to survive clustering threshold for final significance. This was computed, as FDR correction does not consider spurious clustering of data points.

3.3 Results

Behavioural performance

The aim of the experiment was to investigate the effect of cross-modal phase resetting (CMPR) on sensory perceptual performance. To investigate the temporal profile of visual perceptual performance over varying delays, a curve fitting procedure was applied to *d'* accuracy scores. This was used to test for a cyclic modulation in behavioural performance. We tested three different *d*-prime measures based on different signal detection criteria for those trials considered to be Hits Rates (HR) and False Alarms (FA). The first, *d*-prime detection 1 (DP-DT-1), HRs were based on correctly detecting the direction of coherent motion and no-coherent motion, where FAs were based simply on those trials where participants did not accurately detect the direction of motion and did not incorporate performance accuracy on the no-coherent motion trials. Second, *d*-prime detection 2 (DP-DT-2), the same criteria as above, but FAs considers performance on no-coherent motion trials. Finally, *d*-prime discrimination (DP-DS) is based only on those trials where there was coherent motion. HR criteria are based on trials where the correct discrimination in the direction of coherent motion was selected, where FAs consisted of the opposite, not accurately discriminating direction. It is important to note when considering discrimination, this measure is based on fewer trials, and therefore this inherently suffers from higher signal-to-noise (SNR) ratio.

Table 1. DP-DT-1 descriptive statistics. Hit rates (HIT), false alarm rates (FA) and bias criterion (c)

SOA	HIT % (S.E.M.)	FA % (S.E.M.)	c (S.E.M.)
16.67 ms	77 (± 1.03)	7 (± 0.84)	0.35 (± 0.03)
33.34 ms	78 (± 1.02)	7 (± 0.87)	0.37 (± 0.03)
50.01 ms	80 (± 1.01)	7 (± 0.85)	0.32 (± 0.03)
66.68 ms	79 (± 0.89)	8 (± 0.87)	0.31 (± 0.03)
83.35 ms	81 (± 0.99)	6 (± 0.75)	0.33 (± 0.03)
100.02 ms	80 (± 0.91)	7 (± 0.78)	0.32 (± 0.03)
116.69 ms	80 (± 1.26)	9 (± 1.13)	0.23 (± 0.03)
133.36 ms	78 (± 1.02)	10 (± 1.16)	0.26 (± 0.03)
150.03 ms	79 (± 1.36)	9 (± 1.15)	0.26 (± 0.03)
166.70 ms	79 (± 1.24)	9 (± 1.15)	0.26 (± 0.02)
183.37 ms	79 (± 1.28)	9 (± 1.09)	0.27 (± 0.03)
200.04 ms	76 (± 1.72)	11 (± 1.37)	0.26 (± 0.02)
216.71 ms	80 (± 1.4)	7 (± 0.74)	0.31 (± 0.02)
233.38 ms	80 (± 1.46)	6 (± 0.89)	0.35 (± 0.03)
250.05 ms	78 (± 1.57)	7 (± 0.95)	0.35 (± 0.03)
266.72 ms	77 (± 1.64)	7 (± 1.1)	0.39 (± 0.03)
283.39 ms	73 (± 1.32)	7 (± 1.03)	0.44 (± 0.04)
300.06 ms	74 (± 1.26)	7 (± 0.78)	0.43 (± 0.04)

Cells contain the mean and standard error of the mean (S.E.M.) averaged across participants. Trials time-locked to tone onset.

Table 2. DP-DT-2 descriptive statistics. Hit rates (HIT), false alarm rates (FA) and bias criterion (c)

SOA	HIT % (S.E.M.)	FA % (S.E.M.)	c (S.E.M.)
16.67 ms	79 (± 0.95)	17 (± 1.11)	0.07 (± 0.01)
33.34 ms	80 (± 0.89)	15 (± 1.08)	0.08 (± 0.02)
50.01 ms	82 (± 0.91)	15 (± 0.92)	0.05 (± 0.01)
66.68 ms	81 (± 0.87)	16 (± 0.89)	0.06 (± 0.01)
83.35 ms	84 (± 0.77)	13 (± 0.85)	0.05 (± 0.01)
100.02 ms	83 (± 0.68)	14 (± 0.87)	0.04 (± 0.01)
116.69 ms	82 (± 1.07)	15 (± 1.19)	0.07 (± 0.02)
133.36 ms	80 (± 1.05)	16 (± 1.08)	0.05 (± 0.01)
150.03 ms	81 (± 1.19)	15 (± 1.18)	0.05 (± 0.01)
166.70 ms	81 (± 1.21)	16 (± 1.19)	0.04 (± 0.01)
183.37 ms	82 (± 1.13)	15 (± 0.92)	0.03 (± 0)
200.04 ms	78 (± 1.49)	18 (± 1.4)	0.04 (± 0.01)
216.71 ms	82 (± 1.19)	14 (± 0.96)	0.05 (± 0.01)
233.38 ms	82 (± 1.24)	14 (± 1.18)	0.05 (± 0.01)
250.05 ms	81 (± 1.47)	16 (± 1.33)	0.04 (± 0.01)
266.72 ms	80 (± 1.47)	17 (± 1.37)	0.03 (± 0.01)
283.39 ms	76 (± 1.24)	21 (± 1.24)	0.04 (± 0.01)
300.06 ms	77 (± 1.11)	20 (± 1.12)	0.03 (± 0)

Cells contain the mean and standard error of the mean (S.E.M.) averaged across participants. Trials time-locked to tone onset.

Table 3. DP-DS descriptive statistics. Hit rates (HIT), false alarm rates (FA) and bias criterion (c)

SOA	HIT % (S.E.M.)	FA % (S.E.M.)	c (S.E.M.)
16.67 ms	56 (± 1.01)	1 (± 0.23)	0.99 (± 0.02)
33.34 ms	56 (± 1.23)	2 (± 0.31)	0.93 (± 0.02)
50.01 ms	58 (± 1.11)	2 (± 0.22)	0.94 (± 0.02)
66.68 ms	57 (± 0.96)	2 (± 0.32)	0.93 (± 0.02)
83.35 ms	59 (± 1.17)	2 (± 0.42)	0.87 (± 0.02)
100.02 ms	58 (± 0.9)	2 (± 0.39)	0.88 (± 0.02)
116.69 ms	51 (± 1.14)	1 (± 0.33)	1.05 (± 0.02)
133.36 ms	50 (± 0.88)	2 (± 0.47)	1.03 (± 0.03)
150.03 ms	50 (± 1.03)	2 (± 0.39)	1.01 (± 0.02)
166.70 ms	50 (± 0.9)	2 (± 0.35)	1.04 (± 0.02)
183.37 ms	49 (± 1.12)	2 (± 0.58)	1.01 (± 0.03)
200.04 ms	48 (± 1.14)	2 (± 0.38)	1.07 (± 0.02)
216.71 ms	58 (± 1.28)	2 (± 0.43)	0.9 (± 0.03)
233.38 ms	57 (± 1.44)	3 (± 0.4)	0.88 (± 0.02)
250.05 ms	57 (± 1.46)	2 (± 0.3)	0.89 (± 0.02)
266.72 ms	55 (± 1.41)	2 (± 0.43)	0.92 (± 0.03)
283.39 ms	51 (± 1.44)	3 (± 0.43)	0.95 (± 0.03)
300.06 ms	52 (± 1.46)	2 (± 0.38)	0.95 (± 0.02)

Cells contain the mean and standard error of the mean (S.E.M.) averaged across participants. Trials time-locked to tone onset.

Table 4. Grand average. Hit rates (HIT, percentage correct), false alarm rates (FA, percentage) and d' (c, bias response) for each SOA

	HIT % (S.E.M.)	d' (c)	FA % (S.E.M.)
5-Frames	73.3(2.28)	2.39(0.5)	7.05(1.28)
10-Frames	79.76(2.5)	2.71(0.41)	6.0(1.18)
25-Frames	74.83(2.78)	2.44(0.49)	6.91(1.39)

Cells contain the mean and standard error of the mean (S.E.M.) averaged across participants for Hit and FA. Trials time-locked to tone onset.

Table 1-3 displays the Hit Rate, False Alarm, and Response Bias(c) for each SOA across the conditions. A non-parametric contrast (Wilcoxon signed ranks test) between the mean values of c against zero (no response bias) revealed that these were significantly greater than zero for all conditions (DP-DT-1: $Z = -3.725, p < 0.05$; DP-DT-1: $Z = -3.724, p < 0.05$; and DP-DS: $Z = -3.724, p < 0.05$). This indicates that participants were biased to respond that there was coherent motion; however, this bias was the same direction across all conditions indicating that d' scores were not confounded by a difference in response bias. Table 4 shows the results of average apparent motion discrimination accuracy (hit rate and d prime) for each experimental condition. These data indicate that all subjects, including those with high false alarm rates, were nonetheless able to differentiate apparent motion in the three forced choice task.

Table 1 shows the results of average apparent motion discrimination accuracy (hit rate and d-prime) for each d-prime condition. These data indicate that all subjects, including those with high false alarm rates, were nonetheless able to differentiate apparent motion in the three-alternative forced choice. In all three experimental conditions a repeated-measures analyses of variance (RM-ANOVA) was implemented to assess the variability of apparent motion discrimination accuracy (d') across the 18 SOAs as a function over time phase locked to tone onset. Three RM-ANOVA were performed for the three d-primes with factors SOA (18-factors) across subjects (19) there was a significant main effects of SOA for the DP-DT-1 ($F_{17,306} = 2.80$, $p < 0.001, \eta_p^2 = 0.13$), and DP-DT-2 ($F_{17,306} = 4.06$, $p < 0.001, \eta_p^2 = 0.18$), but there was no significant main effect for the DP-DS ($F_{17,306} = 1.35$, $p > 0.05, ns, \eta_p^2 = 0.07$).

Figure 3.4 shows box plots of the d' performance and reaction times (RT) for each subject across the conditions. This enabled visual inspection of the data to identify outliers and determine which data sets to exclude for further analyses. Participants were excluded if the average d' performance was consistently below or above the peri-threshold level set between 65% and 80% accuracy. Based on these criteria subject eighteen was excluded for having consistently low accuracy scores and slow RTs. Individual trials with reaction times outside the specified criterion of 200 and 1400 ms were excluded.
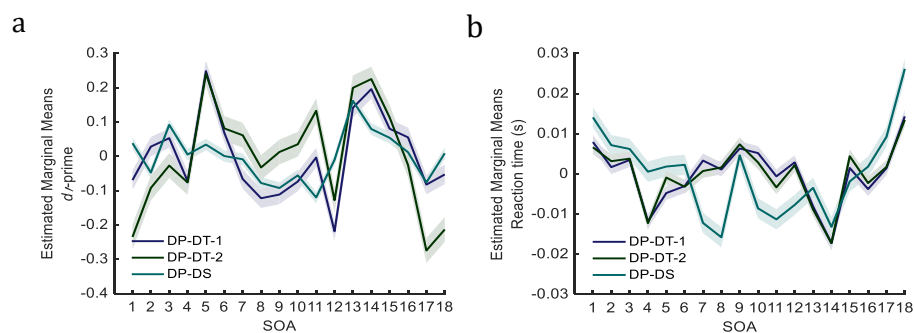
Figure 3.3. Average d' as a function of SOA. Line plots illustrating estimated marginal means at the group-level performance across SOAs. **a)** Accuracy expressed as d' scores SEM = 0.002, SEM = 0.001, SEM = 0.003, respectively and **b)** reaction times. Solid lines show the data where shading demarcates standard error. Standard error for reaction times SEM = 0.039, SEM = 0.035, SEM = 0.039, respectively.
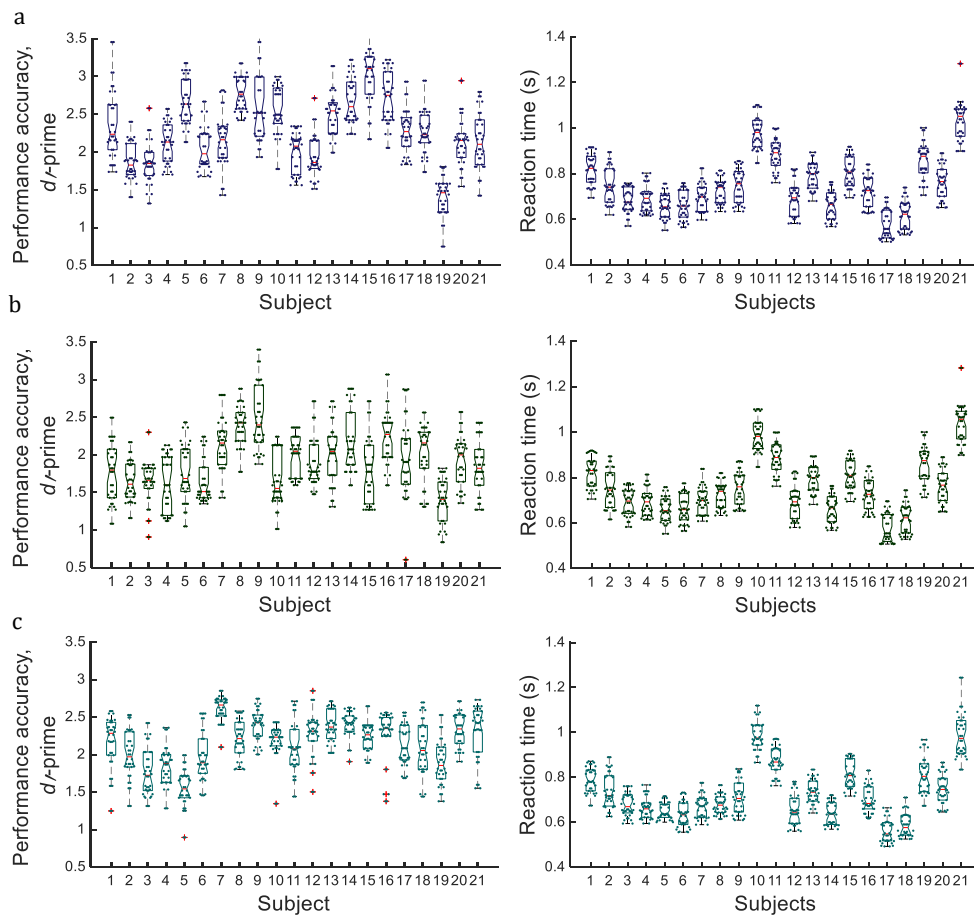
Figure 3.4. Descriptive Statistics. Box plots illustrating the individual subject performance data. Left panel represents the d' accuracy discrimination and detection. Right panel represents ration time (RT) data. a) DP-DT-1, b) DP-DT-2, c) DP-DS. Lines in boxes represent medians, the box ends at the 25th and 75th percentiles, whiskers 10th/90th percentiles. Individual SOA data are superimposed dots for each subject. Outliers (>1.5 times the interquartile distance) are plotted with crosses.

Periodicity in perceptual performance

To investigate the effects of the varying onset of the target stimulus presentation (coherent motion) over the 18 SOAs time-locked to tone-onset, a curve fitting function was applied to data. This test determined if there are periodic fluctuations evident in d' discrimination accuracy as a function over time relative to tone onset. To assess significance of the model fit and the presence of periodicity, a bootstrapping statistical approach were combined with the cosinusoidal model fitting procedures. Critically, this procedure tests the existence of a significant cyclic modulation in sensory perceptual performance, where the periodic fluctuations observed in the data could be attributed to stimulus-locked oscillatory activity. The results revealed a significantly modelled cosine function for all three conditions. Figure 3.5 illustrates the time-course of visual task performance timelocked to tone onset for all three conditions (after linear detrending), with best-fitting cosine models superimposed in red.
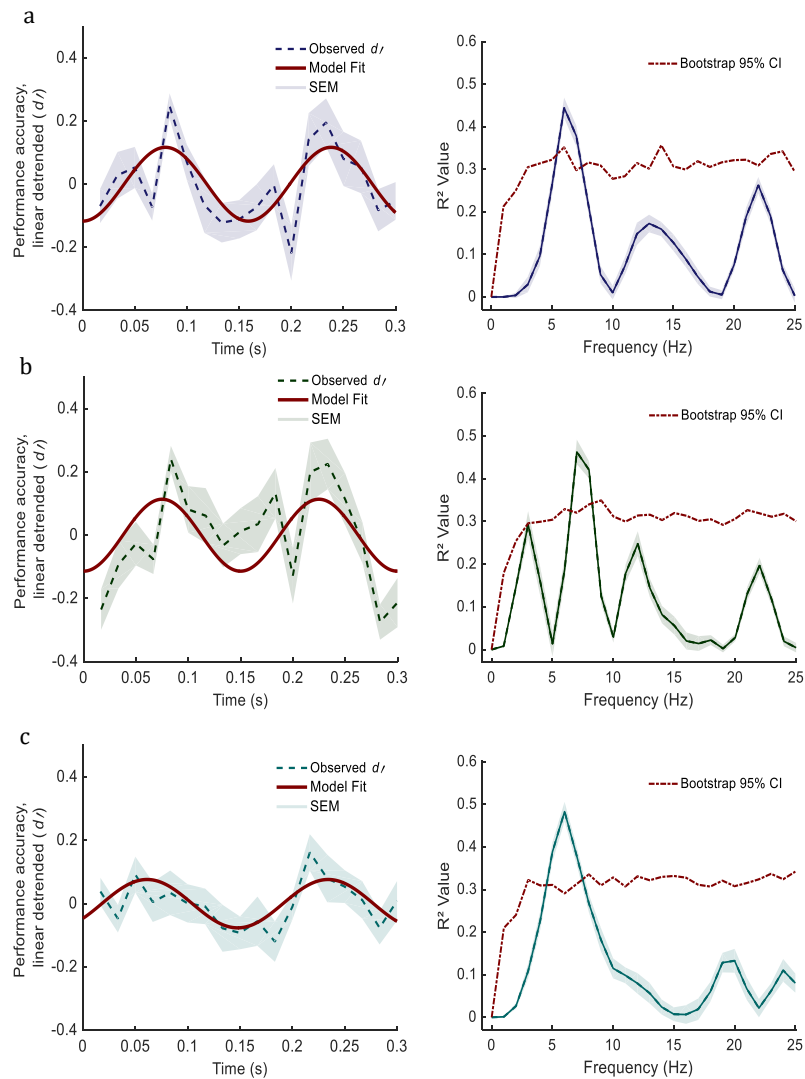
Figure 3.5. Group Avg. Cosine Functions. *Left panel* shows cosine model fits (red sloid line) superimposed on d' data (dotted line). *Right panel* shows the bootstrapping significance r-square model fits. **a)** DP-DT-1, **b)** DP-DT-2, **c)** DP-DS conditions respectively. Group average d' accuracy (linearly detrended) for apparent motion discrimination for all conditions over 2 cycles post-tone onset. The best fitting cosine model superimposed in red. **a)** 6 Hz (r2 = 0.45), **b)** 7 Hz (r2 = 0.46), **c)** 6 Hz (r2 = 0.48), show the optimal significant cosine functions. Shaded area represent standard error of the mean (SEM) after the removal of baseline between subject variance (within-subject error bars (Cousineau, 2005).

statistics. The DP-DT-1 revealed a best fitting cosine model at 6 Hz (r^2 = 0.45) with a range of significant frequencies between 6-7 Hz (95% CI). DP-DT-2 revealed a best fitting cosine model was 7 Hz (r^2 = 0.46) with a range of significant frequencies between 7-8 Hz (95% CI). Finally, the DP-DS, the best significant model fit was 6 Hz (r^2 = 0.48) with a range of significant frequencies between 5-7 Hz (95% CI). These data statistically confirm the presence of a cyclic modulation in visual task performance at group level. Single subject data not shown here, yield similar results.

Power Spectral Density estimate

In order to further assess the existence of periodicity in sensory perceptual performance as evidence of CMPR, the *d'* data were transformed into their frequency-domain representations (see Methods). The short-time FFT method (MATLAB, *spectrum.welch* method) was used to compare the frequency content in the data. Figure 3.6.b illustrates the power spectrum density (PSD) computed on the group average spectrum and ranges from 1-33 Hz. This method uses a standard Fourier transform of the data. For all three *d*-primes the power peaks around the 7-12 Hz frequency band for the grand averaged group data. There is a clear peak in the DP-DT-1 at 8 Hz, whereas for DP-DT-2 there is a peak at 9 Hz and DP-DS a peak at 9 Hz. All three *d*-primes show peaks at higher frequencies between 23-25 Hz, although with lower power than the first peak. Here the frequency spectrum of noise in the data is uniform, where any significant peaks would provide evidence for a consistent periodic component.
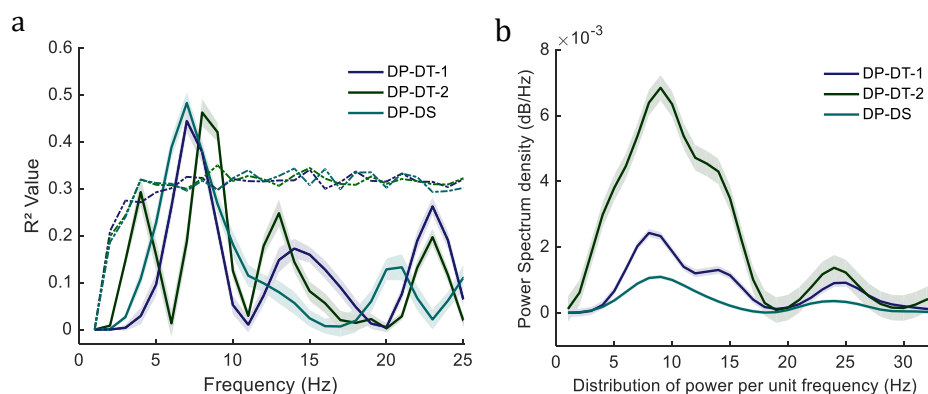
Figure 3.6. Power spectral density and R-square fit. a) R^2 values for cosine model fitting across frequencies. Three conditions superimposed. Peak fitting frequencies at 5-10 Hz. Solid lines indicate the 95% confidence interval bootstrapped permutation. **b)** Using standard short-time Fourier transform, power spectrum of d-prime temporal profile. All the conditions show clear peaks at 6-8 Hz frequency. The 10- and 25-frame conditions show peaks at 24 Hz where the 5-frames conditions shows a strong peak at a 15 Hz frequency.
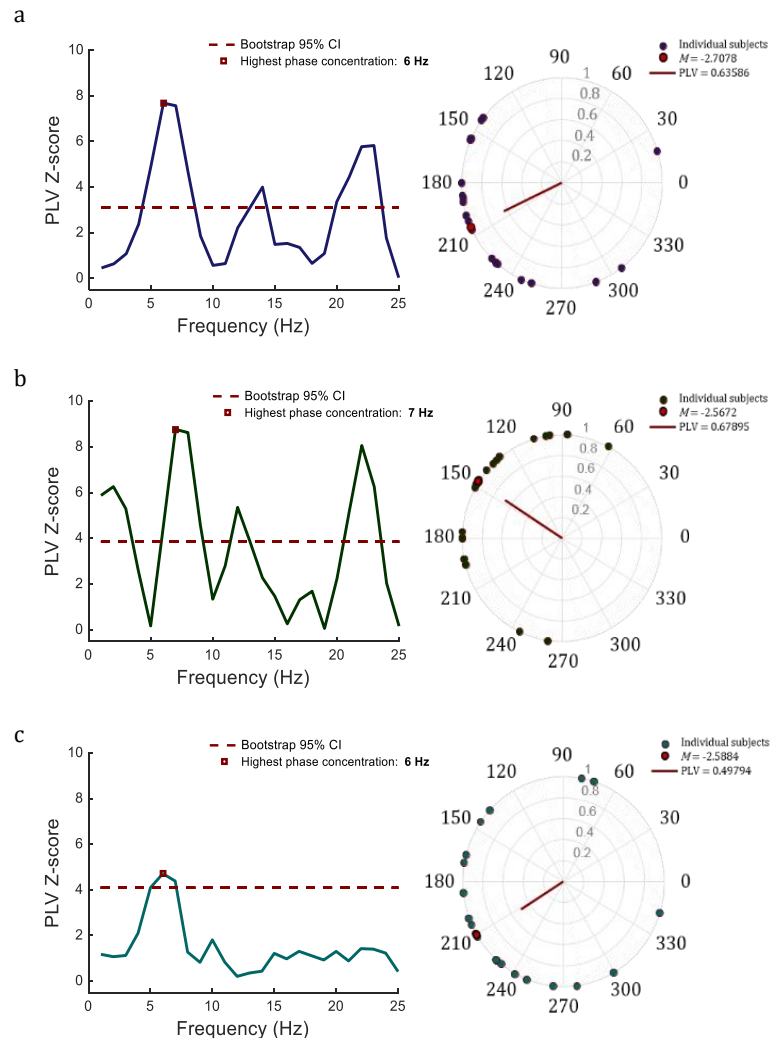
Figure 3.7. Phase concentration. *Left panel;* Rayleigh's Z-scores across subjects on d' cosinusoidal model fits as a function of frequency. Red squares indicate the highest phase concentration. Horizontal red dotted line indicated the 95% confidence interval cut-off (z-score = 3.8) ***Right panel;*** Circular plot representing the highest phase concentration frequency, with individual participants' phase angle values on the circumference of the unit circle (theta phase in degrees). Red dot and line represents the mean and resultant vector length respectively for the phase coherence of d' across participants. The vector length here measures the consistency of phase locking around the mean angle (M), with 0 being random and 1 being zero variance. The vector direction indicates the preferred phase of visual task performance (d'), and length indicates magnitude of phase resetting, the mean resultant (PLV). Peak PLVs reported here; **a)** DP-DT-1, z-score = 6 Hz, PLV = .6 (M = -2.7), **b)** DP-DT-1, Z-score = 7 Hz, PLV = .7 (M = .3), **c)** DP-DS, z-score = 6 Hz, PLV = .5 (M = -2.6).

Oscillatory phase concentration

Across all *d*-primes, there is significant evidence for a phase modulation in visual perceptual performance following tone-onset. The magnitude of phase locking was measured using the mean resultant vector length (MRVL) on a unit circle (figure 3.7, *right panel*), a measure of circular phase concentration derived from the Rayleigh's test for circular uniformity. By this measure, CMPR was determined using phase-locking analyses of the *d*-prime data, time-locked to tone onset as a function over time across SOAs. Here, the data show that ongoing low frequency visual oscillations are reset in all the conditions. A Rayleigh's Z-statistic were assigned to each frequency band (1-33 Hz). This test confirmed statistically significant nonuniformity ($p < 0.05$) in the phase distribution in across all three *d*-primes. The optimal phase concentration DP-DT-1 was 6 Hz with a MRVL = .63 (*z*-score range = .46 – 7.69), DP-DT-2 with 7 Hz, MRVL = .68 (*z*-score range = .26 – 8.76). In the discrimination *d*-prime the optimal phase was 6 Hz with a MRVL = .48 (*z*-score range = .36 – 4.71). Phase locking analyses revealed similar results between both detection *d*-primes, whereas with discrimination, phase locking was weaker and at 6 Hz. These data provide consistent supporting evidence for CMPR across all three *d*-primes.

3.4   MEG sensor-level results

In order to investigate the effects of CMPR in the visual cortex, data were realigned to movement onset. The allowed us the test for modulation effects across the evoked response to the percept of apparent coherent motion in the RDK stimulus. Figure 3.8 shows the alignment of the data time-courses for further analyses. Figure 3.9 shows a summary of the grand average event-related response to auditory and visual stimuli. Event-related fields (ERFs) at putative auditory (superior temporal gyrus) and occipital sensors are shown compared with coherent- and no-coherent motion conditions.

ROI analyses at sensor space

Using non-parametric permutation tests the loci of auditory and visual evoked activation were defined statistically by comparing the difference of the correct trials between coherent-motion and no-coherent-motion conditions. Topographical maps of the planar gradiometer data show the results of the cluster-based statistics. These revealed two significant clusters, one spanning the visual cortex and one over the auditory cortex, a selection of these sensors were chosen to construct the ROIs which were used for further analyses (figures 3.10, and 3.11). The ERF data show that the auditory time-locked data, main significant difference between conditions at approximately 100 – 150 ms in putative auditory sensors. In visual time-locked data (i.e. coherent motion conditions) the main significant difference in the visual sensors appears at 250 – 300 ms, these were later used as time-windows of interest for further analyses.
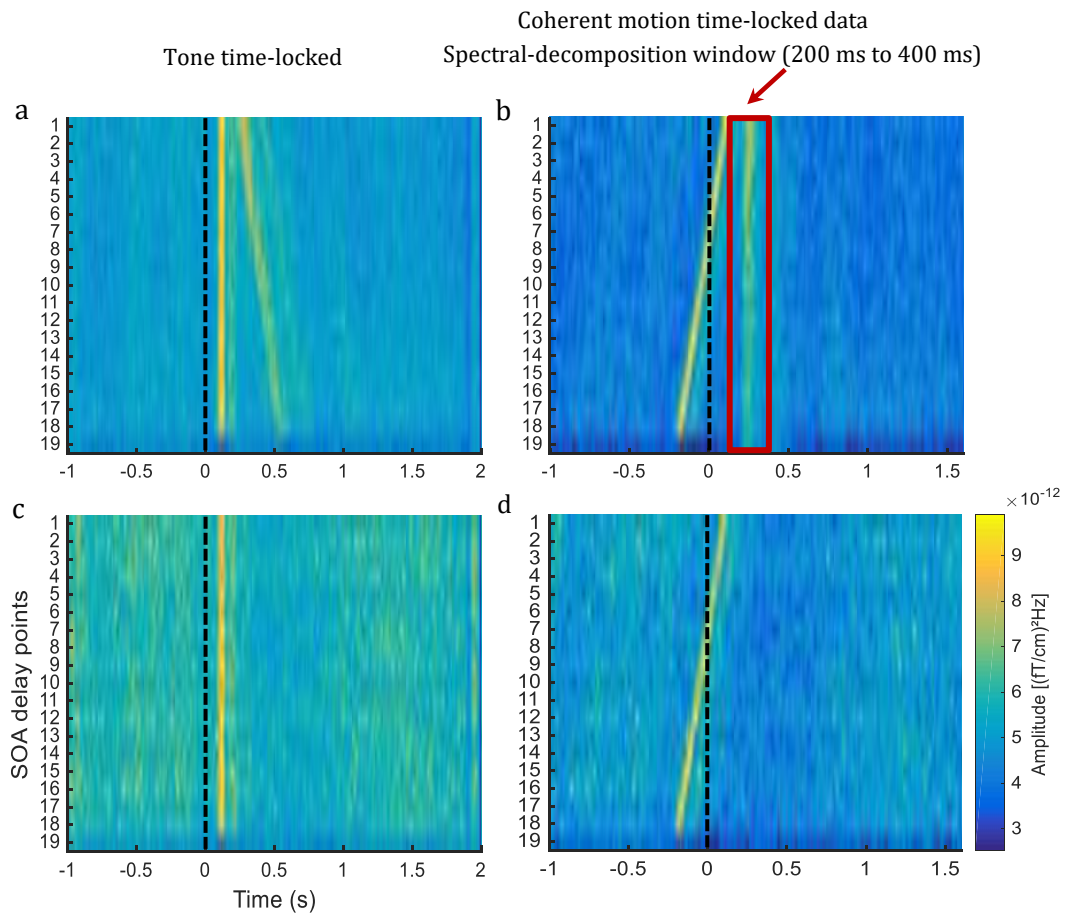
Figure 3.8. Time-course realignment. Power spectrum plots showing the ERFs over time points for each SOA delay point. Each row on the Y-axis represents an SOA. All eighteen SOAs are shown here stacked. The X-axis shows the power over all time points for which each particular SOA occured indexed on the Y-axis **a-b)** Data in the coherent apparent motion condition **c-d)** Data in the coherent apparent motion condition. **a. c.)** Data time-locked tone-onset, **b. d.)** data time-locked to apparent coherent motion. All plots show clear ERFs to tone-onset and in the coherent-motion conditions there are clear ERFs at 300 ms time-locked to tone-onset. SOA 19 on all plots shows the data for the no-tone (baseline) condition. Data from SOA 19 were not included for further analyses, but are shown here for reference.

Cyclic modulation of ERF component

To assess an auditory induced modulation of visual oscillations we used a time-frequency decomposition across the SOAs. It was possible then to establish spectral properties across the SOAs as a function over time. Data time-locked to coherent motion onset revealed, in the visual ROI, a cyclic modulation in ERF components at 300 ms in the 10 Hz frequency, clusters significant at $p<0.05$. For the temporal parietal ROI, there is a significant cluster at 240 – 300 ms around 4 Hz, similarly for the auditory ROI but with a longer window of 240 – 350 ms (figure 3.12.a, and 3.12.b). This data shows that ERF amplitudes are modulated at alpha frequency in the visual cortex.

Pre-stimulus oscillatory phase difference

We would predict that the underlying neural correlates of the observed cyclic modulation in d' performance should reveal evidence for both phase reset, and a pre-stimulus phase difference between hits and misses in the neurophysiological recordings. Across our participants and trials, we investigated if pre-stimulus phase modulates visual sensory performance. Phase analyses was computed by taking the circular average between phase courses of sensors in the visual ROI cluster. Data were separated into correct (hits) and incorrect (misses) trials. By contrasting the phase angle distributions of correct and incorrect trials, using the Watson-Williams test across time-points for each subject in the frequency bands between 1-20 Hz, the effects of pre-stimulus activity on post-stimulus period can be tested. The visual ROI revealed a significant phase distribution between the groups of trials (figure 3.13). The data showed that ~200 ms prior to visual stimulus onset, there was a significant difference in phase concentration in theta (6-8 Hz) frequency bands, and significant broadband clusters at higher frequencies (16-20 Hz) at ~ 100 ms prior to visual target onset which extends into the post stimulus period.

Correlation of behavioural and MEG sprectral profiles

We computed the correlation between the behavioural spectral profiles of DP-DT-1 performance with the MEG spectrum. Figure 3.14 show the results. Analyses with Spearman rho show very strong positive correlations in the time range .29 s to .33 s ($r_s = .83$ $p < 0.001 : r_s = .96$ $p < 0.001$), a strong negative correlation at .23 s ($r_s = -.65$ $p < 0.001$) and becomes positive at .25 s ($r_s = .65$ $p < 0.001$), and a negative correlation between .36 s to .38 s ($r_s = -.4$ $p < 0.001 : r_s = -.45$ $p < 0.001$). We can see a clear positive significant correlation at the critical time window of 300 ms post tone onset. This indicated that the ERF components which represent cortical excitability correlate with the cyclic modulation in behavioural perceptual performance. All results were subjected to multiple comparisons test using the FDR correction.
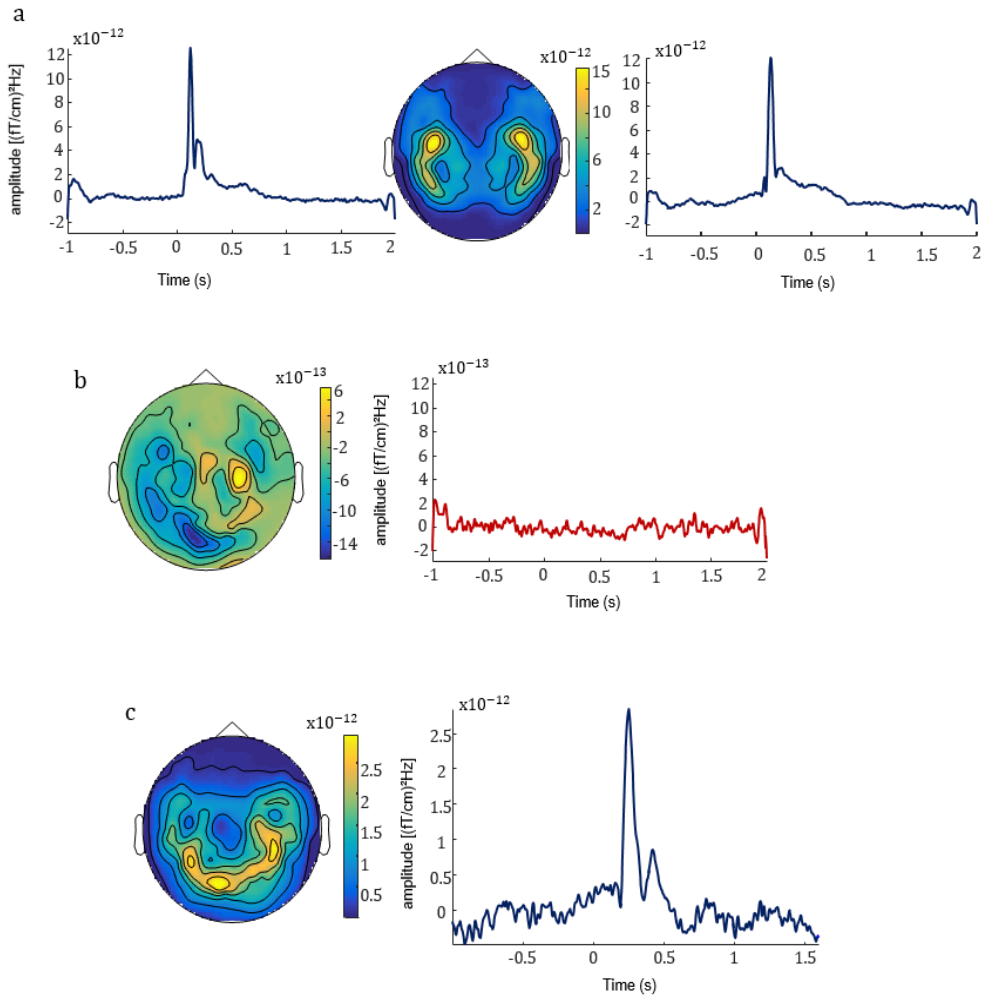
Figure 3.9. Localisation of auditory and visual activation. Topographical representation of average MEG channel activation for localisation for auditory and visual activation. ERF plots show average auditory and visual evoked fields from the highlighted sensors. **a)** Data time-locked to tone onset, **b)** Data from the control condition, no-tone trials **c)** data time-locked to visual target onset.
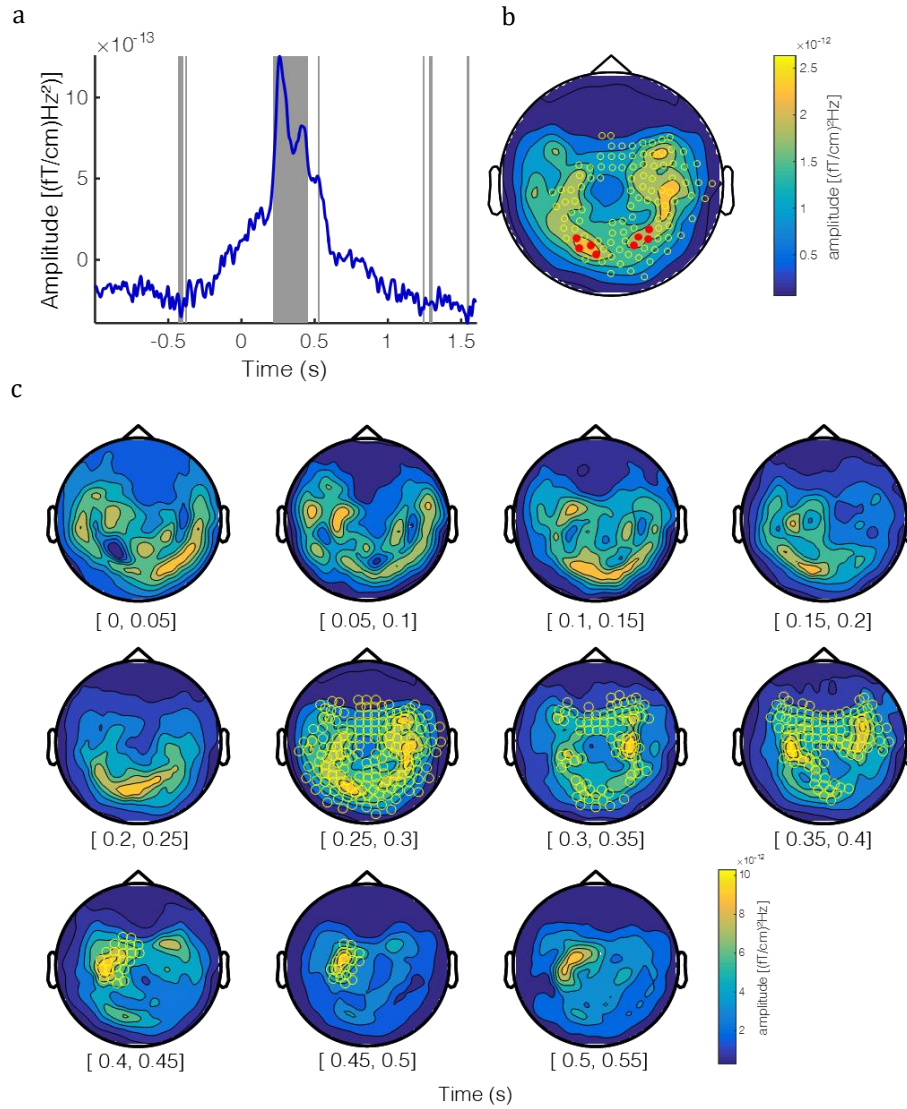
Figure 3.10. Localisation of visual evoked activation. Data time-locked to coherent movement onset. Activation reveals the difference between coherent motion and no-coherent motion conditions. **a)** Topographical cluster plots in a time window from 1-550 ms shifting in windows of 50 ms. **b)** Evoked field component of coherent motion onset. Grey bars demarcate a significant difference between conditions. **c)** Topographical plot showing sensors selected for ROI analyses in black. Nonparametric cluster based statistics show significant cluster channels, shown in yellow circles.
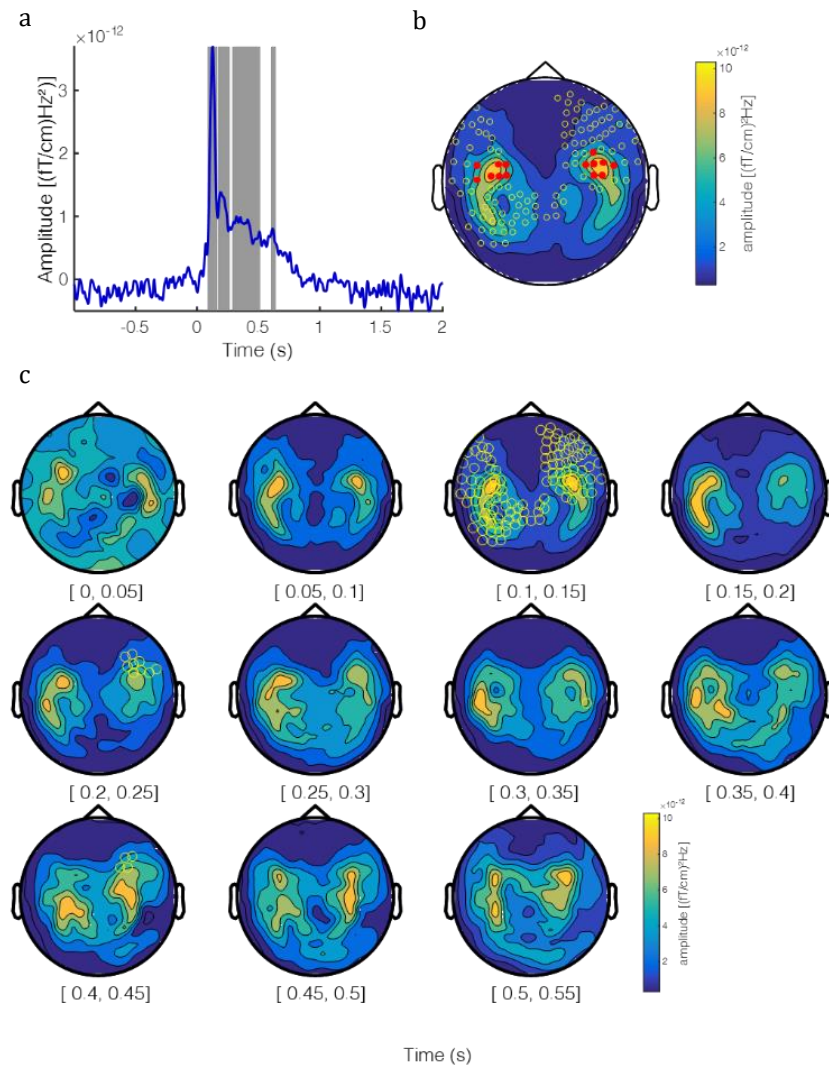
Figure 3.11. Localisation of auditory evoked activation. Data time-locked to tone onset. Activation reveals the statistical difference between coherent motion and no-coherent motion conditions. **a)** Topographical cluster plots spanning a time window from 0-555 ms shifting in 50 ms increments . **b)** Evoked field component of coherent motion onset. Grey bars demarcate a significant difference between conditions. **c)** Topographical plot showing sensors selected for ROI analyses in black. Nonparametric cluster based statistics show significant cluster channels, shown in yellow circles
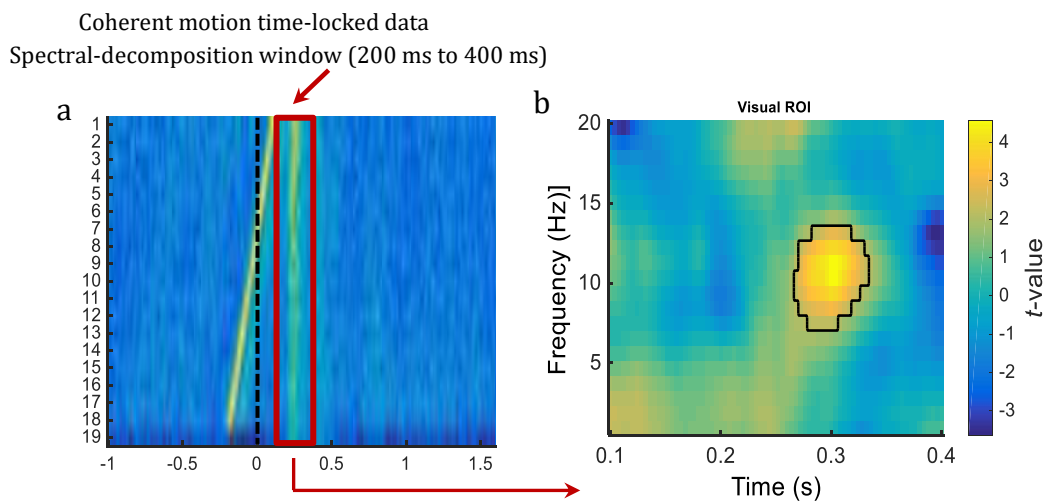
Figure 3.12. Cyclic modulation in ERF component. Time-frequency resolved power changes analyses in visual ROI data. **a)** Schematic of coherent motion time-locked to movement onset. Red box indicated the window of interest which represents the ERF response following auditory stimulus in the visual cortex, **b)** TFR statistics of the visual ERF components timelocked to moment onset, black contours demarcate significant clusters with p < 0.05 threshold, using non-parametric cluster based permutation tests.
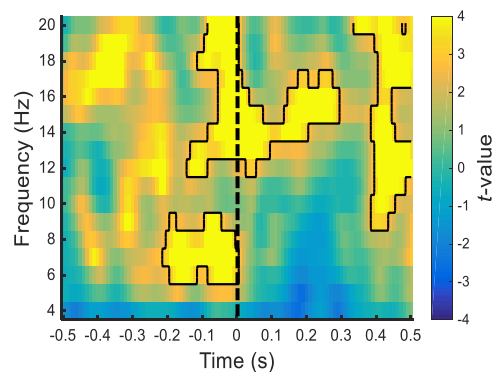
Figure 3.13. Pre-stimulus phase difference. Clusters reveal time-frequency resolved analyses for phase opposition sum statistics (Watson Williams Test) for the visual ROI. Black contours demarcate significant clusters with p < 0.05 threshold, using non-parametric cluster based permutation tests. Black dotted line indicates the onset of apparent coherent motion.
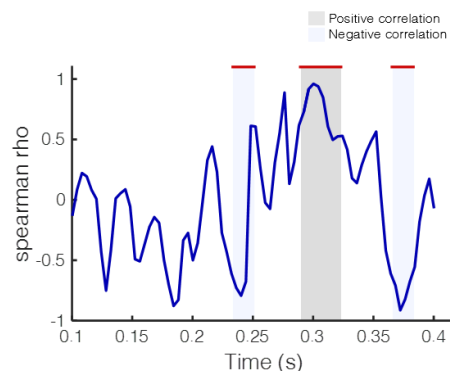
Figure 3.14. Correlation of MEG and behavioural spectral data. Behavioural temporal profile of d-prime accuracy values was correlated with the cyclic modulation observed in the ERF values time-locked to movement onset. A non-parametric Spearman's correlations revealed a significant positive correlation around 300 ms while negatively correlated around 200 ms and 350 ms. Significance is at $p < 0.01$.

3.5 Discussion

Our aim was to investigate an auditory induced modulation of visual cortical excitability to influence early visual sensory-perceptual processing. Using both MEG and psychophysiological methods, it was possible to demonstrate evidence that may support the CMPR mechanism and its perceptual consequences. We assessed the temporal profile of performance over varying delays (SOA), time-locked to a salient auditory stimulus. We predicted that if there were evidence of a transient phase reorganisation in the underlying visual oscillations, this would manifest itself as a cyclic modulation in perceptual performance. Using signal detection theory, we estimated performance accuracy using d' scores, which indexed the sensitivity and discriminability criterion of the target ACM. The results show that this was indeed the case. The behavioural data revealed a clear cyclic modulation in visual motion perception at specific low frequencies in the theta-alpha range.

MEG recordings enable us to probe neural oscillatory phase directly. The data revealed a rhythmic modulation of cortical excitability in theta (1-4) Hz and alpha (8-12 Hz) frequency bands as indexed by ERF amplitude values as a function over time. These findings are in line with the perceptual cycle theory, that the visual system samples incoming stimuli in discrete cycles in the theta (150-200 ms) and in alpha (80-100 ms) frequency ranges (Busch et al., 2009; Lakatos et al., 2005; Vanrullen et al., 2011). We observed pre-stimulus alpha phase differences, which has specific consequences on perceptual outcomes. Here we found that there was significant difference in phase distributions between hits and misses, suggesting that there is a preferred phase for optimal performance. At these preferred phases, there was a higher probability of detecting or discriminating the near-threshold target coherent motion onset. Finally we found brain behaviour correlation between the spectral profiles of d' and ERF as a function of SOA. Our data support findings shown in both animal (e.g., Lakatos et al., 2009, 2007; Magri et al., 2009) and human neurophysiological research (e.g., Busch et al., 2009; Mathewson & Gratton, 2009; Monto & Palva, 2008).

Our data contribute to the existing sparse evidence suggesting that a transient task irrelevant auditory stimulus can modulate visual motion perception. In contrast to previous investigations, here we provide evidence from both electrophysiological and behavioural evidence. The interaction between auditory and visual domains may be achieved through the mechanism of cross-modal phase resetting. This is because, visual motion detection and discrimination accuracy was modulated as a function of SOA time-locked to tone onset further supporting the notion of the perceptual cycles theory. In the majority of cross-modal interaction studies, the visual modality has been shown to predominate (Easton & Moran, 1978; Gibson, 1933; Hay & Keller, 1965). For example, there are numerous studies suggesting a strong visual influence on auditory perception (K. Calvert, Bhattacharjee, & Zegura, 1998;

Driver & Spence, 1998). What is less investigated are studies demonstrating a strong auditory influence on visual perception, or even more so visual motion perception.

Behavioural performance

By varying the onset of the target coherent motion relative to the tone-onset, it is possible to align and systematically sample the time course of performance in order to find signs of behavioural oscillations. Perceptual performance expressed in *d'* scores were analysed as a sample of discrete time-series indexed by SOA values. To this end, curve-fitting procedures revealed a clear rhythmic modulation in visual perception. Importantly, we implemented titration procedures at the start of each block to control for extreme subject variability in discrimination and detection performance. This ensured that performance was kept at individual subjects near-threshold. To this end, if the target near-threshold ACM occurred at SOAs which corresponding to the optimal phase in the visual systems sampling rhythm, this signal will be amplified and increase the probability of accurately detecting or discrimination the true direction of motion. The data revealed significant cosine models in the 5-6 Hz (theta) frequency range across all *d'* conditions. Significance was assessed by comparing the observed results with those obtained from random shuffling of the time points using permutation procedures. Spectral analyses of the detrended temporal profile of *d'*, performed across subjects, revealed oscillations in the frequency range between 5-12 Hz. Subsequent PLV analyses computed on the average *d'* for each subject, indicated that across subjects performance was phase-locked to the tone-onset in the theta frequency band with a clear peak at 6 Hz in all three *d'* conditions. In both detection *d'* conditions there were similar peaks at higher frequencies, around 12-14 Hz and 23 Hz, with an additional phase reset at 2 Hz in the DP-DT-2 condition. We speculate in detail below that these higher frequencies reflect higher-order cognitive processes (Smith & Ratcliff, 2004). Whereas, the lower frequencies (delta, 2 Hz), have been implicated in a role for anticipatory processes (Schroeder & Lakatos, 2009), which can be interpreted here as the period between tone-onset and target delay. We attribute this periodicity to reflect the underlying state of neural activity and accept this as evidence in support for the CMPR mechanism.

The input from the visual system is constantly changing and our perceptual representation must continuously be updated. Given that the external changes in our sensory environment are continuous, we might predict that conscious updating is continuous as well. Alternatively, this gain of information could be periodic, if at the neuronal level this mechanism is employed through oscillatory activity. Using a dynamic RDK stimulus, we were able to investigate the discrete nature of perception under continuous stimulation. In our paradigm in order to perceive global apparent coherent motion in the RDK stimulus participants are required to integrate spatio-temporally information over-time (Casco, Morgan, & Ward, 1988; Fredericksen, Verstraten, & Grind, 1994; Lappin & Bell, 1976; Ramachandran & Anstis, 1983). Specifically, there is a gain of information with each successive frame displacement

that are retrospectively perceived as continuous. Each spatiotemporal frame displacement involves feedforward and re-entrant processing. In natural viewing the world is sampled via eye movements (Wutz, Muschter, van Koningsbruggen, & Melcher, 2014) or shift of attention with an overt sampling of the visual field at a rate of 3-5 times per second (Fiebelkorn et al., 2013; Landau & Fries, 2012; Song et al., 2014). Using a tone to phase-align visual oscillations experimentally is one mechanism whereby we are able to uncover these inherent fluctuations likely tied to perceptual sampling. The cosinusoidal curve-fitting models show that detection and discrimination rate (d') systematically fluctuates at specific low frequencies between theta and low alpha range (5 and 8 Hz). Suggesting that performance was modulated by the delay between tone-onset and SOA, supported by previous findings (e.g., Fiebelkorn et al., 2011; Landau & Fries, 2012).

Cyclic modulation of cortical excitability

We predicted that if there were evidence for CMPR, there would be a response consistent with a reorganisation of ongoing baseline activity that would emerge as an oscillatory pattern. This would be characterised as a modulation in the ERF amplitudes indexed by SOA, where the magnitude and latency would contrast responses evoked by visual stimulation alone. The neurophysiological data revealed that this was indeed the case. Here spectral analyses revealed that ERF amplitudes across the 18 SOAs were modulated phasically at 300 ms following coherent motion onset in two posterior regions, visual alpha and parieto-temporal theta. Interestingly, there is a reciprocal relationship between the rhythmicity observed in ongoing visual oscillations phase-reset by the tone and the modulation seen across ERF amplitude values as a function of SOA. In the former, spectral decomposition analyses is performed on the MEG times-series data which reveals specific oscillations that constitutes the data (Gross et al., 2013). Whereas, performing spectral analysis across the time-locked ERF components as a function of SOA and analysed as a sample of discrete time-series reveals commensurate rhythmicity. Our results show an audio-visual modulation of parieto-occipital low frequency (1-4 Hz) and alpha band (8-12 Hz) power in the occipital regions that is predictive of perceptual multisensory modulation. Previous work has suggested that low-level sensory interactions including the build-up of the decision process can contribute to audio-visual motion perception (Kim et al., 2012; Sekuler, Sekuler, & Lau, 1997; Shams, Kamitani, & Shimojo, 2002; Stein, London, & Wilkinson, 1996; Vroomen & Gelder, 2000; Watkins et al., 2006).

The periodicity in ERF amplitude values are taken as a proxy of underlying cortical excitability, a concept which has previously been supported (Dijk, Werf, & Mazaheri, 2010; Gross et al., 2002; Mazaheri & Jensen, 2008, 2010). These studies show that the amplitude of event related response components vary depending on the performance. For example, Busch et al. (2009) found an increase in ERP amplitude values for hit rates in the detection of brief near-threshold visual stimuli as compared to misses. Specifically, perception was dependent on the stimulus-onset time relative to the phase of

ongoing 5-10 Hz (theta-alpha) oscillations in the frontal cortex (Busch et al., 2009a) or parietal cortex (Mathewson et al., 2009). Taken together, the probability of detecting near-threshold stimuli depends on the neural excitability, which covaried with EEG fluctuations on a fine temporal scale and varies with the phase of theta/alpha band oscillations (Busch et al., 2009a; Dijk et al., 2008; Ergenoglu et al., 2004; Mathewson et al., 2009; Wyart & Sergent, 2009). We correlated the spectral profile across ERFs and d' temporal profile. The data revealed a strong positive correlation at the critical 300 ms time-window post movement onset.

Electrophysiological recordings show that alpha power over posterior cortical regions predict cortical excitability, since it modulates the probability that a TMS pulse will elicit the perception of phosphenes (Romei, Rihs, Brodbeck, & Thut, 2008). These findings demonstrate that ongoing activity is not only characterised by its amplitude, but by its instantaneous phase and is related to the probability of neural firing (Fries, Nikolić, & Singer, 2007; Lakatos, Shah, Knuth, et al., 2005; Lakatos, Shah, & Knuth, 2005; VanRullen, Reddy, & Koch, 2005; Whittingstall & Logothetis, 2009). Research shows the phase of these local field potentials, specifically alpha/theta oscillations are related to the probability of perceiving a near-threshold stimulus (Busch et al., 2009a; Mathewson & Gratton, 2009). Evidence of endogenous neural phase resetting following an exogenous stimulation has been demonstrated using TMS stimulation at the alpha frequency range, has been shown to affect oscillatory activity as measured by EEG (Thut, Schyns, & Gross, 2011), and perception (Romei, Driver, Schyns, & Thut, 2011).

Pre-stimulus phase modulates perception

An increasing number of studies show that stimulus detection is influenced by both oscillatory power and the precise temporal dynamics of an oscillation (i.e., its phase) before the onset of the target stimulus (Busch et al., 2009; Mathewson et al., 2009; Romei et al., 2012). In our study, we use a brief tone to gain systemic control over the instantaneous state of the visual oscillations prior to ACM onset. Our data revealed pre-stimulus phase difference between hits and misses for ACM detection and discrimination in the theta-alpha frequency range. These data support previous findings that occipital alpha oscillations are affected by the auditory input (Mathewson et al., 2009; Mathewson & Lleras, 2011; Romei, Gross, & Thut, 2010). This follows the idea that visual perception operates mechanistically in successive cycles, alternating between phases of optimal and non-optimal excitability, which is associated with stronger or weaker inhibition, where the same stimuli wither more, likely to be perceived or go undetected.

Varela et al (1981) have provided support for this idea; they reported that perception of two flashes separated by approximately 60-80 ms changed as a function of alpha phase (7-13 Hz). Here they found that at one phase the flashes were perceived as simultaneous and at the opposite phase as sequential,

even though the temporal asynchrony of the stimuli were consistent. More recent evidence has demonstrated that posterior pre-stimulus alpha amplitude modulates the perception of visual stimuli (Han & VanRullen, 2016), and there is a relationship between pre-stimulus alpha power and early evoked potentials (Ploner et al., 2006). Furthermore, alpha power has been implicated in the modulation in the precision of predictions about upcoming stimuli (Bauer, Stenner, & Friston, 2014). Our data support the principle that alpha activity operates in a phasic manner (VanRullen & Koch, 2003; Varela, Lachaux, & Rodriguez, 2001) where alpha phase cycles in periods of increased probability of visual detection of near-threshold stimuli, whereas perception is lower at other phases. Furthermore, although not measured in the current paradigm, we could speculate that pre-stimulus alpha/theta phase modulates post-stimulus ERF amplitudes. Taken together, alpha-band oscillations modulate incoming sensory information, whereby a phase correlated inhibitory influence gates neuronal firing in a cyclic manner as a function of time (Busch, Dubois, & VanRullen, 2009; Jensen & Mazaheri, 2010; Klimesch & Schack, 2004; Mathewson & Gratton, 2009; Sauseng, Klimesch, & Gruber, 2007; Sauseng, 2012; Gregor Thut et al., 2006).

In our study, we extend the literature to suggest a role for pre-stimulus theta frequency in the spatiotemporal integration of sensory information, as was required in the RDK paradigm. Other studies have also associated a role for pre-stimulus theta in the modulation of sensory perception. For example, Chakravarthi & Vanrullen (2012) examined the 'flash-lag' effect, a visual illusion whereby a steady moving object is incorrectly perceived ahead of its true location at the moment of flash. This perceptual lag is taken as indirect evidence for updating the conscious representation of the sensory input after the 'flash' signal. Pre-stimulus EEG theta phase determined whether an earlier or later part of the ongoing motion sequence would be temporarily grouped, or 'framed' with the flash. These findings verify the idea that ongoing theta oscillations produce perceptual cycles in which visual inputs are processed periodically. Furthermore, VanRullen et al. suggest that 5-10 Hz oscillations contribute to "top-down" control (Jensen, Bonnefond, & VanRullen, 2012; Vanrullen, 2013), which was motivated by findings based on attentional phase effects on perception (Busch & VanRullen, 2010; Busch et al., 2009a). This is in line with data showing a relationship between pre-stimulus oscillations and a predictive feedback-induced effect, where frontal pre-stimulus theta oscillations and occipital beta-frequency oscillations together determine post-stimulus judgements (Han & VanRullen, 2016). In our data, we see some prestimulus beta activity which extends in the post stimulus period. This could be attributed to higher order cognitive processes as discussed previously or rather a motor preparatory response.

It is noteworthy that our study did not explicitly manipulate attention, whereas this manipulation has been shown to be important for showing pre-stimulus effects occurring in the alpha frequency range (e.g., Busch & VanRullen, 2010; Lakatos et al., 2008; Stefanics & Hangya, 2010). It is possible that

different brain regions and different experimental conditions utilise oscillations occurring at different frequencies. Within this framework, it is possible that alpha oscillations are predominantly influential for modulating early sensory processing and therefore critical for simple detection tasks, whereas other frequency bands may be important in the same or other areas in different tasks.

Spatiotemporal integration

Participants were required to extract a global coherent motion signal embedded in noise in a continuous RDK stimulus. Random dots were displaced from their position in the first pattern for four successive frame rates. In order to perceive a single percept of coherent motion at the target rotation onset, participants must integrate the spatiotemporal information with each successive frame displacement. Spatiotemporal integration defined within this context refers to the accumulation of dynamic information of successive frame displacements in the kinematogram that is integrated across time to form a single coherent perception of motion. Motion perception is an essential aspect of visual perception. The visual systems must detect coherent patterns of stimulation that remain invariant under displacement on the retina. It is widely reported that brief visual stimulation is characterised as a primary visual evoked potential (VEP) as seen around 90-125 ms latency post stimulus onset, with a typical P1 and N1 peak latencies (e.g. Kremláček, Kuba, & Kubova, 2004; Makeig, Westerfield, & Jung, 2002; Schlykowa, Dijk, & Ehrenstein, 1993). These component peaks are likely to reflect crucial junctures in early cortical processing and may be particularly susceptible to differences in pre-stimulus neural excitability indexed by alpha phase. However, in our data we observed late evoked responses at 300 ms (M3 and P3, its electromagnetic counterpart) post ACM-onset. Our data would suggest that much like these early components, late responses are modulated by pre-stimulus activity. However, here we observe this modulation in theta frequency range.

These latencies effects have been reported previously in motion perception (Lappin & Bell, 1976; Mitchell, Sundberg, & Reynolds, 2009), where late components are suggested to reflect higher order cognitive processes rather than a primary evoked response to the onset of a stimulus presentation. We speculate that our data reflects the percept of ACM embedded within the noise rather than any changes in the stimulus properties itself. In the latter, we would expect to see a typical N1 response, which is not the case here. The M300 has primarily been implicated in endogenous cognitive processes (Devrim, Demiralp, Ademoglu, & Kurt, 1999). Devrim et al. further argued that the M3 component constitutes the major component of near-threshold visual ERPs including occipital responses. Similarly, previous findings report a high correlation between the M3 amplitude and the detection and discrimination of near-threshold stimulus (Hillyard, Squires, Bauer, & Lindsay, 1971; Parasuraman & Beatty, 1980; Paul & Sutton, 1972; Schürmann et al., 2001). For example, Haig & Gordon (1998) showed a cyclic modulation of the amplitude of the M3 evoked component that was phase-locked to alpha oscillatory

phase. Their findings show that late ERP components (P3) are influenced by the phase of ongoing oscillations.

Analyses from event-related oscillations (ERO), an alternative theoretical and methodological approach to the analyses of event-related M/EEG responses (W Klimesch, Sauseng, & Hanslmayr, 2007b; W Klimesch et al., 2004; Sauseng, Klimesch, Gruber, et al., 2007), argue that the M3 is elicited through the superposition of delta and theta frequency band oscillatory responses. Intracranial recording methods have identified the temporal-parietal regions are essential generators of the M3 (Jones et al., 2004). Furthermore, Başar et al. (1992) showed an association between delta and theta response with signal detection and decision making process of near-threshold stimuli. They suggested that low frequencies are associated in the M3 response, their findings were based on ERP analyses performed in the frequency domain, and consistently revealed that the primary contribution of the P3 component is concentrated in the theta frequency range (Başar-Eroglu, Başar, & Demiralp, 1992; Demiralp, Ademoglu, & Istefanopulos, 1998; Kolev, Demiralp, Yordanova, & Ademoglu, 1997). Although finding that late components constitute frequencies in the lower spectrum, are not very surprising. ERF events occurring prior to the M3, such as the N1, are typically related early sensory processing, whereas later components are associated with higher-order cognitive processes. This includes, motor planning, decision making, recognition and discrimination, content updating and executive control (Devrim et al., 1999; Donchin & Coles, 1988; Geffen, Wright, Green, & Gillespie, 1997; Nieuwenhuis, Aston-Jones, & Cohen, 2005; Polich, 2007). Studies using apparent motion stimuli have suggested that detection and discrimination of these types of stimuli fall within the remit of higher cognitive processes (Donner, Siegel, Fries, & Engel, 2009; Horwitz & Newsome, 1999; Roitman & Shadlen, 2002; Siegel, Engel, & Donner, 2011).

Our results show that the spatiotemporal integration of information occurred in the visual and parietal ROIs. Most human studies report that motion perception is restricted to V5/MT, with some paradigms using constant random-dot stimulation show responses to correlate with firing in V5 neurons (e.g. Britten, Newsome, & Shadlen, 1996). However, our data is in sensor space and we may only speculate a specific neural substrate for the data recorded at the sensors. Future studies would need to replicate these findings at source space. Here we show neural activity in response to the apparent coherent motion perception of a continuous RDK stimulus in parietal and visual ROIs. This is consistent with findings from Williams et al. (2003) who reported parietal activity for the perception and detection of apparent coherent motion in a random dot pattern. Therefore, we speculate that a neural correlate of the percept of apparent motion need not be restricted to V5 areas. There is a lack of a clear distinction between 'processing' versus 'perceptual' areas of the brain, but recent findings suggest that the areas involved in apparent motion perception is a part of a neural network which is

collectively responsible for its perceptual representation (Moutoussis, Keliris, Kourtzi, & Logothetis, 2005).

Limitations and caveats

As previously noted in Chapter 2, there are some inherent limitation when performing spectral analyses on behavioural data, but this will not be discussion here again. Next methodological consideration concerns measuring phase resetting. In non-invasive human M/EEG recordings it is theoretically impossible to demonstrate that evoked activity results from phase-resetting of ongoing neural oscillators (Telenczuk & Nikulin, 2010). Nonetheless, with sensible inferences on the origins of the signal with adept paradigms and the use of mathematical informed approaches, can provide useful criteria for interpretation (Canavier, 2015). There are two opposing theories that attempt to elucidate the genesis of the ERF. The oscillatory model posits that evoked responses are a consequence of a phase reset of ongoing oscillations (Hanslmayr et al., 2007; Klimesch et al., 2007a; Makeig et al., 2004; Mäkinen et al., 2005; Sayers et al., 1974). Whereas according to the evoked model, evoked responses arise as a fixed-polarity and fixed-latency in each trial which is superimposed on the intrinsic neural oscillations where the averaging of these evoked responses produces the ERF/P (Hillyard & Kutas, 1983; Jervis et al., 1983; Mäkinen et al., 2005; Mazaheri & Jensen, 2006). Unlike previous studies investigating phase resetting, we used a dynamic visual stimulus presented continuously for the duration of a trial and prior to a temporarily informative tone. To this end, we were able to control for sudden changes in the properties of visual stimulus. Effectively we were able to discern the observed responses being a neural signature delineating the percept of coherent motion perception and not a direct consequence of phase resetting induced by transient stimulation. Evoked responses occurring at these ensuing latencies are attributed to higher order cognitive process, such as decision making and visual discrimination (Gold & Shadlen, 2007; Hanslmayr et al., 2005; Hillyard & Kutas, 1983).

3.6 Conclusion

In the present study, we sort to provide both psychophysical and neurophysiological evidence, which may support the CMPR mechanism. Our findings show manifestations of oscillations in behavioural performance at physiologically relevant rhythms. Where low frequency oscillations have a role in the spatiotemporal integration of information. These findings were supported by the MEG data showing a cyclic modulation of ERF amplitude values as a function of SOA following tone-onset, suggesting that an auditory stimulus can modulate cortical excitability in the visual cortex. In addition, the phase of pre-stimulus oscillations predicts perceptual response function. Taken together we extend the literature on CMPR by showing a correlation between the cyclic modulation in behavioural performance and cortical excitability as indexed by late evoked responses in a continuous apparent motion task.

Chapter 4

Cross-modal enhancement for multisensory predictions of self-generated stimuli.

4.1 Introduction

Our sensory systems must continually adapt to receiving varying information from the environment. Sensory input rarely influences a single sensory modality. Therefore, the representation of sensory information requires the integration of responses across distributed sensory systems. This is largely because even rudimentary object features are processed in different specialised modalities in parallel. Cross-modal integration is a candidate mechanism that enables the binding of signals across functionally interconnected cortical regions, including multisensory cortices (Kayser & Logothetis, 2007; Lakatos, Shah, Knuth, & Ulbert, 2005). This is essential, as sensory information comprises a diverse combination of auditory, visual, haptic, and olfactory properties. Across the hierarchy of sensory processing, neural activity is influenced by top-down attentional mechanisms that dynamically interact in the binding and selection of signals through a context-dependent way as a function of predictions and a prior of knowledge (Engel & Singer, 2001; Fries, Neuenschwander, Engel, & Goebel, 2001).

In the first two experiments, I have explored the behavioural and electrophysiological signatures of cross-modal interactions particularly in the context of cross-modal phase resetting (*see* Chapters 3 and 4). As discussed in the previous chapters, CMPR is a versatile, flexible and efficient mechanism for sensory gain control. The process of selective attention is an attribute of the biased completion model (Fries, Reynolds, Rorie, & Desimone, 2001; Mitchell, Sundberg, & Reynolds, 2009) that assumes that attention influences visual processing by enhancing the input gain for the group of low-level neurons associated with an attended behaviourally relevant stimulus over those groups of neurons related to the unattended stimulus. The mechanism of gain control is not specified in the model but may very well be implemented through an enhancement of synchronous neural oscillations among the group of low-level neurons driven by the attended stimulus and a functional connection between them and higher-order neurons (Fries, Neuenschwander, et al., 2001; Fries, 2005; Fries, Womelsdorf, & Oostenveld, 2008). Various oscillations in multiple frequency bands have been attributed to the enhancement of attention (Lakatos et al., 2005; Lakatos et al., 2009; Lakatos, Karmos, Mehta, Ulbert, & Schroeder, 2008). Interestingly, sensory gain control is an essential requirement for almost any

behavioural task and is therefore one of the fundamental operations in the human brain (Friston, 2005).

Another well-studied model case for this fundamental operation (besides the interactions of two sensory modalities) is the interaction between motor and sensory areas. This dynamic coordination of oscillations across sensory modalities and motor areas is described in the terms of predictive coding. Motor action leads to predictable sensory consequences. This predictive coding is associated with attentional neuromodulatory gain control in sensory processing, which reflects a (Bayes-optimal) encoding of precision accuracy in detection via the excitability of neural populations that report prediction errors. The very fact that the sensory consequences are predictable, changes the way they are processed in the brain and the associated percept. Specifically, self-induced sensory stimuli lead to reduced activation in sensory cortex. The exact mechanisms are yet unclear. However, inter-areal phase resetting is a potential mechanism, which may index the forward model account of motor-to-somatosensory prediction (Blakemore, Frith, & Wolpert, 2001; Wolpert et al., 1995) to different sensory modalities (e.g. somatosensory and auditory modalities; Lakatos et al., 2007).

In fact, it has been suggested that two distinct mechanisms might be at play in this motor-sensory interaction. First, during motor preparation the overall excitability of sensory areas could be reduced. This could represent a general unspecific mechanism that is independent of a prediction regarding the exact identify of the expected stimulus. Indeed, increases in the power of alpha oscillations before movement onset have been reported in sensory areas (Müller, Leske, Hartmann, & Szebényi, 2014; Stenner, Bauer, Haggard, & Heinze, 2014). Since alpha power is negatively correlated with cortical excitability this corresponds to an overall increased suppression (Lakatos, Shah, Knuth, et al., 2005; Lange et al., 2013; Vincenzo Romei et al., 2010). Second, more precise predictions regarding stimulus identity could be represented in a temporally more precise control of excitability via phase resetting. Again, there are reports of differences in phase locking following self-induced versus passively perceived sensory stimuli (Liyu Cao, Thut, & Gross, 2016b)

Here, we have studied the interplay of motor and (one or two) sensory areas using the same methodologies (time-frequency analysis of power and phase) as in the previous studies using a well-established paradigm from the sensory attenuation literature (*for a review, see:* Hughes, Desantis, & Waszak, 2013). However, here we contribute to the existing literate in several ways: First, most of the previous electrophysiological studies investigate motor-sensory interactions by looking only at evoked data. We perform spectral analysis with power and phase. Second, most previous studies use EEG. Here, with MEG we avoid the referencing problem (Davidson, 1988; Nunez, 2006; Pascual-Marqui et al., 2011), have denser sensor placement and (by computing planar gradient representation) can get relatively focal estimates of activation from small sensor groups (although we acknowledge that source

localisation would be preferable). Third, for the first time, to our knowledge, we study the motor-sensory interactions simultaneously in up to two sensory modalities. The paradigm therefore represents a novel combination of standard paradigms in two fields, the sensory attenuation field and the multi-sensory field.

Interactions between motor and sensory systems

Our sensory systems have limited processing capacity and our brains must therefore adapt to deal with the surfeit of information arriving at our senses. One method used to manage this information is to predictively amplify sensory inputs carrying relevant information while supressing those which do not (Friston, 2012; Schroeder, Lakatos, Kajikawa, Partan, & Puce, 2008; Schroeder & Wilson, 2010). In principle, stimuli produced by our own self-initiated actions are generally regarded as trivial, as their consequences are largely predictable (Bays, Wolpert, & Flanagan, 2005; Blakemore, Rees, & Frith, 1998; Blakemore, Wolpert, & Frith, 2000). Reducing redundancy associated with self-initiated actions, enables us to focus resources on extracting novel information from stimuli that correspond to biologically significant changes in our surroundings. This ability is important as it enables us to maintain perceptual stability. Conventional views propose that information about motor commands are used to distinguish the sensory consequences of our own actions from externally produced sensations. Predicting the sensory consequences of self-generated movements is an essential component of motor control (Wolpert & Flanagan, 2001).

Von Holst (1954) introduced the notion whereby the brains sensory motor areas send in parallel an efference copy of the same motor commands that are sent to move the eyes, to the visual system. This predicts the sensory consequences as indexed by corollary discharge of the movement, where this prediction allows the visual system to compensate for retinal displacement during voluntary eye movement (Sperry, 1950). In order to determine the location of an object relative to our heads, for example, its retinal location and gaze direction must be determined. Helmholtz (1967) proposed that since the eye muscles are thought not to contain any sensory receptors, gaze direction is determined rather by predicting the eye location based on the efference copy of the motor command going to the extraocular muscles (Bridgeman & Stark, 1991). Consequently, the object's veridical position in space can be determined by both the estimation of the eyes position together with the object's retinal location. Predictions can work in an integrated way by assimilating input from other sensory modalities to filter information, attenuating components produced via our own self-initiated actions (re-afference) from those produced externally. Conceptually, in order to produce predictions, the central nervous system (CNS) must comprise a central monitor (Frith., 1992) or internal "forward model" (Blakemore, Wolpert, & Frith, 1998; Ito & Speer, 2008).

The reduced sensory processing of self-generated stimuli is typically explained by the CNS forward models of motor control (Miall & Wolpert, 1996). This forward model, variously referred to as corollary discharge (Sperry, 1950) or efference copy (von Holst, 1954), of the motor command are used to generate continuously predictions of the sensory consequences of self-initiated movement and the causal relationship between their outcomes (Ito & Speer, 2008; Weiskrantz, Elliott, & Darlington, 1971; Wolpert et al., 1995). These predictions are then compared with the actual sensory feedback (re-afference) from the movement. Subsequently, self-generated actions are reliably predicted on the basis of motor commands, and as a result there is little if any sensory discrepancy between the comparisons of the predictions and the results of the actual sensory feedback. This accurate prediction can be used to attenuate the sensory effects of self-generated movement (P. Bays, Flanagan, & Wolpert, 2006; SJ Blakemore et al., 1998).

In contrast, externally driven sensations are not associated with an efference copy, and therefore the forward model is not able to predict these events. The model attenuates or removes sensory feedback components associated with self-generated movement in order to accentuate more relevant and unpredicted feedback generated through external events. This mechanism acts as a processing filter discerning perhaps those more relevant components of external incoming sensory information. This mechanism of predictive attenuation offers an explanation as to why self-generated tactile stimulation we perceived is weaker than the same stimulus externally imposed (Bays et al., 2006, 2005; Blakemore et al., 1998; Shergill, Bays, Frith, & Wolpert, 2003). The transmission of an efference copy to the appropriate sensory modality may be an emergent property of a self-organising system. Specifically, corollary discharge is related to synchronous neural oscillations. Accomplished through the synchronisation of oscillatory activity among distributed neural assemblies (Singer, 1999). Neural populations could be identified as being a part of the same functional network if their spatiotemporally distributed neural ensembles oscillate in the same synchronous frequencies. The brain optimises efficient processing of limited resources by aligning the internal neurophysiology to the external context of germane stimuli. This mechanism is an index of the active predictive sensing, which can guide the temporal structure of motor-initiated rhythmic events, an example par excellence is audition where continuous speech is sampled at a frequency of about 4-7 Hz (Park, Ince, Schyns, Thut, & Gross, 2015; Schroeder & Wilson, 2010).

Under the assumption that the forward model mechanism involves self-coordinated communication between motor and sensory systems, enhancement of neural synchrony should be evident before execution of motion actions. Consistent evidence has been demonstrated in local field potential recordings from somatosensory cells in rats, which showed neural synchrony that preceded exploratory whisking in both 7-12 Hz (Nicolelis, Baccala, Lin, & Chapin, 1995) and 30-35 Hz (Hamada, Miyashita, & Tanaka, 1999) bands. Hamada et al. (Hamada, Miyashita, & Tanaka, 1999) proposed that

transfer of an efference copy of motor preparation to the somatosensory cortex, taking place within hundreds of milliseconds before the action and observed as oscillations phase-locked to it, might trigger neural oscillations. This is described in much more detail elsewhere (Friston, 2005). Here a conceptual explanation can be derived from the predictive coding theory. The tenant of this model is founded on the idea that sensory cortices receive information about internal predictions, the generative model, about the possible sensory consequences of forthcoming stimuli and these are systematically compared with the actual incoming information.

Within this framework, the evoked response component is an index of prediction error, which is an expression of the discrepancy between predicted sensory outcomes and the actual sensory input. To this end, reduced prediction errors are expressed as a suppression in the magnitude of evoked responses. The difference between top-down expectation and incoming sensory inputs propagate forward throughout the cortical hierarchy in distinct frequency bands. Specifically, sensory predictions are communicated via anatomical feedback connections in the alpha to beta frequency range, whereas prediction errors are communicated along feedforward connections in the gamma frequency range (Arnal & Giraud, 2012; Arnal, Wyart, & Giraud, 2011; Bastos, Litvak, Moran, Bosman, & Fries, 2015).

The sensory attenuation (SA) effect has been reported as a perceptual phenomenon using subjective report (Blakemore, Frith, & Wolpert, 1999). For example, Bays et al. (Bays et al., 2005) demonstrated that the perceived intensity of self-applied tactile stimuli are reduced when compared with identical, externally generated stimuli. Similarly, the SA effect has been shown using signal detection theory methodology. Here it has been shown that there is a reduction of perceived loudness and visual contrast following self-generated auditory stimuli (Weiss, Herwig, & Schütz-Bosbach, 2011) and visual (Cardoso-Leite & Mamassian, 2010) stimuli respectively. Neurophysiological recordings have equally demonstrated the SA effect with ERP/Fs (Aliu, Houde, & Nagarajan, 2009; Baess, Widmann, & Roye, 2009) and neuroimaging methods (Blakemore et al., 1999, 1998).

Studies using EEG and MEG have shown that the auditory cortex response to self-generated auditory tones is supressed relative to the response while passively listening to the same tones. For example, Schafer & Marcus demonstrated that the EEG response was attenuated for self-generated auditory stimuli when compared to externally generated stimuli (Schafer & Marcus, 1973). More recent evidence found similar findings, where the MEG response arising from the auditory cortex were attenuated for self-triggered tones (Martikainen, Kaneko, & Hari, 2005). Evidence for SA has prominently been demonstrated using auditory stimuli (Baess et al., 2009; Knolle, Schröger, Baess, & Kotz, 2012). Taken together these experiments typically observe a significantly reduced N1 (M100, its electromagnetic counterpart) response amplitude for self-generated auditory stimuli around 100 ms after tone onset. Fewer experiments have been conducted in the visual domain, with these experiments

showing a somewhat less reliable modulation over the vertex (Gentsch & Schütz-Bosbach, 2011), or late modulations over frontal and posterior sensors (Hughes & Waszak, 2011).

Auditory SA has been shown repeatedly (Aliu et al., 2009; Baess et al., 2009; L Cao, Thut, & Gross, 2016; Martikainen et al., 2005). The majority of EEG studies reporting a suppression of the N1 response have shown amplitude reductions only at Cz or a subset of frontocentral electrodes and attribute these effects the classical SA effect in the auditory cortex following self-generated tones, arbitrated by corollary discharge. However, contrary evidence from recording at mastoid regions have reported no SA effect (Timm et al., 2013) or an enhancement (Horváth, Maess, Baess, & Tóth, 2012). Few MEG studies have demonstrated attenuation of the M1 response that explain the suppression in the magnitude of equivalent current dipole sources in the auditory cortex (Aliu et al., 2009; Horváth et al., 2012; Martikainen et al., 2005).

A very recent study by Cao, Thut, & Gross (2016) using MEG spectral analyses demonstrated that self-initiated tones were associated with an increase in pre-stimulus alpha power, decrease in gamma power and an alpha/beta phase locking in the auditory cortex. These oscillatory signatures correlated with SA in evoked ERFs. They discussed this as evidence for a close relationship between neural oscillatory events and SA. Moreover, pre- and post-oscillatory changes correlated, a finding, which further supports the notion for the role of distinct frequencies in neural information processing within the context of predictive coding. Specifically, their data contribute to previous literature, which implicates the role of alpha oscillations reflecting feedback and gamma oscillations feedforward. Interestingly, they suggest that pre-stimulus alpha power represents prediction and post-stimulus gamma power represents prediction error. These mechanisms are modulated by post-stimulus alpha/beta phase resetting. These findings offer new insights into the underlying neural oscillatory mechanism involved in SA.

SA effect have been demonstrated across a variety of modalities (Blakemore et al., 2000; Gentsch & Schütz-Bosbach, 2011; Voss, Bays, Rothwell, & Wolpert, 2007; Weiskrantz et al., 1971). However, imaging studies are sparse that would confirm an auditory suppression induced by self-generated stimuli. Furthermore, to our knowledge to date there has been no evidence for the SA effect for self-generated multisensory stimulations, nor with any imaging evidence. Although research has examined tasks that combine the observation of biological actions with auditory consequences. These paradigms demonstrate that watching visual lip movements combined with auditory speech sounds results in suppression of early components of auditory ERP/F (Stekelenburg & Vroomen, 2007; Wassenhove & Grant, 2005). This evidence suggests that N1(m) suppression in these paradigms are a result of internal predictions about the temporal consequences of biological motion (Arnal, Morillon, & Kell, 2009).

The current study

Here we aimed to extend the literature and use the SA effect with both unisensory and multisensory stimulation in an MEG study to perform power and phase analysis and investigate oscillatory phase in sensory-motor interactions. We aimed to replicate the widely reported SA effect in the auditory cortex (Hughes & Waszak, 2011) and extend our investigation into the visual modality. Within this framework when a tone is self-triggered, its timing is largely predictable. Research has demonstrated that the N1 attenuation associated with self-generated tones reflects their predictability. To investigate this possibility, the present study compared the M100 response to self-generated and externally generated stimuli that were produced at a rate of once every three seconds.

First, we expected that the forward-modal mechanisms would result in sensory prediction and in subsequent motor-to-auditory inhibition indexed as a suppression in the auditory cortex to self-generated tones, effectively replicating the classical SA effect. Next, we sought to investigate the effects of multisensory stimulation within the SA framework. Synchronised neural activity prompt temporal windows of communication between task related modalities (Pascal Fries, 2005; Varela, Lachaux, Rodriguez, et al., 2001). We assessed the effects of CMPR of early multisensory integration, for self and externally generated stimulation. Including the effects of visual-alone stimulation in visual cortex and the mechanisms involved for opposite simulation. In the previous two chapters, we demonstrated that a tone could modulate visual oscillations; here we extend our investigations to include a phase-reset of neural oscillations in primary auditory cortex by visual input. These seem to be an important mechanism in sensory perceptual processing (Mercier et al., 2015; Perrodin & Kayser, 2015; Thorne, Vos, & Viola, 2011). To our knowledge, for the first time, we aimed to investigate the motor-sensory interactions simultaneously in up to two sensory modalities. The paradigm therefore represents a novel combination of standard paradigms in two fields, the sensory attenuation field and the multi-sensory field. Furthermore, in the current study we were able to assess the effects of nonlinear multisensory integration. To this end, neural activity evoked by both auditory-alone and visual-alone was compared with that of audiovisual stimulation using the linear additive criterion model (Kayser, Petkov, & Logothetis, 2008; Mercier et al., 2013; Stein, 1998).

Most M/EEG studies investigating SA have restricted their analyses to specific stimulus-evoked responses (Baess et al., 2009; Gentsch & Schütz-Bosbach, 2011; Hesse, Nishitani, Fink, & Jousmäki, 2010; Hughes & Waszak, 2011; Martikainen et al., 2005). Here we focus on neural oscillations in time-frequency domain, motivated by previous findings that induced responses convey a corollary discharge signal. Alpha oscillations in the visual cortex has been attributed as representing a pulsed inhibition by feedback projections that prioritise sensory processing of task relevant (Jensen & Mazaheri, 2010) and salient stimuli (Jensen, Bonnefond, & VanRullen, 2012). It has been previously

suggested that related functions are attributes of sensory attenuation, specifically the prevention of self-initiated desensitisation and prioritising of externally generated stimuli (Lally, Frendo, & Diedrichsen, 2011; Poulet & Hedwig, 2007). To this end, we expect that prediction of self-initiated stimuli would reflect an increase in alpha-amplitude in the visual cortex and predict sensory attenuation at the perceptual level. We further, extend this prediction to the auditory cortex.

Finally, deficits in sensory-predictive processes have been identified as specific symptoms of psychopathology, most notably delusions of control in schizophrenia (ScZ) patients (Frith & Wolpert, 2000; Lindner, Thier, Kircher, Haarmeier, & Leube, 2005; Shergill, Samson, & Bays, 2005; Synofzik, Thier, Leube, & Schlotterbeck, 2010). ScZ patients who express such delusions report their own actions as being made for them by an external agent rather than by their own will. Paradoxically, the actions that are perceived to be forced upon them are in fact in accord with the patient's own intentions. Therefore, these deficits underlying delusions of control are not related to an inability to initiate action but rather the perception of these actions being registered as internally triggered. In principle, a failure to predict self-generated actions leads to prediction-error resulting in sensory feedback that is surprising and the feeling that action was not internally initiated (Fletcher & Frith, 2009). Persistence of prediction-error would lead to a reduced sense of agency. Evidently the majority of first-rank symptoms of ScZ appear to reflect external attributions of internal generated phenomena (Fletcher & Frith, 2009).

Although there is evidence that ScZ patients show deficits in predicting the sensory consequences of self-generated actions, which are often exhibited by subnormal levels of auditory M100 suppression to self-initiated auditory sensations (Ford et al., 2001; Lindner, Thier, Kircher, Haarmeier, & Leube, 2005; Shergill et al., 2005; Synofzik et al., 2010), such case-control studies can be problematic due to medication effects. Here we investigate evidence which may support observing these deficits using a complimentary approach which involves assessing schizotypal characteristics in healthy people, considering ScZ as an extreme expression of a continuous phenotype normally distributed in the population (Chapman, Chapman, & Kwapil, 1994; Claridge, 1994; Peters, Joseph, Day, & Garety, 2004; Peters, Joseph, & Garety, 1999). Measuring such individual differences offers a unique approach to validating models of symptoms in the absence of medication. Given the deficits in sensory prediction observed in ScZ patients, we predicted a negative correlation between levels of sensory prediction (SA effect) and a tendency towards delusion ideation. This subnormal sensory attenuation effect has been similarly taken as evidence for the self-monitoring abnormalities proposed to underlie most characteristic clinical features of disorders (Blakemore et al., 1999; Frith & Wolpert, 2000; Chris Frith, 2005). In addition we administered the systemising quotient (SQ), designed to measure the tendency to use a systematic rule-based approach to understanding experiences.

Hypotheses

The novel combination of concepts from multisensory integration and sensory attenuation in this study led us to derive the following hypothesis: 1) First, we predicted that multi-sensory effects would be evident also in the active condition in measures of power and phase locking. 2) We expect to replicate the effect of reduced M100 component in the active versus passive condition. 3) We hypothesise that sensory attenuation extends to the multisensory condition. 4) Finally, we predicted that self-report questionnaire data would correlate with sensory attenuation.

4.2 Methods

Participants

Twenty-two right-handed volunteers participated in the study (13 male, mean age 24.8 ± 5.3 years). All participants provided informed written consent and received a monetary compensation for their participation. Two participants were excluded for further analysis due to technical issues concerning behavioural threshold performance. None had been diagnosed with a hearing disability or had a history of significant neurological or psychiatric illness. Participants had normal to corrected-to-normal vision. Handedness was defined by the Edinburgh Handedness Test (Oldfield, 1971) were approved by the local ethical committee (University of Glasgow, The College of Science and Engineering) and conducted in conformity with the declaration of Helsinki.

Questionnaires

We administered the Peters Delusion Inventory (PDI-21) to assess Delusional ideation (Peters et al., 2004). Total scores range from 0–336, with higher scores reflecting higher delusional ideation. In addition, we administered the systemising quotient (SQ-R); higher scores indicate an advanced ability for analysing and exploring a system, with a score range 0-80 (Wheelwright, Baron-Cohen, & Goldenfeld, 2006).

Design and procedure

Figure 4.1 shows a schematic of the stimuli and paradigm. The experiment consisted of six experimental condition blocks with ninety trials in each, presented in a randomised order with breaks in between each. In the *active-auditory* (A-Aud) condition, participants were required to make a self-paced finger abduction at a rate of approximately once every three seconds. This movement triggered the onset of a pure auditory tone. Participants fixated a dark grey cross at the centre on a uniform grey background for the duration of the block. In contrast, finger abductions in the *active-visual* (A-Vis) condition, triggered a high contrast black-and-white checkerboard. Whereas a combination of both the

auditory and visual stimuli were presented simultaneously after making finger abductions in the *active-multisensory* (A-Vis) condition, participants were instructed to attend both stimuli. In all the active (self-generated) conditions, participants were required to make the finger abductions at about three second interludes, were to avoid counting intervals, and attend the stimuli. The next three conditions were identical to the self-generated blocks but here stimuli were externally generated (*passive*). In these conditions, participants were instructed to attend to the stimuli passively, which were present at once every 3 s. The three *passive* condition were *passive-auditory* (P-Aud), *passive-visual* (P-Vis), and *passive-multisensory* (P-Vis).

Stimuli

Finger abductions triggered the visual and auditory stimuli. Visual stimuli were presented through a DLP projector (PT-D7700e-K, Panasonic®) placed outside the magnetically shielded room (MSR) onto a screen situated 1.90 m away from the participant via an in-room mirror. Stimuli were generated off-line using Matlab 2013.b (The MathWorks®) and controlled using routines from Psychophysics toolbox (Brainard, 1997). In the auditory alone conditions participants were instructed to fixate a dark grey cross (0.9° x 0.9°) which was presented at the centre on a uniform grey background (3 cd/m^2 background luminance) for the duration of the block. In the visual and audiovisual conditions, a high contrast 5x5 black-and-white checkerboard was presented at the centre of the screen on the uniform grey background. The mean luminance was 50 cd m^{-2} (40-60 cd m^{-2}) and contrast between black and white squares at 80% defined by the *Michelson contrast* (Odom, Bach, Barber, & Brigell, 2004). The finger abduction triggered the onset on the checkerboard for a duration of 50 ms (checkerboard: 4.7° x 4.7 of total visual angle; °24° x 18°). Sound stimuli (pure auditory tone, 1000 Hz, 50 ms in duration, 70-85 dB sound pressure level (SPL)), were delivered binaurally via a sound pressure transducer through two 5 m long plastic tubes terminating in plastic insert earpieces. Sound stimuli levels were calibrated using a condenser microphone and sound level meter.

All responses were made with the right index finger which was placed in front and flush of a fibre-optic laser mounted on a table in the scanner. The fibre-optic laser was an in-house built optoelectronic device. Finger abductions created a break in the laser beam, which sent a trigger to initiate the onset of the stimuli. The timing between finger abduction triggering the onset of the stimuli; either the soundwaves reaching both ears of the participant, and/or the visual checkerboard appearing on screen, was simultaneous within a 350 µs accuracy time difference. We elected to use a fibre-optic laser as a trigger response rather than a button box (Lumitouch), to eliminate the known noise associated with making button box responses. This ensured no contamination of noise in any of the conditions. A training block (50 trials) was used at the start of each session to acquaint participants with executing accurate finger abductions that would trigger a response once every three seconds and to calibrate the sensitivity of the fibre-optic sensor adapted to each participant's performance. During the training

session participants received visual feedback on the timing performance after each trial to ensure responses were made at least once every three seconds. No feedback was giving during the actual experiment.
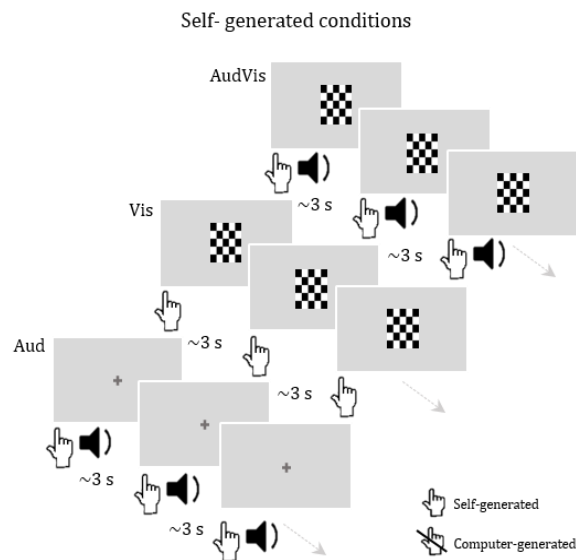
Figure 4.1. Experimental design. Schematic of task and stimuli. For illustrative purposes, only the self-generated (active) conditions are presented. Visual stimuli were a 5x5 high contrast checkerboard and auditory stimuli were brief 1000 Hz tone. All stimuli were presented for 50 ms at onset finger abduction in the self-generated conditions. Participants' right index finger was placed flush with a laser mounted on a table in MEG. To begin the trial, participants made self-paced figure abductions approximately once every 3 s. There were three condition, auditory-alone, visual-alone, and audiovisual. Each condition was presented once in a block of 90 trials. The externally generated condition was identical, expect participants passively viewed all stimuli, which were presented at a rate of approximately once every 3 s.

Neuroimaging acquisition

Neural activity was recorded continuously during each block from participants in a comfortable sitting position using a 4D Neuroimaging Magnes® 3600 WH system (Neuroimaging Inc., San Diego) with 248 magnetometers in a magnetically shielded room. The acquisition sample rate was 1017 Hz, and data were acquired. The MEG signal was high pass filtered at 0.1 Hz and digitised at 508 Hz. Data from three bad channels were excluded from the data. Participants were asked to remain as still as possible and were continuously monitored by video camera. They were also instructed to minimize blinking during the presentation of visual stimuli, and instead to synchronize their blinks with the simultaneous button press for selecting responses. Eye movements were monitored using a SR-research remote Eyelink 1000 system (SR Research Ltd., Ontario Canada), signals were sampled synchronously at 1017.25 Hz, with online 0.1 Hz High-pass filtering. Calibration of eye fixation was performed at the beginning of each run using a 9-point fixation procedure.

MEG-MRI Co-registration

Prior to data acquisition, participants head shape was 3D-digitized using a Polhemus stylus (FASTRAK®, Polhemus Inc., VT, USA digitisation system). This was utilized for accurate co-registration for source space analyses with the landmark locations matched on the individual participants' anatomical magnetic resonance (MR) T1 –weighted structural scan with 1 mm isotropic resolution. This was implemented using a surface-matching technique adapted from Capilla, Schoffelen, Paterson, Thut, & Gross (2014). This semiautomatic procedure provides the best fit between subjects scalp surface extracted from the anatomical MRI image and the head shape digitised in MEG. Five spatially distributed head coils (placed on the right and left pre-auricular locations, Cz, nasion, and inion) provided landmark positions with reference to the MEG sensors and allowed monitoring of head movement. Head movements values were < 0.5 cm in all participants.

The MR structural images were acquired with a 3.0-T Trim Trio Scanner (Siemens, Erlangen, Germany) using a 12-channel head coil. High-resolution T1-weighted structural images were collected in 192 axial slices and isotropic voxels (1 mm³; field of view: 256 × 256 mm² matrix, TR = 1900ms, TE = 2. 92ms, time to inversion = 900ms, FA = 9°). This was subsequently transformed into a standard Montreal Neurological Institute standardised brain (MNI152) (5mm) (Jenkinson & Smith, 2001) to allow for group level analyses.

4.3 MEG Analysis

Data analysis of the MEG signal was performed using the FieldTrip software package (Oostenveld & Fries, 2010); see http://fieldtrip.fcdonders.nl/), in-house Matlab code in accord with current MEG guidelines (Joachim Gross et al., 2013), and CircStat: a Matlab Toolbox for Circular Statistics (Berens, 2009).

Preprocessing

The preprocessing of the MEG signal was performed using the following procedures. First, trials with inter-trial intervals less than 1500 ms were discarded (mean of 4.4 % of trials removed from each condition). The signal was epoched in trials of 2 s in length time-locked to stimulus onset (1 s pre-stimulus). Secondly, before visually inspecting MEG traces for artefacts, the DC offset and linear trends were removed to facilitate visualisation. Four excessively noisy sensors were discarded from all subjects' analysis. Additionally, trials contaminated with physiological (eye blinks, eye movements) or non-physiological (squid jumps) were discarded. Thirdly, signals recorded from by the MEG reference channels were used to linearly remove electromagnetic interference from outside the scanner, implemented using the "ft_denoise_pca" function in FieldTrip (Johnson et al., 2003) and post-acquisition, data were DC offset to ensure a zero mean signal on all sensors. Finally, trials containing

large signal variance that corresponded to cardiac artefacts were projected out of the MEG signal using Independent Component Analyses ("fastica" algorithm implemented in FieldTrip). After all pre-proceeding stages, because trial numbers are known to influence analyses methods crucially (Hanslmayr et al., 2013), trial numbers were equated across the all conditions with the lowest number of trials in any one condition and randomly selecting the same number of trials from the remaining conditions.

Sensor-level analysis

Before calculating the event-related averaging at sensor space, the artefact-free neuromagnetic time series data were bandpass filtered in the range of 1–30 Hz on the preprocessed data. Event-related fields (ERFs) were baseline corrected to the 500 ms period immediately preceding the stimulus onset for each condition. From the fields measured by the magnetometers, the approximation of the MEG planar gradient was computed using Fieldtrip's *ft_megplanar* function. Considering planar gradient data simplifies the interpretation of the sensor-level results, as the maximal signals are located above neural sources (Bastiaansen & Knösche, 2000; Hari et al., 1997). For the ERFs, the combined resulting horizontal and vertical planar gradients were calculated by singular value decomposition per channel location using the fields from the sensors and both first- and second-order neighbouring sensors (maximum distance of 7.4 cm) and using the "sincos" approach implemented in Fieldtrip. This projected the data along the largest magnitude direction above a given source (M Hämäläinen et al., 1993). For the spectral analyses, we computed metrics separately for the horizontal and vertical planar gradients, and combined the two by computing the sum.

Evoked response analysis

All non-rejected trials were sorted according to the respective conditions. The ERFs elicited for each stimulus category were aligned to stimuli onset, then these were computed separately for each participant and averaged in the time range between 700 and 700ms, and subsequently, the grand-average across all participants was computed. Evoked responses were baseline corrected between -700 and 700 ms. Loci of auditory and visual evoked activation were defined statistically by comparing the group-level differences difference between baseline (pre-stimulus) and post-stimulus activity in the passive conditions (as these conditions are hypothesised to produce the largest evoked responses). This was achieved by using nonparametric cluster-based Monte Carlo permutation *t*-tests (Maris & Oostenveld, 2007). To correct for multiple comparisons, the sensors that show the same effect and were exceeding the critical threshold value and neighbouring in the sensor array (separated by <5 cm) were grouped together. This approach is validated due to the principle that a physiological source produces the maximal planar gradient field signals in a contiguous group of sensors that are located

directly above the neural sources (Bastiaansen & Knösche, 2000; Matti Hämäläinen et al., 1993; Hari, 1993).

Sensors were selected for which the t statistics of the difference between conditions exceeded an a priori threshold (corrected $p < 0.05$, two-sided). Next, the selected samples were based on spatial adjacency, and the sum of the t statistics within the cluster was used as the cluster level statistic. Subsequently the cluster with the maximum statistic was used as a cluster level statistic (nonparametric statistics). By randomising the data across the two conditions and repeating the test statistic 2,000 times, we obtained a reference distribution to evaluate the statistic of the actual data. The p value was estimated according to the proportion of randomisations of the reference distribution exceeding the observed maximum cluster-level statistic (the Monte Carlo p value). The results of these statistics would allow the demarcation of significant sensor-clusters to be used as regions of interest (ROI) from which four sensors were chosen to be selected for further analyses. The ROIs were, left- and right- auditory cortex and one in the visual cortex. The sensors were chosen based on their maximal responses at the M100 component latency (95-120 ms post-stimulus). Across subjects, we used data from the MEG sensors with the largest ERF (characterised by the N1m-P2m complex) over the three ROIs.

To test for significant differences between Active and Passive condition in the ERF data, the mean amplitudes of the ERF responses were then computed with a two-way repeated-measures analyses of variance (RM-ANOVA). To this end, a 2 (stimuli generation (GEN) type: Active, Passive) x 3 (stimulation (STIM) type: Auditory, Visual, and Audiovisual) factors design was used. A general alpha criterion of $p < 0.05$ was used for statistical comparisons. p-values we corrected for multiple comparisons using the Bonferroni-Dunn criterion.

Spectral analyses

To measure the time-frequency representation (TFR) of power and linear phase-locking value (LPLV) or linear inter-trial coherence (LITC) (Lachaux & Rodriguez, 2000; Makeig, Westerfield, Jung, et al., 2002b; Tallon-Baudry & Bertrand, 1996) metric, we used a sliding time window fast Fourier transform (FFT) approach. The frequencies of interest ranged from 2 to 30 Hz in steps of 1 Hz. The time window was always such that it fit exactly four cycles of the frequency of interest, and it slid over the time axis in steps of 50 ms. Each instance of the sliding window was multiplied by a Hanning taper and Fourier-transformed, whereby yielding a time-resolved complex Fourier spectrum. Power values $pow_n(f, t)$ for trial n, frequency f, and time point t were computed by squaring the absolute value of the Fourier coefficients $c_n(f, t)$, i.e., $pow_n(f, t) = |c_n(f, t)|^2$ and were averaged over trials. The Fourier analyses revealed the instantaneous phase and amplitude estimates for each single trial. Next, the PLV was calculated (Tallon-Baudry & Bertrand, 1996)(an index that represents the degree of

phase synchrony that is bounded between zero and one). This allows for the distinction between phase-locked (evoked) and non-phase-locked (induced) neural responses. This measures, at a given time point, the variability across trials of the phase difference either within a cortical area or between two sensors across cortical regions. ITLC was computed by taking the absolute value of the mean of the complex Fourier phase ɸ values across N trials, after complex normalising, and taking the absolute value represented by $||$, as follows;

$$lITC = \left| \frac{\sum_{i=1}^{n} c_n\,(f,t)}{\sqrt{n \sum_{i=1}^{n} |c_n\,(f,t)^2|}} \right|$$

(1)

The TFR show power as a function of time and frequency averaged over trials within each condition and a logarithmic transform was applied to reduce inter-subject variability in the power estimates. The difference between two conditions (i.e., active vs. passive) was calculated as a ratio of log-transformed power (log-ratio). Since ratio data are inherently non-normal because of lower bounding, a log transform was used for analysis. A log ratio of less than zero indicates suppression whereas a value of zero indicates no suppression and values greater than zero indicate enhancement.

Spectral statistics

In order to test for significant differences between TFRs of PLVs and log-power between poststimulus and prestimulus (i.e., baseline) activity windows, each were subjected to permutation statistics described above. To this end, the 19 prestimulus windows (-750 ms to 0 ms) and the 19 poststimulus windows (0 ms to 750 ms) of the TFRs from the 19 different subjects were randomly permuted 2,000 times. For each iteration of the test the maximum differences was taken as the threshold for the TFRs. Using the maximum statistics take into consideration multiple comparisons issue (Nichols & Holmes, 2002). The poststimulus outcome for both the ERF and log-power analyses can be either positive or negative relative to baseline. To this end, a two-tailed threshold was used to determine the statistical significance (all p-values were reported as significant if $p \leq 0.05$ or $p \geq 0.95$). For the analyses of phase alignment, a one tailed method was used to determine statistical significance (all p-values were reported as significant if $p \leq 0.05$) as this would enable the identification of increases in poststimulus phase consistency. A similar method was carried out to assess significant differences in the TFRs of PLV and log-power between Active and Passive conditions. Here the 19 Active windows (-750 ms to 750 ms) and the 19 Passive windows (0 ms to 750 ms) of the TFRs from the 19 different subjects were randomly permuted 2,000 times.

Nonlinear multisensory effects

In order to assess whether any unisensory driven modulations interacted non-linearly with multisensory stimulation we applied a variant model of the linear additive criterion model

$[AV \ vs. (A + V)]$ described in Mercier et al., (2015) and discussed in detail in previous studies (Kayser, Petkov, & Logothetis, 2008; Mercier et al., 2013; Stein, 1998). Using the model we could assess if the activity evoked in the multisensory conditions differed from the summation of the activity evoked by the two unisensory stimuli (auditory and visual). It was then possible to measure if these nonlinear multisensory effects were supra additive or subadditive - if the multisensory conditions were larger or smaller, respectively, than the sum of the unisensory conditions. To establish whether the differences between the multisensory conditions and the summation of the two unisensory conditions were statistically significant, a cluster-based nonparametric randomisation procedure described in detail above was used. However, data in the TFR domain were averaged over ROI sensors, and the frequency boundaries of the theta, alpha, and beta bands were based on those widely accepted and published EEG/MEG methodology (Niedermeyer & Silva, 2005). Clusters were selected for which the t statistics of the difference between conditions exceeded an a priori threshold (corrected $p < 0.05$, two-sided).

Brain-behaviour regresion analysis

We conducted regression analyses to test the interactions between modulations in SA effect (i.e., oscillatory power difference between Active vs, Passive) and the questionnaire data scores, and the possibility that the SA effect is mediated by frequency as a function of time. Data from the questionnaire scores and TFRs of SA effect were analysed using procedures in Fieldtrip using the ft_freqstatistics function. The procedure regresses the TFR of SA effect on the predictor, which is the participants' questionnaire scores, at each corresponding temporal-point in the subject-wise activation time course using the independent samples regression coefficient t-statistics. Significance was assessed using non-parametric permutations procedures (2000 Monte Carlo random iterations, α = 0.05) described earlier. Group-level analyses resulted in β weights for each time-frequency (1 to 30 Hz) clusters in a selected ROI.

Robust correlation and SA effect on ERFs

All correlation coefficients and corresponding *p*-values were computed using Spearman correlation. Correlations resulting in significant *p*-values were quantified using Robust Correlation (Rousselet & Pernet, 2012). This stringently assesses for false positive correlations using bootstrap resampling including six additional validation tests (see, Rousselet & Pernet, 2012). Only significant correlations are shown, where significance were corrected for multiple comparisons using a family-wise error rate using maximum statisitcs through permutation tests (Groppe, Urbach, & Kutas, 2011).

4.4 Results

Sensory attenuation of evoked reponses

The auditory evoked fields data replicated the characteristic attenuation effect (SA) in response to both multisensory (MS, audiovisual stimulation) and unisensory auditory stimuli. Figure 4.2 shows the ERFs across conditions, and figure 4.3 shows the RM-ANOVA interactions.

Results for the left auditory ROI (LAC):

The results for the left ROI showed a significant main effect of stimuli generation type (GEN) ($F_{1,19} = 6.35 \ p < 0.05, \eta_p^2 = 0.25$), this revealed that Passive (P) GEN-type was significantly higher than Active (A). There was a significant main effect of stimulus-type (STIM; $F_{2,38} = 26.86, p < 0.001, \eta_p^2 = 0.59$). *Contrasts* revealed that MS had higher amplitude values compared with Aud ($F_{1,19} = 33.38, p < 0.01, \eta_p^2 = 0.38$) whereas Aud ($F_{1,19} = 29.28, p < 0.001, \eta_p^2 = 0.61$) had significantly higher amplitude than Vis, and MS contrasted with Vis showed higher amplitude difference ($F_{1,19} = 28.26, p < 0.001, \eta_p^2 = 0.60$). Finally, there was a significant two-way interaction between the two factors for GEN$^\times$ STIM type ($F_{2,38} = 20.55, p < 0.001, \eta_p^2 = 0.52$). This indicates that Gen-type had different effects on evoked amplitudes depending on the STIM-type. To break down the interaction, *post hoc* c*ontrasts* were performed, this revealed that P-MS had significantly higher amplitude than A-MS ($F_{1,19} = 12.01 \ p < 0.001, \eta_p^2 = 0.39$) this demented that the SA effect in multisensory stimuli conditions, and similarly P-Aud contrasted with A-Aud ($F_{1,19} = 11.92 \ p < 0.01, \eta_p^2 = 0.39$) showing the SA effect. Whereas there was only a trend towards significance, interestingly showing the opposite facilitation effect, with higher amplitude in A-Vis compared with P-Vis ($F_{1,19} = 3.26 \ p = 0.09, \eta_p^2 = 0.15, ns$).

Next, we tested if there were differences between multisensory responses and unisensory responses; first there was significantly higher amplitude in A-MS contrasted with A-Aud ($F_{1,19} = 7.59 \ p < 0.05, \eta_p^2 = 0.29$), and P-MS with P-Aud ($F_{1,19} = 8.83 \ p < 0.01, \eta_p^2 = 0.32$). We did not investigate the contrast of MS responses to visual stimuli in the auditory ROI. Finally, we tested if the magnitude of the SA effect was significantly different in multisensory stimuli compared to unisensory auditory stimuli, the results show that there is no difference ($F_{1,19} = 1.84 \ p = 0.19, \eta_p^2 = 0.09, ns$).
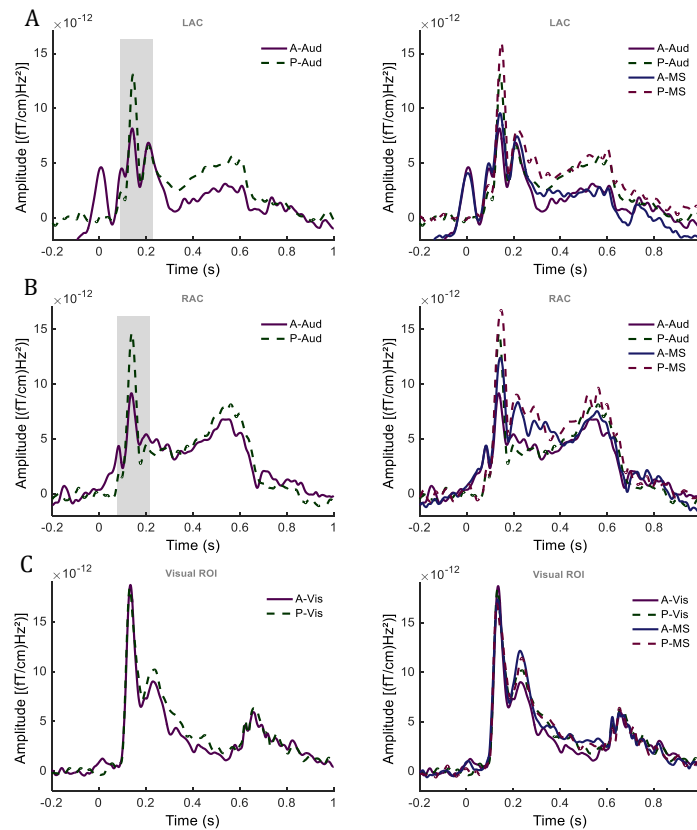
Figure 4.2. Grand average event-related fields. Grand averaged ERF planar gradient waveforms associated with the different conditions superimposed. **A)** LAC, **B)** RAC, **C)** Vis ROIs showing the unisensory Active (solid lines) vs. Passive (dotted lines) conditions left panel and in the right panel but with the multisensory conditions included. ERFs are time-locked to stimulus onset (t = 0). Time t = 0 ms represents stimulus onset. The Passive conditions evoked larger N100 (here, 150 ms) compared to Active conditions, replicating the characteristic SA effect in both LAC and RAC, but not Vis ROI. Grey shaded area demarcates significance at p < 0.05 (FDR corrected).
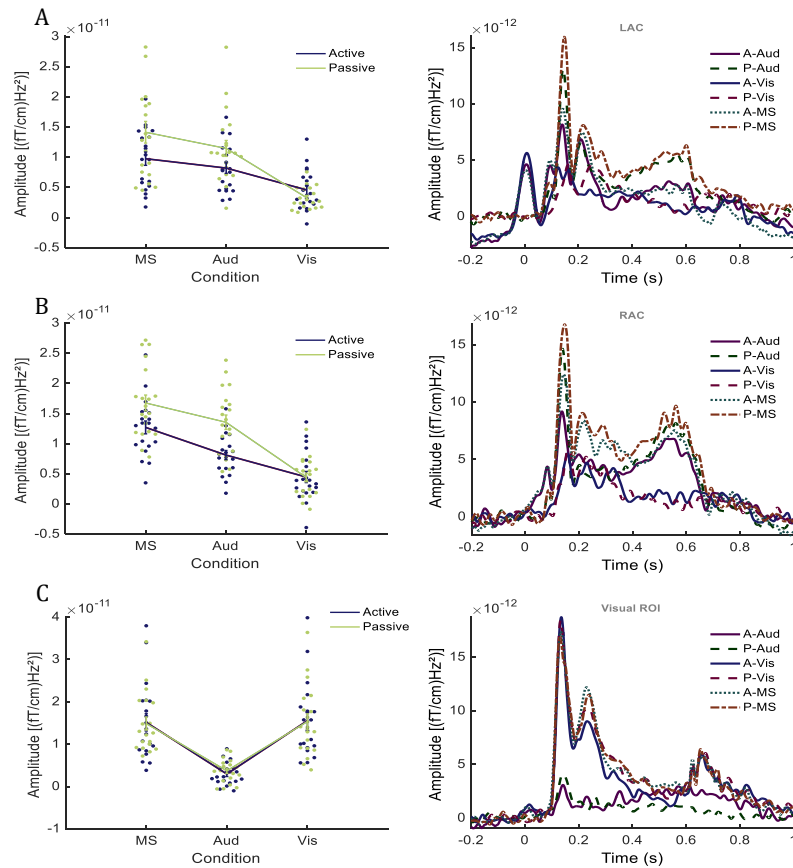
Figure 4.3. RM ANOVA of grand average ERFs. Right panel showing grand averaged ERF planar gradient waveforms associated with the different conditions superimposed. **A)** LAC, **B)** RAC, **C)** Vis ROIs showing the unisensory Active (solid lines) vs. Passive (dotted lines) conditions. ERFs are time-locked to stimulus onset (t = 0). Left panel shows scatter plots with individual participants ERF amplitude values averaged over the N1 component (t = 80-150 ms). Time t = 0 ms represents stimulus onset. Solid lines, blue and green show the results of the RM-ANOVA interaction for Active and Passive conditions respectively. **A)** LAC, **B)** RAC, show significant difference interaction between MS and Aud conditions. Error bars show represent group averages ± SEM. Significant differences in between Active and Passive MS and Aud conditions replicate classical SA effect.

Results for the right auditory ROI (RAC):

In the right ROI there was a significant main effect for GEN ($F_{1,19} = 16.68\ p < 0.001, \eta_p^2 = 0.47$). There was a significant main effect of STIM ($F_{2,38} = 67.76, p < 0.001, \eta_p^2 = 0.78$). Further *contrasts* revealed similar results to the left ROI, with higher amplitude in MS compared to Aud ($F_{1,19} = 98.43, p < 0.001, \eta_p^2 = 0.84$) and Aud contrasted with Vis ($F_{1,19} = 54.35, p < 0.001, \eta_p^2 = 0.74$). There was a significant two-way interaction between GEN×STIM ($F_{2,38} = 7.96, p < 0.01, \eta_p^2 = 0.30$). To unpack this interaction as before, *post hoc contrasts* were performed, this revealed that P-MS had significantly higher amplitude than A-MS ($F_{1,19} = 12.43\ p < 0.01, \eta_p^2 = 0.40$), and P-Aud contrasted with A-Aud ($F_{1,19} = 15.38\ p < 0.01, \eta_p^2 = 0.45$), both these results showing the SA effect. The evoked responses to visual stimuli show the same facilitation effect seen with higher amplitude in A-Vis compared with P-Vis but not significant ($F_{1,19} = 0.01\ p = 0.92, \eta_p^2 = 0.01, ns$). As before, next we tested if there were differences between multisensory responses and unisensory responses; first there was significantly higher amplitude in A-MS contrasted with A-Aud ($F_{1,19} = 30.00\ p < 0.001, \eta_p^2 = 0.61$), and P-MS with P-Aud ($F_{1,19} = 6.89\ p < 0.05, \eta_p^2 = 0.27$). Finally, we tested if the magnitude of the SA effect was significantly different in multisensory stimuli compared to unisensory auditory stimuli, the results show that there is no difference ($F_{1,19} = 0.91\ p = 0.35, \eta_p^2 = 0.05, ns$).

Results for the visual ROI (Vis):

There was no significant main effect for GEN ($F_{1,19} = 0.03\ p = 0.87, \eta_p^2 = 0.02, ns$) but there was a significant main effect for STIM ($F_{2,38} = 45.96, p < 0.001, \eta_p^2 = 0.71$). *Contrasts* revealed that MS was not significantly different from Vis ($F_{1,19} = 0.25\ p = 0.63, \eta_p^2 = 0.01, ns$), but Aud was significantly different from Vis ($F_{1,19} = 49.42, p < 0.001, \eta_p^2 = 0.72$). Finally, there was no significant interaction GEN × STIM ($F_{2,38} = 0.34, p = 0.72, \eta_p^2 = 0.02$). Next we tested if there were differences between multisensory responses and unisensory responses; first there was no significantly higher amplitude in A-MS contrasted with A-Aud ($F_{1,19} = 0.12\ p = 0.73, \eta_p^2 = 0.01$), and P-MS with P-Aud ($F_{1,19} = 0.18\ p = 0.68, \eta_p^2 = 0.01$). With these results showing no difference between multisensory and unisensory responses in the visual ROI, we did not investigate further any difference in SA magnitude differences. Across all three ROIs there is higher ERF magnitude responses to both self and externally generated stimuli for the multisensory conditions as compared to the unisensory conditions.

Sensory attenuation of spectral data

To assess the SA effects in the spectral analyses, the differences between Active and Passive conditions (SA effect) across the three stimulation types (MS, Aud, and Vis) were computed for both linear PLV TFRs and log-power TFRs, and ROI (see Methods for details). All *p*-values for cluster permutation distribution reported as significant at $p < 0.05$, maximum *t*-statistics at specific time

points and frequency are reported in brackets, this give some indication where the main effect occur in the cluster. Positive t-statistics indicates that the Active condition had significantly higher activation (event-related oscillations) compared to the Passive condition, whereas negative t-values indicate lower activation in active compared to passive condition.
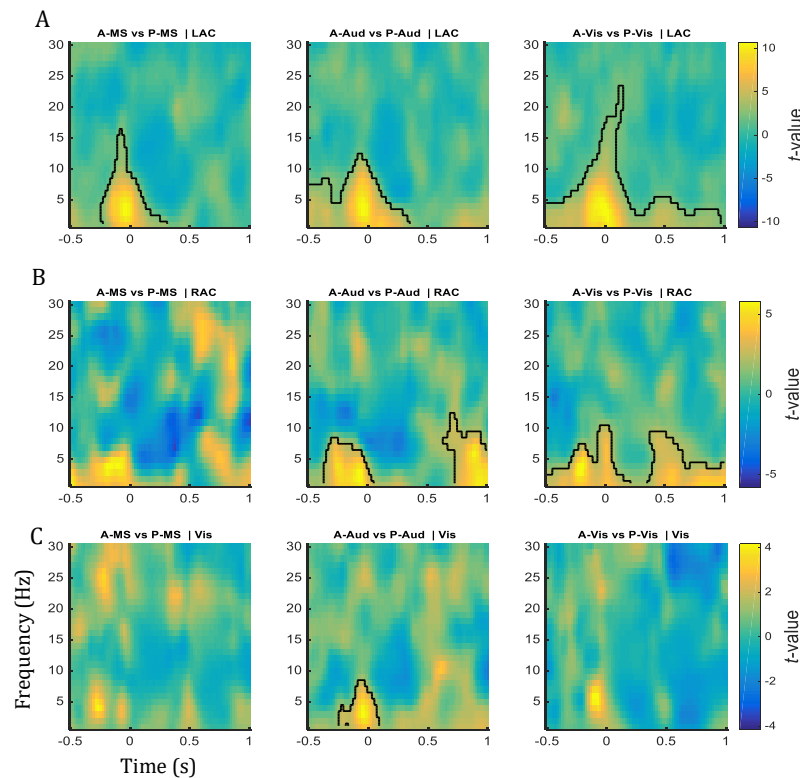
Figure 4.4. Linear PLV- Active vs. Passive. Grand average time-frequency representations (TFR) of non-parametric t-statistics (N=19) for the linear PLV contrast between Active (A-) and Passive (P-) conditions. Data averaged over planar gradient channels in each **A)** LAC, **B)** RAC, and **C)** Vis ROIs. TFR statistics show black contours which demarcate significant clusters with a threshold of p < 0.05 threshold (cluster corrected), using non-parametric cluster permutation tests. Positive t-values (shown in yellow) indicate significantly higher phase concentration between conditions (Active > Passive). Time t = 0 ms represents the position of the onset of stimulus presentation relative to the -500 to 1000 ms analyses window.

Linear Phase-locking

Figure 4.4 shows the results show significant clusters representing a difference between Active vs. Passive linear PLV. Figure 4.4.A shows that all active versus passive contrasts in left auditory cortex are dominated by significantly higher phase locking at the time of movement onset in the active condition. Notably, this effect is absent in the right auditory cortex ROI. This effect can be clearly attributed to the movement related evoked component in left motor cortex (contralateral to the moving finger). No significant and systematic pattern can be observed in visual sensors.
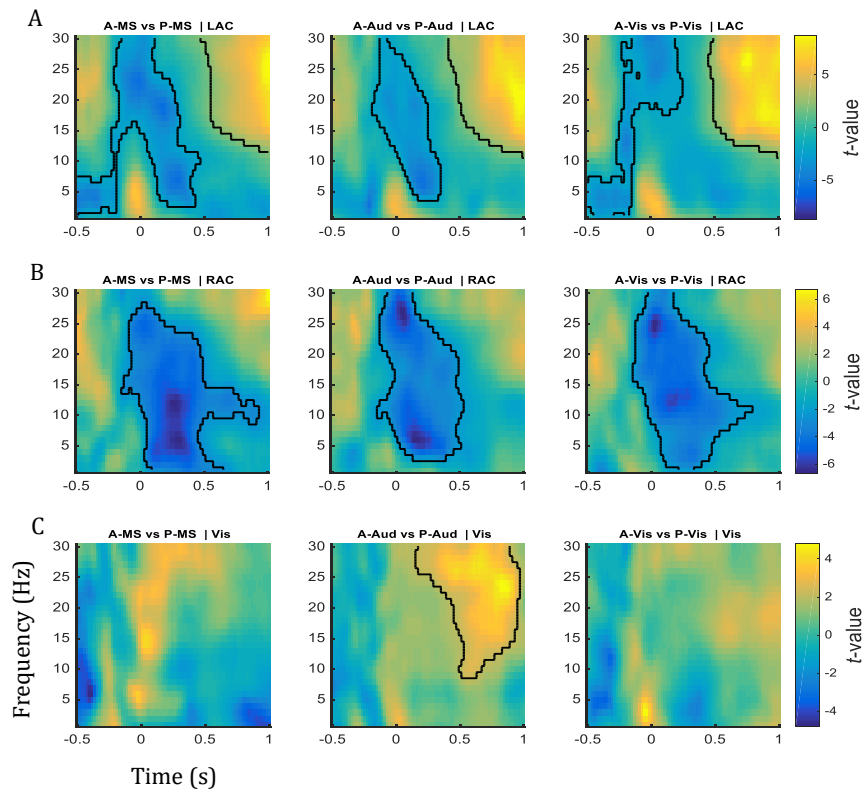
Figure 4.5. Log ratio power - Active vs. Passive. Grand average time-frequency representations (TFR) of non-parametric t-statistics (N=19) for the linear PLV contrast between Active (A-) and Passive (P-) conditions. Data averaged over planar gradient channels in each **A)** LAC, **B)** RAC, and **C)** Vis ROIs. TFR statistics show black contours which demarcate significant clusters with a threshold of p < 0.05 threshold (cluster corrected), using non-parametric cluster permutation tests. Positive t-values (shown in yellow) indicate significantly higher power between conditions (Passive > Active). Time t = 0 ms represents the position of the onset of stimulus presentation relative to the -500 to 1000 ms window analyses window.

Log ratio power

Figure 4.5 shows the results for the contrast of power between Active and Passive conditions reveal generally similar clusters patterns in the LAC and RAC. There is a negative cluster between about 0-500 ms in broad frequency band. In addition, the LAC shows a beta rebound from making finger abductions. This is seen as a positive cluster between 500-1000 ms at 15-30 Hz. This is due to the fact that LAC channel cluster is close to the left motor cortex. In visual sensors, there was only a significant cluster in the A-Aud vs. P-Aud comparison at about 400-1000 ms between 10-30 Hz. These results show that there is consistently lower power in the Active condition compared to the Passive in the auditory ROIs in the post stimulus period (A-MS, A-Aud, A-Vis < P-MS, P-Aud, P-Vis).

Multisensory vs. Unisensory

To assess the SA effects in the spectral analyses, the differences between Active and Passive conditions (SA effect) across the three stimulation types (MS, Aud, and Vis), both linear PLV and log-power TFRs, across ROIs were analysed (see Methods for details). All p-values for cluster permutation distribution reported as significant at $p < 0.05$, maximum t-statistics at specific time points and frequency are reported in brackets, this give some indication where the main effect occur in the cluster. Positive t-statistics indicates that the Active condition had significantly higher activation (event-related oscillations) compared to the Passive condition.

Linear Phase-locking

In figure 4.6 we observed a statistically significant difference in linear PLV between both the A-MS and P-MS vs. the unisensory conditions across the majority of ROIs. The results show that in the comparison between multisensory and auditory-alone conditions across both LAC and RAC, there are similar clusters. This is observed for both active and passive conditions. Specifically, there is a peak in the clusters around alpha (8-12 Hz) around 300 ms to 500 ms time window. Whereas the same comparison of multisensory with visual-alone conditions in both auditory ROIs, we see two peaks in the cluster. One that is in the theta range (7 Hz) appearing after stimulus onset. The other peak appears around 600 ms in the low-theta (4 Hz) frequency range. In the visual sensors, we observed only significant clusters in the multisensory conditions compared to the auditory unisensory conditions. Both showing broad activity differences between 0-1000 ms with broadband low-frequency range between 1-30 Hz.

Log ratio power

Figure 4.7 shows the results for log ration power. Here we observe a consistent pattern of lower power at around 10-30 Hz in the multisensory compared to the auditory unisensory conditions; but higher power just after stimulus onset at around 5 Hz. In the LAC, the comparisons between A-MS vs. A-Aud show a significant cluster around 300-600 ms between 7-30 Hz. In the A-MS vs. A-Vis, there was a positive cluster around 0-300ms between 1-15 Hz. In the passive conditions, P-MS vs. P-Vis there was a significant positive cluster from 0-600 ms around 4 Hz, and a negative cluster around 300-500ms at 7-30 Hz, similar to the active comparison, for the P-MS vs. P-Vis there was a significant positive cluster around 0-600 ms from 1-30 Hz but had a low frequency peak. In the visual sensors, the results reveal similar patterns to that seen in the auditory sensors. However, cluster statistics were not able to detect any significant differences between P-MS and P-Vis conditions.
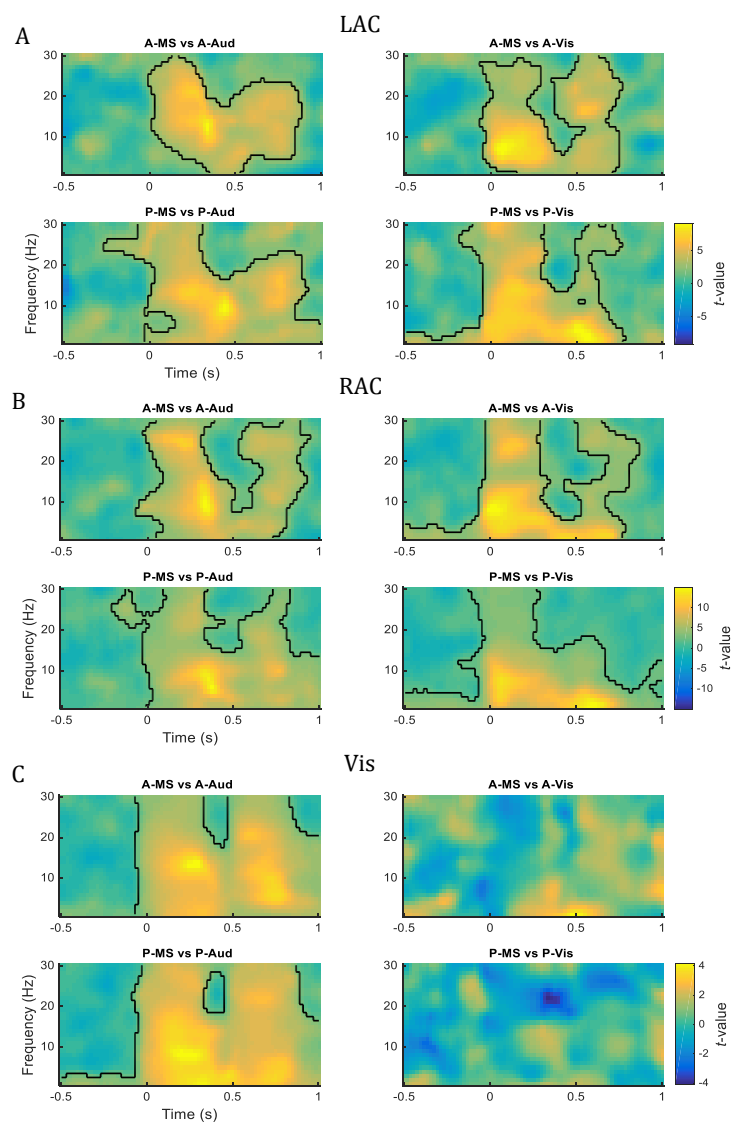
Figure 4.6. Multisensory indices in LPLV. Grand average time-frequency representations (TFR) of non-parametric t-statistics (N=19) for the LPLV contrast between multisensory Active (A-) and Passive (P-) conditions. Data averaged over planar gradient channels in each **A)** LAC, **B)** RAC, and **C)** Vis ROIs. TFR statistics show black contours which demarcate significant clusters with a threshold of p < 0.05 threshold (cluster corrected), using non-parametric cluster permutation tests. Positive t-values (shown in yellow) indicate significantly higher phase concentration between conditions (Multisensory > Unisensory). Time t = 0 ms represents the position of the onset of stimulus presentation relative to the -500 to 1000 ms analyses window.
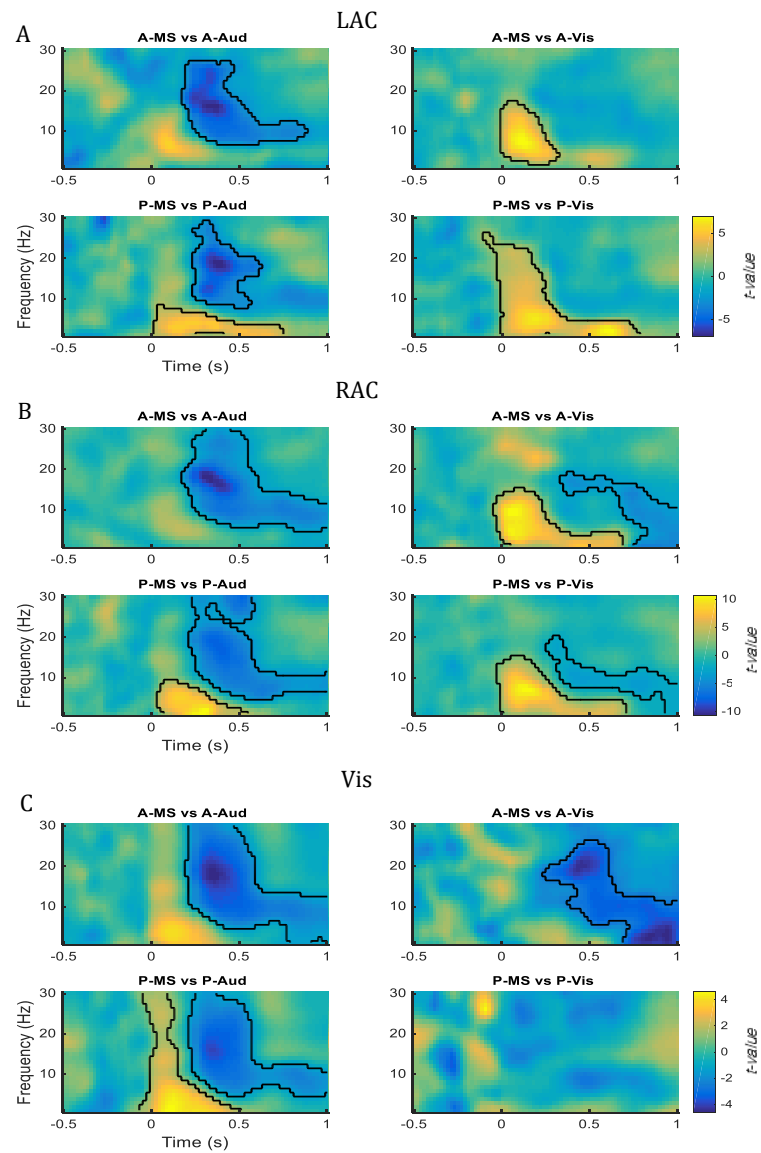
Figure 4.7. Multisensory indices in power. Grand average time-frequency representations (TFR) of non-parametric t-statistics (N=19) for the log power contrast between multisensory Active (A-) and Passive (P-) conditions. Data averaged over planar gradient channels in each **A)** LAC, **B)** RAC, and **C)** Vis ROIs. TFR statistics show black contours which demarcate significant clusters with a threshold of $p < 0.05$ threshold (cluster corrected), using non-parametric cluster permutation tests. Positive t-values (shown in yellow) indicate significantly higher power between conditions (Multisensory > Unisensory). Negative t-values (shown in blue) represent the opposite. Time t= 0 ms represents the position of the onset of stimulus presentation relative to the -500 to 1000 ms window analyses window.

Linear additive model

In order to assess whether any unisensory driven modulations interacted non-linearly with multisensory stimulation we applied a linear additive criterion model $[AV \, vs. \, (A + V)]$. Using this model, we are able to detect if the relative contribution of multisensory stimulation is significantly higher than the addition of the two-unisensory stimulation conditions.

Linear Phase-locking

Figure 4.8., shows the linear PLV results show that this was indeed the case. We observed similar results across all three ROIs, significant positive clusters span broadband low frequency around two windows. One at approximately 100-300 ms and another at 600-800 ms window. In the LAC the active conditions reveal a negative cluster between -100-100 ms around 4 Hz and a large positive cluster, which approximately spans the frequency range between 4-25 Hz at approximately 300ms and 600 ms. In the passive conditions there is a broadband low-frequency positive cluster between 0-700 ms, with highest values around 500 ms at 3 Hz. The results in the RAC yield similar cluster patterns. In both these auditory sensors there is a clear peak around alpha at approximately 300 ms. In visual sensors there is a slightly higher peak at 14 Hz around 300 ms, in the passive conditions there is three peaks mainly around the 300 ms region around 2 Hz, 10 Hz, and 16 Hz. These cluster peaks seem to be representing the evoked component in the comparison.

Log ratio power

Figure 4.9., shows the power results reveal similar patterns across the ROIs that reflect the characteristic signatures of oscillatory evoked responses. These patterns generally consist of a positive cluster around theta to low-alpha frequency followed by a power decrease in slightly higher frequencies around alpha that spans into beta frequency. These results there show that difference of evoked responses in the linear model.

Cross-modal phase resetting

In order to estimate the effects of CMPR across the three ROIs and conditions, we measured if there was significant increase in phase locking from baseline in a non-primary processing modality following stimulation. We sought to quantify if there was significant increase in phase locking in the visual cortex following an auditory-alone stimulation and vice versa. To this end, we estimated the auditory response in the visual ROI and measured the response to visual stimulation in the LAC and RAC. This was done by measuring PLV, which indexes the phase concentration over a set of sensors (Lachaux & Rodriguez, 1999). Therefore, we may then infer possible functional connectivity between two ROIs as indexed by the CMPR model. This was calculated across all conditions and ROIs. Next, we sought to investigate the mechanisms underlying the ERF response components. Using time-frequency data we

could estimate whether increases in phase concentration were accompanied by increases in power. As discussed previously we computed the PLV across trials to reveal whether ongoing oscillations are reset via CMPR in non-primary processing ROIs after stimulation. Next we then assessed concomitant power to investigate whether phase resetting of ongoing oscillations was related to the characteristic ERF response, or occurred in the absence of power increases and reflected rather a modulatory mechanism.

PLV in cross-modal regions

Figures 4.10 - 4.13 show the PLV and power for cross-modal effects. For Active and Passive unisensory conditions (figures 4.10 – 4.11), analyses of PLV, time-locked to stimulus onset, revealed similar significantly strong positive clusters of phase synchrony across the three ROIs. Following visual–alone stimulation in both the Active and Passive conditions, we observed in the auditory ROIs strong phase synchrony in broadband low frequency band (1-30 Hz) across two time windows (~0-350 ms, ~500-800 ms), with the strongest phase-locking occurring around approximately 3-7 Hz. For the auditory response in the visual ROI, there was strong phase locking around 200-400 ms at approximately 4 Hz. The multisensory response in both auditory ROIs had similar pattern in the unisensory conditions. There was strong phase synchrony in broadband low frequency (1-30 Hz) across two time windows (~0-350 ms, ~500-800 ms), with the strongest phase-locking occurring around approximately 3-7 Hz.

Power in cross-modal regions

Power in the LAC and RAC for the active conditions for both multi- and unisensory conditions there is a clear positive cluster following stimulus onset that lasts for about 200ms and is in the range of 1-7 Hz and continues until 1000 ms but is confined to the mu rhythm. A negative cluster folds over the positive regions, revealing a significant decrease in power in all other time ranges and frequencies where there is no power increase. The one exception between the activation patterns between the ROIs is a second positive cluster between 300-1000 ms in the frequency range of 15-30 Hz, with strongest power at 15 Hz that is present only in the LAC. These power results show similar patterns in the Passive conditions for both multisensory and unisensory conditions. Here there is a small positive cluster following stimulus onset that is largest between 0-300 ms in the range of 1-6 Hz (but extends to 30 Hz in the multisensory condition), the cluster then continues until 1000 ms in the mu rhythm. The data revealed a negative cluster, which was largest between 400-600 ms in broadband low-frequency range (5-30 Hz), which then continued until 1000 ms in the frequency range between 5-15 Hz. These patterns of clusters were similar in the visual ROIs.
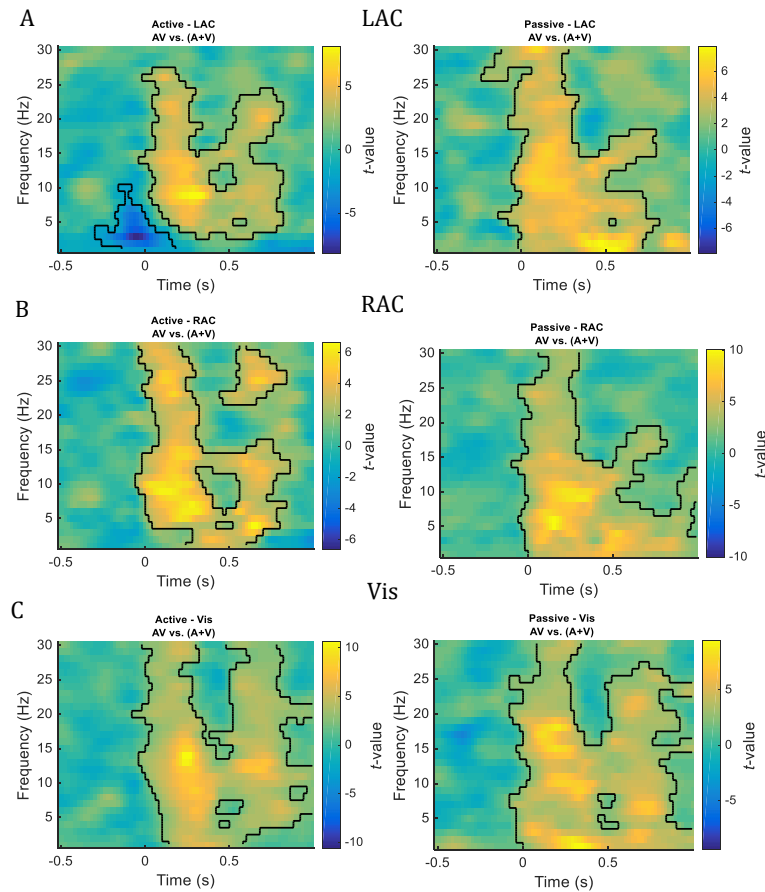
Figure 4.8. Nonlinear multisensory indices in LPLV. Additivity index of multisensory (MSI) effects on unisensory (US) LPLV assessed using the additive model [AV vs. (A+V)]. Grand average TFR of non-parametric t-statistics (N=19). Data averaged over planar gradient channels in each **A)** LAC, **B)** RAC, and **C)** Vis ROIs. TFR statistics show black contours which demarcate significant clusters with a threshold of p < 0.05 threshold (cluster corrected), using non-parametric cluster permutation tests. Positive t-values (shown in yellow) indicate significantly higher MSI indices between UN conditions combined. (MSI > US-Aud + US-Vis). Negative t-values (shown in blue).
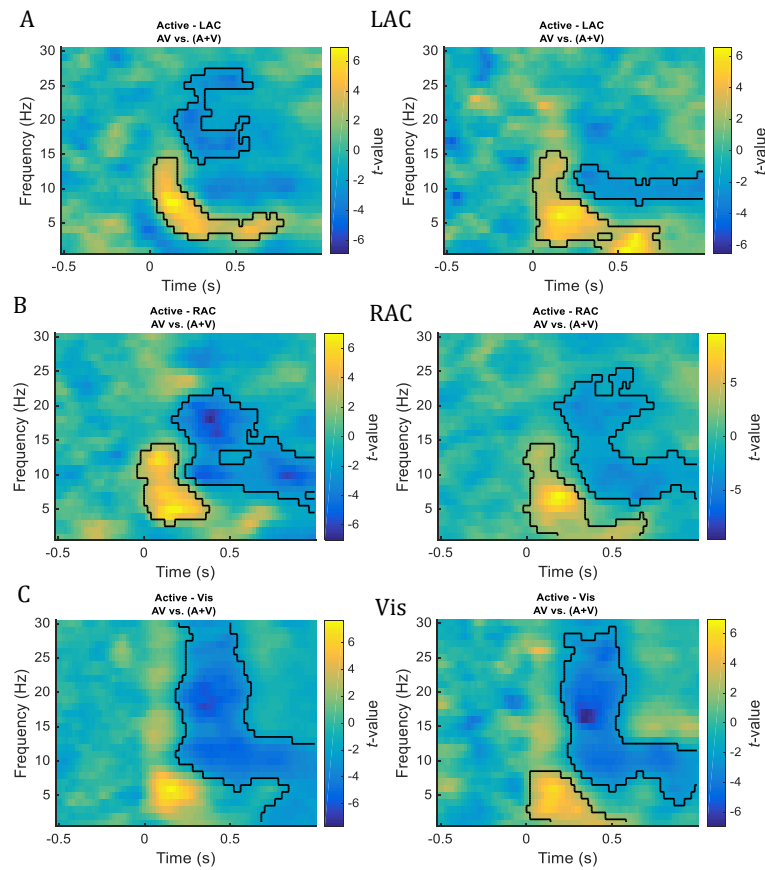
Figure 4.9. Nonlinear multisensory indices in power. Additivity index of multisensory (MSI) effects on unisensory (US) power assessed using the additive model [AV vs. (A+V)]. Grand average TFR of non-parametric t-statistics (N=19). Data averaged over planar gradient channels in each **A)** LAC, **B)** RAC, and **C)** Vis ROIs. TFR statistics show black contours which demarcate significant clusters with a threshold of p < 0.05 threshold (cluster corrected), using non-parametric cluster permutation tests. Positive t-values (shown in yellow) indicate significantly higher MSI indices between UN conditions combined. (MSI > US-Aud + US-Vis). Negative t-values (shown in blue).
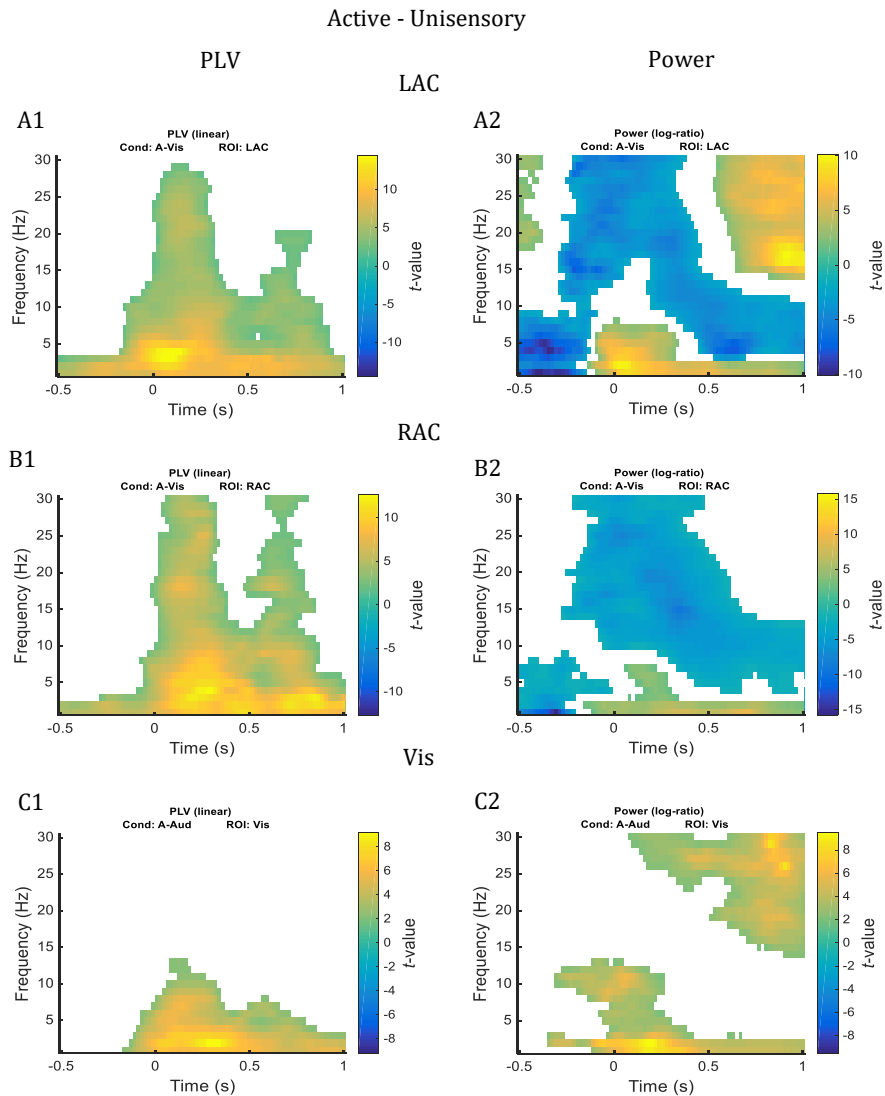
Figure 4.10. Cross modal indices of active unisensory condition. TFR plots show cross-modal phase concentration, with auditory responses in the visual ROI and contrariwise responses. Grand average time-frequency representations (TFR) of non-parametric t-statistics (N=19) for the LPLV contrast with baseline (t =-500 – 100 ms). Data averaged over planar gradient channels in each **A)** LAC, **B)** RAC, and **C)** Vis ROIs. Only significant clusters are shown in colour with a threshold of p < 0.05 threshold (cluster corrected), using non-parametric cluster permutation tests. Positive t-values (shown in yellow) indicate significantly higher phase concentration compared to baseline. Time t= 0 ms represents the position of the onset of stimulus presentation relative to the -500 to 1000 ms window analyses window.

Figure 4.12. Cross modal indices of active multisensory condition. TFR plots show cross-modal phase concentration, with auditory responses in the visual ROI and contrariwise responses. Grand average time-frequency representations (TFR) of non-parametric t-statistics (N=19) for the LPLV contrast with baseline (t =-500 – 100 ms). Data averaged over planar gradient channels in each **A)** LAC, **B)** RAC, and **C)** Vis ROIs. Only significant clusters are shown in colour with a threshold of p < 0.05 threshold (cluster corrected), using non-parametric cluster permutation tests. Positive t-values (shown in yellow) indicate significantly higher phase concentration compared to baseline. Time t= 0 ms represents the position of the onset of stimulus presentation relative to the -500 to 1000 ms window analyses window.

Passive - Multisensory

PLV   Power

LAC

RAC

Vis

Figure 4.13. Cross modal indices of passive multisensory condition. TFR plots show cross-modal phase concentration, with auditory responses in the visual ROI and contrariwise responses. Grand average time-frequency representations (TFR) of non-parametric t-statistics (N=19) for the LPLV contrast with baseline (t =-500 – 100 ms). Data averaged over planar gradient channels in each **A)** LAC, **B)** RAC, and **C)** Vis ROIs. Only significant clusters are shown in colour with a threshold of p < 0.05 threshold (cluster corrected), using non-parametric cluster permutation tests. Positive t-values (shown in yellow) indicate significantly higher phase concentration compared to baseline. Time t= 0 ms represents the position of the onset of stimulus presentation relative to the -500 to 1000 ms window analyses window.

Brain-behaviour regression analysis

Finally, we regressed the data scores from two questionnaires, the PDI and SQ, with the SA effect in the LAC and RAC. Figure 4.14 shows the results from the correlation between the ERF log power differences (SA effect) over the time-window of the M1 component (80 – 150 ms) with the PDI and SQ scores. The data correlated for the PDI scores reveals a significant negative correlation in both ROIs. This is in line with previous findings that report a negative correlation between PDI scores and SA effect.

The correlation for, LAC ($r_s = -.45$, $p < 0.05$, 95% CI $[-0.91\ 0.19]$) and RAC ($r_s = -.46$, $p < 0.05$, 95% CI $[-0.88\ 0.19]$). Correlation for the SQ reveal a negative correlation in both the LAC ($r_s = -.42$, $p < 0.05$, 95% CI $[-0.88\ 0.21]$) and RAC ($r_s = -.47$, $p < 0.05$, 95% CI $[-0.82\ 0.13]$). We did not compute correlations for the VIS ROI conditions, as the SA effect was not significant in this area.
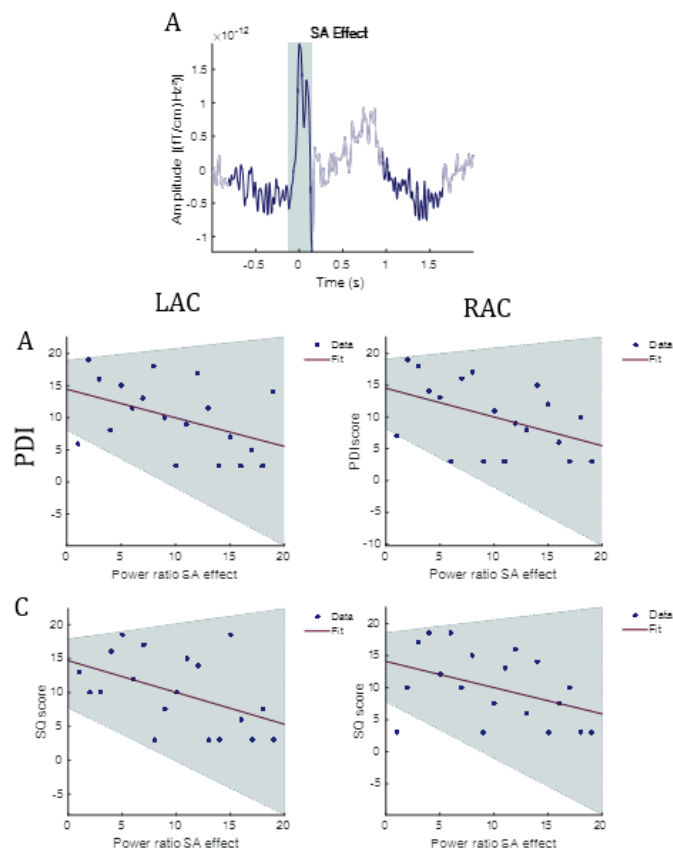
Figure 4.14. Correlation of SA effect and Questionnaires. Scatter plots (rank data) for Spearman's correlation between power SA effect and questionnaires scores (PDI and SQ). A) SA power data calculated as the difference between A-Aud and P-Aud conditions, averaged over sensors in the RAC, and LAC ROIs, for the time window covering the N1 component time window demarcated here as light blue shading in A (80-140 ms). Dark blue lines indicate significant difference between Active and Passive conditions using a paired samples t-test (p < 0.05). B) PDI scores, C) SQ scores.

4.5 Discussion

Here, we investigated the interplay of motor and multiple sensory areas using a well-established paradigm from the sensory attenuation literature (*for a review, see:* Hughes, Desantis, & Waszak, 2013). We contribute to the existing literate by performing spectral analysis with power and phase. Most previous studies use EEG. Here, with MEG we avoid the referencing problem (Davidson, 1988; Nunez, 2006; Pascual-Marqui et al., 2011), have denser sensor placement and (by computing planar gradient representation) can get relatively focal estimates of activation from small sensor groups. For the first time, to our knowledge, we study the motor-sensory interactions simultaneously in up to two sensory modalities. The paradigm therefore represents a novel combination of standard paradigms in two fields, the sensory attenuation field and the multi-sensory field.

Evoked component analyses

Our first hypothesis was confirmed. We were able to replicate the widely reported SA effect by comparing the magnitude differences in N1(m) ERF responses elicited by self-generated and externally generated unisensory stimuli. Interestingly, our second hypothesis was confirmed as well. To the best of our knowledge, we contribute novel findings for SA of motor-sensory interactions in two modalities simultaneously with multisensory stimulation. In both the unisensory and multisensory conditions, there is clear evidence for attenuation of the M1 response in both the LAC and RAC. However, there is no significant difference between, self- versus externally generated responses in the visual cortex.

The magnitude of the M100 component is only indirectly related to inter-areal phase resetting. Therefore, the modulation of M100 amplitude does not provide unambiguous evidence for cross modal (or motor-sensory) phase resetting. However, these suppression effects can be interpreted as being sensitive to cortical excitability and are likely to be at least partially induced by phase resetting. Our data revealed that the magnitude of the ERF amplitude values were significantly greater in the multisensory conditions compared to the unisensory across all three ROIs. Within the framework where the M100 component is an index of phase resetting, we may propose that the greater magnitudes observed in the multisensory conditions are a consequence of CMPR (Mercier et al., 2015; Moore, Bartoli, & Karunakaran, 2015; Schroeder et al., 2008). Interestingly, there is an opposing effect from motor regions, which leads to a reduction in the M100 component also seen in the multisensory condition. The motor-sensory modulation effectively diminishes the multisensory benefit. We speculate that this is a consequence of opposing modulatory effects on oscillatory phase in sensor areas. These concepts are discussed further in detail below.

Sensory attenuation is ubiquitous in the auditory domain. However, our data contribute to the sparse paradigms which investigate the SA effect in the visual domain (Cardoso-Leite & Mamassian,

2010; Gentsch & Schütz-Bosbach, 2011; Stenner et al., 2014). With only four studies to date (to our knowledge) investigating the effect in the visual domain using electrophysiology (Gentsch & Schütz-Bosbach, 2011; Hughes & Waszak, 2011; N. G. Mifsud et al., 2016; Schafer & Marcus, 1973). These studies provide mixed findings and use different experimental protocols. For example, Hughes and Waszal (2011), investigated visual evoked potential (VEP) responses to self-initiated visual checkerboards and reported increased P2 visual evoked amplitudes over an occipital region in contrast the attenuation effect reported in the auditory domain. Gentsch and Schutz-Bosbach (2011) measuring VEPs produced by arrow stimuli of self- and externally generated actions showed evidence for SA. However, the stimuli were embedded in a visual forced-choice response task where stimuli were subliminally primed. Interestingly, both these studies report no evidence for SA effect on N1 in classical visual responses over occipital regions but rather, self-generated visual stimuli resulted in attenuation of responses anterior regions.

In contrast, Benazet et al. (2016) using EEG, argued that they found evidence for attenuation of VEPs following visual feedback of real and delayed hand movements, creating a mismatch between predicted and actual visual consequences. However, this task does not follow the standard protocols of the classical SA paradigms, and this effect could be attributed rather to prediction error than to a difference between active and passive comparison. Interestingly, Mifsud et al. (N. G. Mifsud et al., 2016) found a facilitation of the N145 visual component for self- versus externally generated stimuli. This provides some of the first evidence to support a facilitation effect in VEP using standard protocols.

These inconsistent findings for electrophysiological SA effect in visual regions is in contrast to the large and consistent body of evidence in support for an N1 attenuation in the auditory domain. One possible explanation for not observing an M100 attenuation in the visual domain is the possibility that in contrast to the auditory and somatosensory domains SA may either be a weak response that is spatiotemporally dependent on the specific protocol of a particular paradigm or effectively the mechanism may not occur in the visual domain at all.

Time-frequency analyses

We computed the linear phase coherence between self- and externally generated stimuli. The data clearly shows a pre-to-post stimuli motor effect around stimulus onset around theta frequency range. This is consistent with what would be expected when analysing the phase of evoked potentials (M. Cohen, 2014; Lachaux & Rodriguez, 1999; Makeig et al., 2004). Cluster-based statistics done at sensory space may not be sensitive enough to discern specific localised phase effects related to the M100 evoked components in the these particular comparisons between conditions (Maris & Oostenveld, 2007). However, analyses of power spectrum reveals a clear structure in the data. Moreover, the stimulus phase-locked power responses directly evoked either due to CMPR or to stimulus evoked

effects gives some idea which frequency band could relate to phase resetting (Makeig et al., 2004). In contrast to passive conditions where stimuli are externally generated, in the active self-generated conditions participants were required to make finger abductions. Thus, any differences when comparing activation between active and passive conditions might be contaminated by motor processing. However, we are able to focus on the RAC, as these sensors are spatially distant enough not to avoid any signal leakage from motor activated areas. The RAC reveals a broadband power decrease at 100 ms and strongest T values at approximately 5 Hz, which corresponds to the M100 component. The MS condition show an additional peak around 10 Hz. This might be related to the visual stimulation projecting into auditory areas.

Interestingly, when comparing phase locking differences between multisensory and unisensory conditions we are able to discern the relative contribution of cross-modal effects within a specific sensory modality. As with phase effects discussed previously, we make the distinction here that phase locking differences observed between conditions can be related to phase resetting. The effects in auditory regions in general are quite consistent. While comparing the MS with the Vis condition, this reveals a clear significant difference peaking early at a frequency of 5Hz. This is the typical frequency in which evoked components are expressed. This difference is due to the presence of auditory stimulation from the MS condition that activates the auditory cortex. This pattern is mutually consistent for active and passive conditions across both LAC and RAC. Equally, there are consistent patterns seen for the comparisons between MS and Aud conditions, however, this pattern is dissimilar to the MS versus Vis comparisons. Here the strongest difference is at a higher frequency around 10 Hz and peaks later (300 ms). This is a likely signature of the cross-modal effect. In other words, the visual stimulus is modulating the phase in auditory areas. An effect that has been consistently demonstrated previously (Kayser & Logothetis, 2007; Lakatos et al., 2005; Luo, Liu, & Poeppel, 2010; Thorne & Debener, 2014). Interestingly, as previously seen, this signature is relatively similar in both LAC and RAC for the active and passive conditions.

Cluster statistics (using standard settings) leads to extended clusters in time and frequency that already starts shortly after stimulus onset. Given the inherent temporal smoothing in Hanning tapering in time-frequency analyses (Gröchenig, 2001), it is difficult to specify the exact onset of the cross-modal effect. However, it appears that the effect does begin shortly after stimulus onset and increases in strength until about 300ms. It is noteworthy, that the frequency is higher (10 Hz) compared to previous contrasts (5 Hz). This would suggest a modulatory component. We reason, that an auditory stimulus would indeed elicit a characteristic evoked component in the auditory cortex, that is represented in the time-frequency domain as a low frequency power and phase locking increase with strongest effects significantly below 10 Hz. Here, we observe a different effect of cross-modal integration, which originates from visual stimulation modulating phase locking in the auditory cortex.

This is interesting, because due to the segregation in the frequency domain both effects can be present at the same time, while modulating stimulus processing simultaneously in different ways. These findings are consistent with recent findings from EEG that show visually driven modulatory effects within low-frequency oscillations source localised to the auditory cortex (Thorne, Vos, & Viola, 2011).

Considering that the same signature is evident for both the active conditions suggests that the visual-auditory interaction is preserved. In addition, the motor cortex is activated at the same time, and conjointly modulates auditory evoked components. Could the motor regions modulate the auditory cortex at yet another frequency? Our data provided tentative evidence for this. It appears that in most of the active contrasts in the LAC and RAC, there is stronger phase-locking in the beta band (~ 25 Hz). The beta rhythm is indeed a prominent oscillation in motor areas (Engel & Fries, 2010; Pfurtscheller, Silva, & Lopes da Silva, 1999). However, the effects are seen in the contrast between two active conditions (e.g. active MS versus active Aud) and the evidence here is not fully conclusive. When considering the data from contrasts in the visual areas, it is clear that with the current data analyses methods, we were unable to reveal effects that could provide evidence for cross-modal phase resetting.

Although the cluster statistics did not reveal significant difference effects in visual regions, this does not necessarily dictate there is no evidence for CMPR from auditory-visual interactions. This could be a result of standard cluster statistics not being sensitive enough to reveal these effects at sensor space. Previous research would suggested that auditory responses in the visual cortex may be quantitatively different than visual-auditory interactions (Mercier et al., 2015; Perrodin & Kayser, 2015). Several EEG and MEG studies have reported early latency multisensory interactions that localise best to auditory cortex (Foxe, Morocz, & Murray, 2000; Mishra & Martinez, 2007; Raij et al., 2010; Thorne, Vos, & Viola, 2011), consistent with studies from human neuroimaging (Foxe & Wylie, 2002) and electrophysiological recordings in nonhuman primates (Schroeder & Foxe, 2002). Future, research would explore this further at sensor space.

A phase-reset of neural oscillations in primary auditory cortex by visual input is important underlying mechanism (Mercier et al., 2015; Perrodin & Kayser, 2015; Thorne & Debener, 2014). Recent research suggests that not only the visual, but also the motor system plays a critical role for an efficient adjustment to excitability fluctuation in the auditory cortex to expected upcoming events, which is in line with the forward model account (Doelling, Arnal, Ghitza, & Poeppel, 2014; Fujioka, Trainor, & Large, 2012; Morillon, Hackett, & Kajikawa, 2015). For example, Park et al. (2015), using MEG and transfer entropy measures (Schreiber, 2000) were able to show that frontal and motor area can modulate the phase of delta/theta oscillations in the auditory cortex. Specifically, they identified the left precentral gyrus as a source of top-down control for speech production. These findings support previous studies that show the involvement of motor areas in speech production and perception

(Pickering & Garrod, 2007; Sohoglu, Peelle, & Carlyon, 2012). Wilson et al. (2004) demonstrated that listening to natural speech activates motor areas involved in speech production. Here they proposed that the motor system possesses an efference copy of the expected auditory events and therefore can prepare the auditory cortex in such a way that oscillations arriving in the auditory cortex are at their high excitability phase exactly when relevant upcoming stimuli is expected to be processed (Arnal & Giraud, 2012).

Mercier et al. (2015) using simple detection task were able to provide supporting evidence found in speech perception and production studies. Here they demonstrated oscillatory phase resetting between motor and auditory cortices increased during the time interval between stimulus presentation and self-generated responses. They suggested their data is evidence for active communication between two central nodes of the sensorimotor network, which are recruited to perform the task. Moreover, they found super-additive multisensory effects on phase synchrony between motor and auditory cortices that were a consequence of faster synchronisation in the multisensory condition. This was supported by analysing correlation between phase reset in the auditory cortex and subsequent phase reset between motor and auditory cortices. This would suggest that there is stinger multisensory-driven phase alignment between motor and auditory cortices.

Our present data contribute further yet to reveal the presence of nonlinear multisensory effects in low frequencies. We investigated supra-additive multisensory effects across the conditions. We found consistent findings in both the active and passive conditions. Over the auditory ROIs, there was stronger PLV for the multisensory than the sum of unisensory conditions, which peaked around theta/ alpha and later peak at beta. In the visual cortex, this peak was higher around the beta frequency band. Additionally, in the passive conditions we see another peak around theta frequency at 500 ms time-window. Taken together these findings provide even further evidence to support that CMPR from the motor to sensory areas is a potential mechanism. The phase alignment at these lower frequencies found here in our ROIs may not only be linked with motor cortices as suggested but consist of other beta band networks such as the superior parietal lobule, known to be involved in multisensory integration (Molholm, Sehatpour, & Mehta, 2006).

Our data further revealed supra-additive effects peaking cluster of alpha and some signatures of beta peaking (Figure 4.8, but see Figures 4.10.C, 4.11.C) that were not seen when looking at the statistically significant cross-modal phase reset in both the active (Figure 4.10) and passive (Figure 4.11) visual conditions, which in contrast revealed lower mu/theta frequencies. This observation highlights the possible role that different frequency band have in neural integration. Several studies have now suggested the existence of a parallel between functional hierarchy and distinct frequency

bands using varying cognitive tasks (Bastos et al., 2015; Buschman & Miller, 2007; Lakatos et al., 2005; Rohe & Noppeney, 2016; Schroeder & Foxe, 2005).

Correlation analyses

Finally, we correlated SA with PDI scores. Deficits in sensory-predictive processes have been identified as specific symptoms of psychopathology, most notably delusions of control in ScZ patients (Frith & Wolpert, 2000; Lindner, Thier, Kircher, Haarmeier, & Leube, 2005; Shergill, Samson, & Bays, 2005; Synofzik, Thier, Leube, & Schlotterbeck, 2010). Our data were able to replicate previous studies showing a negative correlation between SA and PDI score (Blakemore, Wolpert, & Frith, 2002; Lindner et al., 2005; Shergill et al., 2005; Teufel, Kingdon, Ingram, Wolpert, & Fletcher, 2010). This suggests that individuals with higher level in delusion ideation showed a small SA effect supporting previous evidence that this delusion-like thinking is associated with a reduced tendency to predict and attenuate the sensory consequences of self-generated actions. Our data although preliminary give some indication that deficits in sensory prediction in ScZ patients may not simply be the consequence of the deluded state or related to the effects of neuroleptic medication. Rather, these appear to be stable trait-like characteristics in individuals score high in self-report measures of schizotypal characteristics. We further provide similar evidence in self-report measure using the Systemising Quotient, which until recently have been investigated together in a cross-cultural study (Cao & Gross, 2015)

Limitations and caveats

As with all studies using MEG at sensory space, data are contaminated by signal leakage from surrounding regions. Furthermore, when assessing the effect of CMPR, which is a measure of functional connectivity between two regions, these are subjected to spurious contributions due to signal leakage between the two regions. Beamformer methods are able to remove signal leakage, which has zero-lag by orthogonalse the time series data (Brookes, Woolrich, & Barnes, 2012; Hipp, Hawellek, Corbetta, & Siegel, 2012). Any subsequent measure cannot be due to signal leakage. Furthermore, here we used standard protocols for time-frequency analyses resulting in large clusters of activity. Future work will address this issue and analyse data using more sophisticated methods.

Next, it is important to clarify that we make assumptions about CMPR here using a simple basic stimuli in a SA task analysed with standard protocols on MEG sensor space, here we provide indirect evidence for this functional connectivity measure. Moreover, the effects seen here may not exclusively be ascribed to phase reset within in a modality or across sensory modalities. Neuroimaging has demonstrated the extensive networks implicated in multisensory processing, even for basic task tasks with simple stimuli (Martuzzi, Murray, Michel, & Thiran, 2007; Molholm et al., 2002; Schroeder & Foxe, 2005).

Future research would benefit from using directed functional connectivity measures at source space to provide stronger supporting evidence for cross-modal effects. Such measure may include Granger causality (e.g., Bressler & Seth, 2011), transfer entropy and mutual information measures (e.g., Lobier, Siebenhühner, Palva, & Palva, 2014), or phase-lag index (e.g., Stam, Nolte, & Daffertshofer, 2007). It is noteworthy, that as discuss in previous chapter it is inherently difficult to provide direct evidence for phase resetting in electrophysiological studies.

4.6 Conclusion

Our data contributes to the theoretical framework of the temporal coding hypothesis, specifically the phase reset mechanism, which predicts that information is encoded in the precise phases at which neuron are active (Canavier, 2015; Makeig, Westerfield, & Jung, 2002; Thorne et al., 2011). Our results support a recent study by Mercier et al. (2015), who demonstrated that temporal alignment of responses to multisensory events would be evident as an increase in oscillatory phase synchrony between unisensory brain regions. Moreover, they propose that phase coherence between motor and auditory cortices is linked to faster behavioural performance. A mechanism, which may be controlled via CMPR and is in line with our interpretations here. Although, their evidence may be confounded by recordings from electrocorticographic (ECoG) recording from epilepsy patients. Here we provide similar arguments in healthy subjects using MEG.

The forward model as described by the corollary discharge, describes a mechanism which supresses sensations that match anticipatory consequences of self-generated motor actions (Helmholtz, 1924; Helmholtz, 1867; von Holst & E., 1954). CMPR may be a candidate mechanism, which may index the forward model account of motor-to-somatosensory prediction account (Blakemore, Frith, & Wolpert, 2001; Wolpert et al., 1995) to another sensory modalities. This mechanism provides an interpretation for the integration of cortical information processing between primary and associative cortical areas (e.g. primary visual and middle temporal cortical regions; Chen, Lakatos, Shah, & Mehta, 2007) and different sensory modalities (e.g. somatosensory and auditory modalities; Lakatos et al., 2007). As suggested in the previous chapters, simple detected and discrimination tasks involve recurrent interactions between multiple cortical and subcortical regions. This is most likely achieved through the coordination of fluctuations in neural oscillatory activity. Oscillatory phase is able to mediate such interactions by inducing a mechanism of optimal temporal windows of communication between distant neural ensembles involved in a task (Engel & Singer, 2001; Pascal Fries, 2005; Varela et al., 2001). This is even shown to involve regions thought to be unrelated to the task modality (Kayser & Logothetis, 2007; Romei, Gross, & Thut, 2012; Schroeder & Lakatos, 2009; Thorne & Debener, 2014).

Chapter 5

5.1 General discussion

The coordination of oscillations across anatomical and temporal scales has gained prominence as a fundamental principle in functional connectivity underlying cognition and behaviour (Buzsaki, 2006; Fries, 2005; Siegel, Donner, & Engel, 2012; Thut et al., 2012a; Voloh & Womelsdorf, 2016). Oscillatory phase resetting is a measurable marker of the changing dynamics that underlie such coordination, and is a fundamental transition from the notion of static snapshots of brain activity and towards dynamically evolving neural circuits (Kopell, Ermentrout, Whittington, & Traub, 2000). Oscillatory phase provides the neural architecture for encoding and transmission of stimulus information across diverse brain systems. Specifically, this thesis investigates the modulation of neural oscillatory phase across sensory modalities as well as motor-sensory domains, within the framework of cross-modal phase resetting.

The phase reset hypothesis for multisensory integration details that cross-modal interactions are evoked by the occurrence of a sensory event on one modality realigning or shifting the phase of ongoing oscillations in another modality to a specific value; such that the processing of a subsequent event in that modality is either supressed or facilitated, depending on the exact relation between the phase of the neural activity and the occurrence of the second stimulus. However, the majority of studies investigating this mechanism within the framework multisensory integration use brief, momentary stimuli, and focus either on the spatial domain or detection of a single transient near-threshold stimulus. What is far less investigated is the interaction of the auditory modality and dynamic visual motion perception. Although prior studies have demonstrated that different presentations of sounds can affect the precision or quality of a visual motion percept, similarly when the sound is not task relevant (Kim, Peters, & Shams, 2012; Sekuler, Sekuler, & Lau, 1997). These studies have not provided evidence for this interaction between modalities being a consequence of CMPR. Moreover, behavioural studies have failed to find conclusive evidence for sensory interaction between the two modalities within the framework of auditory to visual motion perception. Taken together, the data presented in this thesis offer new insights into the role that neural oscillations play in visual motion perception and how this can be modulated via CMPR. These data are in line with prior investigations supporting the CMPR hypothesis and the sensory perceptual consequences following multisensory integration. Specifically an auditory induced modulation of ongoing visual oscillations (Diederich et al., 2012; Diederich et al., 2014; Fiebelkorn, Foxe, & Butler, 2011; Lakatos et al., 2009; Mercier et al., 2013; Naue et al., 2011; Romei et al., 2012b).

Periodicities between modalities, at least in the visual domain, appear to be synchronised not only with sensory events in other sensory modalities but also with motor-events. In addition to investigation the interaction between sensory modalities, this thesis explored the possibility that the interaction between the motor cortex and sensory modalities can be operated via CMPR. In addition, for the first time to our knowledge, we investigate sensory-motor interaction in up to two sensory modalities. Our data contributes to the theoretical framework of the temporal coding hypothesis, specifically the phase reset mechanism, which predicts that information is encoded in the phases at which neuron are active (Canavier, 2015; Makeig, Westerfield, & Jung, 2002; Thorne et al., 2011).

Varying information from the environment is continually bombarding our senses, our brain needs to select, filter and prioritise these inputs. Additionally, these processes may be modulated through feedback connections which further necessitate inter-regional communication. There is a large body of research suggesting that neural oscillations, which are an index of the fluctuation in cortical excitability of neural populations, are the brain's principle mechanism to achieve this information processing and transmission. To this end, events that coincide with a high excitability state of an oscillation will be amplified whereas events occurring during a low excitability phase are supressed (Schroeder & Lakatos, 2009a). This was observed in **Chapter 2** and **Chapter 3**, where the detection and discrimination of near-threshold visual motion had a higher probability of being accurate at certain SOAs and not others. The ability of the brain to drive or control these oscillations, phase aligning high and low excitability states with relevant and irrelevant events, respectively, makes this a powerful mechanism for sensory gain control for the gating and filtering of inputs (Fries, Neuenschwander, et al., 2001; Fries, 2005; Fries, Womelsdorf, & Oostenveld, 2008). These chapters demonstrated that CMPR is a versatile mechanism for sensory gain control, where selective sustained attention can influence visual processing in a rhythmic way. In addition, prior investigations have shown that attention can achieve such dynamic routing of sensory information in the cortex through both the enhancement of spike rates of neurons and also the enhancement of precise synchronisation of neuronal groups activated by the attended stimulus (Fries, Reynolds, et al., 2001; Womelsdorf & Fries, 2006).

Auditory modulation of the visual cortex

The existing literature demonstrates a variety of methodologies that have elucidated evidence for a modulatory role of cross-sensory interactions on ongoing cortical oscillations and its impact on neural response (Canavier, 2015). These are described in primary auditory cortex of nonhuman primates (Kayser, 2009; Lakatos et al., 2009) and in visual and auditory cortices in humans (Fiebelkorn, Foxe, & Butler, 2011; Fiebelkorn et al., 2013; Perrodin & Kayser, 2015; Romei et al., 2012b), including somatosensory (Foxe et al., 2000; Lakatos et al., 2007). Specifically, a number of investigations suggest that auditory stimulation can modulate visual response in the visual cortex to

influence early sensory-perceptual processing (Fiebelkorn et al., 2011; Fort et al., 2002; Giard & Peronnet, 1999; Mishra & Martinez, 2007; Molholm et al., 2002; Naue et al., 2011; Romei et al., 2012b). The majority of studies investigating these cross sensory interactions have focused on using brief, momentary stimuli, and focus either on the spatial domain (Eimer & Driver, 2000; Landau & Fries, 2012a) or detection of a single transient near-threshold stimulus (Fiebelkorn et al., 2011; Kayser et al., 2008; Naue, Rach, Strüber, & Huster, 2011; Romei, Gross, & Thut, 2012). To date, however, there has been sparse evidence suggesting that an axillary (task irrelevant) tone can modulate visual motion perception. To this end, **Chapter 2** and **Chapter 3**, sought to investigate these cross-sensory interactions using multisensory stimulation. Here the results provide novel findings from both electrophysiological evidence form MEG recording and psychophysical measures demonstrating that theta-alpha frequency oscillations play a key role in the integration of information over time in a visual motion discrimination and detection task. Prior studies have similarly suggested that low-frequency (theta-alpha) oscillations play a key role in the phase resetting mechanisms to align cortical excitability to important events in the stimulus stream (Ng, Schroeder, & Kayser, 2012; Schroeder et al., 2008; Thorne et al., 2011; Weise, Hartmann, Schröger, Weisz, & Ruhnau, 2016).

Recent evidence suggests that sustained attention in one location is not static, but rather appears to happen rhythmically. For example, Busch and VanRullen (2010) using EEG demonstrated that the detection of a visual target presented at threshold was systematically related to the phase of ongoing theta oscillation (~7 Hz). This phase behaviour relationship was contingent on the allocation of attentional resources following a cue and was absent at other location in the visual field. To this end, the cue served not only to guide the deployment of attention but also cause the timing of the high- and low-excitability states of the oscillation to phase reset across trials (see also Lakatos et al., 2009). Therefore, it appears that the selection mechanism periodically samples the attended location, with the degree of selective fluctuating with the phase of the neural rhythms. These findings would suggest that visual selective attention is a rhythmic behaviour that is dynamic and flexible. The neural basis of these rhythmic properties of selective attention is unclear but taken together with the findings from **Chapter 2** and **Chapter 3** suggest that selective attentional resources modulate sensory gain control via cross-modal interactions. In other words, phase resetting may be a mechanism for supramodal attentional control (Kayser, 2009; Lakatos et al., 2009). Specifically, a task irrelevant tone can modulate the sustained attention of continuous stimulation in a visual motion detection and discrimination task.

Frequency of sensory processing

Research that investigates the role of different oscillatory frequency bands in sensory information processing suggests that different functional roles for higher and lower frequencies. Due to their cycles length, slower oscillations support better functional coupling of networks over much larger distances

due to conduction delay properties (Kopell et al., 2000). This concept is evident in the data presented in this thesis, specifically theta-alpha frequency bands appear to be involved in auditory modulation of visual cortical activity, which requires long distance communication.

The vast majority of established research has attributed alpha frequency band (7-12 Hz) as the principle frequency range of visual stimulus processing. From the early foundations of EEG recordings, Hans Berger in 1929 (Berger, 1929) reported the dependence of alpha power on visual input. Here Berger found that alpha power in EEG increased when participants closed their eyes. Ever since these findings, both theoretical and empirical approaches have provided convincing evidence that alpha band is related to an inhibition (disengagement) of brain regions (Foxe & Snyder, 2011; Jensen & Mazaheri, 2010; Klimesch, Sauseng, Hanslmayr, et al., 2007; Klimesch et al., 2011). For example, alpha is implicated in visual perception, both for the detection of visual target and the likelihood of the perception of TMS induced phosphenes, that depends of EEG alpha phase (Busch et al., 2009; Mathewson et al., 2009; Romei et al., 2010), and power (Hanslmayr et al., 2007; Romei, Brodbeck, et al., 2008). Similar results are found following rhythmic visual stimulation, with a neural resonance of alpha, indicating that the intrinsic frequency of neurons (Hutcheon & Yarom, 2000) in the visual system is indeed located predominantly in the alpha frequency band. Furthermore, alpha is implicated in the probability of detecting a visual target after a cue and observed in behavioural oscillations following reaction times which fluctuate periodically (Landau & Fries, 2012a; Song et al., 2014). It is noteworthy to mention that these have been reported at a frequency of 4 Hz per visual hemifields, indicating an overall rhythmicity of 8 Hz, thus lying within the alpha range.

In **Chapter 3**, the data revealed that visual motion detection and discrimination varies strongly as a function of prestimulus phase on multiple temporal scales, from low delta in the temporal parietal, and alpha in the visual regions. The MEG electrophysiological data significantly correlate with the behavioural spectral profile of *d'* across subjects. These data therefore extend previous findings that describe a relationship between phase, within defined frequency bands and either behavioural and neurophysiological outcomes (Busch et al., 2009; Dugué et al., 2011; Haig & Gordon, 1998; Jansen & Brandt, 1991; Kayser et al., 2008; Kruglikov & Schiff, 2003; Lakatos et al., 2007, 2009; Makeig, Westerfield, & Jung, 2002; Mathewson et al., 2009; Monto & Palva, 2008; Scheeringa, Mazaheri, & Bojak, 2011). The majority of these studies emphasis the role of theta/alpha oscillations. The data presented here confirm the importance of this frequency bands, but together with the behavioural findings from Chapter 2, suggest also a role for delta oscillations as predictive indicators of visual target detection.

A wealth of research that demonstrates that top-down processes can modulate the phase and consequently cognitive processing (Fiebelkorn, Foxe, & Butler, 2011; Lakatos et al., 2009, 2008) and

cortical excitability (Fries, 2005; Fries, Reynolds, et al., 2001; Friston, 2005b; Snyder & Foxe, 2010). Our data further revealed a cyclic modulation in ERF amplitudes as a function of SOA in theta and alpha, over the temporal parietal and visual regions respectively These modulations occurred at 300 ms post motion onset, indicating that the evoked responses where a reflection of the decision-making process. Components at these latencies represent high-order cognitive processes rather than low level visual processing that are influence by top-down regions. These results suggest that theta-alpha power, an index of cortical excitability, has an influence on visual motion perception. Taken together, these data are in line with prior studies that demonstrated a negative relationship between instantaneous alpha oscillations and perceptual performance (Ergenoglu et al., 2004; Hanslmayr et al., 2005b; Thut et al., 2006), indicating that low prestimulus alpha promotes good visual perception performance. Furthermore, prior investigation demonstrate that brain rhythms operate interactively on multiple temporal and spatial scales (Canolty & Knight, 2010; Jensen & Colgin, 2007). A large number of these studies show that the phase of theta oscillations modulate the amplitude of gamma (> 30 Hz) oscillations (Canolty et al., 2006; Lakatos, Shah, Knuth, et al., 2005a; Whittingstall & Logothetis, 2009). Our investigations were focused on frequencies below 25 Hz; future work would investigate the phase-detection relationships at higher frequencies and the dependence on the phases of lower frequencies that affect the perception of visual motion.

Although the alpha (8-12 Hz) rhythm remains widely implicated in visual perception, progressively more research is demonstrating functional associations of perception involving other frequency bands, as reported here in 4-8 Hz theta frequency range (Diederich et al., 2014; Dugué et al., 2015; Vanrullen, 2013; VanRullen & Dubois, 2011; Mathewson & Lleras, 2011). For example, VanRullen and colleagues have demonstrated the relative contribution that ongoing pre-stimulus EEG oscillations have on perceptual consequences. In one of their studies (Busch et al., 2009), they presented brief flashes of light at near-threshold detection, where the luminance of the flashes were calibrated so that the exact same stimulus would be perceived on approximately half of the trials, but go undetected on the other half. They found significant pre-stimulus phase concentration at ~7 Hz (theta range) on those trials where flashes were accurately detected. In **Chapter 2,** it was investigated if the visual systems sampling frequency would adapt to the length of coherent visual motion as a mechanism to achieve optimal sensory perceptual performance. The data would suggest that the visual system seems to reveal a constant sampling frequency around theta-alpha range (with optimal fitting around 6-9 Hz).

The results from both **Chapter 2** and **Chapter 3**, demonstrate that the discrete sampling of the visual environment is not disruptive to stimulus processing even when it is operationally independent of the visual input. In other words, the systems subsamples "blindly" or irrespectively of the content of the visual input (i.e., "snapshots" ate taken independently of the content of the visual input). This is evident in our task where the visual system maintains its rhythm of stimulus processing even when it

cannot be adjusted in such a way during continuous stimulation (coherent visual motion) of events that have an unpredictable sequence (direction of coherent motion or no motion). Our data provides a novel contribution to the literature suggesting that theta-alpha frequency range seems to be dominant for stimulus processing, more specifically the integration of information over time in visual motion perception. Taken together, auditory-driven modulations in phase concentration over visual cortices observed in theta-alpha frequency range strongly suggest a central role for this frequency range in mediating communication between auditory and visual cortices. The pattern of results in sensory cortex through cross-modal phase resetting are analogous to the findings reported for non-human primates (Kayser et al., 2008; Lakatos et al., 2007).

Evidence for an involvement of alpha activity in information processing has been provided by numerous studies using a variety of methods (Mazaheri, Schouwenburg, & Dimitrijevic, 2014). Furthermore, there is evidence for a relationship between long-range coherence in the alpha frequency band and perceptual and cross-modal binding (Thorne et al., 2011). Prior studies reporting oscillations occurring in the alpha band have been reported to adjust when the onset of a spatial location of expected upcoming events in known. For example, alpha lateralisation was observed to be influenced by the predictability of the spatial location of a visual target , indicating an active adjustment of alpha power base on anticipatory spatial attention (Bonnefond & Jensen, 2012; Haegens, Nácher, & Luna, 2011). Furthermore, the processing of the uncertainty about when events are likely to occur is facilitated by phase resetting in theta activity before the event occurs to enhance their processing and detection (Lakatos et al., 2008; Stefanics & Hangya, 2010). The role of alpha in sensory predication have also been observed in research investigating the theories of sensorimotor control (Miall & Wolpert, 1996; Wolpert & Flanagan, 2001). The prominent "forward modal" theory proses that the underlying mechanisms of action prediction send an efference copy of the motor command to generate prediction about the sensory consequences of those self-generated actions (**Chapter 4**). Within this framework, research suggests that predictions are communicated along anatomical feedback connection via alpha oscillations (Bastos et al., 2015; Wang, 2010). Recent evidence shows that prior to stimulus onset, alpha power controls the gain control of local neural populations reflecting precision of the predication about the incoming events (Cao et al., 2016a). These mechanisms may be implemented by modulating local neural excitability levels, known to be indexed by alpha (Romei, Brodbeck, et al., 2008).

Taken together, these and other findings suggest that there may not be a single common sampling rhythms affecting all our perceptions, but rather many simultaneous rhythms that periodically modulate various cognitive and perceptual functions in distinct modalities at independent rates (VanRullen, 2016b; VanRullen & Dubois, 2011). A review of the literature highlights that the frequency

of these periodicities are very diverse, but reveal clear peaks at alpha (10 Hz) and theta (7 Hz), which are tentatively attributed to sensory and attentional sampling rhythms respectively.

Motor-sensoy interactions

Another established model case for this fundamental operation is the interaction between motor and sensory areas. The coordination of oscillation across sensory modalities and motor domains are described in terms of the predictive coding theory. Motor action leads to predictable sensory consequences. Within this framework, predictive encoding is associated with attentional neuromodulatory gain control in sensory processing, which reflects the modulation of neural excitability changes, which may be an index of reporting prediction error (Logothetis, 2008). The exact mechanisms between motor and sensory modalities are yet unclear, but in **Chapter 4**, we propose that inter-areal phase resetting is be a potential mechanism that may index the forward model account of motor-somatosensory perdition account (Blakemore, Frith, & Wolpert, 2001; Wolpert et al., 1995) to different sensory modalities (e.g. somatosensory and auditory modalities; Lakatos et al., 2007). To this effect, a predictive influence can be exerted if one event resets the phase of ongoing excitability fluctuations and thereby influence the processing of upcoming events in the same or different modalities. There the phase resetting mechanism is not specific to multisensory interactions, but rather represents a more general mechanism through which different sensory, motor, and top-down attentional control can modulate the ongoing processing across domains. Taken together, cross-modal phase resetting provides a canonical operation enabling the flexible integration of multiple sensory, motor and top-down modulations.

Within this framework, we investigated the prediction context of multisensory consequences following self-generated actions using both unimodal and bimodal visual and auditory stimuli. The data here suggests that an internal model generates temporal predictions for at least two modalities. This sensorimotor synchronisation can be indexed by theta frequency range (3-7 Hz). Another attribute of this operation is that of oscillatory power, which may impact the overall responsiveness of a given brain region, a process that has been associated with the modulation of neural firing (Haegens, Nácher, & Luna, 2011; Jensen et al., 2012). These novel findings are in line with previous reports in unisensory paradigms showing evidence for temporal predictions in visual (Gentsch & Schütz-Bosbach, 2011; Hughes & Waszak, 2011; Knolle et al., 2012), auditory (Cao et al., 2016a; Ford et al., 2001;Ford, Roach, & Faustman, 2007; Hughes et al., 2013; Shergill et al., 2005), and somatosensory (Bays, Wolpert, & Flanagan, 2005; Hesse et al., 2010; Weiskrantz et al., 1971) system, although investigated separately. Although there is a large body of research that focused on the role of the forward model in predicting visual consequences of actions, several studies have also demonstrated the importance in tactile predictions (Blakemore et al., 1998). Taken together, this suggests that

sensory consequences of forward model predictions in different modalities are based on similar mechanisms. What is less clear, however, is the mechanisms involved in multisensory predictions.

Importantly, in contrast to previous studies which manipulate temporal prediction when investigating sensory attenuation here, in self-generated (active trials) conditions, participants have a better temporal prediction about upcoming stimuli, since these actions are decided voluntarily. Whereas, in the externally generated (passive trials) conditions, there is an uncertainty about the onset of the stimulus as these are jittered, and therefore are unpredictable. Consequently, due to this unpredictability difference, these paradigms are unable to discern whether the effects are due solely to an efference copy mechanism, differences in predictability, or both. In the **Chapter 4** however, we avoid this potential confound by presenting the passive stimuli at the same rate on every trial. To this end, not only was it possible to suggest the results are a consequence of an efference copy mechanism but it was also possible to investigate the difference in processing unimodal versus multimodal action consequences generated either actively or passively.

Neural correlates of crossmodal modulation

Although the current methods of this thesis do not allow us to determine the pathway though which auditory-driven influences occurred, there are several highly plausible possibilities to consider. These include a direct cortico-cortical auditory to visual pathway (Cappe & Barone, 2005; Clavagnier, Falchier, & Kennedy, 2004; Falchier, Clavanier, & Barone, 2002), subcortical thalamic influence (C. Schroeder & Lakatos, 2009a; Sherman & Guillery, 2002; Sherman, 2007), or mediating higher-order multisensory region such as posterior superior temporal gyrus (Tyll, Bonath, Schoenfeld, Heinze, & Ohl, 2013; Werner & Noppeney, 2010), or the intra-parietal sulcus (Leitão, Thielscher, Werner, & Pohmann, 2013).

The neural circuitry implicated in the effective transmission of the efference copy signal is largely under dispute, including but not exclusive to the motor cortex (Ford, Palzes, Roach, & Mathalon, 2013; Reznik, Henkin, Levy, & Mukamel, 2015), prefrontal cortex (Müller et al., 2014), and inferior frontal gyrus (Wang, Mathalon, Roach, Reilly, & Keedy, 2014), that have been proposed as advocates in the generation of the efference copy signal. It seems irrefutable to suggest the involvement of the motor cortex in generating the efference copy signal as it is originally proposed as a copy of the motor command (Holst & Mittelstaedt, 1950). Evidence from *in vivo* intracellular recordings demonstrated a particular neural circuit that connects the motor and auditory domains, providing a potential neural basis for the efference copy (Schneider, Nelson, & Mooney, 2014). Future studies are needed with a focus on disentangling the anatomical origins of phase-aligned activation, microcircuits that can be preferentially targeted to adjust phase, the effect of noise either in the stimulus or in endogenous

oscillatory activity, and methods of manipulating neural populations in order to affect computation and behaviour.

Evidence for sensory attenuation in the visual cortex is sparse, with one study reporting rather an enhancement over occipital sensors (Mifsud, Oestreich, Jack, & Ford, 2016). A similar effect is observed in our data (**Chapter 4**), although the effects are not significant. These differences between the effects observed in different modalities poses an interesting question. Are there different neural systems specialised for the transmission of different efference copies, which are independent? Misfud et al were unable to find a correlation between auditory sensory attenuation and visual facilitation effects, which tentatively suggests the existence of two independent systems, one for motor-auditory and another motor-visual. Interestingly, Williamson, et al. (2015) reported differential modulatory effects in the auditory and visual regions of the thalamus in mice. While, Zhang et al. (2016) found that both auditory and somatosensory cortices of mice are connected to motor cortex, whereas visual cortex is predominantly connected to anterior cingulate cortex. Taken together these offer some new insight into the possibility that there are different neural circuitry implicated in processing what seems to be qualitatively different efference copies with the same motor origin but with differing connections to different modalities.

5.2 Limitations, caveats and future directions

Psychophysics of behavioural oscillations

In recent years, there has been an increase in measuring behavioural oscillations and making inferences about these periodicities to those of the underlying cortex. To this end, several psychophysical studies using time-resolved behavioural measurements reveal rhythmic fluctuations (de Graaf et al., 2013; Diederich, Schomburg, & Colonius, 2012; Fiebelkorn, Foxe, & Butler, 2011; Landau & Fries, 2012; Song, Meng, Chen, Zhou, & Luo, 2014; VanRullen & Busch, 2011). It is important to note, the inherent temporal limitations of conventional spectral methods that can be applied to behavioural data (*for a technical note see;* Forrest & Suter, 1994). The one major concern is the limitations imposed due to sampling (aliasing) and truncation (leakage). However, these limitations can be minimised if applied with due care. Perpetual cycles appear to be limited to lower frequencies, especially when considering findings reported in behavioural studies (Song et al., 2014). This bias is partly a consequences of the technical constraints imposed on the methods for investigating oscillations. For example, behavioural oscillations are often reported below 20 Hz by the limited number of trials or as previously mention a limited number of sampling points. While these limitations are inherent in behavioural paradigms, limitation are imposed in studies using M/EEG, her the signal-to-noise declines rapidly with frequency. Prior knowledge of the frequency of interest of the to-be-observed behavioural oscillation will not ensure that that spectral decomposition will not produce

aliasing (frequencies sampled above the Nyquist frequency). The majority of studies assess fluctuations in perception at a much coarser temporal scale and therefore are limited in their capacity to use spectral analyses to measure oscillations in behavioural data (Theunissen & Doupe, 1998; Vanrullen & Dubois, 2011b). It is important to note, that in our paradigm inferences are made on few repeating cycles of behavioural rhythms. Potentially this could be avoided by increasing the number of observations (SOAs). However, in the current paradigm this was not possible, because increasing the number of SOA would substantially increase the number of trails needed, resulting in an increase in the total recording time.

The problems with leakage are inherent in spectral decomposition analyses, since most behavioural oscillations will probably not fit the harmonic requirements of the measurement. Usually the main aim of the analyses is to discern a particular peak to be different from that expected in a spectrum derived from random data, windows should increase the detection of peaks for components that are not harmonics in the spectrum. Hamming windows (as used in in the current data) are particularly effective in these instances as they distort harmonic and non-harmonic components less than other commonly used windows (Cohen, 2014; Forrest & Suter, 1994). Considering these limitations, however, the current methods do minimise potential confounds. In addition, the finding reported in the behavioural analyses correlate with those found with direct measures recorded in MEG.

Task affects d-prime values

In **Chapter 3**, *d′* measures where used to quantify the sensitivity accuracy of detection and discrimination. The observed *d′* responses in the data are slightly higher than standard reports, including those reported in **Chapter 2**. However, higher values have been associated with tasks that introduce a wait time before responding (Reuss, Kiesel, Kunde, & Hommel, 2011; Vorberg, Mattler, & Heinecke, 2003), as were the case in the MEG task. In this task once participants made a response experiment would move onto the next trial. As a way to minimise artefacts caused by eye movements at the start of each trial, participants were requested to use the time interval before responding to make eye blinks. By introducing a delay the response in the *d′* are not only influenced by the conscious processes, but also by unconscious information (Kiesel, Wagener, Kunde, & Hoffmann, 2006; Reuss et al., 2011; Schlaghecken & Eimer, 2004). These studies suggest that unconscious processes exert their influence over a very short time window, the delay would diminish the influence of these unconscious processes and lead to smaller *d′* values. Our data is in line with these assumptions.

Measuring phase resetting

The question of how to accuracy measure phase resetting. Phase resetting is a measure of the concentration of phase after a reference point across trials. One of the most commonly used methods to quantify the phase consistency across trials is the inter-trial coherence (ITC; Makeig, Westerfield, &

Jung, 2002) also commonly reference to as phase-locking value (PLV; (Tallon-Baudry & Bertrand, 1996). The term 'inter-trial coherence' refers to its interpretation as the event-related phase concentration (ITPC) or event-related linear coherence (ITLC) between the recorded MEG activity and the event-phase indicator. The ITC is calculated by taking, for each time point, the modulus of the circular phase average across trials. Statistical significance can be measured via permutation testing, or via Rayleigh's test for circular uniformity.

One advantage that MEG has over EEG, is circumventing the reference electrode problem (Cohen, 2014). However, in either case, a signal recorded from a sensor may have multiple components contributing to the activation of the waveform. This could include oscillatory activity in multiple frequency bands, as well as evoked activity. As introduced in the **Main Introduction (see section, conceptual issues);** there has been a long withstanding debate in the M/EEG literature on whether the evoked potential observed in relation to variable task contexts is primary a result of oscillatory phase reset or evoked activity and methods have been proposed to differentiate the two (Makeig et al., 2004b; Sauseng, Klimesch, Gruber, et al., 2007; Shah, Bressler, & Knuth, 2004). One primary method used to determine if phase resetting has occurred is by analysing both power and phase concurrently, averaged across trials, then if the power remain constant in the response to a stimulus, but the phase becomes more consistent (across trials), then there is a higher probability that an oscillations been reset (Sauseng, Klimesch, Gruber, et al., 2007). However, recently it was shown that the "total power" (power calculated on each trial, then averaged) is statistically relatively weaker than phase consistency at detecting changes in a stimulus synchronised activity (Ding & Simon, 2013). Whereas, "evoked power" (waveforms averaged over trials, then power calculated) was to a similar degree as good as phase consistency measure at detecting such activity. In other words, the power signature averaged over trials does not show a stimulus-driven change, and a new phase (consistent over trials) is established that is locked to a stimulus, then this would constitute strong evidence that a phase reset has occurred (Voloh & Womelsdorf, 2016).

When analysing neural oscillatory signatures, considering both the phase and power together may provide evidence to suggest a phase reset, however it remains important to consider the electrophysiological modality used to make such recordings. The vast majority of studies on neural oscillations, recorded signals represent spatially synchronised activity (LFP, M/EEG). When considering measurements recorded with these neuroimaging tools, it is important to consider some potential mechanism that could lead to the observed phase reset: First, a single oscillator that is reset by a stimulus, secondly, many individual oscillation generators that becomes spatially synchronised, or finally the recruitment of newly generated oscillations. Taken together it is possible for power to change, even in the presence of phase reset. For example, amplitude may increase following a phase reset of a single oscillator, while the latter two mechanisms, spatial synchronisation raises the signal-

to-noise-ratio for a particular frequency band, which will manifest as a concurrent increase in power (Telenczuk & Nikulin, 2010). This highlights a major point to consider when measuring neurophysiological circuits, is that our knowledge is limited, which fundamentally restricts the ability to make strong inferences about the presence of oscillations (Cohen, 2014). Although, neural recordings from single cell studies can help to discern the spatial component of phase reset. In non-invasive human M/EEG recordings it is theoretically impossible to demonstrate that evoked activity results from phase-resetting of ongoing neural oscillators (Telenczuk & Nikulin, 2010). Nonetheless, with sensible inferences on the origins of the signal with adept paradigms and the use of mathematical informed approaches, can provide useful criteria for interpretation (Canavier, 2015).

Next, another point to consider is the interpretation of the functional connectivity between modalities. In all three experimental chapters, our interpretations are not founded on direct evidence of one modality driving or modulating another but rather these are based on indirect measures. For example, many empirical studies support the view that the motor cortex is principally involved in the generation of the efference copy (Ford et al., 2013; Voss et al., 2007), however, our methods do not allow us to reveal the directed functional connectivity between the motor cortex and other sensory modalities. Similarly, our interpretation of the data are based on the assumption that the auditory cortex aligns visual oscillations through the mechanism of cross-modal phase resetting. Future, research would investigate the mechanism further using more direct and sophisticated measures of functional connectivity. These may include but not restricted to, granger causality or mutual information measures.

Interestingly, future research would benefit from investigating the possibility that perceptual cycles may have spatial specificity. Considering the existing literature, it would seem that the cyclic modulation of perceptual performance is not necessarily uniform over different sensory modalities. One possibility is that the sampling phase propagates efficiently across space, as in traveling waves (see, Ermentrout & Kleinfeld, 2001). The majority of experiments aim to investigate the temporal dynamics of perception, future studies would benefit from additionally investigating the spatial dimension.

MEG signal leakage

Many previous studies introduced earlier have provided support for an auditory induced modulation in visual perception, including others that support the view that the motor cortex is involved in generating an efference copy signal that may interact with other sensory modalities (e.g. auditory cortices). However, with the current methods used it would not be possible to measure true functional connectivity between these modalities. Furthermore, the activation observed in each region of interest may be a combination of signals from other regions, a consequences of field spread. As with

all studies using MEG in sensory space, data are contaminated by signal leakage from surrounding regions. Furthermore, when assessing the effect of CMPR, which is a measure of functional connectivity between two regions, these are subjected to spurious contributions due to signal leakage between the two regions. Beamformer methods are able to reduce the influence signal leakage, which has zero-lag by orthogonalse the time series data (Brookes et al., 2012; Hipp et al., 2012). Any subsequent measure cannot be due to signal leakage. Furthermore, here we used standard protocols for time-frequency analyses resulting in large clusters of activity. Future work will address this issue and analyse data using more sophisticated methods. Another point to consider is that of anatomical differences in cortical folding which lead to considerable variability in the signals recorded at the sensor-level.

Nonlinear multisensory interactions

One particular challenge when conducting human multisensory research, within the context of cross-modal interactions, it determining the appropriate statistical quantification for identifying these interactions within primary sensory cortices, including higher order regions in the brain (Calvert, 2001; Laurienti, Perrault, Stanford, Wallace, & Stein, 2005). One fundamental problem is the inherent difficulty in transposing established principles of cross-sensory interactions, founded on the basis of single-unit recording in animals (Stein & Meredith, 1993), to that of the macroscopic level recording of neural population responses and behavioural responses in humans. **Chapter 4** highlights another point to consider, the ability to differentiate between understanding the nature of super-additive and sub-additive nonlinear responses. In other words, multisensory responses that are greater than or less than the summed unisensory responses, respectively (see Laurienti et al., 2005)

5.3 Conclusion

Oscillations provide the neural architecture that may support the effective communication within and between cortices. Oscillatory activity has be linked to a variety of phenomena, and the phase of these oscillations are fundamentally linked to perception. The exact underlying dynamics of neural transmission and perceptual processing are yet fully understood. However, cross-modal phase resetting may be a candidate mechanism that may explain the interaction between different modalities. Investigating the spatial and temporal dynamics of this process will further our understanding of the neural mechanisms that govern not only sensory perceptual processing but also other processes that are involved predictive code framework. This thesis provides novel evidence that supports this theory.

References

Akam, T., Oren, I., Mantoan, L., & Ferenczi, E. (2012). Oscillatory dynamics in the hippocampus support dentate gyrus-CA3 coupling. *Nature*.

Alais, D., & Burr, D. (2004). No direction-specific bimodal facilitation for audiovisual motion detection. *Cognitive Brain Research*.

Aliu, S., Houde, J., & Nagarajan, S. (2009). Motor-induced suppression of the auditory cortex. *Journal of Cognitive Neuroscience*.

Annett, M. (1970). A classification of hand preference by association analysis. *British Journal of Psychology*, *61*(3), 303–321. https://doi.org/10.1111/j.2044-8295.1970.tb01248.x

Aoyagi, M., Kiren, T., Kim, Y., Suzuki, Y., Fuse, T., & Koike, Y. (1993). Optimal modulation frequency for amplitude-modulation following response in young children during sleep. *Hearing Research*.

Arnal, L., & Giraud, A. (2012). Cortical oscillations and sensory predictions. *Trends in Cognitive Sciences*.

Arnal, L., Morillon, B., & Kell, C. (2009). Dual neural routing of visual facilitation in speech processing. *The Journal of*.

Arnal, L., Wyart, V., & Giraud, A. (2011). Transitions in neural oscillations reflect prediction errors generated in audiovisual speech. *Nature Neuroscience*.

Baess, P., Widmann, A., & Roye, A. (2009). Attenuated human auditory middle latency response and evoked 40-Hz response to self-initiated sounds. *European Journal of*.

Barry, R. (2009). Evoked activity and EEG phase resetting in the genesis of auditory Go/NoGo ERPs. *Biological Psychology*.

Barry, R., Blasio, F. De, & Pascalis, V. De. (2014). Preferred EEG brain states at stimulus onset in a fixed interstimulus interval equiprobable auditory Go/NoGo task: a definitive study. *International Journal of*.

Barry, R., Pascalis, V. De, Hodder, D., & Clarke, A. (2003). Preferred EEG brain states at stimulus onset in a fixed interstimulus interval auditory oddball task, and their effects on ERP components. *International Journal of*.

Bartos, M., Vida, I., & Jonas, P. (2007). Synaptic mechanisms of synchronized gamma oscillations in inhibitory interneuron networks. *Nature Reviews Neuroscience*.

Başar, E. (1980). *EEG-brain dynamics : relation between EEG and Brain evoked potentials*. Amsterdam ;;New York ;New York N.Y.: Elsevier/North-Holland Biomedical Press.

Başar, E. (1992). Brain natural frequencies are causal factors for resonances and induced rhythms. *Induced Rhythms in the Brain*.

Başar, E. (1998). Brain Dynamics and Brain Codes. *Brain Function and Oscillations*.

Başar, E., Başar-Eroğlu, C., Karakaş, S., & Schürmann, M. (1999). Are cognitive processes manifested in event-related gamma, alpha, theta and delta oscillations in the EEG? *Neuroscience Letters*.

Basar, E., & Schurmann, M. (1997). Alpha oscillations in brain functioning: an integrative theory. *International Journal of ….*

Başar-Eroglu, C., Başar, E., & Demiralp, T. (1992). P300-response: possible psychophysiological correlates in delta and theta frequency channels. A review. *International Journal of*.

Bastiaansen, M., & Knösche, T. (2000). Tangential derivative mapping of axial MEG applied to event-related desynchronization research. *Clinical Neurophysiology*.

Bastos, A., Litvak, V., Moran, R., Bosman, C., & Fries, P. (2015). A DCM study of spectral asymmetries in feedforward and feedback connections between visual areas V1 and V4 in the monkey. *Neuroimage*.

Bauer, M., Stenner, M., & Friston, K. (2014). Attentional modulation of alpha/beta and gamma oscillations reflect functionally distinct processes. *The Journal of*.

Baule, G., & McFee, R. (1963). Detection of the magnetic field of the heart. *American Heart Journal*.

Bays, P., Flanagan, J., & Wolpert, D. (2006). Attenuation of self-generated tactile sensations is predictive, not postdictive. *PLoS Biol*.

Bays, P. M., Wolpert, D. M., & Flanagan, J. R. (2005). *Perception of the Consequences of Self-Action Is Temporally Tuned and Event Driven*. *Current Biology* (Vol. 15). https://doi.org/10.1016/j.cub.2005.05.023

Bays, P., Wolpert, D., & Flanagan, J. (2005). Perception of the consequences of self-action is temporally

tuned and event driven. *Current Biology*.

Benazet, M., Thénault, F., Whittingstall, K., & Bernier, P.-M. (2016). Attenuation of visual reafferent signals in the parietal cortex during voluntary movement. *Journal of Neurophysiology*, *116*(4).

Benedetto, A., & Spinelli, D. (2016). Rhythmic modulation of visual contrast discrimination triggered by action. *Proc. R. Soc.*

Benjamini, Y., & Hochberg, Y. (1995). Controlling the false discovery rate: a practical and powerful approach to multiple testing. *Journal of the Royal Statistical Society. Series B (*.

Benjamini, Y., & Yekutieli, D. (2001). The control of the false discovery rate in multiple testing under dependency. *Annals of Statistics*.

Berens, P. (2009). CircStat: a MATLAB toolbox for circular statistics. *J Stat Softw.*

Berger, H. (1929). Über das elektrenkephalogramm des menschen. *European Archives of Psychiatry and Clinical*.

Besle, J., Schevon, C. A., Mehta, A. D., Lakatos, P., Goodman, R. R., McKhann, G. M., … Schroeder, C. E. (2011). Tuning of the human neocortex to the temporal dynamics of attended events. *The Journal of Neuroscience : The Official Journal of the Society for Neuroscience*, *31*(9), 3176–85. https://doi.org/10.1523/JNEUROSCI.4518-10.2011

Bishop, G. (1932). Cyclic changes in excitability of the optic pathway of the rabbit. *American Journal of Physiology--Legacy*.

Blakemore, S., Frith, C., & Wolpert, D. (1999). Spatio-temporal prediction modulates the perception of self-produced stimuli. *Journal of Cognitive Neuroscience*.

Blakemore, S., Frith, C., & Wolpert, D. (2001). The cerebellum is involved in predicting the sensory consequences of action. *Neuroreport*.

Blakemore, S., Rees, G., & Frith, C. (1998). How do we predict the consequences of our actions? A functional imaging study. *Neuropsychologia*.

Blakemore, S., Wolpert, D., & Frith, C. (1998). Central cancellation of self-produced tickle sensation. *Nature Neuroscience*.

Blakemore, S., Wolpert, D., & Frith, C. (2000). Why can't you tickle yourself? *Neuroreport*.

Blakemore, S., Wolpert, D., & Frith, C. (2002). Abnormalities in the awareness of action. *Trends in Cognitive Sciences*.

Bonnefond, M., & Jensen, O. (2012). Alpha oscillations serve to protect working memory maintenance against anticipated distracters. *Current Biology*.

Braddick, O. (1974). A short-range process in apparent motion. *Vision Research*.

Brainard, D. H. (1997, January 1). The Psychophysics Toolbox. *Spatial Vision*. Brill.

Brandt, M. (1997). Visual and auditory evoked phase resetting of the alpha EEG. *International Journal of Psychophysiology*.

Brandt, M., & Jansen, B. (1991). The relationship between prestimulus alpha amplitude and visual evoked potential amplitude. *International Journal of Neuroscience*.

Bressler, S. L., & Seth, A. K. (2011). Wiener–Granger causality: a well established methodology. *Neuroimage*, *58*(2), 323–329. Journal Article. https://doi.org/10.1016/j.neuroimage.2010.02.059

Britten, K., Newsome, W., & Shadlen, M. (1996). A relationship between behavioral choice and the visual responses of neurons in macaque MT. *Visual*.

Brookes, M., Woolrich, M., & Barnes, G. (2012). Measuring functional connectivity in MEG: a multivariate approach insensitive to linear source leakage. *Neuroimage*.

Bruns, A. (2004). Fourier-, Hilbert-and wavelet-based signal analysis: are they really different approaches? *Journal of Neuroscience Methods*.

Busch, N., Dubois, J., & VanRullen, R. (2009). The phase of ongoing EEG oscillations predicts visual perception. *The Journal of Neuroscience*.

Busch, N. N. A., & VanRullen, R. (2010). Spontaneous EEG oscillations reveal periodic sampling of visual attention. *Proceedings of the National …*, *107*(37), 16048–16053. Journal Article.

Busch, N., & VanRullen, R. (2010). Spontaneous EEG oscillations reveal periodic sampling of visual attention. *Proceedings of the National …*.

Buschman, T., & Miller, E. (2007). Top-down versus bottom-up control of attention in the prefrontal and posterior parietal cortices. *Science*.

Buschman, T., & Miller, E. (2009). Serial, covert shifts of attention during visual search are reflected by

the frontal eye fields and correlated with population oscillations. *Neuron*.

Buzsaki, G. (2006). *Rhythms of the Brain*.

Buzsáki, G., & Draguhn, A. (2004). Neuronal oscillations in cortical networks. *Science*, *304*(5679), 1926–1929. Journal Article.

Buzsáki, G., & Draguhn, A. (2004). Neuronal oscillations in cortical networks. *Science*.

Calvert, G. (2001). Crossmodal processing in the human brain: insights from functional neuroimaging studies. *Cerebral Cortex*.

Calvert, K., Bhattacharjee, S., & Zegura, E. (1998). Directions in active networks. *IEEE*.

Canavier, C. (2015). Phase-resetting as a tool of information transmission. *Current Opinion in Neurobiology*.

Canolty, R. R. T., & Knight, R. R. T. (2010). The functional role of cross-frequency coupling. *Trends in Cognitive Sciences*, *14*(11), 506–15. https://doi.org/10.1016/j.tics.2010.09.001

Canolty, R. T., Edwards, E., Dalal, S. S., Soltani, M., Nagarajan, S. S., Kirsch, H. E., … Knight, R. T. (2006). High Gamma Power Is Phase-Locked to Theta Oscillations in, *313*(September), 1626–1628.

Cao, L., & Gross, J. (2015). Cultural Differences in Perceiving Sounds Generated by Others: Self Matters. *Frontiers in Psychology*, *6*, 1865. https://doi.org/10.3389/fpsyg.2015.01865

Cao, L., Thut, G., & Gross, J. (2016a). The role of brain oscillations in predicting self-generated sounds. *NeuroImage*. https://doi.org/10.1016/j.neuroimage.2016.11.001

Cao, L., Thut, G., & Gross, J. (2016b). The role of brain oscillations in predicting the sensory consequences of your actions. *bioRxiv*.

Cao, L., Thut, G., & Gross, J. (2016). The role of brain oscillations in predicting the sensory consequences of your actions. *bioRxiv*.

Capilla, A., Schoffelen, J.-M., Paterson, G., Thut, G., & Gross, J. (2014). Dissociated α-band modulations in the dorsal and ventral visual pathways in visuospatial attention and perception. *Cerebral Cortex (New York, N.Y. : 1991)*, *24*(2), 550–61. https://doi.org/10.1093/cercor/bhs343

Cappe, C., & Barone, P. (2005). Heteromodal connections supporting multisensory integration at low levels of cortical processing in the monkey. *European Journal of Neuroscience*.

Cardoso-Leite, P., & Mamassian, P. (2010). A new look at sensory attenuation action-effect anticipation affects sensitivity, not response bias. *Psychological*.

Casco, C., Morgan, M., & Ward, R. (1988). Spatial properties of mechanisms for detection of moving dot targets in dynamic visual noise. *Perception*.

Cavanagh, P., & Mather, G. (1989). Motion: The long and short of it. *Spatial Vision*.

Chakravarthi, R., & Vanrullen, R. (2012). Conscious updating is a rhythmic process. *Proceedings of the National Academy of Sciences of the United States of America*, *109*(26), 10599–604. https://doi.org/10.1073/pnas.1121622109

Chapman, L., Chapman, J., & Kwapil, T. (1994). Putatively psychosis-prone subjects 10 years later. *Journal of Abnormal*.

Chen, C., Lakatos, P., Shah, A., & Mehta, A. (2007). Functional anatomy and interaction of fast and slow visual pathways in macaque monkeys. *Cerebral*.

Chen, C., Mathalon, D., Roach, B., & Cavus, I. (2011). The corollary discharge in humans is related to synchronous neural oscillations. *Journal of Cognitive*.

Claridge, G. (1994). Single indicator of risk for schizophrenia: probable fact or likely myth? *Schizophrenia Bulletin*.

Clavagnier, S., Falchier, A., & Kennedy, H. (2004). Long-distance feedback projections to area V1: implications for multisensory integration, spatial awareness, and visual consciousness. *Cognitive, Affective, & Behavioral*.

Cleary, R., & Braddick, O. (1990). Masking of low frequency information in short-range apparent motion. *Vision Research*.

Cohen, D. (1972). Magnetoencephalography: detection of the brain's electrical activity with a superconducting magnetometer. *Science*.

Cohen, D. (2004). Boston and the history of biomagnetism. *Neurology and Clinical Neurophysiology*.

Cohen, M. (2014). *Analyzing neural time series data: theory and practice*.

David, O., Harrison, L., & Friston, K. (2005). Modelling event-related responses in the brain. *NeuroImage*.

David, O., Kilner, J. M., & Friston, K. J. (2006). Mechanisms of evoked and induced responses in

MEG/EEG. *NeuroImage*, *31*(4), 1580–1591. https://doi.org/10.1016/j.neuroimage.2006.02.034

Davidson, R. J. (1988). EEG Measures of Cerebral Asymmetry: Conceptual and Methodological Issues. *International Journal of Neuroscience*, *39*(1–2), 71–89. https://doi.org/10.3109/00207458808985694

Delorme, A., & Makeig, S. (2004). EEGLAB: an open source toolbox for analysis of single-trial EEG dynamics including independent component analysis. *Journal of Neuroscience Methods*.

Demiralp, T., Ademoglu, A., & Istefanopulos, Y. (1998). Analysis of event-related potentials (ERP) by damped sinusoids. *Biological Cybernetics*.

Devrim, M., Demiralp, T., Ademoglu, A., & Kurt, A. (1999). A model for P300 generation based on responses to near-threshold visual stimuli. *Cognitive Brain Research*, *8*(1), 37–43. https://doi.org/10.1016/S0926-6410(99)00007-5

Diederich, A., Schomburg, A., & Colonius, H. (2012). Saccadic reaction times to audiovisual stimuli show effects of oscillatory phase reset. *PloS One*.

Diederich, A., Schomburg, A., van Vugt, M., Senkowski, D., Schneider, T., Foxe, J., … Kastern, S. (2014). Fronto-Central Theta Oscillations Are Related to Oscillations in Saccadic Response Times (SRT): An EEG and Behavioral Data Analysis. *PLoS ONE*, *9*(11), e112974. https://doi.org/10.1371/journal.pone.0112974

Dijk, H. Van, Schoffelen, J., & Oostenveld, R. (2008). Prestimulus oscillatory activity in the alpha band predicts visual discrimination ability. *The Journal of*.

Dijk, H. van, Werf, J. van der, & Mazaheri, A. (2010). Modulations in oscillatory activity with amplitude asymmetry can produce cognitively relevant event-related responses. *Proceedings of the*.

Ding, N., & Simon, J. (2013). Power and phase properties of oscillatory neural responses in the presence of background activity. *Journal of Computational Neuroscience*.

Doelling, K., Arnal, L., Ghitza, O., & Poeppel, D. (2014). Acoustic landmarks drive delta–theta oscillations to enable speech comprehension by facilitating perceptual parsing. *Neuroimage*.

Donchin, E., & Coles, M. (1988). Is the P300 component a manifestation of context updating. *Behavioral and Brain Sciences*.

Donner, T., Siegel, M., Fries, P., & Engel, A. (2009). Buildup of choice-predictive activity in human motor cortex during perceptual decision making. *Current Biology*.

Driver, J., & Spence, C. (1998). Attention and the crossmodal construction of space. *Trends in Cognitive Sciences*.

Dugué, L., Marque, P., & VanRullen, R. (2011). The phase of ongoing oscillations mediates the causal relation between brain excitation and visual perception. *The Journal of Neuroscience*, *31*(33), 11889–11893. Journal Article.

Dugué, L., Marque, P., & VanRullen, R. (2011). The phase of ongoing oscillations mediates the causal relation between brain excitation and visual perception. *The Journal of Neuroscience*.

Dugué, L., Marque, P., & VanRullen, R. (2015). Theta oscillations modulate attentional search performance periodically. *Journal of Cognitive Neuroscience*.

Eagle, R. A., & Rogers, B. J. (1996). Motion detection is limited by element density not spatial frequency. *Vision Research*, *36*(4), 545–558. https://doi.org/10.1016/0042-6989(96)89252-2

Easton, R., & Moran, P. (1978). A quantitative confirmation of visual capture of curvature. *The Journal of General Psychology*.

Eimer, M., & Driver, J. (2000). An event-related brain potential study of cross-modal links in spatial attention between vision and touch. *Psychophysiology*, *37*(5), 697–705.

Engel, A., Gerloff, C., Hilgetag, C., & Nolte, G. (2013). Intrinsic coupling modes: multiscale interactions in ongoing brain activity. *Neuron*.

Engel, A. K., & Fries, P. (2010). Beta-band oscillations—signalling the status quo? *Current Opinion in Neurobiology*, *20*(2), 156–165. https://doi.org/10.1016/j.conb.2010.02.015

Engel, A., & Singer, W. (2001). Temporal binding and the neural correlates of sensory awareness. *Trends in Cognitive Sciences*.

Ergenoglu, T., Demiralp, T., Bayraktaroglu, Z., Ergen, M., Beydagi, H., & Uresin, Y. (2004). Alpha rhythm of the EEG modulates visual detection performance in humans. *Brain Research. Cognitive Brain Research*, *20*(3), 376–83. https://doi.org/10.1016/j.cogbrainres.2004.03.009

Ermentrout, G. B., & Kleinfeld, D. (2001). Traveling Electrical Waves in Cortex: Insights from Phase Dynamics and Speculation on a Computational Role. *Neuron*, *29*(1), 33–44.

https://doi.org/10.1016/S0896-6273(01)00178-7

Falchier, A., Clavanier, S., & Barone, P. (2002). Anatomical Evidence of Multimodal Integration in Primate Striate Cortex. *Journal of*.

Farries, M., & Wilson, C. (2012). Phase response curves of subthalamic neurons measured with synaptic input and current injection. *Journal of Neurophysiology*.

Fell, J., Dietl, T., Grunwald, T., Kurthen, M., Klaver, P., Trautner, P., ... Fernández, G. (2004). Neural bases of cognitive ERPs: more than phase reset. *Journal of Cognitive Neuroscience*, *16*(9), 1595–1604. Journal Article.

Fiebelkorn, I. C., Foxe, J. J., Butler, J. S. J., Mercier, M. R., Snyder, A. C., & Molholm, S. (2011). Ready, Set, Reset: Stimulus-Locked Periodicity in Behavioral Performance Demonstrates the Consequences of Cross-Sensory Phase Reset. *Journal of Neuroscience*, *31*(27), 9971–9981. https://doi.org/10.1523/JNEUROSCI.1338-11.2011

Fiebelkorn, I. C. I., Saalmann, Y. B. Y., & Kastner, S. (2013). Rhythmic sampling within and between objects despite sustained attention at a cued location. *Current Biology*, *23*(24), 2553–8. https://doi.org/10.1016/j.cub.2013.10.063

Fiebelkorn, I. C., Snyder, A. C., Mercier, M. R., Butler, J. S., Molholm, S., & Foxe, J. J. (2013). Cortical cross-frequency coupling predicts perceptual outcomes. *Neuroimage*, *69*, 126–137. Journal Article.

Fiebelkorn, I., Foxe, J., & Butler, J. (2011). Ready, set, reset: stimulus-locked periodicity in behavioral performance demonstrates the consequences of cross-sensory phase reset. *The Journal of*.

Fiebelkorn, I., Foxe, J., Butler, J., & Molholm, S. (2011). Auditory facilitation of visual-target detection persists regardless of retinal eccentricity and despite wide audiovisual misalignments. *Experimental Brain Research*.

Fiebelkorn, I., Saalmann, Y., & Kastner, S. (2013). Rhythmic sampling within and between objects despite sustained attention at a cued location. *Current Biology*.

Fisher, N. I. (1995). *Statistical Analysis of Circular Data*. Cambridge University Press.

Fletcher, P., & Frith, C. (2009). Perceiving is believing: a Bayesian approach to explaining the positive symptoms of schizophrenia. *Nature Reviews Neuroscience*.

Ford, J. M., Mathalon, D. H., Heinks, T., Kalba, S., Faustman, W. O., & Roth, W. T. (2001). Neurophysiological Evidence of Corollary Discharge Dysfunction in Schizophrenia. *American Journal of Psychiatry*, *158*(12), 2069–2071. https://doi.org/10.1176/appi.ajp.158.12.2069

Ford, J., Palzes, V., Roach, B., & Mathalon, D. (2013). Did I do that? Abnormal predictive processes in schizophrenia when button pressing to deliver a tone. *Schizophrenia Bulletin*.

Ford, J., Roach, B., & Faustman, W. (2007). Synch before you speak: auditory hallucinations in schizophrenia. *American Journal of*.

Forrest, T. G., & Suter, R. B. (1994). The Discrete Fourier Transform (DFT) in Behavioural Analysis. *Journal of Theoretical Biology*, *166*(4), 419–429. https://doi.org/10.1006/jtbi.1994.1037

Fort, A., Delpuech, C., Pernier, J., & Giard, M. (2002). Early auditory–visual interactions in human cortex during nonredundant target identification. *Cognitive Brain Research*.

Foxe, J., Morocz, I., & Murray, M. (2000). Multisensory auditory–somatosensory interactions in early cortical processing revealed by high-density electrical mapping. *Cognitive Brain ....*

Foxe, J., & Snyder, A. (2011). The role of alpha-band brain oscillations as a sensory suppression mechanism during selective attention. *Frontiers in Psychology*.

Foxe, J., & Wylie, G. (2002). Auditory-somatosensory multisensory processing in auditory association cortex: an fMRI study. *Journal of ....*

Fredericksen, R., Verstraten, F., & Grind, W. Van De. (1994). Temporal integration of random dot apparent motion information in human central vision. *Vision Research*.

Fries, P. (2005). A mechanism for cognitive dynamics: neuronal communication through neuronal coherence. *Trends in Cognitive Sciences*.

Fries, P. (2005). A mechanism for cognitive dynamics: neuronal communication through neuronal coherence. *Trends in Cognitive Sciences*, *9*(10), 474–480. Journal Article.

Fries, P. (2009). Neuronal gamma-band synchronization as a fundamental process in cortical computation. *Annual Review of Neuroscience*.

Fries, P. (2015). Rhythms for cognition: communication through coherence. *Neuron*.

Fries, P., Neuenschwander, S., Engel, A., & Goebel, R. (2001). Rapid feature selective neuronal synchronization through correlated latency shifting. *Nature*.

Fries, P., Nikolić, D., & Singer, W. (2007). The gamma cycle. *Trends in Neurosciences*, *30*(7), 309–16. https://doi.org/10.1016/j.tins.2007.05.005

Fries, P., Reynolds, J., Rorie, A., & Desimone, R. (2001). Modulation of oscillatory neuronal synchronization by selective visual attention. *Science*.

Fries, P., Womelsdorf, T., & Oostenveld, R. (2008). The effects of visual stimulation and selective visual attention on rhythmic neuronal synchronization in macaque area V4. *The Journal of ….*

Friston, K. (2005). A theory of cortical responses. *Transactions of the Royal Society B: ….*

Friston, K. (2012). Prediction, perception and agency. *International Journal of Psychophysiology*, *83*(2), 248–252. Journal Article.

Frith, C. (2005). The neural basis of hallucinations and delusions. *Comptes Rendus Biologies*, *328*(2), 169–175. https://doi.org/10.1016/j.crvi.2004.10.012

Frith, C., & Wolpert, D. (2000). Abnormalities in the awareness and control of action. *Of the Royal ….*

Fujioka, T., Trainor, L., & Large, E. (2012). Internalized timing of isochronous sounds is represented in neuromagnetic beta oscillations. *The Journal of.*

Geffen, G., Wright, M., Green, H., & Gillespie, N. (1997). Effects of memory load and distraction on performance and event-related slow potentials in a visuospatial working memory task. *Journal of Cognitive.*

Gentsch, A., & Schütz-Bosbach, S. (2011). I did it: unconscious expectation of sensory consequences modulates the experience of self-agency and its functional signature. *Journal of Cognitive Neuroscience.*

Giard, M. H., & Peronnet, F. (1999). Auditory-visual integration during multimodal object recognition in humans: a behavioral and electrophysiological study. *Journal of Cognitive Neuroscience*, *11*(5), 473–490. https://doi.org/10.1162/089892999563544

Gibson, J. (1933). Adaptation, after-effect and contrast in the perception of curved lines. *Journal of Experimental Psychology.*

Gold, J. I., & Shadlen, M. N. (2007). The Neural Basis of Decision Making. *Annual Review of Neuroscience*, *30*(1), 535–574. https://doi.org/10.1146/annurev.neuro.29.051605.113038

Golumbic, E., Ding, N., Bickel, S., & Lakatos, P. (2013). Mechanisms underlying selective neuronal tracking of attended speech at a 'cocktail party'. *Neuron.*

Gomez-Ramirez, M., Kelly, S., & Molholm, S. (2011). Oscillatory sensory selection mechanisms during intersensory attention to rhythmic auditory and visual inputs: a human electrocorticographic investigation. *The Journal of.*

Graaf, T. De, Gross, J., Paterson, G., & Rusch, T. (2013). Alpha-band rhythms in visual task performance: phase-locking by rhythmic sensory stimulation. *PloS One.*

Graaf, T. De, Gross, J., Paterson, G., Rusch, T., de Graaf, T. a, Gross, J., … Thut, G. (2013). Alpha-band rhythms in visual task performance: phase-locking by rhythmic sensory stimulation. *PloS One*, *8*(3), e60035. https://doi.org/10.1371/journal.pone.0060035

Green, D., & Swets, J. (1966). *Signal detection theory and psychophysics.*

Gröchenig, K. (2001). *Foundations of Time-Frequency Analysis.*

Groppe, D., Urbach, T., & Kutas, M. (2011). Mass univariate analysis of event-related brain potentials/fields I: A critical tutorial review. *Psychophysiology.*

Gross, J., Baillet, S., Barnes, G. R., Henson, R. N., Hillebrand, A., Jensen, O., … Schoffelen, J.-M. (2013). Good practice for conducting and reporting MEG research. *NeuroImage*, *65*, 349–63. Journal Article. https://doi.org/10.1016/j.neuroimage.2012.10.001

Gross, J., & Schmitz, F. (2004). Modulation of long-range neural synchrony reflects temporal limitations of visual attention in humans. *Proceedings of the ….*

Gross, J., Schnitzler, A., Timmermann, L., & Ploner, M. (2007). Gamma Oscillations in Human Primary Somatosensory Cortex Reflect Pain Perception. *PLoS Biology*, *5*(5), e133. https://doi.org/10.1371/journal.pbio.0050133

Gross, J., Timmermann, L., Kujala, J., Dirks, M., Schmitz, F., Salmelin, R., & Schnitzler, A. (2002). The neural basis of intermittent motor control in humans. *Proceedings of the National Academy of Sciences of the United States of America*, *99*(4), 2299–302. https://doi.org/10.1073/pnas.032682099

Gruber, W., Klimesch, W., & Sauseng, P. (2005). Alpha phase synchronization predicts P1 and N1 latency and amplitude size. *Cerebral.*

Haegens, S., Händel, B., & Jensen, O. (2011). Top-down controlled alpha band activity in somatosensory areas determines behavioral performance in a discrimination task. *The Journal of Neuroscience*.

Haegens, S., Nácher, V., & Luna, R. (2011). α-Oscillations in the monkey sensorimotor network influence discrimination performance by rhythmical inhibition of neuronal spiking. *Proceedings of the ….*

Haig, A., & Gordon, E. (n.d.). EEG alpha phase at stimulus onset significantly affects the amplitude of the P3 ERP component.

Hamada, Y., Miyashita, E., & Tanaka, H. (1999). Gamma-band oscillations in the 'barrel cortex' precede rat's exploratory whisking. *Neuroscience*.

Hämäläinen, M., Hari, R., & Ilmoniemi, R. (1993). Magnetoencephalography—theory, instrumentation, and applications to noninvasive studies of the working human brain. *Reviews of Modern ….*

Hämäläinen, M., Hari, R., Ilmoniemi, R. J. R., Knuutila, J., & Lounasmaa, O. V. (1993). Magnetoencephalography—theory, instrumentation, and applications to noninvasive studies of the working human brain. *Reviews of Modern Physics*, *65*(2), 413–497. https://doi.org/10.1103/RevModPhys.65.413

Han, B., & VanRullen, R. (2016). The rhythms of predictive coding: pre-stimulus phase modulates the influence of shape perception on luminance judgments. *bioRxiv*.

Hanslmayr, S., Aslan, A., Staudigl, T., Klimesch, W., Herrmann, C. S., & Bäuml, K.-H. (2007). Prestimulus oscillations predict visual perception performance between and within subjects. *NeuroImage*, *37*(4), 1465–73. https://doi.org/10.1016/j.neuroimage.2007.07.011

Hanslmayr, S., Gross, J., Klimesch, W., & Shapiro, K. (2011). The role of alpha oscillations in temporal attention. *Brain Research Reviews*.

Hanslmayr, S., Klimesch, W., & Sauseng, P. (2007). Alpha phase reset contributes to the generation of ERPs. *… Cortex*.

Hanslmayr, S., Klimesch, W., Sauseng, P., Gruber, W., Doppelmayr, M., Freunberger, R., & Pecherstorfer, T. (2005a). *Visual discrimination performance is related to decreased alpha amplitude but increased phase locking*. *Neuroscience Letters* (Vol. 375). https://doi.org/10.1016/j.neulet.2004.10.092

Hanslmayr, S., Klimesch, W., Sauseng, P., Gruber, W., Doppelmayr, M., Freunberger, R., & Pecherstorfer, T. (2005b). Visual discrimination performance is related to decreased alpha amplitude but increased phase locking. *Neuroscience Letters*, *375*(1), 64–8. https://doi.org/10.1016/j.neulet.2004.10.092

Hanslmayr, S., Volberg, G., & Wimber, M. (2013). Prestimulus oscillatory phase at 7 Hz gates cortical information flow and visual perception. *Current Biology*.

Hari, R. (1993). Magnetoencephalography as a tool of clinical neurophysiology. *Electroencephalography. Baltimore, Williams & Wilkins*.

Hari, R., Salmelin, R., & Makela, J. (1997). Magnetoencephalographic cortical rhythms. *International Journal of ….*

HARTER, M. (1967). Excitability cycles and cortical scanning: a review of two hypotheses of central intermittency in perception. *Psychological Bulletin*.

Harter, M., & White, C. (1968). Periodicity within reaction time distributions and electromyograms. *The Quarterly Journal of Experimental*.

Hay, I., & Keller, A. (1965). Polymer deformation in terms of spherulites. *Colloid & Polymer Science*.

Helmholtz, H. (1924). *Helmholtz's treatise on physiological optics,*. [Rochester N.Y.]: Optical Society of America.

Helmholtz, H. Von. (1867). *Handbuch der physiologischen Optik*.

Henry, M. M. J., & Obleser, J. (2012). Frequency modulation entrains slow neural oscillations and optimizes human listening behavior. *Proceedings of the National Academy of Sciences*, *109*(49), 20095–20100. Journal Article.

Hesse, M., Nishitani, N., Fink, G., & Jousmäki, V. (2010). Attenuation of somatosensory responses to self-produced tactile stimulation. *Cerebral*.

Hillyard, S., & Kutas, M. (1983). Electrophysiology of cognitive processing. *Annual Review of Psychology*.

Hillyard, S., Squires, K., Bauer, J., & Lindsay, P. (1971). Evoked potential correlates of auditory signal detection. *Science*.

Hipp, J., Hawellek, D., Corbetta, M., & Siegel, M. (2012). Large-scale cortical correlation structure of

spontaneous oscillatory activity. *Nature*.

Holst, E., & Mittelstaedt, H. (1950). Das reafferenzprinzip. *Naturwissenschaften*.

Horváth, J., Maess, B., Baess, P., & Tóth, A. (2012). Action–Sound Coincidences Suppress Evoked Responses of the Human Auditory Cortex in EEG and MEG. *Journal of Cognitive Neuroscience*, *24*(9), 1919–1931. https://doi.org/10.1162/jocn_a_00215

Horwitz, G., & Newsome, W. (1999). Separate signals for target selection and movement specification in the superior colliculus. *Science*.

Hughes, G., Desantis, A., & Waszak, F. (2013). Mechanisms of intentional binding and sensory attenuation: The role of temporal prediction, temporal control, identity prediction, and motor prediction. *Psychological Bulletin*.

Hughes, G., & Waszak, F. (2011). ERP correlates of action effect prediction and visual sensory attenuation in voluntary action. *Neuroimage*.

Hutcheon, B., & Yarom, Y. (2000). Resonance, oscillation and the intrinsic frequency preferences of neurons. *Trends in Neurosciences*.

Ito, K., & Speer, S. R. (2008). Anticipatory effects of intonation: Eye movements during instructed visual search. *Journal of Memory and Language*, *58*(2), 541–573. Journal Article.

Jacobs, J., Kahana, M., & Ekstrom, A. (2007). Brain oscillations control timing of single-neuron activity in humans. *The Journal of*.

Jansen, B., & Brandt, M. (1991). The effect of the phase of prestimulus alpha activity on the averaged visual evoked response. *Electroencephalography and Clinical*.

Jensen, O., Bonnefond, M., & VanRullen, R. (2012). An oscillatory mechanism for prioritizing salient unattended stimuli. *Trends in Cognitive Sciences*.

Jensen, O., & Colgin, L. L. L. (2007). Cross-frequency coupling between neuronal oscillations. *Trends in Cognitive Sciences*, *11*(7), 267–269. Journal Article.

Jensen, O., & Mazaheri, A. (2010). Shaping functional architecture by oscillatory alpha activity: gating by inhibition. *Frontiers in Human Neuroscience*.

Jensen, O., & Mazaheri, A. (2010). Shaping functional architecture by oscillatory alpha activity: gating by inhibition. *Frontiers in Human Neuroscience*, *4*(November), 186. https://doi.org/10.3389/fnhum.2010.00186

Jervis, B., Nichols, M., Johnson, T., & Allen, E. (1983). A fundamental investigation of the composition of auditory evoked potentials. *IEEE Transactions on*.

Johnson, R., Hirschkoff, E., & Buchanan, D. (2003). Full-sensitivity biomagnetometers: Sam Williamson's vision brought to life. *Magnetic Source Imaging of the Human Brain*, 217–229. Journal Article.

Jones, K. A., Porjesz, B., Almasy, L., Bierut, L., Goate, A., Wang, J. C., … Begleiter, H. (2004). Linkage and linkage disequilibrium of evoked EEG oscillations with CHRM2 receptor gene polymorphisms: implications for human brain dynamics and cognition. *International Journal of Psychophysiology*, *53*(2), 75–90. https://doi.org/10.1016/j.ijpsycho.2004.02.004

Kayser, C. (2009). Phase resetting as a mechanism for supramodal attentional control. *Neuron*, *64*(3), 300–302. Journal Article.

Kayser, C., & Logothetis, N. K. N. (2007). Do early sensory cortices integrate cross-modal information? *Brain Structure & Function*, *212*(2), 121–32. https://doi.org/10.1007/s00429-007-0154-0

Kayser, C., Petkov, C. I. C., & Logothetis, N. K. N. (2008). Visual modulation of neurons in auditory cortex. *Cerebral Cortex*, *18*(7), 1560–1574. Journal Article.

Kayser, C., Petkov, C., & Logothetis, N. (2008). Visual modulation of neurons in auditory cortex. *Cerebral Cortex*.

Kiesel, A., Miller, J., Jolicœur, P., & Brisson, B. (2008). Measurement of ERP latency differences: A comparison of single-participant and jackknife-based scoring methods. *Psychophysiology*.

Kiesel, A., Wagener, A., Kunde, W., & Hoffmann, J. (2006). Unconscious manipulation of free choice in humans. *Consciousness and*.

Kim, R., Peters, M. A. K., & Shams, L. (2012). 0 + 1 > 1: How adding noninformative sound improves performance on a visual task. *Psychological Science*, *23*(1), 6–12. https://doi.org/10.1177/0956797611420662

Kim, R., Peters, M., & Shams, L. (2012). 0+ 1> 1 how adding noninformative sound improves performance on a visual task. *Psychological Science*.

Klimesch, W., Fellinger, R., & Freunberger, R. (2011). Alpha oscillations and early stages of visual encoding. *Frontiers in Psychology*, *2*, 118. https://doi.org/10.3389/fpsyg.2011.00118

Klimesch, W., Hanslmayr, S., Sauseng, P., & Gruber, W. (2006). Distinguishing the evoked response from phase reset: A comment to Mäkinen et al. *Neuroimage*.

Klimesch, W., Sauseng, P., & Hanslmayr, S. (2007a). EEG alpha oscillations: the inhibition–timing hypothesis. *Brain Research Reviews*.

Klimesch, W., Sauseng, P., & Hanslmayr, S. (2007b). Event-related phase reorganization may explain evoked neural dynamics. *Neuroscience & ….*

Klimesch, W., Sauseng, P., Hanslmayr, S., & Gruber, W. (2007). Event-related phase reorganization may explain evoked neural dynamics. *Neuroscience & ….*

Klimesch, W., Schack, B., & Schabus, M. (2004). Phase-locked alpha and theta oscillations generate the P1–N1 complex and are related to memory performance. *Cognitive Brain ….*

Kline, K., & Eagleman, D. (2008). Evidence against the temporal subsampling account of illusory motion reversal. *Journal of Vision*.

Knolle, F., Schröger, E., Baess, P., & Kotz, S. (2012). The cerebellum generates motor-to-auditory predictions: ERP lesion evidence. *Journal of Cognitive*.

Kolev, V., Demiralp, T., Yordanova, J., & Ademoglu, A. (1997). Time–frequency analysis reveals multiple functional components during oddball P300.

Kopell, N., Ermentrout, G. B., Whittington, M. A., & Traub, R. D. (2000). Gamma rhythms and beta rhythms have different synchronization properties. *Proceedings of the National Academy of Sciences*, *97*(4), 1867–1872. https://doi.org/10.1073/pnas.97.4.1867

Kremláček, J., Kuba, M., & Kubova, Z. (2004). Motion-onset VEPs to translating, radial, rotating and spiral stimuli. *Documenta*.

Kruglikov, S., & Schiff, S. (2003). Interplay of electroencephalogram phase and auditory-evoked neural activity. *The Journal of Neuroscience*.

Lachaux, J., & Rodriguez, E. (1999). Measuring phase synchrony in brain signals. *Human Brain ….*

Lachaux, J., & Rodriguez, E. (2000). Studying single-trials of phase synchronous activity in the brain. *… Journal of Bifurcation ….*

Lakatos, P., Chen, C.-M., O'Connell, M. N., Mills, A., & Schroeder, C. E. (2007). Neuronal oscillations and multisensory interaction in primary auditory cortex. *Neuron*, *53*(2), 279–292. Journal Article.

Lakatos, P., Karmos, G., Mehta, A. D. A., Ulbert, I., & Schroeder, C. E. (2008). Entrainment of neuronal oscillations as a mechanism of attentional selection. *Science*, *320*(5872), 110–113. Journal Article.

Lakatos, P., Musacchia, G., O'Connel, M. N., Falchier, A. Y., Javitt, D. C., & Schroeder, C. E. (2013). The spectrotemporal filter mechanism of auditory selective attention. *Neuron*, *77*(4), 750–61. https://doi.org/10.1016/j.neuron.2012.11.034

Lakatos, P., O'Connell, M. N., Barczak, A., Mills, A., Javitt, D. C., & Schroeder, C. E. (2009). The leading sense: supramodal control of neurophysiological context by attention. *Neuron*, *64*(3), 419–430. Journal Article.

Lakatos, P., Schroeder, C., & Leitman, D. (2013). Predictive suppression of cortical excitability and its deficit in schizophrenia. *The Journal of*.

Lakatos, P., Shah, A. A. S., Knuth, K. K. H., Ulbert, I., Karmos, G., & Schroeder, C. E. (2005). An oscillatory hierarchy controlling neuronal excitability and stimulus processing in the auditory cortex. *Journal of …*, *94*(3), 1904–1911. Journal Article.

Lakatos, P., Shah, A., & Knuth, K. (2005). An oscillatory hierarchy controlling neuronal excitability and stimulus processing in the auditory cortex. *Journal of ….*

Lakatos, P., Shah, A., Knuth, K., & Ulbert, I. (2005). An oscillatory hierarchy controlling neuronal excitability and stimulus processing in the auditory cortex. *Journal of*.

Lally, N., Frendo, B., & Diedrichsen, J. (2011). Sensory cancellation of self-movement facilitates visual motion detection. *Journal of Vision*.

Landau, A., & Fries, P. (2012). Attention samples stimuli rhythmically. *Current Biology*.

Landau, A. N. A., & Fries, P. (2012). Attention samples stimuli rhythmically. *Current Biology*, *22*(11), 1000–1004. https://doi.org/10.1016/j.cub.2012.03.054

Lange, J., Oostenveld, R., & Fries, P. (2013). Reduced occipital alpha power indexes enhanced excitability rather than improved visual perception. *The Journal of Neuroscience*.

Lappin, J., & Bell, H. (1976). The detection of coherence in moving random-dot patterns. *Vision*

Research.

Latour, P. (1967). Evidence of internal clocks in the human operator. *Acta Psychologica*.

Laurienti, P. J., Perrault, T. J., Stanford, T. R., Wallace, M. T., & Stein, B. E. (2005). On the use of superadditivity as a metric for characterizing multisensory integration in functional neuroimaging studies. *Experimental Brain Research*, *166*(3–4), 289–297. https://doi.org/10.1007/s00221-005-2370-2

Leitão, J., Thielscher, A., Werner, S., & Pohmann, R. (2013). Effects of parietal TMS on visual and auditory processing at the primary cortical level–a concurrent TMS-fMRI study. *Cerebral*.

Liebe, S., Hoerzer, G., Logothetis, N., & Rainer, G. (2012). Theta coupling between V4 and prefrontal cortex predicts visual short-term memory performance. *Nature Neuroscience*.

Lindner, A., Thier, P., Kircher, T., Haarmeier, T., & Leube, D. (2005). Disorders of agency in schizophrenia correlate with an inability to compensate for the sensory consequences of actions. *Current Biology*.

Lindner, A., Thier, P., Kircher, T. T. J., Haarmeier, T., & Leube, D. T. (2005). *Disorders of Agency in Schizophrenia Correlate with an Inability to Compensate for the Sensory Consequences of Actions*. *Current Biology* (Vol. 15). https://doi.org/10.1016/j.cub.2005.05.049

Llinás, R. (1988). Central Nervous System Function.

Lobier, M., Siebenhühner, F., Palva, S., & Palva, J. M. (2014). Phase transfer entropy: A novel phase-based measure for directed connectivity in networks coupled by oscillatory interactions. *Neuroimage*, *85*, 853–872. Journal Article.

Lőrincz, M., Kékesi, K., Juhász, G., & Crunelli, V. (2009). Temporal framing of thalamic relay-mode firing by phasic inhibition during the alpha rhythm. *Neuron*.

Luo, H., Liu, Z., & Poeppel, D. (2010). Auditory cortex tracks both auditory and visual stimulus dynamics using low-frequency neuronal phase modulation. *PLoS Biology*, *8*(8), e1000445. https://doi.org/10.1371/journal.pbio.1000445

Macmillan, N., & Creelman, C. (2005). Detection Theory: A User's Guide Lawrence Erlbaum Associates. *New York*.

Magri, C., Whittingstall, K., Singh, V., Logothetis, N. K., & Panzeri, S. (2009). A toolbox for the fast information analysis of multiple-site LFP, EEG and spike train recordings. *BMC Neuroscience*, *10*, 81. https://doi.org/10.1186/1471-2202-10-81

Makeig, S., Debener, S., Onton, J., & Delorme, A. (2004). Mining event-related brain dynamics. *Trends in Cognitive Sciences*.

Makeig, S., Westerfield, M., & Jung, T. (2002). Dynamic brain sources of visual evoked responses. *Science*.

Makeig, S., Westerfield, M., Jung, T., & Enghoff, S. (2002a). Dynamic brain sources of visual evoked responses.

Makeig, S., Westerfield, M., Jung, T., & Enghoff, S. (2002b). Dynamic brain sources of visual evoked responses. *Science*.

Mäkinen, V., Tiitinen, H., & May, P. (2005). Auditory event-related responses are generated independently of ongoing brain activity. *NeuroImage*.

Maloney, R., Mitchison, G., & Barlow, H. (1987). Limit to the detection of Glass patterns in the presence of noise. *JOSA A*.

Maris, E., & Oostenveld, R. (2007). Nonparametric statistical testing of EEG- and MEG-data. *Journal of Neuroscience Methods*, *164*(1), 177–90. https://doi.org/10.1016/j.jneumeth.2007.03.024

Marois, R., & Ivanoff, J. (2005). Capacity limits of information processing in the brain. *Trends in Cognitive Sciences*.

Martikainen, M., Kaneko, K., & Hari, R. (2005). Suppressed responses to self-triggered sounds in the human auditory cortex. *Cerebral Cortex*.

Martuzzi, R., Murray, M., Michel, C., & Thiran, J. (2007). Multisensory interactions within human primary cortices revealed by BOLD dynamics. *Cerebral*.

Mathewson, K., Gratton, G., & Fabiani, M. (2009). To see or not to see: prestimulus α phase predicts visual awareness. *The Journal of …*.

Mathewson, K., & Lleras, A. (2011). Pulsed out of awareness: EEG alpha oscillations represent a pulsed-inhibition of ongoing cortical processing. *Frontiers in …*.

Mazaheri, A., & Jensen, O. (2006). Posterior α activity is not phase-reset by visual stimuli. *… Academy*

of Sciences of the United ....

Mazaheri, A., & Jensen, O. (2008). Asymmetric amplitude modulations of brain oscillations generate slow evoked responses. *The Journal of Neuroscience*.

Mazaheri, A., & Jensen, O. (2010). Rhythmic pulsing: linking ongoing brain activity with evoked responses. *Front Hum Neurosci*.

Mazaheri, A., & Picton, T. (2005). EEG spectral dynamics during discrimination of auditory and visual targets. *Cognitive Brain Research*.

Mazaheri, A., Schouwenburg, M. van, & Dimitrijevic, A. (2014). Region-specific modulations in oscillatory alpha activity serve to facilitate processing in the visual and auditory modalities. *Neuroimage*.

McDonald, J. J., Störmer, V. S., Martinez, A., Feng, W., & Hillyard, S. A. (2013). Salient sounds activate human visual cortex automatically. *The Journal of Neuroscience : The Official Journal of the Society for Neuroscience*, *33*(21), 9194–201. https://doi.org/10.1523/JNEUROSCI.5902-12.2013

McDonald, J., Teder-Sälejärvi, W., & Hillyard, S. (2000). Involuntary orienting to sound improves visual perception. *Nature*.

McNicol, D. (2005). *A primer of signal detection theory*.

Mercier, M. M. R., Foxe, J. J. J., Fiebelkorn, I. C. I., Butler, J. S. J., Schwartz, T. H., & Molholm, S. (2013). Auditory-driven phase reset in visual cortex: Human electrocorticography reveals mechanisms of early multisensory integration. *Neuroimage*, *79*, 19–29. Journal Article. https://doi.org/10.1016/j.neuroimage.2013.04.060

Mercier, M. R., Molholm, S., Fiebelkorn, I. C., Butler, J. S., Schwartz, T. H., & Foxe, J. J. (2015). Neuro-oscillatory phase alignment drives speeded multisensory response times: an electro-corticographic investigation. *The Journal of Neuroscience : The Official Journal of the Society for Neuroscience*, *35*(22), 8546–57. https://doi.org/10.1523/JNEUROSCI.4527-14.2015

Miall, R., & Wolpert, D. (1996). Forward models for physiological motor control. *Neural Networks*.

Mifsud, N. G., Oestreich, L. K. L., Jack, B. N., Ford, J. M., Roach, B. J., Mathalon, D. H., & Whitford, T. J. (2016). Self-initiated actions result in suppressed auditory but amplified visual evoked components in healthy participants. *Psychophysiology*, *53*(5), 723–732. https://doi.org/10.1111/psyp.12605

Mifsud, N., Oestreich, L., Jack, B., & Ford, J. (2016). Self-initiated actions result in suppressed auditory but amplified visual evoked components in healthy participants.

Miles, R. (1990). Synaptic excitation of inhibitory cells by single CA3 hippocampal pyramidal cells of the guinea-pig in vitro. *The Journal of Physiology*.

Miller, J., Ulrich, R., & Schwarz, W. (2009). Why jackknifing yields good latency estimates. *Psychophysiology*.

Miller, K., Honey, C., Hermes, D., Rao, R., & Ojemann, J. (2014). Broadband changes in the cortical surface potential track activation of functionally diverse neuronal populations. *Neuroimage*.

Miller, R. (1991). *Cortico-Hippocampal Interplay and the Representation of Contexts in the Brain* (Vol. 17). Berlin, Heidelberg: Springer Berlin Heidelberg. https://doi.org/10.1007/978-3-662-21732-0

Min, B., Busch, N., Debener, S., & Kranczioch, C. (2007). The best of both worlds: Phase-reset of human EEG alpha activity< i> and</i> additive power contribute to ERP generation. *International Journal of ....*

Mishra, J., & Martinez, A. (2007). Early cross-modal interactions in auditory and visual cortex underlie a sound-induced visual illusion. *The Journal of ....*

Mitchell, J. F., Sundberg, K. A., & Reynolds, J. H. (2009). Spatial attention decorrelates intrinsic activity fluctuations in macaque area V4. *Neuron*, *63*(6), 879–88. https://doi.org/10.1016/j.neuron.2009.09.013

Molholm, S., Ritter, W., & Murray, M. (2002). Multisensory auditory–visual interactions during early sensory processing in humans: a high-density electrical mapping study. *Cognitive Brain ....*

Molholm, S., Sehatpour, P., & Mehta, A. (2006). Audio-visual multisensory integration in superior parietal lobule revealed by human intracranial recordings. *Journal of*.

Monto, S., & Palva, S. (2008). Very slow EEG fluctuations predict the dynamics of stimulus detection and oscillation amplitudes in humans. *The Journal of ....*

Moore, B., Bartoli, E., & Karunakaran, S. (2015). Multisensory Integration Reveals Temporal Coding

across a Human Sensorimotor Network. *The Journal of.*

Morand, S., Gross, J., & Thut, G. (2015). Temporal framing in apparent motion perception cycles with a 12Hz (alpha) rhythm. *Journal of Vision.*

Morillon, B., Hackett, T., & Kajikawa, Y. (2015). Predictive motor control of sensory dynamics in auditory active sensing. *Current Opinion in.*

Moutoussis, K., Keliris, G., Kourtzi, Z., & Logothetis, N. (2005). A binocular rivalry study of motion perception in the human brain. *Vision Research*, *45*(17), 2231–2243. https://doi.org/10.1016/j.visres.2005.02.007

Movshon, J., & Thompson, I. (1978). Spatial summation in the receptive fields of simple cells in the cat's striate cortex. *The Journal of Physiology.*

Müller, N., Leske, S., Hartmann, T., & Szebényi, S. (2014). Listen to yourself: the medial prefrontal cortex modulates auditory alpha power during speech preparation. *Cerebral.*

Naruse, Y., Matani, A., Hayakawa, T., & Fujimaki, N. (2006). Influence of seamlessness between pre-and poststimulus alpha rhythms on visual evoked potential. *Neuroimage.*

Naue, N., Rach, S., Strüber, D., & Huster, R. (2011). Auditory event-related response in visual cortex modulates subsequent visual responses in humans. *The Journal of.*

Naue, N., Rach, S., Strüber, D., Huster, R. J., Zaehle, T., Körner, U., & Herrmann, C. S. (2011). Auditory event-related response in visual cortex modulates subsequent visual responses in humans. *The Journal of Neuroscience : The Official Journal of the Society for Neuroscience*, *31*(21), 7729–36. https://doi.org/10.1523/JNEUROSCI.1076-11.2011

Neuling, T., Rach, S., Wagner, S., Wolters, C. C. H., & Herrmann, C. S. (2012). Good vibrations: oscillatory phase shapes perception. *Neuroimage*, *63*(2), 771–778. https://doi.org/10.1016/j.neuroimage.2012.07.024

Ng, B., Schroeder, T., & Kayser, C. (2012). A precluding but not ensuring role of entrained low-frequency oscillations for auditory perception. *The Journal of Neuroscience.*

Nichols, T., & Holmes, A. (2002). Nonparametric permutation tests for functional neuroimaging: a primer with examples. *Human Brain Mapping.*

Nicolelis, M., Baccala, L., Lin, R., & Chapin, J. (1995). Sensorimotor encoding by synchronous neural ensembly activity at multiple levels of the somatosensory system. *Science.*

Niedermeyer, E., & Silva, F. da. (2005). *Electroencephalography: basic principles, clinical applications, and related fields.*

Nieuwenhuis, S., Aston-Jones, G., & Cohen, J. (2005). Decision making, the P3, and the locus coeruleus--norepinephrine system. *Psychological Bulletin.*

Noesselt, T., Tyll, S., Boehler, C. N., Budinger, E., Heinze, H.-J., & Driver, J. (2010). Sound-Induced Enhancement of Low-Intensity Vision: Multisensory Influences on Human Sensory-Specific Cortices and Thalamic Bodies Relate to Perceptual Enhancement of Visual Detection Sensitivity. *Journal of Neuroscience*, *30*(41).

Nunez, P. L. (2006). *Electric fields of the brain: the neurophysics of EEG.* Book, Oxford University Press.

Odom, J., Bach, M., Barber, C., & Brigell, M. (2004). Visual evoked potentials standard (2004). *Documenta.*

Oldfield, R. (1971). The assessment and analysis of handedness: the Edinburgh inventory. *Neuropsychologia.*

Oostenveld, R., & Fries, P. (2010). FieldTrip: open source software for advanced analysis of MEG, EEG, and invasive electrophysiological data. *Computational ….*

Parasuraman, R., & Beatty, J. (1980). Brain events underlying detection and recognition of weak sensory signals. *Science.*

Park, H., Ince, R. A. A., Schyns, P. G., Thut, G., & Gross, J. (2015). Frontal top-down signals increase coupling of auditory low-frequency oscillations to continuous speech in human listeners. *Current Biology : CB*, *25*(12), 1649–53. https://doi.org/10.1016/j.cub.2015.04.049

Pascual-Marqui, R. D., Lehmann, D., Koukkou, M., Kochi, K., Anderer, P., Saletu, B., … Kinoshita, T. (2011). Assessing interactions in the brain with exact low-resolution electromagnetic tomography. *Philosophical Transactions. Series A, Mathematical, Physical, and Engineering Sciences*, *369*(1952), 3768–84. https://doi.org/10.1098/rsta.2011.0081

Paul, D., & Sutton, S. (1972). Evoked potential correlates of response criterion in auditory signal detection. *Science.*

Pelli, D. G. (1997, January 1). The VideoToolbox software for visual psychophysics: transforming numbers into movies. *Spatial Vision*. Brill.

Penny, W., Kiebel, S., Kilner, J., & Rugg, M. (2002). Event-related brain dynamics. *Trends in Neurosciences*.

Percival, D. B., & Walden, A. T. (1993). *Spectral Analysis for Physical Applications*. Cambridge University Press.

Perrodin, C., & Kayser, C. (2015). Natural asynchronies in audiovisual communication signals regulate neuronal multisensory interactions in voice-sensitive cortex. *Proceedings of the*.

Peters, E., Joseph, S., Day, S., & Garety, P. (2004). Measuring delusional ideation: the 21-item Peters et al. Delusions Inventory (PDI). *Schizophrenia Bulletin*.

Peters, E., Joseph, S., & Garety, P. (1999). Measurement of delusional ideation in the normal population: introducing the PDI (Peters et al. Delusions Inventory). *Schizophrenia Bulletin*.

Pfurtscheller, G., Silva, F. Da, & Lopes da Silva, F. H. (1999). Event-related EEG/MEG synchronization and desynchronization: basic principles. *Clinical Neurophysiology*, *110*(11), 1842–1857. Journal Article.

Pickering, M., & Garrod, S. (2007). Do people use language production to make predictions during comprehension? *Trends in Cognitive Sciences*.

Pitts, W., & McCulloch, W. (1947). How we know universals the perception of auditory and visual forms. *The Bulletin of Mathematical Biophysics*.

Ploner, M., Gross, J., Timmermann, L., & Pollok, B. (2006). Pain suppresses spontaneous brain rhythms. *Cerebral*.

Polich, J. (2007). Updating P300: an integrative theory of P3a and P3b. *Clinical Neurophysiology*.

Poulet, J., & Hedwig, B. (2007). New insights into corollary discharges mediated by identified neural pathways. *Trends in Neurosciences*.

Poppel, E., & Logothetis, N. (1986). Neuronal oscillations in the human brain. *Naturwissenschaften*, *73*(5), 267–268. https://doi.org/10.1007/BF00367781

Purves, D., & Paydarfar, J. (1996). The wagon wheel illusion in movies and reality. *Proceedings of the*.

Quyen, M. L. Van, & Bragin, A. (2007). Analysis of dynamic brain oscillations: methodological advances. *Trends in Neurosciences*.

Rahn, E., & Basar, E. (1993a). Enhancement of visual evoked potentials by stimulation during low prestimulus EEG stages. *International Journal of Neuroscience*.

Rahn, E., & Basar, E. (1993b). Prestimulus EEG-activity strongly influences the auditory evoked vertex response: a new method for selective averaging. *International Journal of Neuroscience*.

Raij, T., Ahveninen, J., Lin, F., Witzel, T., Jääskeläinen, I. P., Letham, B., … Stufflebeam, S. (2010). Onset timing of cross-sensory activations and multisensory interactions in auditory and visual sensory cortices. *European Journal of Neuroscience*, *31*(10), 1772–1782. Journal Article.

Ramachandran, V., & Anstis, S. (1983). Displacement thresholds for coherent apparent motion in random dot-patterns. *Vision Research*.

Ramachandran, V., & Anstis, S. (1986). The perception of apparent motion. *Scientific American*.

Ramachandran, V. V. S., & Anstis, S. S. M. (1986). The perception of apparent motion. *Scientific American*.

Raymond, J., Shapiro, K., & Arnell, K. (1992). Temporary suppression of visual processing in an RSVP task: An attentional blink? *Journal of Experimental ….*

Reuss, H., Kiesel, A., Kunde, W., & Hommel, B. (2011). Unconscious activation of task sets. *Consciousness and Cognition*.

Reznik, D., Henkin, Y., Levy, O., & Mukamel, R. (2015). Perceived loudness of self-generated sounds is differentially modified by expected sound intensity. *PloS One*.

Rinzel, J., & Ermentrout, G. B. (1998). Analysis of neural excitability and oscillations. *Methods in Neuronal Modeling*, *2*, 251–292. Journal Article.

Rizzuto, D. S., Madsen, J. R., Bromfield, E. B., Schulze-Bonhage, A., Seelig, D., Aschenbrenner-Scheibe, R., & Kahana, M. J. (2003). Reset of human neocortical oscillations during a working memory task. *Proceedings of the National Academy of Sciences of the United States of America*, *100*(13), 7931–6. https://doi.org/10.1073/pnas.0732061100

Rohe, T., & Noppeney, U. (2016). *Distinct Computational Principles Govern Multisensory Integration in Primary Sensory and Association Cortices*. *Current Biology* (Vol. 26).

https://doi.org/10.1016/j.cub.2015.12.056

Roitman, J., & Shadlen, M. (2002). Response of neurons in the lateral intraparietal area during a combined visual discrimination reaction time task. *The Journal of Neuroscience*.

Romei, V., Brodbeck, V., Michel, C., & Amedi, A. (2008). Spontaneous fluctuations in posterior α-band EEG activity reflect variability in excitability of human visual areas.

Romei, V., Brodbeck, V., Michel, C., Amedi, A., Pascual-Leone, A., & Thut, G. (2008). Spontaneous fluctuations in posterior alpha-band EEG activity reflect variability in excitability of human visual areas. *Cerebral Cortex (New York, N.Y.: 1991)*, *18*(9), 2010–8. https://doi.org/10.1093/cercor/bhm229

Romei, V., Driver, J., Schyns, P. G., & Thut, G. (2011). Rhythmic TMS over parietal cortex links distinct brain frequencies to global versus local visual processing. *Current Biology: CB*, *21*(4), 334–7. https://doi.org/10.1016/j.cub.2011.01.035

Romei, V., Gross, J., & Thut, G. (2010). On the role of prestimulus alpha rhythms over occipito-parietal areas in visual input regulation: correlation or causation? *The Journal of Neuroscience: The Official Journal of the Society for Neuroscience*, *30*(25), 8692–7. https://doi.org/10.1523/JNEUROSCI.0160-10.2010

Romei, V., Gross, J., & Thut, G. (2010). On the role of prestimulus alpha rhythms over occipito-parietal areas in visual input regulation: correlation or causation? *The Journal of Neuroscience*.

Romei, V., Gross, J., & Thut, G. (2012). Sounds reset rhythms of visual cortex and corresponding human visual perception. *Current Biology*, *22*(9), 807–813. Journal Article. https://doi.org/10.1016/j.cub.2012.03.025

Romei, V., Gross, J., & Thut, G. (2012). Sounds reset rhythms of visual cortex and corresponding human visual perception. *Current Biology*.

Romei, V., Murray, M., Cappe, C., & Thut, G. (2009). Preperceptual and stimulus-selective enhancement of low-level human visual cortex excitability by sounds. *Current Biology*.

Romei, V., Murray, M., & Merabet, L. (2007). Occipital transcranial magnetic stimulation has opposing effects on visual and auditory stimulus detection: implications for multisensory interactions. *The Journal of*.

Romei, V., Rihs, T., Brodbeck, V., & Thut, G. (2008). Resting electroencephalogram alpha-power over posterior sites indexes baseline visual cortex excitability. *Neuroreport*.

Romei, V., Rihs, T., Brodbeck, V., & Thut, G. (2008). Resting electroencephalogram alpha-power over posterior sites indexes baseline visual cortex excitability. *Neuroreport*, *19*(2), 203–8. https://doi.org/10.1097/WNR.0b013e3282f454c4

Rousselet, G., & Pernet, C. (2012). Improving standards in brain-behavior correlation analyses. *Frontiers in Human Neuroscience*.

Sachdev, R., & Ebner, F. (2004). Effect of subthreshold up and down states on the whisker-evoked response in somatosensory cortex. *Journal of*.

Sauseng, P. (2012). Brain oscillations: phase-locked EEG alpha controls perception. *Current Biology*.

Sauseng, P., & Griesmayr, B. (2010). Control mechanisms in working memory: a possible function of EEG theta oscillations. *… & Biobehavioral Reviews*.

Sauseng, P., Klimesch, W., & Gruber, W. (2007). Are event-related potential components generated by phase resetting of brain oscillations? A critical discussion. *Neuroscience*.

Sauseng, P., Klimesch, W., Gruber, W., & Hanslmayr, S. (2007). Are event-related potential components generated by phase resetting of brain oscillations? A critical discussion. *Neuroscience*.

Sayers, B., Beagley, H., & Henshall, W. (1974). The mechanism of auditory evoked EEG responses. *Nature*.

Schafer, E., & Marcus, M. (1973). Self-stimulation alters human sensory brain responses. *Science*.

Scheeringa, R., Mazaheri, A., & Bojak, I. (2011). Modulation of visually evoked cortical FMRI responses by phase of ongoing occipital alpha oscillations. *The Journal of*.

Schellart, N., Trindade, M., Reits, D., & Verbunt, J. (2004). Temporal and spatial congruence of components of motion-onset evoked responses investigated by whole-head magneto-electroencephalography. *Vision Research*.

Schlaghecken, F., & Eimer, M. (2004). Masked prime stimuli can bias 'free' choices between response alternatives. *Psychonomic Bulletin & Review*.

Schlykowa, L., Dijk, B. Van, & Ehrenstein, W. (1993). Motion-onset visual-evoked potentials as a

function of retinal eccentricity in man. *Cognitive Brain Research*.

Schneider, D., Nelson, A., & Mooney, R. (2014). A synaptic and circuit basis for corollary discharge in the auditory cortex. *Nature*.

Schnitzler, A., & Gross, J. (2005). Normal and pathological oscillatory communication in the brain. *Nature Reviews Neuroscience*, *6*(4), 285–296. Journal Article.

Schreiber, T. (2000). Measuring Information Transfer. *Physical Review Letters*, *85*(2), 461–464. https://doi.org/10.1103/PhysRevLett.85.461

Schroeder, C. C. E., & Lakatos, P. (2009). Low-frequency neuronal oscillations as instruments of sensory selection. *Trends in Neurosciences*, *32*(1), 9–18. Journal Article.

Schroeder, C. C. E., Lakatos, P., Kajikawa, Y., Partan, S., & Puce, A. (2008). Neuronal oscillations and visual amplification of speech. *Trends in Cognitive Sciences*, *12*(3), 106–113. Journal Article. https://doi.org/10.1016/j.tics.2008.01.002

Schroeder, C. E., & Foxe, J. (2005). Multisensory contributions to low-level, 'unisensory' processing. *Current Opinion in Neurobiology*, *15*(4), 454–8. https://doi.org/10.1016/j.conb.2005.06.008

Schroeder, C. E., & Lakatos, P. (2009). The gamma oscillation: master or slave? *Brain Topography*, *22*(1), 24–26. Journal Article.

Schroeder, C., & Foxe, J. (2002). The timing and laminar profile of converging inputs to multisensory areas of the macaque neocortex. *Cognitive Brain Research*.

Schroeder, C., & Foxe, J. (2005). Multisensory contributions to low-level,'unisensory'processing. *Current Opinion in Neurobiology*.

Schroeder, C., & Lakatos, P. (2009). Low-frequency neuronal oscillations as instruments of sensory selection. *Trends in Neurosciences*.

Schroeder, C., Lakatos, P., & Kajikawa, Y. (2008). Neuronal oscillations and visual amplification of speech. *Trends in Cognitive ….*

Schroeder, C., & Wilson, D. (2010). Dynamics of active sensing and perceptual selection. *Current Opinion in ….*

Schürmann, M., Başar-Eroglu, C., Kolev, V., & Başar, E. (2001). Delta responses and cognitive processing: single-trial evaluations of human visual P300. *International Journal of Psychophysiology*, *39*(2), 229–239. https://doi.org/10.1016/S0167-8760(00)00144-6

Sekuler, R., Sekuler, A. B., & Lau, R. (1997). Sound alters visual motion perception. *Nature*, *385*(6614), 308–308. https://doi.org/10.1038/385308a0

Sekuler, R., Sekuler, A., & Lau, R. (1997). Sound alters visual motion perception. *Nature*.

Shah, A. A. S., Bressler, S. S. L., Knuth, K. K. H., Ding, M., Mehta, A. D., Ulbert, I., & Schroeder, C. E. (2004). Neural dynamics and the fundamental mechanisms of event-related brain potentials. *Cerebral Cortex*, *14*(5), 476–483. Journal Article.

Shah, A., Bressler, S., & Knuth, K. (2004). Neural dynamics and the fundamental mechanisms of event-related brain potentials. *Cerebral ….*

Shams, L., Kamitani, Y., & Shimojo, S. (2002). Visual illusion induced by sound. *Cognitive Brain Research*.

Shergill, S., Bays, P., Frith, C., & Wolpert, D. (2003). Two eyes for an eye: the neuroscience of force escalation. *Science*.

Shergill, S., Samson, G., & Bays, P. (2005). Evidence for sensory prediction deficits in schizophrenia. *American Journal of*.

Sherman, S., & Guillery, R. (2002). The role of the thalamus in the flow of information to the cortex. *Of the Royal ….*

Sherman, S. M. (2007). The thalamus is more than just a relay. *Current Opinion in Neurobiology*, *17*(4), 417–422. https://doi.org/10.1016/j.conb.2007.07.003

Shimojo, S., & Shams, L. (2001). Sensory modalities are not separate modalities: plasticity and interactions. *Current Opinion in Neurobiology*, *11*(4), 505–509. https://doi.org/10.1016/S0959-4388(00)00241-5

Shimojo, S., Watanabe, K., & Scheier, C. (2001). 12 The Resolution of Ambiguous Motion: Attentional Modulation and Development. *Visual Attention and Cortical*.

Siegel, M., Donner, T. H., & Engel, A. K. (2012). Spectral fingerprints of large-scale neuronal interactions. *Nature Reviews Neuroscience*, *13*(2), 121–134. Journal Article.

Siegel, M., Engel, A. K., & Donner, T. H. (2011). Cortical network dynamics of perceptual decision-making in the human brain. *Frontiers in Human Neuroscience*, *5*, 21.

https://doi.org/10.3389/fnhum.2011.00021

Singer, W. (1999). Neuronal synchrony: a versatile code for the definition of relations? *Neuron*, *24*(1), 49–65, 111–25.

Singer, W. (2013). Cortical dynamics revisited. *Trends in Cognitive Sciences*, *17*(12), 616–26. https://doi.org/10.1016/j.tics.2013.09.006

Smith, P., & Ratcliff, R. (2004). Psychology and neurobiology of simple decisions. *Trends in Neurosciences*.

Smulders, F. (2010). Simplifying jackknifing of ERPs and getting more out of it: retrieving estimates of participants' latencies. *Psychophysiology*.

Snyder, A., & Foxe, J. (2010). Anticipatory attentional suppression of visual features indexed by oscillatory alpha-band power increases: a high-density electrical mapping study. *The Journal of Neuroscience*.

Sohoglu, E., Peelle, J., & Carlyon, R. (2012). Predictive top-down integration of prior knowledge during speech perception. *The Journal of*.

Song, K., Meng, M., Chen, L., Zhou, K., & Luo, H. (2014). Behavioral oscillations in attention: rhythmic α pulses mediated through θ band. *The Journal of Neuroscience : The Official Journal of the Society for Neuroscience*, *34*(14), 4837–44. https://doi.org/10.1523/JNEUROSCI.4856-13.2014

Spaak, E., Lange, F. de, & Jensen, O. (2014). Local entrainment of alpha oscillations by visual stimuli causes cyclic modulation of perception. *The Journal of Neuroscience*.

Sperry, R. (1950). Neural basis of the spontaneous optokinetic response produced by visual inversion. *Journal of Comparative and Physiological Psychology*.

Stam, C. J., Nolte, G., & Daffertshofer, A. (2007). Phase lag index: assessment of functional connectivity from multi channel EEG and MEG with diminished bias from common sources. *Human Brain Mapping*, *28*(11), 1178–93. https://doi.org/10.1002/hbm.20346

Stefanics, G., & Hangya, B. (2010). Phase entrainment of human delta oscillations can mediate the effects of expectation on reaction speed. *The Journal of ….*

Stein, B. E. (1998). Neural mechanisms for synthesizing sensory information and producing adaptive behaviors. *Experimental Brain Research*, *123*(1–2), 124–135. https://doi.org/10.1007/s002210050553

Stein, B. E., & Meredith, M. A. (1993). *The merging of the senses.* The MIT Press.

Stein, B., London, N., & Wilkinson, L. (1996). Enhancement of perceived visual intensity by auditory stimuli: a psychophysical analysis. *Journal of Cognitive*.

Stein, A. Von, & Sarnthein, J. (2000). Different frequencies for different scales of cortical integration: from local gamma to long range alpha/theta synchronization. *International Journal of Psychophysiology*.

Stekelenburg, J., & Vroomen, J. (2007). Neural correlates of multisensory integration of ecologically valid audiovisual events. *Journal of Cognitive Neuroscience*.

Stenner, M., Bauer, M., Haggard, P., & Heinze, H. (2014). Enhanced alpha-oscillations in visual cortex during anticipation of self-generated visual stimulation. *Journal of Cognitive*.

Stroud, J. M. (1956). The fine structure of psychological time. Journal Article.

Swettenham, J. B., Anderson, S. J., & Thai, N. J. (2010). MEG responses to the perception of global structure within glass patterns. *PloS One*, *5*(11), e13865. https://doi.org/10.1371/journal.pone.0013865

Synofzik, M., Thier, P., Leube, D., & Schlotterbeck, P. (2010). Misattributions of agency in schizophrenia are based on imprecise predictions about the sensory consequences of one's actions. *Brain*.

Tallon-Baudry, C., & Bertrand, O. (1996). Stimulus specificity of phase-locked and non-phase-locked 40 Hz visual responses in human. *The Journal of ….*

Telenczuk, B., & Nikulin, V. (2010). Role of neuronal synchrony in the generation of evoked EEG/MEG responses. *Journal of Neurophysiology*.

Teufel, C., Kingdon, A., Ingram, J. N., Wolpert, D. M., & Fletcher, P. C. (2010). *Deficits in sensory prediction are related to delusional ideation in healthy individuals*. *Neuropsychologia* (Vol. 48). https://doi.org/10.1016/j.neuropsychologia.2010.10.024

Theunissen, F. E., & Doupe, A. J. (1998). Temporal and spectral sensitivity of complex auditory neurons in the nucleus HVc of male zebra finches. *The Journal of Neuroscience : The Official Journal of the Society for Neuroscience*, *18*(10), 3786–802.

Thorne, J. D., De Vos, M., Viola, F. C., & Debener, S. (2011). Cross-modal phase reset predicts auditory task performance in humans. *The Journal of Neuroscience: The Official Journal of the Society for Neuroscience*, *31*(10), 3853. Journal Article.

Thorne, J. D., & Debener, S. (2014). Look now and hear what's coming: On the functional role of cross-modal phase reset. *Hear Res*, *307*, 144–152. Journal Article. https://doi.org/10.1016/j.heares.2013.07.00210.1016/j.heares.2013.07.002. Epub 2013 Jul 12.

Thorne, J., & Debener, S. (2014). Look now and hear what's coming: on the functional role of cross-modal phase reset. *Hearing Research*.

Thorne, J. J. D., & Debener, S. (2014). Look now and hear what's coming: On the functional role of cross-modal phase reset. *Hearing Research*, *307*, 144–152. Journal Article. https://doi.org/10.1016/j.heares.2013.07.00210.1016/j.heares.2013.07.002. Epub 2013 Jul 12.

Thorne, J., Vos, M. De, & Viola, F. (2011). Cross-modal phase reset predicts auditory task performance in humans. *The Journal of*.

Thut, G., Miniussi, C., & Gross, J. (2012). The functional importance of rhythmic activity in the brain. *Current Biology*.

Thut, G., Nietzel, A., Brandt, S. A., & Pascual-Leone, A. (2006). Alpha-band electroencephalographic activity over occipital cortex indexes visuospatial attention bias and predicts visual target detection. *The Journal of Neuroscience : The Official Journal of the Society for Neuroscience*, *26*(37), 9494–502. https://doi.org/10.1523/JNEUROSCI.0875-06.2006

Thut, G., Schyns, P., & Gross, J. (2011). Entrainment of perceptually relevant brain oscillations by non-invasive rhythmic stimulation of the human brain. *Front. Psychol*.

Timm, J., SanMiguel, I., Saupe, K., Schröger, E., Wolpert, D., Ghaharamani, Z., … Echallier, J. (2013). The N1-suppression effect for self-initiated sounds is independent of attention. *BMC Neuroscience*, *14*(1), 2. https://doi.org/10.1186/1471-2202-14-2

Todd, J., & Norman, J. (1991). The visual perception of smoothly curved surfaces from minimal apparent motion sequences. *Perception & Psychophysics*.

Todd, J., & Norman, J. (1995). The effects of spatiotemporal integration on maximum displacement thresholds for the detection of coherent motion. *Vision Research*.

Traub, R., Whittington, M., Stanford, I., & Jefferys, J. (1996). A mechanism for generation of long-range synchronous fast oscillations in the cortex. *Nature*.

Tyll, S., Bonath, B., Schoenfeld, M., Heinze, H., & Ohl, F. (2013). Neural basis of multisensory looming signals. *Neuroimage*.

Uhlhaas, P., Roux, F., & Singer, W. (2009). The development of neural synchrony reflects late maturation and restructuring of functional networks in humans. *Proceedings of the*.

Uitert, R. Van, & Johnson, C. (2004). Influence of head tissue conductivity in forward and inverse magnetoencephalographic simulations using realistic head models. *IEEE Transactions on*.

VanRullen, R. (2006). The continuous Wagon Wheel Illusion is object-based. *Vision Research*, *46*(24), 4091–5. https://doi.org/10.1016/j.visres.2006.07.030

Vanrullen, R. (2013). Visual attention: a rhythmic process? *Current Biology : CB*, *23*(24), R1110-2. https://doi.org/10.1016/j.cub.2013.11.006

VanRullen, R. (2016a). How to Evaluate Phase Differences between Trial Groups in Ongoing Electrophysiological Signals. *Frontiers in Neuroscience*, *10*, 426. https://doi.org/10.3389/fnins.2016.00426

VanRullen, R. (2016b). Perceptual Cycles. *Trends in Cognitive Sciences*, *20*(10), 723–735. https://doi.org/10.1016/j.tics.2016.07.006

VanRullen, R., & Busch, N. (2011). Ongoing EEG phase as a trial-by-trial predictor of perceptual and attentional variability. *Frontiers in ….*

VanRullen, R., Busch, N. A., Drewes, J., & Dubois, J. (2011). Ongoing EEG phase as a trial-by-trial predictor of perceptual and attentional variability. *Frontiers in Psychology*, *2*, 60. Journal Article. https://doi.org/10.3389/fpsyg.2011.00060

VanRullen, R., Busch, N., & Drewes, J. (2011). Ongoing EEG phase as a trial-by-trial predictor of perceptual and attentional variability. *Frontiers in*.

VanRullen, R., Carlson, T., & Cavanagh, P. (2007). The blinking spotlight of attention. *Proceedings of the National Academy of Sciences of the United States of America*, *104*(49), 19204–9. https://doi.org/10.1073/pnas.0707316104

VanRullen, R., & Dubois, J. (2011). The Psychophysics of Brain Rhythms. *Frontiers in Psychology*, *2*, 203. https://doi.org/10.3389/fpsyg.2011.00203

VanRullen, R., & Dubois, J. (2011). The psychophysics of brain rhythms. *Frontiers in Psychology*.

Vanrullen, R., & Dubois, J. (2011). The psychophysics of brain rhythms. *Frontiers in Psychology*, *2*(August), 203. https://doi.org/10.3389/fpsyg.2011.00203

VanRullen, R., Guyonneau, R., & Thorpe, S. J. (2005). Spike times make sense. *Trends in Neurosciences*, *28*(1), 1–4. Journal Article.

VanRullen, R., & Koch, C. (2003). Is perception discrete or continuous? *Trends in Cognitive Sciences*.

VanRullen, R., & Koch, C. (2003). Is perception discrete or continuous? *Trends in Cognitive Sciences*, *7*(5), 207–213. Journal Article.

VanRullen, R., Reddy, L., & Koch, C. (2005). Attention-driven discrete sampling of motion perception. *Proceedings of the National Academy of Sciences of the United States of America*, *102*(14), 5291–6. https://doi.org/10.1073/pnas.0409172102

VanRullen, R., Reddy, L., & Koch, C. (2006). The continuous wagon wheel illusion is associated with changes in electroencephalogram power at~ 13 Hz. *The Journal of Neuroscience*.

Varela, F., Lachaux, J. P., Rodriguez, E., & Martinerie, J. (2001). The brainweb: phase synchronization and large-scale integration. *Nature Reviews. Neuroscience*, *2*(4), 229–39. https://doi.org/10.1038/35067550

Varela, F., Lachaux, J., & Rodriguez, E. (2001). The brainweb: phase synchronization and large-scale integration. *Nature Reviews*.

Venables, P. (1960). Periodicity in reaction time. *British Journal of Psychology*.

Vinck, M., Lima, B., Womelsdorf, T., Oostenveld, R., Singer, W., Neuenschwander, S., & Fries, P. (2010). Gamma-Phase Shifting in Awake Monkey Visual Cortex. *Journal of Neuroscience*, *30*(4), 1250–1257. https://doi.org/10.1523/JNEUROSCI.1623-09.2010

Voloh, B., & Womelsdorf, T. (2016). A Role of Phase-Resetting in Coordinating Large Scale Neural Networks During Attention and Goal-Directed Behavior. *Frontiers in Systems Neuroscience*, *10*, 18. https://doi.org/10.3389/fnsys.2016.00018

von Holst, E., & E. (1954). Relations between the central Nervous System and the peripheral organs. *The British Journal of Animal Behaviour*, *2*(3), 89–94. https://doi.org/10.1016/S0950-5601(54)80044-X

Vorberg, D., Mattler, U., & Heinecke, A. (2003). Different time courses for visual perception and action priming. *Proceedings of the*.

Voss, M., Bays, P., Rothwell, J., & Wolpert, D. (2007). An improvement in perception of self-generated tactile stimuli following theta-burst stimulation of primary motor cortex. *Neuropsychologia*.

Vroomen, J., & Gelder, B. (2000). Sound enhances visual perception: cross-modal effects of auditory organization on vision. *Journal of Experimental Psychology: Human*.

Wang, J., Mathalon, D., Roach, B., Reilly, J., & Keedy, S. (2014). Action planning and predictive coding when speaking. *NeuroImage*.

Wang, S., Musharoff, M., & Canavier, C. (2013). Hippocampal CA1 pyramidal neurons exhibit type 1 phase-response curves and type 1 excitability. *Journal of*.

Wang, X. (2010). Neurophysiological and computational principles of cortical rhythms in cognition. *Physiological Reviews*.

Ward, L. (2003). Synchronous neural oscillations and cognitive processes. *Trends in Cognitive Sciences*.

Wassenhove, V. Van, & Grant, K. (2005). Visual speech speeds up the neural processing of auditory speech. *Proceedings of the*.

Watanabe, K. (2001). CROSSMODAL INTERACTION IN HUMANS.

Watanabe, K., & Shimojo, S. (2001). When sound affects vision: effects of auditory grouping on visual motion perception. *Psychological Science*.

Watkins, S., Shams, L., Josephs, O., & Rees, G. (2007). Activity in human V1 follows multisensory perception. *Neuroimage*.

Watkins, S., Shams, L., Tanaka, S., Haynes, J., & Rees, G. (2006). Sound alters activity in human V1 in association with illusory visual perception. *Neuroimage*.

Weise, A., Hartmann, T., Schröger, E., Weisz, N., & Ruhnau, P. (2016). Cross-modal distractors modulate oscillatory alpha power: the neural basis of impaired task performance. *Psychophysiology*, *53*(11), 1651–1659. https://doi.org/10.1111/psyp.12733

Weiskrantz, L., Elliott, J., & Darlington, C. (1971). Preliminary observations on tickling oneself.

Weiss, C., Herwig, A., & Schütz-Bosbach, S. (2011). The self in action effects: Selective attenuation of self-generated sounds. *Cognition*.

Werner, S., & Noppeney, U. (2010). Distinct functional contributions of primary sensory and association areas to audiovisual integration in object categorization. *The Journal of Neuroscience*.

Wheelwright, S., Baron-Cohen, S., & Goldenfeld, N. (2006). Predicting autism spectrum quotient (AQ) from the systemizing quotient-revised (SQ-R) and empathy quotient (EQ). *Brain Research*.

Whittingstall, K., & Logothetis, N. K. (2009). Frequency-band coupling in surface EEG reflects spiking activity in monkey visual cortex. *Neuron*, *64*(2), 281–9. https://doi.org/10.1016/j.neuron.2009.08.016

Wikswo, J. (1995). SQUID magnetometers for biomagnetism and nondestructive testing: important questions and initial answers. *IEEE Transactions on Applied Superconductivity*.

Williams, Z., Elfar, J., Eskandar, E., & Toth, L. (2003). Parietal activity and the perceived direction of ambiguous apparent motion. *Nature*.

Wilson, H., & Cowan, J. (1972). Excitatory and inhibitory interactions in localized populations of model neurons. *Biophysical Journal*.

Wilson, S., Saygin, A., Sereno, M., & Iacoboni, M. (2004). Listening to speech activates motor areas involved in speech production. *Nature Neuroscience*.

Wolpert, D., & Flanagan, J. (2001). Motor prediction. *Current Biology*.

Wolpert, D., Ghahramani, Z., & Jordan, M. (1995). An internal model for sensorimotor integration. *Science*.

Womelsdorf, T., & Fries, P. (2006). Neuronal coherence during selective attentional processing and sensory–motor integration. *Journal of Physiology-Paris*.

Womelsdorf, T., Schoffelen, J., & Oostenveld, R. (2007). Modulation of neuronal interactions through neuronal synchronization.

Wuerger, S., Hofbauer, M., & Meyer, G. (2003). The integration of auditory and visual motion signals at threshold. *Perception & Psychophysics*.

Wutz, A., Muschter, E., van Koningsbruggen, M., & Melcher, D. (2014). Saccades reset temporal integration windows. *Journal of Vision*, *14*(10), 584–584.

Wyart, V., & Sergent, C. (2009). The phase of ongoing EEG oscillations uncovers the fine temporal structure of conscious perception. *The Journal of Neuroscience*.

Zar, J. (1999). Biostatistical analysis.

Zhang, C., & Lewis, T. (2013). Phase response properties of half-center oscillators. *Journal of Computational Neuroscience*.